Pathways Regulating Inflammation in Microglia and Ageing

Lily Keane

A thesis submitted for the degree of Doctor of Philosophy at Queen Mary, University of London
June 2016

Centre for Cancer and Inflammation
Bart's and The London
Queen Mary's School of Medicine and Dentistry
Charterhouse Square
London, EC1M6BQ

Statement of originality

I, Lily Keane, confirm that the research included within this thesis is my own work or that where it has been carried out in collaboration with, or supported by others, that this is duly acknowledged below and my contribution indicated. Previously published material is also acknowledged below.

I attest that I have exercised reasonable care to ensure that the work is original, and does not to the best of my knowledge break any UK law, infringe any third party's copyright or other Intellectual Property Right, or contain any confidential material.

I accept that the College has the right to use plagiarism detection software to check the electronic version of the thesis.

I confirm that this thesis has not been previously submitted for the award of a degree by this or any other university.

Signature:

Date:

Details of collaboration and publications:

1. RNA sequencing was carried out by a company called Oxford Gene Technology (OGT), Begbroke Hill, Woodstock Road, Begbroke, Oxfordshire

2. RNA sequencing analysis and generation of graphs relating to this data was carried out by Dr. Raphael Zollinger at the centre of Cancer and Inflammation, Barts Cancer Institute, Queen Mary University of London, London

Abstract

Inflammation is implicated in a wide array of diseases and is associated with the ageing process: 'inflammageing' is the low-grade inflammation that occurs as an organism ages. I was particularly interested in age-related inflammation of the brain, thought to be mediated by microglia, the immune cells of the central nervous system (CNS). To this end, I carried out RNA sequencing of microglia from young (6 months) and aged mice (23 months). I found that microglia from aged mice have a very distinct transcriptome signature. Interestingly, pathways associated with mTOR signalling and inflammation were upregulated. Given the evidence that mTOR is a key modulator of ageing, I investigated its role in inflammation in microglia. Using a mouse model in which Rheb, a positive regulator of mTORC1, was knocked out in Csf1r-expressing cells (microglia and macrophages), I found that *in vivo* LPS stimulation caused a significant increase in the transcription of inflammatory genes in microglia from mTORC1-deficient mice compared to controls. The effect was further exaggerated in mTORC1-deficient aged mice, suggesting a role for mTORC1 in the priming of aged microglia. However, these transcriptome changes were not translated into protein; indeed, *Csf1r-Cre; Rheb f/f* mice showed reduced overall inflammation, as measured by sickness behaviour in the open-field test and by plasma cytokine levels. On the other hand, long-term treatment with rapamycin *in vivo* showed a very distinct phenotype, with reduced inflammation following LPS stimulation in young mice but no effect in aged ones. This PhD thesis sheds new light on pathways regulating microglia in ageing and has clinical implications for pathologies in which inflammation plays a major role.

Dedication

I dedicate this thesis to my family:

To my father, Patrick, the rock of our family,

To my mother, Lilian, the heart of our family,

To my sister, Jennifer, the heroine of our family,

To my brother, Rory, the kindness of our family,

Acknowledgements

I have no doubt that without the help of a number of people; I wouldn't have been able to accomplish this study or become the scientist that I am today. The most important person for me to thank is my supervisor Dr. Melania Capasso for always supporting, inspiring, motivating and continually pushing me to challenge myself and grow as a scientist.

At the beginning of my PhD, I was incredibly lucky to work with two Postdoctoral researchers, Cristina Ghirelli and Raphael Zollinger, who both spent considerable time training me on how to set up and properly control experiments as well as teaching me about the importance of scientific integrity. I must especially thank Raphael for his help in my RNA sequencing study. Raphael helped me to carefully design these experiments as well as doing all the analysis. I always enjoyed discussing my results with both Cristina and Raphael and found their support particularly at the beginning of my PhD invaluable. I would also like to thank all the other members of my lab (past and present) who have all in someway helped me during my PhD, be it practically or in a supporting capacity.

I must also thank my wonderful friends at the Barts Cancer institute who have showed me continual support during the course of my PhD. I especially have to thank my thesis readers Dr. Caroline Besley, Emma Uthaya Vilventhraraja, Arran Dokal and Dr. Nia Emami.

I must also thank my wonderful family who always show me uncompromising support and practical advice. I must particularly acknowledge my Dad, who has always believed in me and my Mum who is always on my side even when I'm wrong!

Last but not least I must thank my funding body Age Uk. This work would have been impossible without the financial support from them. I would like to thank all the people who fundraised so that I could carry out my research.

List of Figures

List of Tables

Abbreviations

Adenosine monophosphate-activated protein kinase	AMPK
Adenosine triphosphate	ATP
Antigen presenting cells	APCs
Bone-marrow derived dendritic cells	BMDC
Bone-marrow derived macrophages	BMDM
Bovine serum albumin	BSA
Brain-derived neuotrophic factor	BDNF
Caloric restriction	CR
Central nervous system	CNS
Cluster of differeniation	CD
Complement receptor 3	CR3
Cyclooxygenase-2	COX-2
Danger assoicated molecular patterns	DAMPS
Dendritic cells	DCs
Ethylenediaminetetraacetic acid	EDTA
Eukaryotic translation initiation factor 4E	eIF4E
Eukaryotic translation initiation factor 4E-binding protein	4E-BP1
Eukaryotic translation initiation factor 4G	eIF4G
Fetal bovine serum	FBS
Fluorescence-activated cell sorting	FACS
Forkhead Box O	FOXO
Fragments per kilobase of exon per million fragments mapped	FPKM
Gene-set enrichment analysis	GSEA
General control protein 4	GCN4
GTPase activating protein	GAP
Guanosine diphosphate	GDP
Guanosine triphosphate	GTP
Hank's balanced salt solution	HBSS
Hypoxia-inducible facotr 1 α	HILF1α
IKappaB kinase alpha	IKK-α
Ingenuity Pathway Analysis	IPA
Insulin growth factor	IGF
Insulin receptor 1	IRS1
Interferon induced transmembrane proteins	IFITMS
Interferon-γ	IFN-γ
Lipopolysaccaride	LPS
Major histocompatibility complex	MHC
Mammalian target of rapamycin	mTOR
Mitogen-activated protein kinases	MAPK
NLR-related apoptosis inhibitory protein	Naip
Nod-like receptors	NLRs
Nuclear factor kappa beta	NF-κB
Nucleotide-binding oligomerization domain	NOD

Open-field test	OFT
Oxford gene technology	OGT
Parts per million	PPM
Pattern assoicated molecular patterns	PAMPS
Peripheral blood mononuclear cell	PBMC
Peroxisome proliferator activator receptor	PPAR
Phosphate-buffered saline	PBS
Phosphatidylserine	PS
Phosphoinositide 3-kinase	PI3K
PPARγ coactivator 1	PGC-1
Protein kinase C	PKC
Quantiative real time polymerase chain reaction	qPCR
Reactive oxygen species	ROS
RNA integrity number	RIN
Senescence-assoicated secretory phenotype	SASP
Sialic acid binding Ig-like lectins	SIGLECs
Sodium dodecyl sulfate,	SDS
Specific pathogen free	SPF
Sterol regulatory element-binding protein-1	SREBP-1
Straphloccus aureus cowan 1	SAC
Tamoxifen	TAM
Terminal oligopyrimidiine	TOP
Toll-like receptor	TLR
Tricarboxylic acid cycle	TCA
Triggering receptor expressed by myeloid cells-2	TREM2
Tuberous sclerosis complex	TSC
Tumour necrosis factor	TNF
Urinary tract infection	UTI
Wild-type	WT

Table of Contents

1 Introduction

1.1 Life expectancy

World life expectancy has more than doubled over the past two centuries, rising from 25 to 65 years in men and 25 to 70 years in women, resulting in a 2.5 year increase in lifespan per decade, as depicted in **Fig. 1.1**[1]. This figure represents global life expectancy, whereas for example, in the U.K., the average life expectancy is much higher, ranging from 79.1 years for men to 82.8 years for women[2]. The United Nations (UN) has estimated that by 2050 the number of people over 60 years of age will exceed the number of people under 60 years of age in the western world[3].

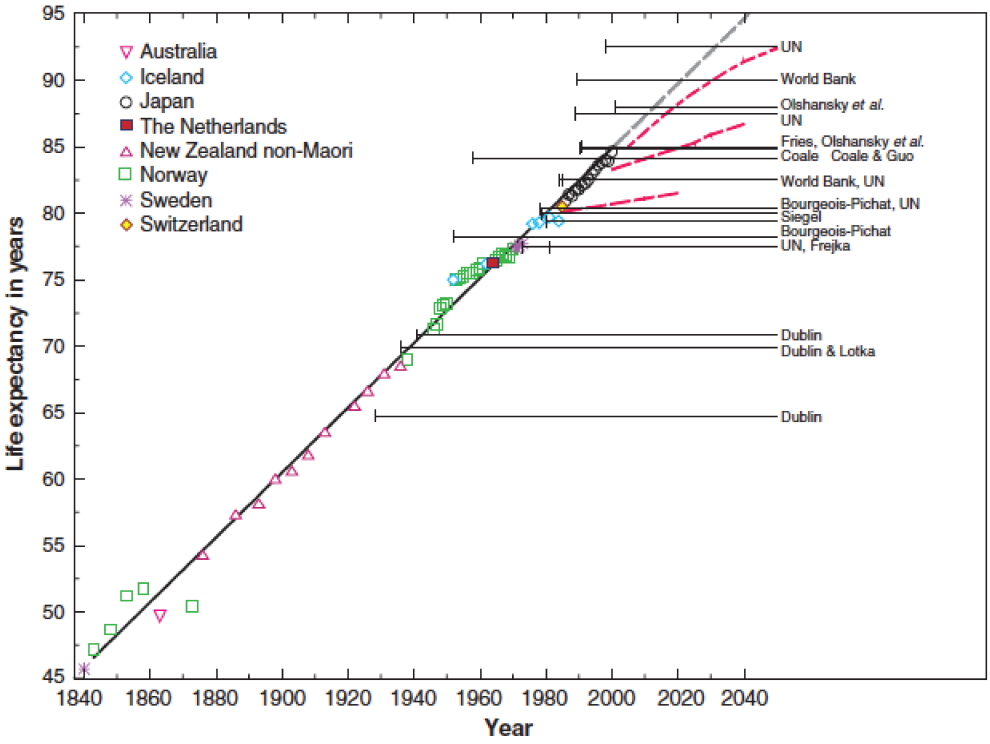

Figure 1.1 Female lifespan expectancy recorded from 1840. The linear regression trend is depicted by a bold black line and the extrapolated trend by a dashed grey line. The horizontal black and grey lines show asserted ceilings on life expectancy, with a short vertical line indicating the study year of publication[1].

1.2 Ageing

Ageing is defined as the gradual decline and functional deterioration of the body, leading to increased vulnerability to death[4]. While lifespan is clearly increasing, as described in **Fig 1.1**, the number of people ageing and therefore affected by age-related

diseases is also increasing. This is because ageing is a major risk factor for a number of chronic illnesses such as diabetes and cardiovascular diseases[5], as well as cancer (**Fig. 1.2**). Ageing is also a primary risk factor for a number of neurodegenerative pathologies, such as Alzheimer's[5].

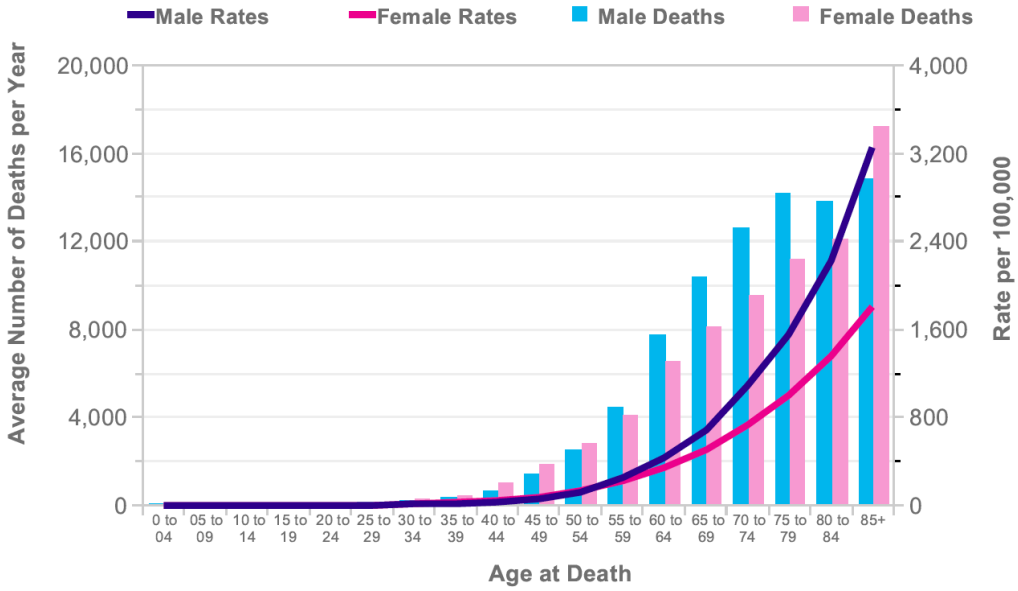

Figure 1.2 The average number of cases of all cancers (excluding non-melanoma skin cancer). The graph shows incidence rates of cancer per 100,000 (blue and pink lines for males and females, respectively) and cancer-related deaths/year (blue and pink bars). Data refer to cases in the United Kingdom from 2011 to 2013. Graph adapted from Cancer Research UK.

The correlation between age and illness has also been shown for dementia, as depicted by **Fig. 1.3** in the world Alzheimer's report in 2015, which showed that the incidence of dementia exponentially increases with age, doubling with every 6.3-year increase in age[6].

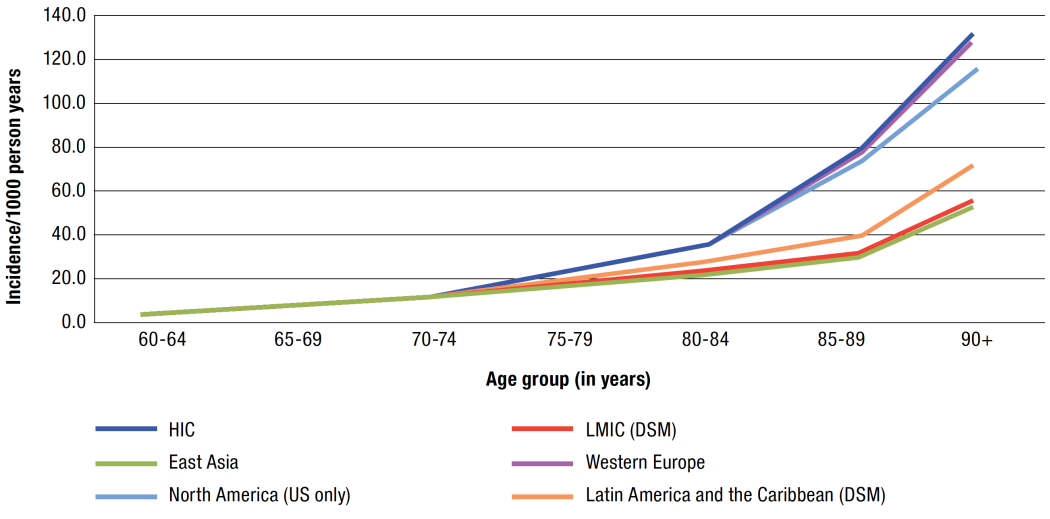

Figure 1.3 Estimated age–specific annual incidence of dementia in different regions across the globe. Incidence is given per 1000 persons per year on the x-axis, with each region depicted by a coloured line. Age groups are shown in years on the y-axis. High- and low-income countries are represented by the blue and red lines, respectively. Data was obtained from the World Alzheimer's report 2015[6].

It is clear that the burden of chronic illnesses is strongly correlated with age; it is therefore a major aim of ageing research to understand how we age and to try and treat age-related illnesses to potentially reduce this burden. "Researchers are learning about the molecular basis of ageing and finding clues about how to treat diseases in the process" Katherine Bourzac, Nature Outlook, 2012[7].

1.3 The Hallmarks of Ageing

In 2000 Hanahan and Weinberg described the six hallmarks of cancer, defining the key characteristics acquired by cancer cells, categorising the cancer research field into subfields that are still of extreme importance today[8]. A similar breakthrough publication was published in *Cell* in 2012 entitled "The Hallmarks of Ageing", whereby the authors attempted to define the common denominators of ageing as shown in **Fig. 1.4**. The hallmarks were categorised into nine groups: 1) genomic instability – the accumulation of different types of DNA damage over time; 2) telomere attrition – the progressive loss of sequences from the ends of chromosomes as we age; 3) epigenetic alterations, such as histone modifications, DNA methylation and chromatin remodelling; 4) loss of proteostasis – the progressive loss of stability of the cell's proteome, which leads to the accumulation of misfolded or aggregated proteins; 5) deregulated nutrient sensing – deregulation of many pathways that sense changes in the availability of nutrients, such as the Insulin Growth Factor (IGF), mammalian target of rapamycin (mTOR), AMP-activated kinase (AMPK) or sirtuin-regulated pathways; 6) mitochondrial dysfunction – which may lead to an increased production of reactive oxygen species (ROS), known to accompany ageing and promoting the deterioration of mitochondria and other cell organelles; 7) cellular senescence – whereby cells exit the cell cycle and change their phenotype; 8) stem cell exhaustion – where tissues lose their ability to regenerate, this also includes the reduction of both haematopoiesis and the production of adaptive immune cells (Immunosenescence); 9) altered intercellular communications, such as "inflamm-ageing", the low grade pro-inflammatory phenotype that accompanies ageing

in mammals[4]. Inflamm-ageing will be the focus of my PhD thesis and will therefore be discussed in more detail.

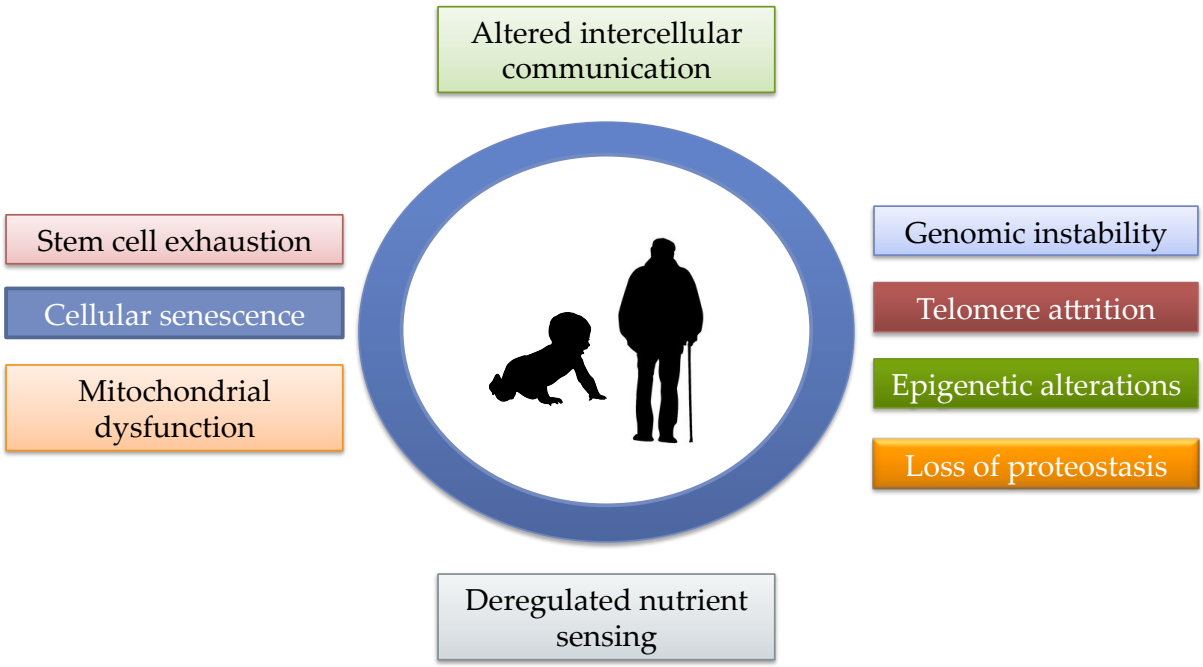

Figure 1.4 The Hallmarks of Ageing - schematic showing "The Nine Hallmarks of Ageing", adapted from Lopez –Otin *et al.*[4].

1.3.1 Inflamm-ageing

A consequence of ageing is the increase in the inflammatory response that can often lead to tissue damage[9]. This damage can itself drive further inflammation in the form of cytokine secretion and ROS production. This perpetual cycle of damage and cytokine release can lead to chronic inflammation with age. This phenomenon was first described as inflamm-ageing in 2000 by Franceschi *et al.*[10]. In this paper, the authors proposed that "inflamm-ageing" is the combination of a progressive increase in pro-inflammatory status and a decreased ability to cope with a number of stressors. Furthermore, they postulated that the persistent pro-inflammatory phenotype that ensues over time is the first phenomenon that eventually leads to increased susceptibility to age-related illnesses. They suggest that genetic factors (loss of robust gene variants or gain of fragile gene variants) may be the second hit that contributes to the development of

diseases with an inflammatory pathogenesis, for example Alzheimer's disease or many types of cancer[9].

1.3.2 Factors that contribute to inflamm-ageing

A number of potential factors contribute to the induction of a more pro-inflammatory phenotype, for example impaired autophagy or inflammasome activation.

Autophagy is the mechanism by which a cell digests its own cytoplasmic contents, it can be a survival pathway in the absence of nutrients but it is also required for the stead-state removal of damaged organelles, which are eventually degraded in lysosomes. This process has been shown to decline with age[11] and the accumulation of damaged organelles can lead to the activation of intracellular sensors such as inflammasomes, leading to increased inflammation. Inflammasomes are multiprotein complexes with different core components (Nod-like receptors – NLRs or AIM2) that assemble in response to a number of different danger signals and lead to the activation of caspase-1; once active, caspase-1 cleaves the inactive pro-IL-1 into its active form IL-1β, contributing to overall inflammation. For example, the NLRP3 inflammasome can be activated by ROS that are generated by an accumulation of dysfunctional mitochondria[12]. The NLRP3 inflammasome, in particular, has been associated with a number of age-related illnesses, such as Alzheimer's disease[13]. The accumulation of amyloid beta in the Alzheimer's brain is linked to a defective neuronal autophagy mechanism[14]; its accumulation activates the NLRP3 inflammasome in microglia cells, leading to the production of IL-1β, which contributes to neuroinflammation in Alzheimer's disease[13,15]. In fact, NLRP3 -/- and Casp1 -/- mice, crossed with models of familial Alzheimer's disease, were largely protected from spatial memory loss and had an enhanced capacity to clear amyloid β[13], implicating the NLRP3 inflammasome as a key player in the pathogenesis of Alzheimer's disease. Caspase-1 has also been shown to cleave pro-IL-18 into it's active form IL-18 and therefore, it's production must also be considered as a consequence of NLRP3 inflammasome activation[16].

1.3.3 Senescence Associated Secretory Phenotype (SASP)

The factors described in the previous paragraph are also key stressors that can drive cellular senescence. The senescence programme initiates cell-cycle arrest in order to

prevent cells from dividing and spreading damage to daughter cells. Once a certain threshold of damage is reached within the cell, the senescence programme is activated[17]. Senescent cells are characterized by the secretion of a number of factors, which have been collectively called the Senescence Associated Secretory Phenotype (SASP)[17]. The SASP was recently characterized by Coppe *et al.* using antibody arrays to measure the secretome of human fibroblast and epithelial cells that had been exposed to genotoxic stess[18]. They found that the secretome of senescent cells was complex and contained multiple factors that related to inflammation, including many interleukins, chemokines and growth factors[18]. There is a lot of interest on fully elucidating the SASP, as these factors may have an impact on surrounding cells that lead to multiple pathologies, for example cancer[19].

1.4 Ageing interventions

1.4.1 Caloric restriction

It was published for the first time in 1935 that restricting the number of calories, while retaining "adequate levels of all other constituents", resulted in the extension of lifespan in white rats[20], although it was not until the early 1990s that further studies showed that this was also evident in other model organisms such as yeast, worms, flies and mice[21]. In 2009 this was further supported by a report in *Science* which showed that caloric restriction (CR) could also extend lifespan in Rhesus monkeys[22]. This study was conducted over a 20-year period and included both male and female Rhesus monkeys. Monkeys were only enrolled in the study once they had reached adulthood and during the study they were continually monitored for signs of illnesses. The cause of death for each monkey was assessed by a pathologist; this allowed the authors to assess not only the effect of CR on lifespan but also to determine its impact on age-related illnesses. They found that monkeys, whose calories were not restricted, had three times the rate of death from age-related diseases, compared to monkeys who had calories restricted since adulthood. The authors identified long-term health benefits in monkeys on a calorie-restricted diet, including a 50% reduction in the incidence of cancer and heart disease, as well as reduced brain atrophy, a sign normally associated with ageing. Strikingly, CR monkeys seemed to be completely protected from diabetes, with all experimental monkeys maintaining glucose homeostasis throughout their lifespan. Overall, CR

appeared to promote survival, reduce age-related illnesses and improve overall metabolic function[22].

Both the extension of lifespan and prevention of age-related illnesses are now widely accepted outcomes of CR. In recent years, it has been proposed that CR may exert some of these anti-ageing properties by relieving oxidative stress and reducing chronic inflammation, two processes that increase with age. Evidence suggests that CR can in fact suppress the activation of the nuclear factor kappa beta (NF-κB) transcription factor[23], a major player in the pro-inflammatory response, while promoting the activation of the peroxisome proliferator-activator receptor family (PPARs) of transcription factors[24]. The activity of PPARs have been shown to decline with age and recently PPARα and PPARγ, in particular, have been shown to inhibit inflammatory cytokine production and promote an anti-inflammatory phenotype[24].

Downregulation of mitogen-activated protein kinase (MAPK) family members ERK, JNK and p38 MAPK, modulation of the forkhead box O (FOXO) transcription factors and activation of sirtuins have all been linked to the anti-inflammatory effects of CR. It has been proposed that these mechanisms could at least in part explain the effects on health and lifespan exerted by CR[25].

1.4.2 mTOR inhibition

The link between dietary restriction and the mTOR pathway in extending lifespan has become clearer in the past ten years. mTOR is a serine/threonine kinase that plays an essential role in cell growth and response to nutrients. A full description of mTOR, and the two complexes containing it, mTORC1 and mTORC2, is provided on pages 22-27 of this introduction, here I only report evidence that mTOR inhibition is beneficial in lifespan extension.

In 2006, Kaeberlein *et al.*[26] conducted a large-scale experiment using 564 strains of *Saccharomyces cerevisiae*, each containing a single gene deletion. They identified ten strains out of 564 that showed a 30% increase in lifespan compared to wild-type (WT) yeast. Of these ten genes, six were related to the yeast homolog of mTOR known as TOR and the Sch9 pathway. The Sch9 gene encodes a protein kinase homologous to the mammalian protein kinase B/AKT and p70S6 kinase. In yeast, Sch9 is important for

regulating cell growth in response to nutrients[27]. Calorie restriction failed to extend lifespan in the TOR-deleted yeast strain, further suggesting that TOR is a target of CR[26]. These findings were further supported by a number of studies in which mTOR was genetically inhibited in other model organisms. For instance, Hansen *et al.*[28] found that reducing levels of ribosomal proteins, S6 kinase or translation initiating factors, all downstream targets of TOR, extended lifespan in *Caenorhabditis elegans*[29]. Like in the yeast study, the authors found that reducing the levels of these factors by RNA interference in calorie-restricted worms did not extend lifespan further[29]. Overall, these studies lead to the view that inhibition of TOR in lower organisms and mTOR in mammals, specifically the mTORC1 complex, was responsible for the extended lifespan caused by CR, although the effect on mTORC1 mediated by CR is likely to be very complex and warrants further investigation[30].

Given that genetic inhibition of mTOR was shown to extend lifespan in a number of model organisms, as shown in **Tab. 1.1**, there is significant interest in targeting mTOR as an anti-ageing intervention. In 2012, a study was published showing that mTOR inhibition with the drug rapamycin could extend lifespan in mice[31]. This pivotal study was carried out by the National Institute on Ageing Interventions Testing Program and tested rapamycin at three independent sites. Rapamcyin extended the median and maximum lifespan of both males and females at all three sites involved in the experiment. Rapamycin was encapsulated and incorporated into the diet and was given to mice starting from 600 days of age. The authors found that this lead to a 9% increase in male lifespan and a 14% increase in female lifespan[31].

There are a number of potential mechanisms that have been suggested to extend lifespan via mTOR inhibition. One of the primary functions of mTORC1 is to promote cell growth and proliferation in response to nutrients, an effect mediated by regulation of both the initiation and elongation steps of protein translation, through its downstream targets S6K and the eukaryotic translation initiation factor 4E-binding protein 1 (4E-BP1)[32].

A global reduction in protein translation could be beneficial in ageing. For example, it could be particularly important when considering age-related pathologies in which protein translation becomes deregulated, for example in many types of cancers.

However, recent evidence suggests that it is not the global reduction in protein translation that mediates overall lifespan extension, rather the promotion of translation of specific mRNAs. For example, it was recently shown in yeast that genetic or pharmacological reduction of the 60S ribosomal subunit extends lifespan[33]. In this study, the authors found that 60S reduction lead to an increase in the activation of general control protein 4 (Gcn4), a transcription factor that is regulated by nutrient availability. Interestingly, they showed that this factor alone appeared to be essential for lifespan extension. In fact, in a number of long-lived mutant strains, this effect was abolished when Gcn4 was deleted. Gcn4 regulates the expression of many genes relating to both lifespan extension and autophagy and appears to be preferentially translated when mTORC1 is inhibited, due to structural features in its 5' region[34]. The idea that a subset of mRNAs is preferentially translated upon mTOR inhibition and that this may influence lifespan extension is further supported by evidence that downregulation of the eukaryotic translational initiation factor 4G (eIF4G) in *C. elegans* lead to an increase in lifespan, which is mediated by an increase in translation of genes relating to the stress response[33].

The activation of autophagy has also been suggested as a potential mechanism that affects lifespan after mTOR inhibition, since mTOR is a negative regulator of this process[35]. When nutrient availability is limited, cells initiate autophagy, a lysosomal-dependent process of self-digestion, as mentioned previously. In this process, damaged organelles are hydrolysed, so that energy can be produced and used for other processes. ATG1 is an important kinase that forms a complex with ATG13 and ATG17 to initiate autophagy[35]. Autophagy declines with age and this has been implicated in a number of age-related illnesses, as previously discussed in the context of inflamm-ageing[36]. In a study in fruit flies, rapamycin caused an increase in lifespan that was accompanied by an increase in the number of lysosomes and autolysosomes, which indicated activation of autophagy. The authors used RNA interference to downregulate the autophagy gene ATG5 in rapamycin-treated flies and found that this completely abrogated lifespan extension, suggesting that, at least in Drosophila, the induction of autophagy was essential for mediating an increase in lifespan[37]. This report was further supported by a similar study in *C. elegans* in which TOR inhibition was also associated with an induction of autophagy and the autophagy genes bec-1 and vps-34 were shown to be required for longevity[28].

Other mechanisms that have been linked to extension of lifespan via mTOR inhibition include enhanced stress resistance and improved mitochondrial function, as well as possible links to inflammation[30]. The potential role of mTOR in the regulation of the inflammatory response will be further discussed in a later section.

	S. cerevisiae	C. elegans	D. melanogaster	M. musculus
Rapamycin	**YES**	**YES**	**YES**	**YES**
mTOR gene mutation or knockdown	**YES**	**YES**	**YES**	**YES**
Raptor gene mutation or knockdown	Not reported	**YES**	Not reported	Not reported
Tsc1 and Tsc2 activation	Not applicable	Not applicable	**YES**	Not reported
S6K gene mutation or knockdown	**YES**	**YES**	**YES**	**YES**
4E-BP activation	Not applicable	Not applicable	**YES**	Not reported
Translation initiation factor knockdown	**YES**	**YES**	Not reported	Not reported
Ribosmal protein knockdown	**YES**	**YES**	Not reported	Not reported

Table 1.1 Summary of studies on TOR signalling pathway and lifespan extension. The table provides a comparison of studies in which the mTOR pathway was either genetically or pharmacologically inhibited and then lifespan extension was assessed. The table includes studies carried out in four different model organisms; yeast, worms, flies and mice. Table 1 is adapted from a review by Johnson *et al.*[30].

1.5 Microglia

1.5.1 Microglia origin and discovery

Microglia are immune cells that derive from myeloid progenitors residing in the brain during development[38,39]. They play an important role in the development, repair, response to injury and maintenance of the neural environment[40]. Pio del Rio Hortega first introduced microglia as morphologically distinct from astrocytes and neurons in a breakthrough publication in 1932, in which he made several observations that are still relevant today[41] (**Fig. 1.5**).

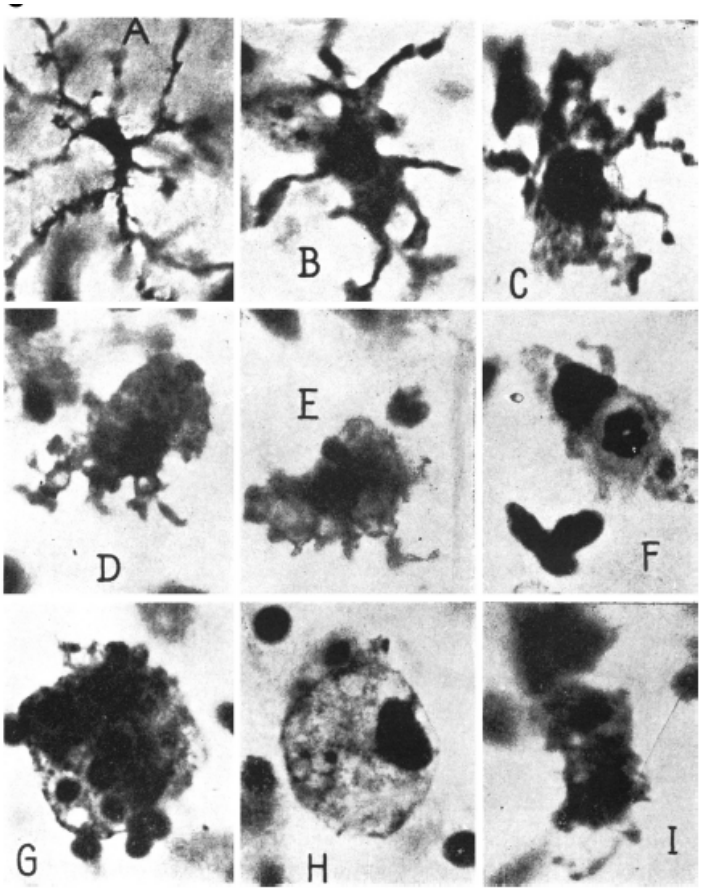

Figure 1.5 Microglia cells as described by Rio Hortega in 1932. Photomicrographs showing the evolution of microglia during phagocytic activity. **A**) A cell with thick, rough prolongations; **B**) a cell with short prolongations and enlarged cell body; **C**) an hypertrophic cell with pseudopodia; **D**) and **E**), amoeboid and pseudopodic forms; **F**) a cell with phagocytosed leukocyte; **G**) a cell with numerous phagocytosed erythrocytes; **H**) a fat-granule cell; **I**) a cell in mitotic division[41].

1.5.2 Microglia function

Microglia share both phenotypic and functional characteristics with other mononuclear phagocytes. Phenotypically, they express major histocompatibility complex (MHC) molecules I and II, as well as several cluster of differentiation (CD) proteins[42-44]. Functionally they are able to carry out myeloid-specific functions including antigen presentation and phagocytosis as well as contribute to inflammation[45]. However, microglia are also quite distinct from other tissue-resident macrophages due to their neural environment[46]. While there have been many studies focusing on the role of microglia in CNS pathology, it is only becoming apparent that these cells play a vital role in CNS homeostasis[47], participating in functions such as phagocytosis of apoptotic neurons, synaptic pruning[48], reorganisation of neuronal circuitry, as well as regulation

of neurons and their numbers in the developing and adult CNS. They carry out this function by phagocytosing neurons with an "eat me" signature and also by triggering programmed cell death in neurons by the release of neurotoxic substances[49]. One possible "eat me" signal detected by microglia is phosphatidylserine (PS), expressed on the plasma membrane of dying cells. One study showed that primary rat cultures of neurons co-cultured with microglia and stimulated with lipopolysaccaride (LPS) lead to neurons exposing PS, resulting in phagocytosis of dying neurons by microglia. In fact the authors showed that up to 90% of neurons in this system could be rescued by blocking the microglia receptor for PS, the vibronectin receptor[50]. Another possible "eat me" signal is the cellular ligand for TREM2 (triggering receptor expressed by myeloid cells-2) that is upregulated on dying neurons. It has been suggested that this interaction promotes microglia-mediated phagocytosis[51].

There are also important neuronal "don't eat me" signals that can inhibit phagocytosis in microglia, for example, CD47 is expressed on cells and myelin in the brain and binds to SIRPα expressed on microglia. It has been shown that binding of CD47 to this receptor inhibits phagocytosis in microglia[52]. Another example of a "don't eat me" signal is polysialylated proteins that are expressed on the surface of neurons. These proteins have been shown to bind to sialic acid-binding immunoglobulin-like lectins known as SIGLECs. The binding of these proteins can active SIGLEC-E expressed on mouse neurons and can also inhibit phagocytosis[53]. It has also been shown that neurons can secrete the chemokine CX3CL1, known as fractalkine. This chemokine can suppress the microglia-mediated inflammatory response by binding to it's receptor CX3CR1 expressed on the surface of microglia and in this way can provide another signal preventing the phagocytosis of the neurons by microglia[54].

Microglia also play a role in adult neurogenesis by either phagocytosing neural progenitor cells[55] or by stimulating the proliferation of progenitor cells through the secretion of soluble factors such as the protease inhibitor, TIMP-1, chemokines such as CXCL1 and RANTES and pro-inflammatory cytokines such as IL-6[56].

Evidence is also emerging that microglia monitor and maintain synapses in the uninjured brain. Two-photon imaging has shown that microglia cells are highly active and motile even in their resting state. They are highly branched and continually survey

their microenvironment[57,58], which results in frequent and persistent contact with synapses[47]. During early development, new neurons and synapses are made at a very high rate, resulting in more neurons and synapses than required. Synaptic pruning is a process by which these "excessive" synapses are removed. Overgrowing synapses followed by their pruning was first shown to be important for optimal memory performance[59]. Paolicelli *et al.*[48] showed through the use of immunohistochemistry and electron microscopy that uninjured brain microglia engulfed synaptic material in the process described as synaptic pruning[48]. The authors suggested that microglia exerted a central role in the accurate maturation of synapses and that a deficit in this process could lead to neurodevelopmental disorders[48].

Recently a number of signals have been identified that may trigger the process of synaptic pruning by microglia. One of the best described is the complement proteins C1q and C3. These proteins have been shown to be expressed in a variety of regions in the healthy postnatal brain mainly localising to immature synapses in these regions[60]. Microglia are known to express the receptor for these complement proteins known as complement receptor 3 (CR3) and in fact the engulfment of synapses by these cells has been shown to be significantly reduced in both C3 and CR3 KO mice suggesting that microglia are targeted to immature synapses by the complement proteins[61]. The CX3CL1-CX3CR1 signalling axis between neurons and microglia has also been implicated in the process of synaptic pruning. Most of evidence for this comes from KO models where CX3CR1 was deleted. One study showed that CX3CR1 KO mice had an accumulation of immature dendritic spines in the developing hippocampus[48]. A similar study showed an increase in immature synapses in the cortex of CX3CR1 KO mice[62]. Both the complement system and the CX3CR1 signalling axis have both been implicated in the process of synaptic pruning during brain development; however, other molecules have been implicated in this process in the adult brain. One example is ATP, which has been shown to be important for purinergic signalling, as well as enhancing the outgrowth of microglia processes during times of high neuronal activity[63]. Other molecules implicated in the adult brain include cytokines such as TNF which has been shown to modify the strength of synapses[64] as well as brain-derived neurotropic factor (BNDF)[48,65].

1.5.3 Microglia activation

One of the characteristic features of microglia is their rapid activation in response to minor changes in the CNS. Given the appropriate stimuli, microglia undergo a morphological shift from a highly branched and ramified morphology to an activated amoeboid morphology with retracted processes and enlarged cell bodies[66]. This phenotypic shift is different to other antigen presenting cells (APCs) such as dendritic cells and splenic macrophages, which extend their dendrites upon antigen stimulation[67]. Microglia activation proceeds through a series of steps (**Fig. 1.5**)[68]. Their activation involves two mechanisms: the loss of inhibitory signals received from neurons or the triggering of receptors by a range of stimuli[69] (**Fig. 1.6**).

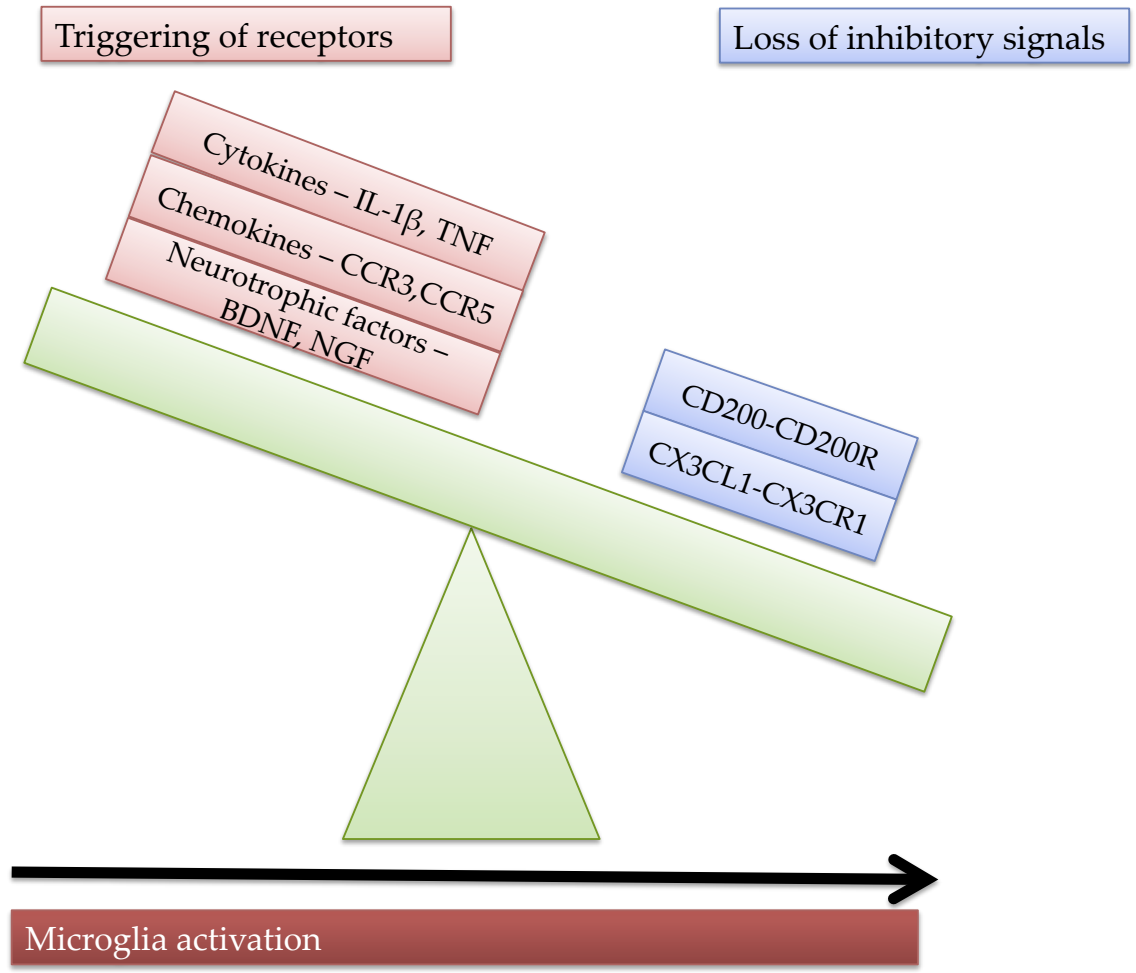

Figure 1.6 Illustration depicting the fine balance between inhibitory and activating signals in microglia based on several published studies[54,69-71].

1.6 Microglia and ageing

To date, the majority of studies on microglia have focused on the adult brain, yet it appears that the function and phenotype of these cells changes over the entire lifespan. For example, during development, microglia clear unnecessary debris, aberrant proteins[42] and apoptotic cells[72]. They exert an important function in pruning excess neurons in the developing brain[73], eliminating synapses[74] and possibly influencing the formation of neural circuits and the correct development of the brain[75,76], as previously mentioned. In the adult brain, resting microglia are continuingly surveying the brain[58] and play an important part in maintaining CNS homeostasis[47].

1.6.1 Morphology and distribution

While it is known that microglia activation becomes deregulated in the course of diseases such as Alzheimer's, during which they become reactive and inflammatory[13], less is known about microglia function during the process of "healthy" brain ageing. A study by Tremblay *et al.*[77] showed that microglia increase in numbers and become unevenly distributed throughout the cortices in two inbred strains of mice as they aged[77]. This agreed with an earlier study that examined the cortex region of the brain in rats, reporting a similar increase in numbers and shape alterations in aged microglia[78]. Aged microglia in the human brain demonstrated a change in morphology including de-ramification, loss of protrusions and branches, spheroid formation and fragmentation of processes[40]. These findings were confirmed using time-lapse live-cell confocal imaging of resting retinal microglia in the mouse eye, where aged microglia appeared significantly smaller and less branched than their younger counterparts[79]. This dystrophic change in morphology has been suggested as an indication of microglial cell senescence[80], whereas other studies suggest that the changes are a reflection of a more active phenotype[81].

1.6.2 Microglia activation markers

Other studies that have investigated changes in microglia in the ageing brain have looked at the expression of activation markers. Ogura *et al.* showed that the number of MHC II-positive microglia increased in older (12 month) rats compared to their younger counterparts (3 months)[82]. This observation was further supported by a later study that isolated microglia from the hippocampus of 3- and 24-month old rats. Here, the authors

showed, by quantitative real-time PCR (qPCR), an increase in expression of MHC II and also of another microglia activation marker, CD86[83]. Letiembre *et al.* also used qPCR but this time using RNA from the whole brain to show an increase in the expression of the microglia activation marker CD14[84].

1.6.3 Microglia regulation of inflammation

Several studies have focused on microglia in the ageing brain and whether they contribute to "inflamm-ageing"[10]. One study used immunohistochemical analysis and qPCR to show that, in human brain samples, there was an increase in the number of IL-1α positive microglia in the ageing brain[85]. Another study showed an increase in the levels of the pro-inflammatory cytokine IL-6 in protein extracts from different regions of the brain, such as the cortex and cerebellum, in 24-month old mice compared to young counterparts. The authors also reported a spontaneous increase in the expression of IL-6 in microglia cultures prepared from aged mice, as well as an increase in the number of IL-6+ microglia cells. Therefore, they suggested that microglia might be responsible for the increase in IL-6 in the ageing brain[86]. While these two studies suggest an increase in basal levels of pro-inflammatory cytokines in the ageing brain, other studies have also shown a more profound activation of the inflammatory response in aged rodents upon peripheral LPS challenge, which appeared to be attributed to more active microglia[87]. Henry *et al.*[88] further supported this hypothesis by showing that peripheral LPS caused an overactive response in microglia from aged mice. A specific increase in IL-1β production was observed in the microglia from aged mice compared to younger mice upon LPS administration[88].

It has been suggested that, with ageing, microglia become "primed" and more sensitive to a second "triggering" stimulus. In the above study, this is demonstrated by the administration of LPS, which then lead to an increase in pro-inflammatory cytokine production in the aged mice, as explained in the schematic in **Fig 1.7**[89]. Other studies also support the age-related inflammatory response in microglia, for example a recent publication in the journal *Nature* suggested a critical signalling axis whereby soluble TNFα, a major pro-inflammatory cytokine, mediated microglia-neuron crosstalk via IkappaB kinase-alpha (IKK-β) and NF-κB[90]. In this study, Zhang *et al.* showed that TNFα produced by microglia had an impact not only on cognitive function but also seemed to exhibit some control over systemic ageing, given its action on neurons in the

hypothalamus and regulation of their Gonadotropin Releasing Hormone (GnRH) production, highlighting the importance of both microglia and the key regulator of inflammation, NF-κB[90].

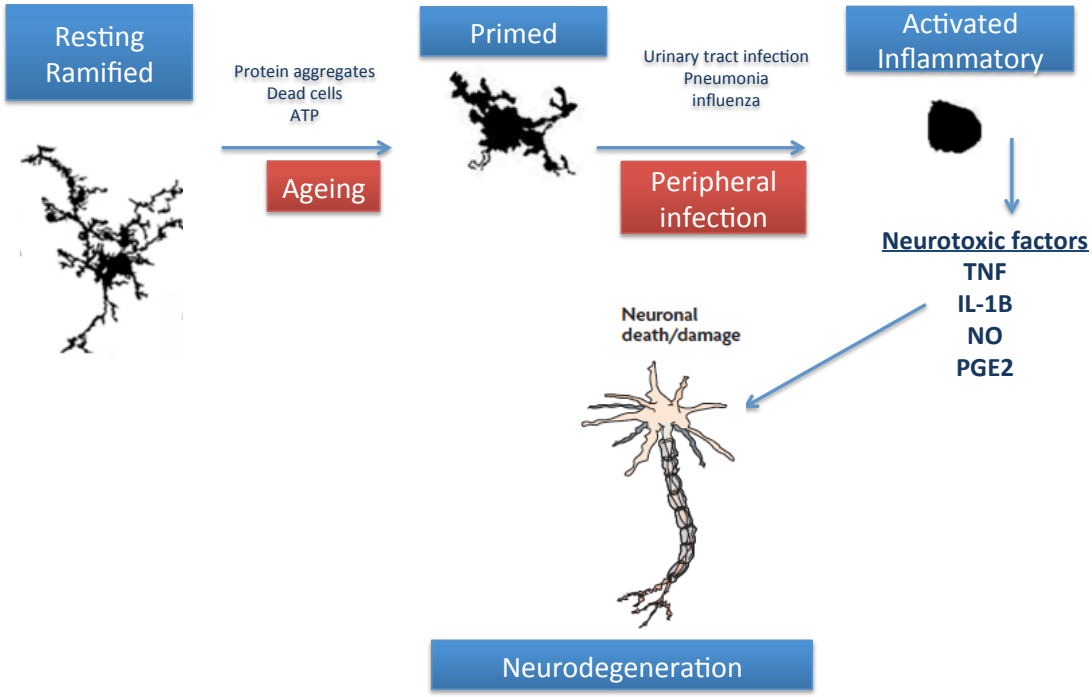

Figure 1.7 Schematic showing how microglia in the ageing brain may contribute to neurodegeneration. Microglia become primed by endogenous proteins in the brain that accumulate with age. This priming causes the microglia to become over-responsive to a peripheral infection. This increase in neurotoxic factors may then contribute to the overall degeneration of the ageing brain, leading to cognitive decline[91]. TNFα, tumour necrosis factor-α; Il-1β, Interleukin 1β; NO, nitric oxide; PGE2, prostaglandin E2. This figure is based on reports from the literature[42,92,93].

1.6.4 Loss of regulatory signals in microglia with ageing

It has been suggested that the priming of microglia depends on the loss of regulatory signals in the ageing brain (as previously described in **Fig. 1.7**). This is supported by studies that have shown that the receptors CX3CR1[94] and CD200R[83] are decreased on microglia with age, suggesting a loss of regulation from neurons to keep microglia in a quiescent state[40].

1.7 The transcriptome of ageing microglia

Four independent papers have investigated age-related changes in gene expression in microglia. They have all demonstrated that the gene expression profile of microglia from the ageing brain changes considerably when compared to microglia isolated from young brains.

Ma *et al.*[91] isolated microglia from the retina of wild type C57BL/6J mice of 3, 12, 18 and 24-months of age. Affymetrix gene chip technology was used to profile changes in gene expression as the age of the mice progressed. The authors identified 719 genes with a fold change of 1.5 or greater that were differentially expressed between at least two of the three age groups compared. Among the top genes, they identified the chemokine and neuroinflammatory biomarker *Cxcl13*, with a 15-fold change in old versus young microglia. They also observed changes in expression in the complement protein *C3* and the positive regulator of complement *Cfb*, which were validated at protein level with immunohistochemical staining. Using pathway analysis, they identified a number of deregulated inflammatory pathways, including IL-1 and MAPK signalling pathway, as well as pathways involved in lipid biosynthesis, angiogenesis and neurotrophin signalling. The authors suggested that deregulation of these pathways may indicate a more active phenotype[91].

Orre *et al.*[95] isolated microglia and astrocytes from the cortices of C57BL/6 mice of 2.5 months and 15-18 months of age and used microarrays to profile changes in gene expression. In this study, they identified 482 genes with a fold change of 2 or greater differentially expressed in old versus young microglia. Among the most differentially expressed genes were *Ccl3*, *Pik3cd*, *Lyzl* and genes within the TNF (Tumour necrosis factor) ligand family. They also found an enrichment of genes related to cytoskeletal protein binding and phagocytosis[95].

Hickman *et al.*[96] isolated microglia from the whole brain from 5-month and 24-month old C57BL/6J mice and they carried out transcriptome profiling by direct RNA sequencing, which is done without prior cDNA amplification. The authors identified a set of genes which they define as the microglia "sensome", determined by using gene ontology analysis and comparing adult microglia with the whole adult brain. In doing so, they identified 1,299 genes that may be involved in sensing the neural environment

and selected the top 100 differentially expressed to describe the microglia sensome, which included many purinergic receptors, chemokine receptors, members of the Siglec family and Toll-like receptor 2 (*Tlr2*). They then assessed changes that occurred in the microglia sensome between young and aged mice. They found that 31% (31 of 100) of the sensome genes were significantly downregulated, including genes involved in sensing endogenous ligands. On the other hand, 13% (13 of 100) of the sensome genes were upregulated; many were involved in sensing microbial agents such as bacteria or fungi and included genes such as *Tlr2*, *CD74*, *Clec7a*, *Cxcl16* and *Ifitm6*. Looking at the entire transcriptome between old and young microglia, they identified 1,832 transcripts to be upregulated in aged microglia and 1,672 to be downregulated. Gene set enrichment analysis (GSEA) was then used to identify pathways that were also affected by age. They found oxidative phosphorylation, which they describe as potentially neurotoxic, to be downregulated and several pathways that have been linked to neuroprotection to be upregulated, such as the Stat3 and Neuroegulin-1 pathway[96].

Grabert *et al.*[97] carried out transcriptional profiling of microglia from discrete brain regions including the cerebellum, cerebral cortex, hippocampus and striatum. This paper addressed two questions. Firstly the consistency of the microglia transcriptome across different brain regions in 4-month old mice and secondly how microglia change with age, using 12-month and 22-month old mice. They found that the microglia transcriptome was in fact regionally heterogeneous. Their analysis suggested that the majority of genes expressed by microglia are fairly consistent between the cerebral cortex and striatum but the expression profiles from the cerebellum and hippocampus were more distinct. In young mice, the major differences appeared to fall into two major categories; bioenergetics/metabolic processes and those related to immune function. Microglia from young mice had higher expression of genes relating to immune function such as antigen presentation, chemotaxis and cell adhesion in the cerebellum, whereas genes relating to energy metabolism were enriched in both the cerebellum and hippocampus. One such example was the transcription factor and mTOR target, PPAR-γ, which is known to be involved in lipid biosynthesis and mitochondrial function. Overall it appeared that microglia from the cerebellum and hippocampus have transcriptome profiles that indicate they are in a more immune vigilant state and possibly, as a consequence, they express higher levels of bioenergetics genes compared to microglia from the cortex and striatum[97].

To understand if the impact of ageing on microglia was consistent among the identified brain regions, the authors also looked at the microglia transcriptome from aged mice and found that 50% of the region-defining transcripts from young mice were deregulated with age. However, these differences appeared to be due to changes in expression of genes relating to immune regulation, rather than the bioenergetics cluster of genes previously described. Interestingly, it seemed there was a region-dependent influence on microglia with age, most notably a reduction in the distinction of hippocampus microglia and an increase in the immunophenotype associated with the cerebellum microglia. Microglia in the cerebellum appeared to be more immune alert with age. The authors speculate that this heightened alertness is important and could be detrimental if poorly controlled. However, it could also confer protective functions by increasing vigilance and potentially clearing harmful agents more efficiently[97].

1.8 mTOR signalling structure, organisation and activation

mTOR is a 298-kDa serine/threonine kinase of the phosphoinositide 3-kinase (PI3K) related family, a master regulator of cellular growth and metabolism, which is deregulated in a number of human diseases, including type 2 diabetes and cancer[98]. mTOR forms the catalytic subunit of two distinct complexes known as mTORC1 and mTORC2 that differ in their composition, substrates, activation and functions. mTORC1 is composed of three core components: Raptor, mLST8 and mTOR itself, plus two distinct negative regulatory components known as Deptor and PRAS40. The roles of both Raptor and mLST8 are relatively unknown, although it has been suggested that Raptor acts as a scaffolding protein essential for mTORC1 assembly[99]. mTORC2 comprises six components; Rictor, mSIN1, Protor-1, mLST8 and Deptor[100]. Deptor is a negative regulatory subunit of both mTORC1 and mTORC2, whereas mSIN1 and Rictor are necessary for the assembly of mTORC2[101].

mTOR acts as a rheostat, sensing both extracellular and intracellular changes and regulating how the cell responds. mTORC1 plays an important role in sensing alterations in growth factors, energy status, amino acids and oxygen. The tuberous sclerosis complex (TSC), which is constituted of two components, TSC1 and TSC2, is an important sensor of these signals and can regulate mTORC1 activity accordingly. The TSC complex negatively regulates mTOR through the small GTPase known as the

ras homolog in brain (Rheb). It has recently been identified that the TSC complex regulates Rheb by acting as a GTPase-activating protein (GAP) towards Rheb. When the TSC complex is active, it causes hydrolysis of guanosine triphosphate (GTP) by Rheb, which leads to the conversion of active GTP to inactive guanosine diphosphate (GDP). This renders Rheb inactive and therefore it can no longer interact and activate mTORC1. However, when PI3K is activated, this will lead to phosphorylation of its downstream target AKT by PDK1. Activated AKT can then phosphorylate TSC2 at S939, S1130 and T462, which leads to a complete inhibition of the TSC complex, allowing Rheb to remain in its active GTP state and fully activate mTORC1 (**Fig 1.8**)[102].

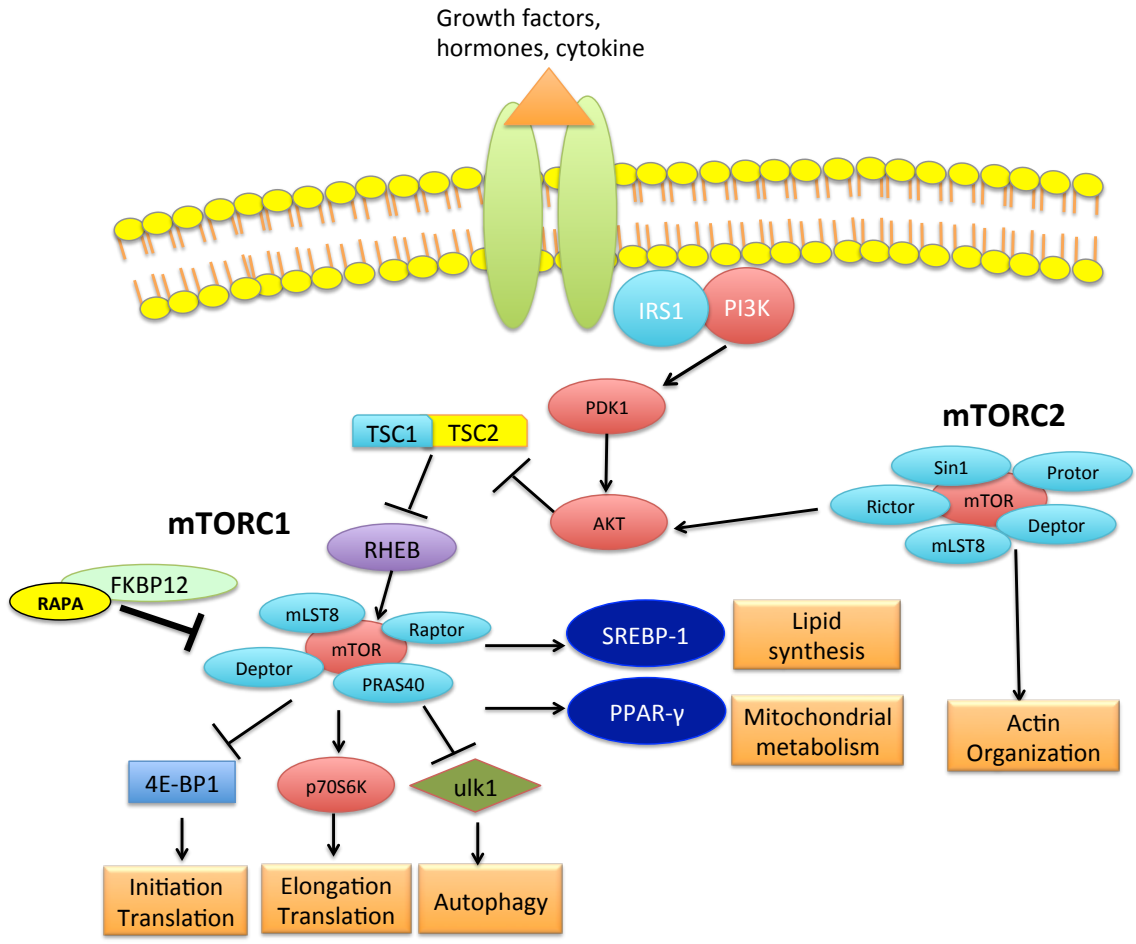

Figure 1.8 Structure and function of mTOR. Growth factors, cytokines and hormones can bind to the IGF/Insulin receptor and drive the activation of PI3K leading to activation of PDK1 and subsequent phosphorylation of AKT at threonine 308. When AKT is active, it can phosphorylate TSC2 rendering the TSC1/TSC2 complex inactive. This results in the GTPase Rheb to remain in its GTP-bound active state, therefore positively regulating mTORC1. mTORC1 can then phosphorylate a number of downstream substrates and regulate different cellular processes. Figure adapted from Sabatini *et al.*[98].

1.8.1 mTOR regulation by growth factors

The mechanism by which AKT inactivates the TSC complex has been demonstrated to occur in response to growth factor activation[103]. However, other mechanisms have also been described that are independent of the TSC complex. Vander Haar *et al.* described a mechanism by which the mTOR binding partner PRAS40 was phosphorylated by AKT, reducing its binding and therefore inhibitory capacity towards mTORC1. This was shown in cells lacking TSC2, emphasising that PRAS40 is an important regulator of insulin sensitivity independent of the TSC complex[104]. Activation of mTORC1 by growth factors leads to a negative feedback mechanism by which PI3K activation is inhibited. This is probably a mechanism evoked by the cell to prevent chronic activation of mTORC1. This inhibitory loop occurs through phosphorylation of Insulin Receptor Substrate 1 (IRS-1) by S6K1, a downstream target of mTORC1. IRS-1 becomes phosphorylated at multiple tyrosine residues when the IGF/Insulin receptor is appropriately engaged and its phosphorylation leads to the recruitment and activation of PI3K. However, when IRS-1 is phosphorylated at certain serine residues, like Ser-270[105], its stability is reduced and this leads to a downregulation of PI3K signalling[106].

1.8.2 Regulation of mTOR by energy status

AMP-dependent kinase (AMPK) is important for maintaining a homeostatic level of adenosine triphosphate (ATP) within the cell. When energy demands increase, cells activate processes that drive energy production, such as autophagy and inhibit energy consuming processes, such as the synthesis of new proteins[107]. AMPK is a critical regulator in the maintenance of ATP levels and it regulates these functions at least in part through inhibition of mTOR[108]. When intracellular ATP is low, AMPK is activated and phosphorylates TSC2, in a manner that enhances its suppression of mTOR. It has also been shown that AMPK can directly phosphorylate Raptor on two well-conserved serine residues that lead to inhibition of mTORC1. Therefore, during times of energy stress, AMPK act as a metabolic checkpoint through inhibition of mTORC1[107].

1.8.3 Regulation of mTOR by amino acids

Availability of amino acids also affects mTORC1 activation. This phenomenon appears independent of insulin and TSC and is therefore mechanistically different from the insulin/PI3K pathway that is normally activated by growth factors[109]. A small group of GTPases, known as the Rag proteins, are key mediators of amino acid-mTORC1 signalling. mTOR is normally localised to the endomembrane, which consists of the endoplasmic reticulum, golgi apparatus and endosomes. However, one group showed that under amino acid deprivation, mTOR was found in tiny punta throughout the cytoplasm but relocated to the perinuclear region of the cell, following just three minutes of amino acid stimulation. The authors showed that this re-localisation required the expression of the Rag proteins and Raptor. They also showed that amino acids appear to regulate the nucleotide loading and subsequent activation of the Rag proteins and further suggested that the re-localisation of the mTORC1 complex to the perinuclear region takes place in order to direct mTOR to the same intracellular compartment as its activator Rheb[110].

1.8.4 Regulation of mTOR by oxygen levels

Oxygen levels have also been shown to activate and regulate mTORC1. Oxygen is essential for regulating metabolism and in hypoxia, when oxygen levels are low, cells activate a number of mechanisms that reduce energy expenditure and protein synthesis. For example, hypoxia has been shown to inhibit mTORC1 through TSC1/2 and REDD1. REDD1 activity allows the TSC complex to be released from its association with the inhibitory 14-3-3 proteins, therefore it can resume its negative regulation of mTOR during hypoxic conditions[111].

1.9 mTORC1 function

Much of our knowledge about the functions of mTORC1 comes from the use of its inhibitor rapamycin. Rapamycin is a lipophilic macrolide, originally isolated from *Streptomyces hygrocropicus* by Suren Sehgal and given the name of rapamycin (from Rapa Nui, the Polynesian name of Easter island)[112]. Rapamycin functions by binding to a small protein known as FKBP12. When rapamycin is bound, FKBP12 cannot interact with mTORC1 and therefore mTORC1 activation is prevented. It was originally thought

that rapamycin was specific to mTORC1 as this FKBP12-rapamycin complex cannot interact with mTORC2, however in recent years it has been shown that the duration and concentration of rapamycin can result in inhibition of mTORC2, as well as mTORC1. This is due to the fact that rapamycin can bind newly synthesised molecules of mTOR, preventing its recruitment in the mTORC2 complex[113]. It is important to note that some functions of mTORC1 are rapamycin-resistant, for example translation of certain transcripts[114,115], this must be taken into account when assessing mTORC1 function based on the use of this drug.

1.9.1 mTOR regulation of protein synthesis

One of the main functions of mTOR is to drive cell growth and proliferation. It does so by regulating different aspects of protein synthesis through a number of mechanisms. Active mTORC1 phosphorylates the translational repressor 4E-BP1. Upon phosphorylation, 4E-BP1 releases the eukaryotic translation initiation factor eIF4E, allowing it to interact with other eIF proteins and drive the initiation of cap-dependent translation[114]. mTOR can also phosphorylate p70 S6 kinase (p70S6K), also involved in protein synthesis, particularly in regulating the elongation phase of protein translation as described in **Fig. 1.8**. Recently, it has been shown that the subset of mRNAs that appear to be specifically regulated by mTORC1 are transcripts that have a 5'-terminal oligopyrimidine (TOP) motif[114,115].

1.9.2 mTOR regulation of lipid synthesis

Lipid biosynthesis is extremely important for the maintenance of homeostasis in the cell. Lipids such as fatty acids, cholesterol and phospholipids are essential for a number of functions, for example, to act as an energy source, signalling molecules or for the assembly of new organelles and plasma membrane upon cell division[116]. There is growing evidence that mTORC1 may play a very important role in lipid synthesis. It has been shown that the PI3K/AKT/mTOR pathway positively regulates the transcription factor PPARγ (**Fig. 1.8**), therefore regulating the expression of genes involved in adipogenesis[117]. There is also evidence that mTORC1 positively regulates the activity of the transcription factor sterol regulatory element-binding protein-1 (SREBP-1). SREBP-1 controls the expression of genes involved in lipid homeostasis such as those relating to cholesterol, fatty acid and phospholipid synthesis[118].

1.9.3 mTOR and autophagy

Autophagy, as previously discussed in the paragraph on inflamm-ageing, is an important process by which dysfunctional organelles and cellular components are degraded by lysosomes. While this is important for maintaining homeostasis, it also provides biological material to sustain processes such as the synthesis of new lipids, carbohydrates and proteins as a source of energy[35]. It is well accepted that inhibition of mTORC1 leads to induction of autophagy, suggesting that mTOR negatively regulates this process. Recently, it was shown that the autophagy factor Atg13 forms a complex with unc-51-like kinase 1 (ULK1) and focal adhesion kinase family interacting protein (FIP200). mTOR phosphorylates ULK1 and Atg13 in a nutrient dependent manner, blocking the induction of autophagy[119] (**Fig. 1.8**).

1.9.4 mTOR and mitochondria metabolism

It has been shown that mTORC1 plays a role in mitochondrial function and biogenesis. For example, Sieke *et al.* showed that mTORC1 regulates oxygen consumption as well as oxidative capacity, as inhibiting mTOR with rapamycin had a significant impact on ATP synthetic capacity and lowered both mitochondrial membrane potential and oxygen consumption. Interestingly, the authors also found that inhibiting mTORC1 had a dramatic effect on the mitochondrial phosphoproteome[120]. Another study provided supporting evidence that mTORC1 is important for mitochondrial function[121]. The authors showed that inhibition of mTOR with rapamycin in skeletal muscle resulted in a decrease in the expression of the PPARγ coactivator 1, known as PGC1-α. This transcription factor is an important regulator that controls mitochondrial oxidative function and sustains energy levels in response to nutrients and hormones. mTORC1 inhibition by rapamycin lead to a decrease in mitochondrial gene expression and oxygen consumption[121].

1.10 mTORC2 function and activation

mTORC1 is the mTOR complex more intensely studied, on the other hand, relatively little is known about mTORC2 in comparison. This may be caused by a lack of specific inhibitors of mTORC2, therefore most of the research to date has been carried out with genetic models in which elements of the complex were deleted. The main downstream substrate of mTORC2 is AKT. AKT is phosphorylated by PDK1 on threonine 308 when

PI3K signalling is activated, however full activation of AKT requires an additional phosphorylation on serine 473, which is mediated by mTORC2 (**Fig. 1.8**)[122]. Through its regulation of AKT, mTORC2 regulates the phosphorylation of the transcription factors FOXO1 and FOXO3a, which causes their inhibition. These transcription factors are involved in multiple cellular processes including cell-cycle arrest, apoptosis, autophagy and inflammation[123]. Besides a potential role of mTORC2 in cell survival and metabolism, it has been shown to regulate the organisation of the cytoskeleton, since knock down of components of the mTORC2 complex appeared to affect actin polymerisation, possibly through phosphorylation of protein kinase C alpha (PKCα)[124].

1.11 Regulation of inflammation in innate immune cells by mTOR

The mTOR pathway plays an important role in regulating immune cell function. This is well established, especially in T cells, which has lead to the use of mTOR inhibitors to suppress T cell function in transplantation[125]. However, there is evidence that mTOR regulates inflammation and metabolic processes also in myeloid cells, which is the focus of my PhD project.

The first evidence that PI3K was involved in the regulation of myeloid inflammatory responses came in 2002, when a group investigated the role of PI3K in regulating IL-12 production in dendritic cells (DCs)[126]. In this *Nature Immunology* paper, Fakao *et al*.[126] studied DCs isolated from the spleens of PI3K -/- mice, characterised by deletion of the gene for the p85α regulatory subunit. They stimulated PI3K -/- and wild-type DCs with Staphylococcus Aureus Cowan 1 (SAC) and anti-CD40 to trigger the induction of IL-12, in the presence or absence of factors that enhance IL-12 production, such as interferon-γ (IFN-γ) and IL-4. They found in all conditions tested that splenic DCs from PI3K -/- mice produced significantly larger amounts of IL-12 compared to wild-type counterparts. They confirmed these findings in DCs generated from bone-marrow cells, known as bone marrow derived dendritic cells (BMDCs) and also by using the PI3K inhibitor wortmannin. These results suggested that PI3K negatively regulated IL-12 production in mouse splenic DCs and BMDCs. The increased IL-12 production correlated with an increase at transcriptional level of the two subunits for IL-12, known as p35 and p40. They found that the kinetics of cytokine production was not altered but that gene expression for both p35 and p40 was significantly increased in PI3K-/- BMDCs, suggesting that the increase in IL-12 production is due to enhanced transcription rather than post-transcriptional modifications. Mechanistically, the authors showed that activation of the MAPK p38 was higher in wortmannin-treated BMDCs following LPS stimulation and a selective inhibitor of p38 caused a reduction in IL-12. Finally, the study assessed if mice infected with *Leishmania major* which requires an effective Th1 response to clear the infection, were protected when PI3K was inhibited. It has previously been established that Balb/c mice are susceptible to *L. major* infection, since they cannot mount an effective Th1 response; this is normally rescued by the administration of IL-12. Indeed, infected Balb/c PI3K -/- mice were resistant to the

infection, as indicated by a significant reduction in the number of parasites in the popliteal lymph nodes 6-weeks post infection. This resistance was accompanied by an increase in Th1 cytokines IFN-γ and TNF[126]. These experiments highlighted the biological relevance of IL-12 regulation by PI3K.

These findings were further supported by Martin *et al.*[127] that found IL-12 production was enhanced in human monocytes following PI3K inhibition and that IL-10 production was suppressed[127]. This is consistent with a report by Aksoy *et al.*[128] who showed that DCs from mice with a knock-in mutation in the p110δ isoform (rendering it inactive) of PI3K had augmented cytokine production[128]. The authors went on to explain that this is due to differences in TLR4 internalisation and downstream consequences on alternative TLR signalling.

Weichhart *et al.*[129] went on to investigate the role of mTOR in these processes. This paper demonstrated that inhibition of mTOR by rapamycin lead to the production of pro-inflammatory cytokines (IL-12p40, IL-12p70, IL-6 and TNF) and a decrease in IL-10 in human peripheral blood mononuclear cells (PBMCs) and monocytes upon stimulation by LPS or SAC. Upon LPS stimulation, TSC2 was phosphorylated in an AKT dependent manner and phosphorylation of mTOR and its downstream targets was observed. These events could be prevented by treatment with wortmannin, suggesting that PI3K signalling is upstream of mTOR in LPS signalling in human monocytes. These findings were confirmed in TSC2 -/- murine embryonic fibroblasts (MEFs) transfected with an IL-12p40 plasmid. TSC2 is important for negatively regulating mTOR activation; therefore the mTOR pathway is constitutively active in cells lacking TSC2. IL-12p40 could not be induced in TSC -/- MEFs upon LPS stimulation compared to wild-type MEFs, which supported the idea that mTOR negatively regulates IL-12 production. To understand how mTOR regulates the expression of inflammatory cytokines, the authors examined the effect of mTOR inhibition on the activity of the transcription factor NF-κB. NF-κB is a master regulator of inflammatory responses and controls the expression of many pro-inflammatory cytokines[130]. Indeed, mTOR inhibition with rapamycin lead to enhanced activation of NF-κB upon LPS stimulation, as demonstrated by the electromobility shift assay. Consistent with this, TSC2 -/- showed a decreased ability to activate NF-κB. These findings, and the relevant molecular interactions, are exemplified in the schematic in **Fig. 1.9**. Furthermore, the

authors found that mTOR inhibition lead also to a decrease in IL-10 production. Since STAT3 regulates IL-10 expression, STAT3 phosphorylation was assessed and found to be reduced when mTOR was inhibited.

Finally, similarly to Fakao *et al.*[126] the authors wanted to assess the biological relevance of these findings and used a *Listeria monocytogenes* infection in Balb/c mice, which usually are unable to produce sufficient amounts of IL-12, IFN-γ and IL-6. Strikingly, a 3-day pre-treatment with rapamycin, given by intraperitoneal injection, was enough to improve survival, an effect abolished by macrophages and DCs depletion with clodronate. Mice treated with rapamycin had a reduced bacterial burden in the liver and an increase in nitric oxide production, which is critical for clearing *L. monocytogenes*. Furthermore, there was an increase in IL-12p70, IL-6 and IFN-γ in the blood of rapamycin-treated mice. Overall, mTOR inhibition by rapamycin caused an increased production of key factors needed to clear the infection[129]. This paper was important in highlighting both the molecular mechanisms that underlie the increased cytokine production but also the biological relevance of these findings. The authors concluded that the mTOR signalling pathway plays a major role in limiting excessive inflammation during infection.

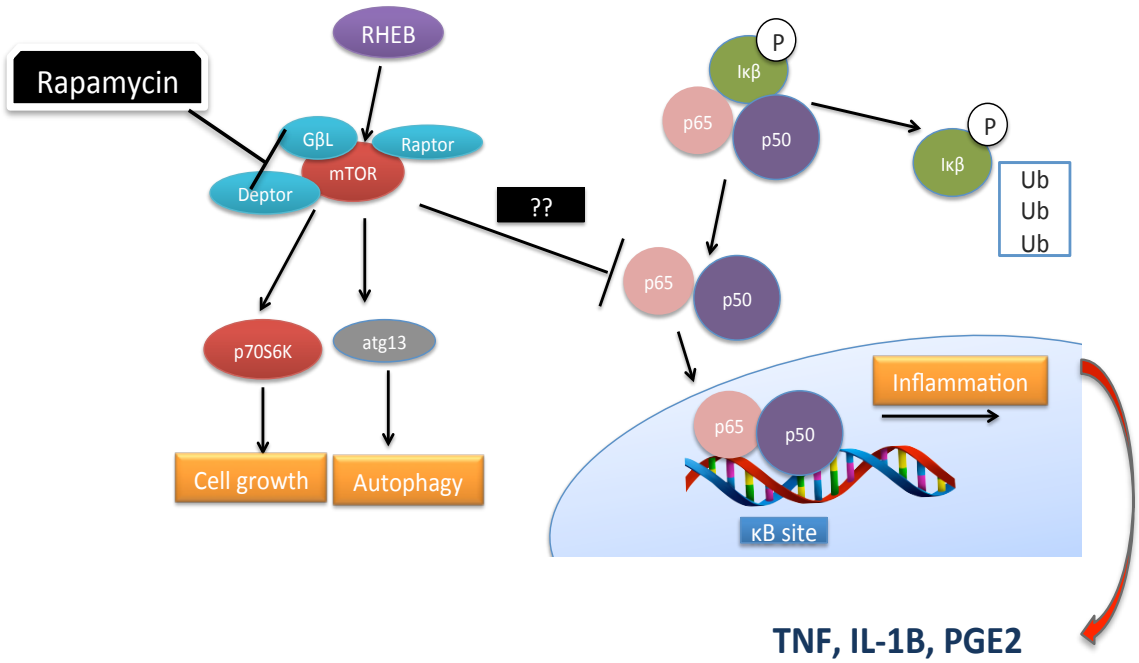

Figure 1.9 Schematic of how mTORC1 inhibition by the drug rapamycin can lead to an increase in NF-κb signaling and subsequent increase in inflammation. mTORC1 negatively regulates NF-κB and therefore inhibition of the mTORC1 complex by

rapamycin leads to an increase in NF-κb activation, measured by translocation of the p65/p50 complex into the nucleus of myeloid cells, This results in an increase in the transcription of inflammatory genes and an overall augmentation of the inflammatory response, However, the molecular link has not been elucidated. Figure based on findings from Weichhart *et al.*[129].

Other studies have also provided evidence that mTOR inhibition leads to an increase in inflammatory responses, for example, mice lacking the mTORC1 scaffolding protein Raptor specifically in DCs showed increased susceptibility to colitis induced by dextran sodium sulphate. The study suggested that this severe inflammatory response is due to a DC-mediated suppression of IL-10[131].

Studies have indicated that inflammation associated with transplantation may be mTOR mediated. Gallon *et al.*[132] profiled biopsies taken from transplanted kidneys. In patients taking rapamycin as an immunosuppressant, they found increased IL-12 signalling as well as an increase in inflammatory and immune responses[132]. This observation was further supported by another study in which the blood from kidney transplant patients was examined. Similarly, expression profiles obtained from the blood of rapamycin-treated patients appeared to be dominated by innate immune cell transcripts, as well as NF-κB-related inflammatory genes[133].

Another study in 2011 by Weichhart *et al.* showed that renal transplant patients receiving rapamycin presented with a phenotype of activated immune cells, despite having combination therapy with anti-inflammatory glucocorticoids. PBMCs from these patients produced elevated levels of IL-12, IL-6, TNFα and IL-1β *ex vivo* compared to patients on other regimens. In fact, rapamycin and Torin 1 (an inhibitor of mTORC1 and mTORC2) blocked the anti-inflammatory effect of glucocorticoids in both human monocytes and myeloid DC *in vitro*[134].

The reports described so far all indicate that mTOR inhibition leads to an increase in pro-inflammatory cytokines such as IL-12 and TNF and a suppression of IL-10 in monocytes, BMDMs and DC both *in vitro* and *in vivo*. The proposed mechanism of action is through NF-κB activation. However, there are other reports that conflict with these observations. For example, an article published in 2011 demonstrated that TSC1 deficiency in BMDMs resulted in increased production of the pro-inflammatory cytokines TNFα, IL-12p40, IL-6 and increased nitric oxide production when stimulated

with LPS. This appears to be contrary to what has been previously described: as TSC1 is known to negatively regulate mTORC1, its deficiency should result in an increase in mTOR activation. However, TSC1 KO BMDMs did not have an increase in NF-κB activation but rather an increase in JNK1/2 phosphorylation that accompanied mTORC1 activation. The authors showed that either a JNK1/2 inhibitor or rapamycin could partly rescue the inflammatory phenotype, whereas the combination almost restored normal responses. The authors suggested that mTORC1 acts as an upstream regulator of JNK1/2 activation during TLR signalling in BMDMs[135].

This study was supported by Byles *et al.* who found that TSC1f/f LysM-Cre BMDMs also displayed an increase in pro-inflammatory cytokines IL-6 and TNFα upon LPS stimulation compared with controls. Furthermore, TSC1 KO BMDMs failed to polarise to an M2 phenotype when stimulated with IL-4/IL-13. This study indicated that the defect was caused by a reduction in AKT phosphorylation as a consequence of chronic activation of mTORC1, which lead to a decrease in mTORC2 activation and subsequently reduced phosphorylation of the transcription factor FOXO1, which regulates some of the M2 genes such as *Fizz1* and *Arg1*[136]. Phosphorylation of FOXO1 causes its inhibition as it results in its sequestration into the cytoplasm, where FOXO1 can no longer drive the transcription of target genes[137].

A more recent study by Zhu *et al.*[138] sheds light on these apparent discrepancies. The authors also used the TSC1f/f; LysM-Cre mice and showed that both peritoneal macrophages and BMDMs produced significantly more pro-inflammatory cytokines IL-12 and TNFα compared to controls. However, treatment with high or low doses of rapamycin failed to inhibit this enhanced cytokine production. Furthermore, they showed that genetic deletion of mTOR promoted rather than reversed the increase in TNF and IL-12 in TSC1 KO BMDMs. These results suggested that the increase in pro-inflammatory responses associated with TSC1 deletion are either mTOR-independent or might depend on downstream signalling pathways that are regulated in a similar fashion upon mTOR inhibition or loss of TSC1, like increased PI3K or AKT activation. In addition, the authors showed that TSC1 can inhibit Ras GTPase activity, similarly to Rheb, and this leads to a reduction in activation of the RAF-MEK-ERK signalling pathway and subsequent cytokine production. Therefore, this process was hyperactivated in TSC1 KO BMDMs and resulted in an increase in cytokine

production. Interestingly, germline TSC1 KO mice spontaneously develop inflammatory disorders and have reduced survival, indicating the importance of this potential signalling axis in maintaining homeostasis. This paper was important in highlighting that TSC1 may have additional targets other than mTOR and that, at least in this instance, the increase in inflammatory responses governed by TSC1 deletion was not mTOR-mediated[138].

The idea that inactivation of TSC1 and TSC2 could lead to an increase in the inflammatory response, through inhibition of mTORC2, has also been suggested by a study in 2011 published in the *Journal of Biological Chemistry*. In this study mTORC2 was inhibited through the deletion of a key component of the complex, Rictor, in MEFs. Rictor KO MEFs showed a hyperinflammatory phenotype upon LPS stimulation, accompanied by a reduction in AKT phosphorylation, as well as reduced phosphorylation of the transcription factor FOXO1. Therefore, in RICTOR KO MEFS, a reduction in AKT and consequently FOXO1 phosphorylation results in elevated nuclear FOXO1 levels and increased cytokine production of IL-6 and IL-8[139]. The notion that mTORC2 negatively regulates the inflammatory response was further supported by *in vivo* evidence that Rictor deletion in the myeloid compartment caused an increased response to LPS injection. As expected, these mice displayed a higher sensitivity to septic shock, accompanied by an increase in TNFα levels in the plasma[140]. Therefore, it is possible to conclude that mTORC1 and mTORC2 inhibition both lead to an increase in inflammatory responses, however, they seem to be mediated by different mechanisms. While mTORC1 inhibition leads to NF-κB activation, mTORC2 inhibition does not.

One interesting study emphasised the importance of mTOR on the production of inflammatory cytokines in response to pathogenic and non-pathogenic microbes. This study suggested that infection with certain pathogens can result in a translational bias toward pro-inflammatory cytokines, through the regulation of translation by mTORC1. The authors compared the effects on macrophages with an infection with either a fully virulent strain of *Legionella pneumophilia* or a non-pathogenic strain, in which the effector system that delivers proteins to the host cell, the Dot/ICM system, is inactivated. Only the infection with the virulent strain, and not the Dot/ICM defective strain, resulted in the suppression of mTOR function, which was accompanied by a

robust pro-inflammatory response at an RNA and protein level. mTOR regulates the initiation of translation through negative regulation of 4E-BP1. In its unphosphorylated state, 4E-BP1 binds to eIF4E. When 4E-BP1 becomes phosphorylated by mTORC1, it releases eIF4E, which then forms a complex with other eIF proteins to initiate translation. The bias in cytokine production observed in macrophages infected with the virulent strain appeared to be inhibited upon blocking this interaction. The authors went on to show that this bias in cytokine production could be mimicked in the Dot/ICM strain using rapamycin, further proving that suppression of the mTOR pathway was responsible for this effect. The authors speculated that this abundance in pro-inflammatory cytokine transcripts upon infection with a pathogen such as *legionella* could have evolved as a mechanism that allows the cells of the innate immune system to mount an inflammatory response even under conditions in which mTOR function is suppressed[141].

Another study that also highlights the importance of translation when considering mTOR inhibition and cytokine production was carried out examining the effects of rapamycin on the SASP. The group, led by Jesus Gil, showed that mTOR inhibition prevents the induction of the SASP in a model of oncogene-induced senescence (IMR90 ER:RAS). mTOR appears to suppresses the SASP through the translation of MAPKAPK2 kinase, which is dependent on 4E-BP1. When mTOR is inhibited, 4E-BP1 phosphorylation is lost and 4E-BP1 remains in a complex with eIF4E, preventing the initiation of translation. Therefore, mTOR inhibition in senescent cells leads to a reduction in the translation and overall activity of MAPKAPK2 kinase. ZFP36L1, a zinc finger protein that destabilizes mRNAs, is a known substrate of MAPKAPK2 and becomes phosphorylated during oncogene-induced senescence, which prevents it from degrading transcripts of numerous SASP components. Therefore, inhibition of mTOR leads to phosphorylation and consequently activation of ZFP36L1 by MAPKAPK2, which leads to degradation of SASP transcripts and overall reduction in the SASP. This study may offer some explanations as to how rapamycin appears to exert anti-ageing properties, by reducing the production of inflammatory genes associated with ageing, at least in certain cell types[142].

1.11 Regulation of microglia function by mTOR

The first evidence that mTOR might regulate microglia function was published in 2005[143]. In this article, the authors investigated the effect of the cellular antioxidant enzyme catalase on the induction of cyclooxygenase-2 (COX-2) and iNOS in the microglia cell line, BV-2, by treating the cells for four hours with this antioxidant. They found that catalase induced activation of the mTOR pathway, as demonstrated by the increase in phosphorylation of p70S6K as well as upregulation of COX-2 and iNOS at protein level, which appeared to be associated with NF-κB activation. Treatment with either rapamycin, a PI3K inhibitor or an NF-κB inhibitor reversed the induction of COX2 and iNOS in the BV-2 cell line upon catalase treatment. This report appears contradictory to earlier reports that associated mTOR inhibition with an increase in NF-κB activation, however it must be considered that it is not known which receptors are activated by catalase. Therefore, the mechanism of action in this setting could be very different to TLR-mediated mTOR activation previously described[143].

Another study that appears to complement this report investigated the effect of hypoxia on microglia activation. The hypoxia-inducible factor-1α (Hif1α), which is involved in sensing the level of oxygen within the cell, plays a central role in the adaptation the cell makes to survive in hypoxia. In this study, the authors investigated the induction of iNOS in both primary rat microglia and the BV-2 microglia cell line under hypoxic conditions. As previously reported, it appeared that hypoxia caused an upregulation of Hif1α in a time-dependent manner that was dependent on the PI3K/AKT/mTOR pathway. Interestingly, inhibitors of PI3K and mTOR abolished the induction of Hif1α as well as the associated iNOS expression under hypoxic conditions, suggesting, for the first time, that the PI3K/mTOR/HIF1α signalling is in involved in regulating iNOS production in microglia under hypoxic conditions[144].

Chong *et al.* also showed that the activation of the PI3K/mTOR pathway in primary microglia and the EOC2 microglia cell line was protective during oxygen and/or glucose deprivation. This was evident as inhibition of mTOR in these conditions lead to significantly more microglia apoptosis, DNA fragmentation and membrane phosphatidylserine exposure[145].

These articles suggest that the mTOR pathway plays a role in different aspects of microglia function, such as survival and NOS2 expression. Another study investigated the activation of mTOR in response to either LPS or a mixture of cytokines that were biologically relevant to the pathogenesis of MS referred to as TII (TNFα, IL1β and IFN-γ) in primary cultures of rat cortical microglia. They found that mTOR was activated by both stimuli, as measured by the phosphorylation of mTOR at S2448. NOS2 expression was also induced by both stimuli but with very different kinetics. Interestingly, pre-treatment with rapamycin blocked the production of NO in the TII treated cells but not in the LPS-treated microglia cells. mTOR inhibition lead to an increase in NOS2 mRNA levels in LPS-treated cells at 24 hours after stimulation, although there was no difference in the protein levels in LPS-treated cells with and without rapamycin. mTOR inhibition in TII treated cells resulted also in diminished production of COX1, COX2 and prostaglandin E2. All three of these factors are increased under inflammatory conditions and are generally associated with a pro-inflammatory phenotype. Lastly, the authors showed that mTOR inhibitors also affected microglia proliferation and viability. This paper highlighted how mTOR inhibition can have differential effects, depending on the type of stimulation and downstream signalling pathways[146].

One interesting study that suggested a possible role for mTOR in the chronic activation state of microglia was carried out in a mouse model of chronic neuroinflammation, the germline multifunctional protein 2 (MFP2) knock out mouse. MFP2 is an important enzyme in peroxisomal β-oxidation and its deletion results in inflammation and a neurological phenotype characterized by motor and cognitive impairments, leading to eventual death by 6-months of age. The study sought to understand the role microglia may play in the pathogenesis of this disease. To this end, the authors carried out microarray analysis to characterise the microglia transcriptome in this disease. Interestingly, they found that the most upregulated pathways were related to protein translation, cellular growth and proliferation such as eIF2, mTOR, p70S6K and eIF4E signalling. The activation of mTOR as well as the upregulation of one of its downstream targets, HIF1α, was validated by IHC. Microglia appeared to be in a primed state, as they produced more pro-inflammatory cytokines upon in vivo LPS stimulation compared to WT microglia, However, they also lacked signs of phagocytic or neurotoxic activity. The authors hypothesise that the activation of the transcription

factor HIF1α might be important in the primed state of MFP2 -/- brain and the chronic neuroinflammatory phenotype observed with the disease[147].

In conclusion, it seems that mTOR plays an important role in regulating the inflammatory response in myeloid cells and is also a key pathway implicated in the ageing brain. Given how microglia changes with age remain understudied and the importance of mTOR in regulating inflammatory processes, I set out to investigate microglia in ageing, with a particular focus on the mTOR pathway.

Aim

Based on the evidence provided so far, the aim of my PhD thesis was to profile transcriptome changes occurring in microglia with age and to elucidate the molecular mechanisms underlying these changes.

2 Methods

2.1 Mice

For the microglia transcriptome experiment, cells were isolated from three different age groups of mice: young (6 months), middle aged (15 months) and old (23 months). Mice were C57BL/6J, female and ex-breeders. They were obtained from Charles River and were housed according to Home Office guidelines. Mice with a transgenic construct containing a Cre recombinase coding sequence under the control of the promoter for the murine colony stimulating factor 1 receptor (Csf1r-Cre) were obtained from Jackson laboratories. LoxP-flanked Rheb alleles were generated in the laboratory of P.F. Worley[148]. In this model, exon 3 of Rheb is floxed. This exon encodes the critical GTP binding domain. This is an out-of-frame deletion and therefore the protein is not produced[148]. All experiments carried out with mice were in accordance with the Home Office licence PPL 70/7411.

2.2 Organ processing

Cells were obtained from the blood, bone marrow and spleen. The processing of each organ is briefly described below.

2.2.1 Blood

Blood was obtained by cardiac puncture using a 27G needle and 1 mL syringe coated in 0.5 M Ethylenediaminetetraacetic acid (EDTA). It was then transferred into a 1.5 mL eppendorf tube and placed on ice. To obtain plasma for cytokine analysis, blood was spun three times with increasing speed in a microfuge, with the supernatant being removed each time. The first speed used was 200 x g for 10 minutes, followed by 2,300 x g for 5 minutes and finally 16,100 x g for 3 minutes. Plasma was then aliquoted and snap frozen before being stored at -80°C until cytokine assessment was carried out. Following the first spin, the pellet of blood cells was kept for flow cytometry analysis. They were placed in a 50 mL falcon with 20 mL of PBS and centrifuged at 300 x g for 10 minutes at 4°C. Red blood cell lysis was carried out by using 10X red blood cell lysis buffer (eBioscience, Cat. No. 00-4300-54), diluted 1:10 in distilled water. Cell pellet was resuspended in 10 mL of 1X lysis buffer and placed in the dark for 10

minutes at room temperature. Following this incubation, cells were washed twice with incubation buffer and a cell count was performed. Cells were resuspended at 2 x 10^7 cells/ mL in incubation buffer [phosphate buffered saline (PBS) + 0.5% bovine serum albumin (BSA) + 2 mM EDTA].

2.2.2 Spleen

Spleens were harvested, placed in 10 mL of PBS and kept on ice until further processing. Afterwards, they were placed on a 70 μm cell strainer from Fisher Scientific (Cat. No. 11597522). They were gently mashed through the strainer using a 5 mL syringe plunger. 10 mL of PBS was added to the cell suspension before centrifugation at 300 x g for 10 minutes at 4°C. To remove red cells, 10 mL of 1X red blood cell lysis buffer was added to the pellet and incubated for 10 minutes at room temperature in the dark. Cells were then washed twice with PBS and resuspended at 2 x 10^7 cells/ mL in incubation buffer.

2.2.3 Bone Marrow

Cells were obtained from the bone marrow by flushing the femurs and tibia with Dulbecco's Modified Eagle Medium (DMEM, Sigma, D5768) supplemented with 10% Foetal Bovine Serum (FBS, Life Technology, Cat. No. 10500-064) and 1% penicillin/streptomycin (Sigma, Cat. No. P4333). This is referred to as complete media. 1 mL of complete media was flushed through the bone marrow using a 27G needle, several times. Cells were then strained through a 70 μm cell strainer before 20 mL of PBS was added to the cell suspension and cells were spun at 300 x g for 10 minutes 4°C. Red cell lysis was carried out as described for spleen and blood and cells were resuspended at 2 x 10^7 cells/ mL.

2.3 Flow cytometry Staining

Flow cytometry staining was carried out in 96-well V-bottom plates from Thermo Fisher (Cat. No. 2605). For each stain performed, 2 x 10^6 cells were used, therefore 100 μl of a 20 X 10^6 cells/ mL cell suspension was added to appropriate wells and then the plate was spun at 320 x g for 5 minutes at 4°C. The cells were then resuspended in 30 μl of CD16/CD32 FcR block (eBioscience, Cat. No. 14-0161-86) for 15 minutes at 4°C.

CD16 and CD32 are FcRIII and FcRII receptors, respectively, which are expressed by a range of immune cells including monocytes/macrophages and B cells. It is important to block these receptors as antibodies used for flow cytometry can non-specifically bind to these receptors and affect the results. Following FcR block, a 2X antibody mix was prepared using Incubation buffer and 30 µl was added to each well. All relevant information regarding the panel of antibodies used (manufacturer, clone and dilutions) is summarised in **Tab. 2.1**. Cells were incubated with antibodies used for flow cytometry for 20-30 minutes at 4°C in the dark. Following this incubation, cells were washed twice with 150 µl of incubation buffer before being resuspended in 150 µl of incubation buffer, which was transferred to 1.2 mL tubes (Star lab, Cat. No. I1412-7400). Data acquisition was carried out with a 4-laser LSR-Fortessa (BD Biosciences) and data analysis was done using Flowjo software.

Antibody	Manufacturer	Cat Number	Clone	Dilution
CD4	eBioscience	17-0041-83	GK1.5	1 in 100
CD8	eBiosceince	46-0081-80	53-6.7	1 in 100
CD45	eBiosceince	9047-9459-120	2D1	1 in 100
CD62L	eBiosceince	12-0621-85	MEL-14	1 in 100
CD11b	eBiosceince	25-0112-82	M1/70	1 in 200
Ly6C	eBiosceince	48-5932-82	HK1.4	1 in 100
Ly6G	eBiosceince	17-5931-81	RB6-8C5	1 in 100
F4/80	eBiosceince	11-4801-85	BM8	1 in 100
CLEC7A	eBiosceince	17-5859-80	bg1fpj	1 in 100
TLR2	eBiosceince	12-9021-80	6C2	1 in 200
Dapi	Cambridge Bioscience	40043-BT	NA	2.5 µg/ml
Fixable viability dye (FVD)	eBiosceince	65-0863-18	NA	1 in 200

Table 2.1 List of antibodies used for flow cytometry including clone, manufacturer, dilution and catalogue number.

2.4 Isolation of microglia

Microglia for RNA sequencing were isolated as follows: brain and spinal cord were dissected following perfusion with 35 mL of ice-cold Hank's balanced salt solution (HBSS) for 5 minutes. The perfusion step was carried out in order to remove any blood cells, particularly monocytes, which express the same markers as microglia. Tissues were then digested using a neuronal dissociation kit (Miltenyi Biotec, Cat. No. 130-092-628), which is based on the enzyme papain, in order to obtain a single cell suspension. Next, cells were washed twice in HBSS and myelin was removed by negative selection

using myelin removal beads (Miltenyi Biotec, 130-094-060) in MACS LS columns (Miltenyi Biotec, Cat. No. 140-096-433). Briefly, 1.8 mL of incubation buffer and 200 µl of myelin removal beads were added to each brain cell suspension and incubated at 4°C in the dark for 15 minutes. Following this incubation, 18 mL of incubation buffer was added to each sample in order to wash the cells, which were centrifuged for 10 minutes at 300 x g. Using three LS columns per brain, 1 of 3 mL of beads/cell suspension were loaded onto each column placed in a MidiMACS separator magnet (Miltenyi Biotec, Cat No. 130-042-302). This step was required to separate bead-bound myelin from the cell suspension. Each LS column was washed twice with incubation buffer and each time the flow-through was collected. Cells were then incubated with the microglia marker antibodies CD11b and CD45 for 20 minutes at 4°C in the dark, prior to being washed twice in incubation buffer and then sorted on a LSR-Fortessa (BD Biosciences). A DAPI suspension (2.5 µg/ml, Cambridge Bioscience, Cat. No. 40443) was used to exclude dead cells and was added just prior to flow sorting.

For experiments using *Csf1r-Cre; Rheb f/f* mice and rapamycin-treated mice, in which microglia were used for quantitative PCR analysis, microglia cells were isolated in a similar manner as described above. However, CD11b microbeads instead of FACS sorting were used to enrich microglia following myelin removal. Briefly, 500 µl of incubation buffer and 40 µl of CD11b microbeads (Miltenyi Biotec, Cat. No. 130-093-636) were added to each cell suspension and incubated at 4°C in the dark for 15 minutes. Following this incubation, 3 mL of incubation buffer was added to each sample in order to wash the cells, which were centrifuged for 10 minutes at 300 x g at 4°C. Using one MS column (Miltenyi Biotec, Cat. No. 130-042-201) per sample, 500 µl of bead/cells were loaded onto each column placed in an OctoMACS separator magnet (Miltenyi Biotec, Cat. No. 130-042-108). This is a positive selection whereby CD11b microglia bind to the column via the CD11b microbeads. Each MS column was washed twice with incubation buffer and then 1 mL of incubation buffer was used to flush the contents of the column using the plunger provided. This positive fraction contained CD11b positive microglia. The purity of the microglia obtained was assessed by flow cytometry analysis by staining an aliquot of cells with the microglia-specific markers CD11b and CD45.

2.5 RNA extraction

For RNA sequencing experiments, microglia were lysed in 120 µl RLT lysis buffer (Qiagen, Cat. No. 74004) and stored at -80°C. Three lysates per replicate were then pooled and RNA was extracted according to the manufacturers guidelines using the RNeasy microkit from Qiagen (Cat. No. 74004). Samples were not randomised for RNA sequencing experiments, however samples that were FACS sorted on the same day were not used for pooling of RNA. Therefore each of the three samples used per RNA extraction were all sorted on different days to eliminate a same day bias. For qPCR experiments, cells were lysed in 350 µl of RLT buffer and were not pooled. RNA was extracted in the same way.

2.6 RNA assessment

The quality and quantity of RNA was measured by Agilent Bioanalyzer 2100 RNA pico chip. Briefly, pico dye (1:65) was added to an aliquot of filtered gel. The gel/dye mix was spun for 10 minutes at room temperature at 13,000 x g and then allowed to equilibrate at room temperature for a further 30 minutes. The gel was then dispensed into a RNA pico chip. Pico conditioning solution, pico marker and pico ladder were dispensed into the appropriate wells.

From each sample, 1 µl was dispensed into appropriate wells and after 60 seconds the chip was inserted into the Agilent 2100 Bioanalyzer. RNA quality was assessed by the presence of the two ribosomal peaks (18S and 28S). The 2100 expert software was then used to calculate RNA concentrations and RNA integrity numbers (RIN) for each sample. Only samples with a RIN>7 were subjected to RNA sequencing.

2.7 RNA Sequencing

Samples were prepared in house up to the point of RNA extraction and assessment. They were then sent to Oxford Gene Technology (OGT) where they were prepared for RNA sequencing using the SMARTer Ultra Low RNA kit for Illumina sequencing (Clontech Laboratories, Inc, Cat. No. 634936). OGT also performed initial analysis on the samples, where they used Boxtie2 and Tophat2 to align reads to the reference

sequences. Transcripts were assembled and quantified using Cufflinks. Cufflinks measures transcript abundances in Fragments Per Kilobase of exon per Million fragments mapped (FPKM) values. These values were received from OGT and then subjected to further statistical analysis.

2.8 Protocol used by OGT to prepare samples for sequencing

SMARTer cDNA synthesis allows the amplification of cDNA with as little as 10 pg of total starting RNA. An oligo (dT) primer is used to prime the first strand reaction. The SMARTer reverse transcriptase used in this protocol reverse transcribes the RNA from the 3' -5' primed end of the mRNA. It also has terminal transferase activity, which means it can add additional nucleotides when it reaches the end of the mRNA. The smarter oligonucleotide is then designed to base-pair with this nucleotide stretch, which allows the creation of an extended template. This results in a full-length cDNA being transcribed containing the complete mRNA as well as anchor sequences, that then serves as a priming site for second-strand synthesis. Following first-strand DNA synthesis, SPRI beads were used to purify the cDNA, as the cDNA will bind to the beads leaving any impurities in the remaining solution. cDNA amplification was achieved using the Advantage 2 PCR kit (part of the Clontech Ultra Low kit) . The amplified cDNA was validated using the Agilent 2100 BioAnalyzer and the high sensitivity DNA chip from Agilent (Cat. No. 5067-4626). Before a library can be generated for Illumina sequencing, the full-length cDNA must be sheared into smaller fragments of roughly 200-500 bp in size. This was done using the Covaris System, an acoustic shearing instrument. Following fragmentation of double-stranded cDNA, the Low Input Library Prep kit from Clontech (Cat. No. 634947) was used to generate a sequencing library. Sequencing was then done on the Illumina Hiseq 200, with each sample being sequenced with 100 bp paired ends at a depth of 33 million reads.

2.9 cDNA synthesis and Quantitative Real-Time Polymerase Chain Reaction (qPCR)

Following RNA extraction, RNA was reverse transcribed into cDNA using the High Capacity cDNA Reverse Transcription kit from Applied Biosystems (Cat. No. 436-

8814). Briefly, a master mix was prepared that contained (per reaction): 1X RT buffer, 1X random hexamers, 4 mM dNTP, 1 µl of reverse transcriptase (50 U/ml) and 2.2 µl of nuclease-free water. This master mix was added to the extracted RNA, contained in 12 µl, therefore the final volume per reaction was 20 µl. All samples were then incubated in a thermocycler using the following programme; 25°C for 10 minutes, 37°C for 120 minutes, 85°C for 5 minutes and held at 4°C.

Following cDNA synthesis, 130 µl of nuclease-free water was added to each sample to dilute the enzymes used in the cDNA synthesis. A master mix was then prepared for the qPCR for each gene of interest, which included per reaction: 10 µl of Biorad iTaq master mix (Biorad, Cat. No. 436-814) and 1 µl of each FAM labelled gene of interest. This master mix was added to wells on a qPCR plate and 9 µl of diluted cDNA was added to each corresponding well. The Step One Plus Real Time PCR machine from Applied Biosystems was used to carry out the qPCR. The PCR programme included an initial denaturation cycle that lasted for 10 minutes at 95°C, followed by 40 cycles of amplification that included 15 seconds at 95°C and one minute at 60°C; the last part of the programme included one more cycle at 25°C for 15 seconds. All primers used are summarised in **Tab. 2.2.**

Primer	Manufacturer	Cat Number
P2ry12	Applied Biosystems	Mm01950543_s1
P2ry13	Applied Biosystems	Mm01951265_s1
Tlr2	Applied Biosystems	Mm00442346_m1
Clec7a	Applied Biosystems	Mm01183349_m1
Cox6a2	Applied Biosystems	Mm00438295_g1
Atp6v1b2	Applied Biosystems	Mm00431987_m1
Hprt1	Applied Biosystems	Mm01545399_m1
Mmp12	Applied Biosystems	Mm00500554_m1
Spp1	Applied Biosystems	Mm00436767_m1
Cst7	Applied Biosystems	Mm00438349_m1
Cxcl13	Applied Biosystems	Mm00444534_m1
Gpnmb	Applied Biosystems	Mm01328587_m1
Apoe4	Applied Biosystems	Mm00545713_m
Mir-155	Applied Biosystems	Mm03306395_pri
Tnf	Applied Biosystems	Mm00443258_m1
Il1b	Applied Biosystems	Mm00434228_m1
Il12a	Applied Biosystems	Mm00434169_m1
Il12b	Applied Biosystems	Mm01288989_m1
Il10	Applied Biosystems	Mm00439614_m1
Il6	Applied Biosystems	Mm00446190_m1
Rela	Applied Biosystems	Mm00501346_m1

Table 2.2 List of qPCR primers used including manufacturer and catalogue number.

2.10 Differentiation of bone marrow derived macrophages (BMDMs)

Bone marrow cells were obtained as previously described for the processing of the bone marrow for flow cytometry analysis. Cells were obtained by flushing the tibia and femur from both legs of a mouse. These cells were then pelleted and resuspended in 20 mL of complete media containing 20 ng/mL of M-CSF (eBioscience, Cat. No. 34-8983-85). M-CSF is a growth factor essential for the differentiation of bone marrow progenitors into macrophages. Approximately 6 x 10^7 cells were obtained from one mouse and they were then split equally into two 15 mm Petri dishes (Falcon, Cat. No. 351058) and allowed to differentiate for 8 days. Following this differentiation step, the BMDMs were re-plated for subsequent experiments. Briefly, the media was removed from each Petri dish and cells were washed once with 10 mL of PBS. Cell Dissociation buffer (Gibco Life Technologies, Cat. No. 13151014) was used to detach the macrophages from the petri dishes by incubating each plate in 10 mL of buffer for 10 minutes at 37°C. Following this incubation, cells were gently scraped off using a 1.8 cm

blade cell scraper from Falcon (Cat. No. 353085). Cells were then placed in complete media before being centrifuged at 300 x g for 10 minutes at 4°C. After this step, they were resuspended in complete media at a concentration of 1 x 10^6 cells per mL. For signalling experiments, 1 mL of cell suspension was used per time-point in a 6-well plate. For qPCR or ELISA experiments, 500 µl of cell suspension was used in a 12-well plate. BMDMs were stimulated with 200 ng/mL of LPS from Escherichia coli 0111:B4 (Sigma, Cat. No. 297-473-0) diluted in complete medium.

2.11 Preparation of protein lysates and protein quantification

Cells were stimulated with LPS for a variety of time points (0,5,15,30 or 60 minutes) in 6-well plates and then placed on ice immediately; media was removed and each well was washed with ice-cold PBS. PBS was aspirated and 80 µl of ice-cold protein lysis buffer was added to each well and left to incubate on ice for 60 minutes. Lysis buffer was made using 10 mL of Ripa buffer (Sigma, Cat. No. R0278) supplemented with 1 tablet of Complete Mini, EDTA-Free Protease Inhibitor (Roche, Cat. No. 12371700), Phosphatase Inhibitor Cocktail 2 (1:100, Sigma, Cat. No. P5726) and Phosphatase Inhibitor Cocktail 3 (1:100, Cat. No. Sigma, P0044). Following incubation with lysis buffer, macrophages were scraped vigorously before cellular material was transferred to 1.5 mL eppendorf tubes. Lysed cells were centrifuged at 16,100 x g for 30 minutes at 4°C. The supernatant was then removed and snap-frozen on dry ice and stored at -80°C. Five µl were kept for protein quantification using the Bicinchoninic Acid assay (BCA). This assay includes the generation of a protein standard curve using bovine serum albumin to determine the protein concentration in the samples. Standards and samples (10 µl) were prepared in PBS and added to a 96-well plate. A solution containing 50 parts Bicinchoninic Acid solution (Sigma, Cat. No. B9643-L) and 1 part of Copper (II) solution (Sigma, Cat. No. C2284) was made and added to each sample and standard (final volume of 200 µl). The plate was then incubated at 37°C for 30 minutes. The colorimetric change caused by the presence of proteins was quantified using a plate reader to read the optical density at 595 nm.

2.12 Western blot

Western blot was used to detect specific proteins based on their size. Proteins were first denatured and then separated by the length of their polypeptide by gel electrophoresis. Proteins were then transferred to a polyvinylidene difluoride (PVDF) membrane, which was incubated with specific antibodies in order to identify proteins of interest.

All samples were thawed on ice. Each sample containing 15 µg of proteins was resuspended to a final volume of 13 µl, prior to the addition of 5 µl 4x NuPAGE LDS Sample buffer (Invitrogen, Cat. No. NP007) and 2 µl 10x NuPAGE Sample Reducing Agent (Invitrogen, Cat. No. NP004). Samples were vortexed and then placed at 70°C for 10 minutes before being loaded on a 4-12% NuPAGE Bis-Tris (Invitrogen, Cat. No. NP0336BOX), 1.5 mm, 15-well pre-cast gel in a running chamber containing 500 mL of 1x MOPS SDS Running buffer (Invitrogen, Cat. No. NP001). SeeBlue Plus2 1X ladder (Invitrogen, Cat. No. LC5925) was loaded with each gel as a molecular weight protein standard. Gels were allowed to run for approximately 90 minutes at 150 V until the blue bands reached the bottom of the gel. The Invitrogen Transfer System was used to transfer proteins from the gel onto PVDF membranes. 1X NuPAGE Transfer buffer (Invitrogen, Cat. No. NP0006), containing 20% methanol (50 mL of 20x NuPAGE Transfer buffer diluted in 750 mL of deionised water and 200 mL of methanol) and Invitrolon™ PVDF/Filter Paper Sandwich (Thermo Fisher Scientific, Cat. No. LC2005) were used. The PVDF membrane was activated in 100% methanol before being equilibrated in deionised water followed by transfer buffer. In a transfer cassette, the activated PVDF membrane was placed on the gel and sandwiched between mattresses and Whatman paper (pre-soaked in transfer buffer). The cassette was then placed in the running chamber, which was filled with running buffer. The entire chamber was placed in a box of ice and an ice pack was also placed in the running chamber to keep the apparatus cold. The transfer was carried out for 2 hours at 65 V. The following step was incubation with a blocking buffer to avoid non-specific binding. The blocking buffer consisted of 5% w/v skimmed milk (Marvel) made in TBST (50 mM Tris-HCl, 150 mM NaCl, 0.1% Tween-20) for 1 hour at room temperature. The membrane was then incubated in primary antibody overnight on a roller at 4°C. Primary antibodies were

diluted in blocking buffer and were all obtained from Cell Signalling. Phospho-S6 Ribosomal Protein (Ser240/244) (1:1000, Cat. No. 5364), S6 Ribosomal Protein (1:1000, Cat. No. 2217) and Total Rheb (1:500, Cat. No. 4935). Following overnight incubation with primary antibodies, membranes were washed 3 times in TBST for 5 minutes at room temperature and then placed in secondary antibody solution – horseradish peroxidase (HRP) conjugated antibodies diluted 1:3000 in blocking buffer – for 1 hour at room temperature. Membranes were then washed again 3 times with TBST. Specific proteins were visualised using the ECL Western Blot Detection System from Amersham (Cat. No. RPN2106) and Hyperfilm ECL (Amersham).

2.13 *In vitro* LPS stimulation of primary adult microglia

Microglia were isolated as described above from adult mice (3-6 months). Following CD11b enrichment, microglia cells were incubated with 100 ng of LPS or complete media for 2 hours. This stimulation was performed in 1.5 mL eppendorf tubes in a water bath at 37°C. Following stimulation, cells were spun at 300 x g for 10 minutes at 4°C to obtain a cell pellet. The supernatant was then discarded and the cells were lysed in 350 µl of RLT buffer. The cells were vortexed for 1 minute to obtain complete lysis before the lysate was snap frozen on dry ice and stored at -80°C until RNA extraction was performed.

2.14 ELISA

ELISA kits were obtained from BD Biosciences: IL-12p40 (Cat. No. 555165), IL-6 (Cat. No. 555240) and TNFα (Cat. No. 558534). ELISA was performed according to the manufacturer's guidelines; however, half-surface area 96-well plates were obtained from Costar (Cat. No. 3690) and used for the assay. The wells in these plates are half the volume of standard 96-well plates, allowing the use of a reduced amount of samples and reagents. This was particularly important for plasma cytokine levels, as the amount of plasma obtained from each mouse was potentially a limiting factor. Briefly, capture antibody was diluted in PBS and added to each well of a 96-well plate. The plate was then incubated overnight at 4°C, prior to being washed three times with wash buffer (PBS with 0.05% Tween-20). The plate was then incubated with assay diluent (PBS with 10% FBS) for 1 hour, in order to block non-specific binding and washed three

times with wash buffer. The highest concentration of standards (1000 pg/mL) were made using a stock solution of each cytokine and then a serial dilution was performed on a separate plate to obtain the remaining standards (500, 250, 125, 62.5, 31.3 and 15.6 pg/mL). Samples and standards were then added to the ELISA plate and incubated for 2 hours at room temperature. Samples that required dilution were diluted in assay diluent. Following incubation, the plate was washed 5 times with wash buffer and then the working detector solution (detection antibody and HRP) was added to the plate and it was incubated at room temperature for 1 hour. The plate was then washed 7 times before the substrate solution [Tetramethylbenzidine (TMB) and hydrogen peroxide from the TMB Substrate Reagent Set (BD Pharmingen, Cat. No.555214)] was added and incubated in the dark for a maximum of 30 minutes. Following the appropriate colour change, 25 ml of 1M H_3PO_4 was added to stop the reaction. Plates were analysed on a plate reader plate reader to read the optical density at 450 nm.

2.15 Open field test protocol and analysis

Wild-type mice were given an intraperitoneal injection of either LPS (0.33 mg/kg) or PBS before being assessed in an open-field test 6 hours post injection. Mice were brought into the testing room 30 minutes prior to the test, so that they could acclimatise to their new surroundings. The test was conducted in a 15-square gridded box. The box was cleaned with ethanol prior to the first mouse being tested and in between each mouse. Each mouse was placed in the left corner of the gridded box at the start of the test and was recorded for a total of 5 minutes. The test was performed so that the analyser was blind to the genotype and treatment group of each mouse. Analysis was conducted by counting the number of times the mouse passed through each square during the 5-minute test (distance travelled). All four paws of the mouse were required to pass within each square to be counted. The number of times the mouse reared (both paws) was counted as another measure of locomotion. Anxiety or stress-like behaviour was also assessed by measuring the number of times the mouse passed through any of the 3 central squares (time in centre) or the first time the mouse passed through one of these central squares (time to centre).

2.16 Rapamycin diet

Rapamycin was first obtained from Rapamycin Holdings in San Antonio, Texas and then microencapsulated with an enteric coating called Eudragit S100. This material was used because it increases the amount of the drug that survives the food preparation and also prevents the drug from being prematurely digested in the stomach. Microencapsulated rapamycin and Eudragit (serving as a control) were then incorporated into separate LabDiets on a 5058 base by Purina labs. The base diet was the same used in our Biological Services Unit and therefore eliminated potential confounding factors. The amount of rapamycin used corresponded to 152 ppm, which resulted in 14 ppm active rapamycin. This diet was similar to the diet used in several of the ageing studies, including the 2012 *Nature* paper by Harrison *et al.* which showed that rapamyin extended lifespan in mice[31].

2.17 LPS injection *in vivo*

For all *in vivo* experiments mice were injected using a 27G needle and 1 mL syringe intraperitoneally with either 200 µl of E. *coli* 0111:B4 (Sigma, Cat. No. 297-473-0) or PBS as control. For Rheb ageing experiments, all mice received 5 mg/kg of LPS. This is a high dose of LPS that induces a robust inflammatory response and mice were culled after 3.5 hours. For sickness behaviour experiments in Rheb KO mice, 0.33 mg/kg of LPS was used to induce transient sickness behaviour and mice were culled after 48 hours. Finally for the rapamycin ageing study, 2 mg/kg of LPS was used and mice were culled after 5 hours.

2.18 Experimental design and statistical analysis

Number of animals were kept to the minimum required for experiments, calculated by power analysis where possible using the software available at www.biomath.info. For RNA sequencing experiments, n=3 was used for each of the three age groups (young, middle and old), where each replicate consisted of 3 pooled samples. This number of replicates was chosen, as there was no prior data available to predict statistical variability at the time of experimental design. For Rheb *in vivo* experiments, this was

also true, so it was difficult to predict the number of mice needed to achieve significance. However we used the power analysis calculator to calculate how many mice to use for the rapamycin ageing study based on observations from the Rheb *in vivo* experiments.

For RNA sequencing experiments data was analysed using an uncorrected one-way ANOVA or unpaired T-test where appropriate. For all other experiments a two-tailed unpaired student T-test was used to calculate significance between two groups or populations. All data was represented with error bars representing the standard error of the mean (of a group). All p values obtained>0.05 were considered significant with an an asterisk indicating the following: * $p<0.05$, ** $p<0.01$ and *** $p<0.001$.

Chapter 3: Characterisation of the Immune System in Ageing

3.1 Naive T cells decline with age

The immune system is known to deteriorate with age in a process known as Immunosenescence and this deterioration is thought to contribute to the overall burden of chronic illness that accompanies ageing[149]. I therefore wanted to profile the changes in the immune system with age. I was particularly interested in changes in the myleoid compartment, as this is less studied than lymphocytes in ageing. Firstly, I assessed T lymphocytes, which form an essential part of the adaptive immune response and can be broadly divided into two main subclasses based on their surface expression of CD4 and CD8 glycoproteins. I used flow cytometry analysis to profile these lymphocyte populations in the bone marrow, blood and spleen from mice of different age groups. Positive populations were obtained for all data using floresence minus one (FMO) and unstained controls.

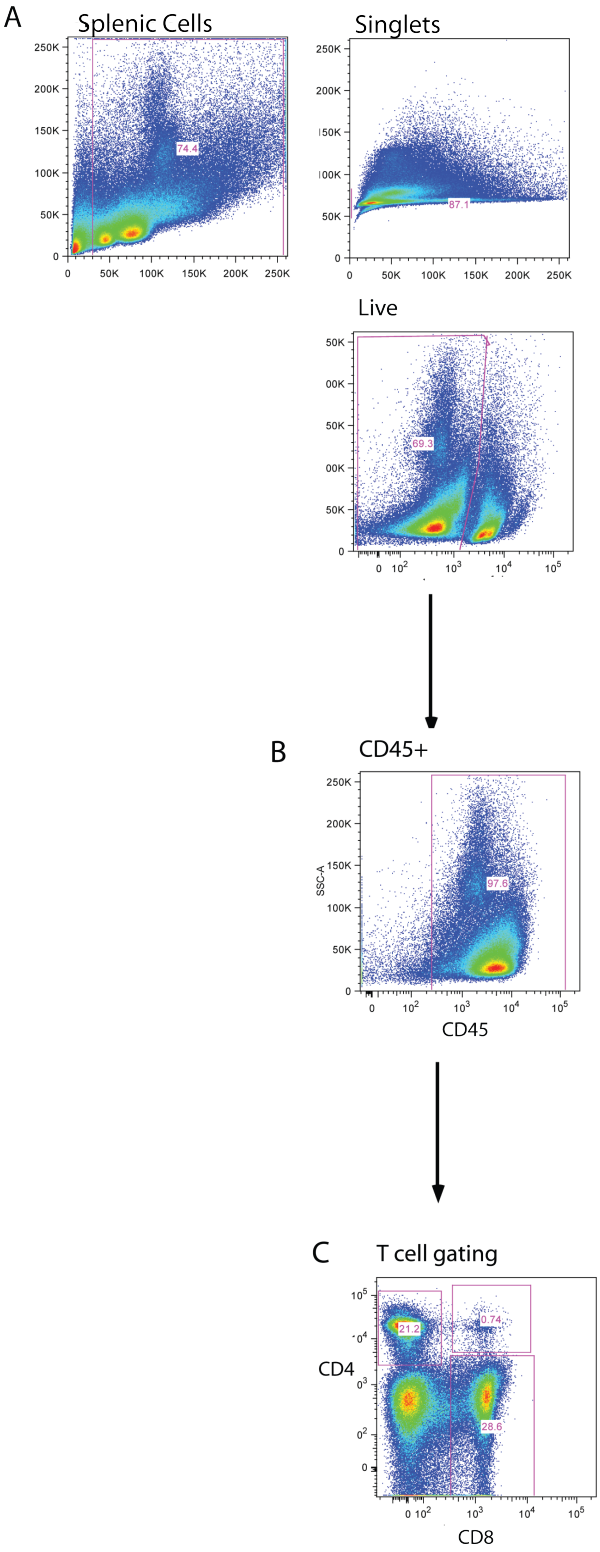

Figure 3.1 Gating strategy used to profile T lymphocytes in the spleen. A) Cells were first gated by their size (forward scatter) and granularity (sideward scatter), then duplets were excluded by gating on cells by their sideward area against their sideward width. Dead cells were excluded by using a viability dye that stains dead cells; therefore live cells are negative for this stain. Finally, immune cells are identified by gating on the **B)** CD45+ population, and **C**) T cell subpopulations, identified by CD4 and CD8 markers.

I stained spleen, bone marrow and blood cells with antibodies to CD45 to identify leukocytes and CD4 and CD8 to assess T cell subsets. It would have been advisable to include CD3 in this analysis, which is a pan marker that stains all T cells, as there are small subsets of other immune cells that express CD4 and CD8 besides T cells. However, to avoid over complicating the flow cytometry staining, CD3 was not included in this analysis.

An example of the gating strategy used is depicted in (**Fig. 3.1A**); briefly, cells were first gated by their forward and sideward scatter. These parameters provide information about the size and overall granularity of the cells. It also allows the exclusion of debris. Next, clumped cells forming doublets were excluded by gating on the sideward width against the sideward area. Dead cells were excluded by gating on the population that is negative for a viability dye. Finally, leukocytes were identified as CD45+ cells (**Fig. 3.1B**) and T cell subsets were assessed by CD4 and CD8 positivity (**Fig. 3.1C**).

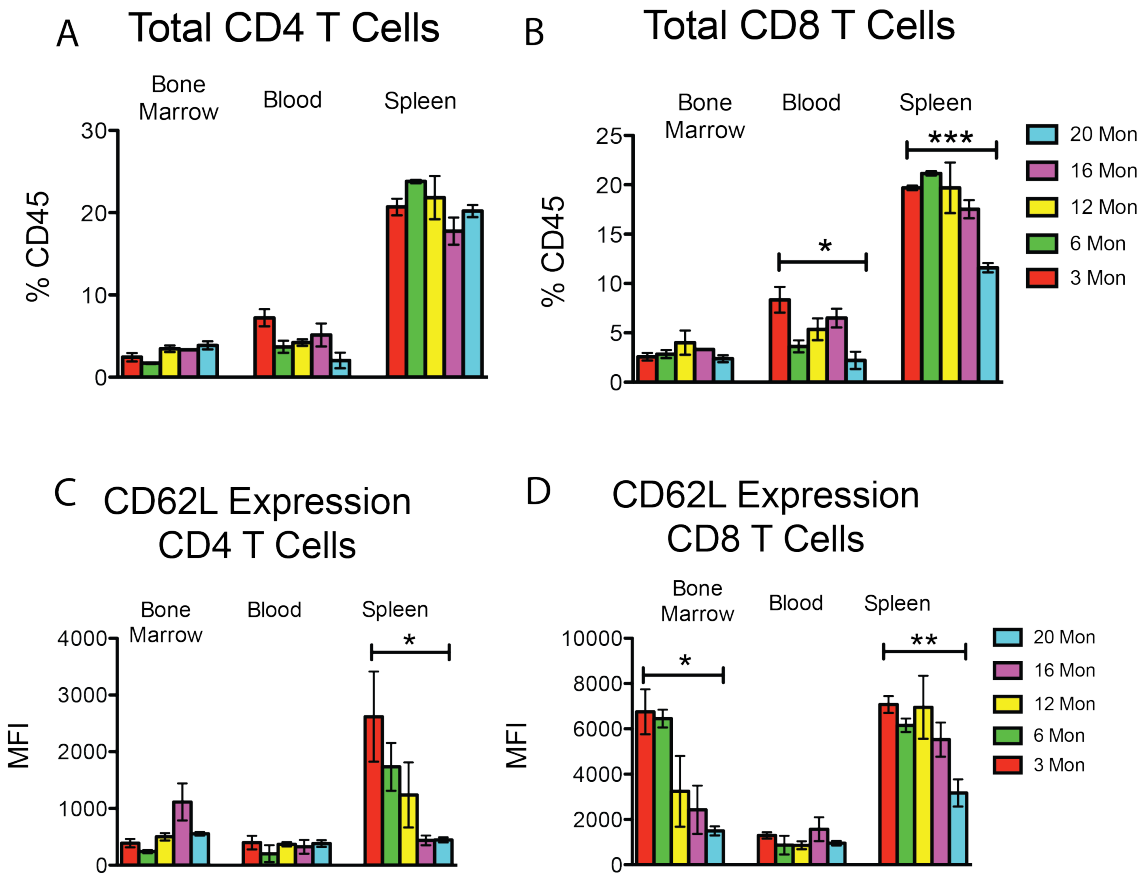

Figure 3.2 Naïve T-lymphocyte populations decline with age. The blood, spleen and bone marrow from 3, 6, 12, 16 and 20-month old mice was assessed by flow cytometry analysis, stained for CD4, CD8 and the naïve T-cell marker CD62L. **A)** Total CD4 T cells **B)** total CD8 T cells are shown as a % of CD45 cells for all three organs. The surface expression of CD62L on CD4 T cells **(C)** and CD8 T cells **(D)** is shown for all three organs as the MFI (median florescence intensity). The data shown are from one experiment, where n=3 for each group and * $p<0.05$, ** $p<0.01$. Significance was calculated using the unpaired two tailed student T-test between individual groups.

I carried out this staining on the blood, bone marrow and spleen from five different age groups of mice that ranged from young to old age. These included 3, 6, 12, 16 and 20-months of age. I found that the total number of CD4 T cells did not appear to change in the blood, spleen or bone marrow with age (**Fig. 3.2A**). However, I did observe a trend with regards to CD8 T cells, which appeared to decrease with age in the blood and spleen (**Fig 3.2B**). This decrease was significantly different between the youngest age group (3 months) and the oldest age group (20 months) and suggested an overall decrease in circulating CD8 T cells, as previously reported[149].

I next looked at the expression of L-selectin also known as CD62L. CD62L is an adhesion molecule that is expressed on naïve T cells that have not yet encountered an antigen and is not expressed by effector memory cells[150]. In the bone marrow, the expression of L-selectin is associated with cells that are committed to lymphoid differentiation. I therefore used CD62L to measure loss of naïve T cells with age. I found that the expression of CD62L on both CD4 and CD8 T cells steadily declined in the spleen over the five age groups tested (**Fig 3.2B** and **Fig. 3.2D**). I found that the entire population of both CD4 or CD8 T cells showed a decrease in expression of CD62L with age, therefore I show changes as MFI rather than percentage of cells. Both CD4 and CD8 T cells from 20-month old mice expressed significantly less CD62L compared to CD4 and CD8 cells from 3-month old mice. On the other hand, T cells in the blood did not show differences in CD62L expression with age, in either CD4 or CD8 cells (**Fig. 3.2C** and **3.2D**). In the bone marrow, CD4 T cells did not show differences in CD62L expression with age but there was a steady decrease in CD62L on CD8 T cells in the bone marrow, significantly different between 3 and 20 months of age (**Fig. 3.2D**). This finding might suggest that fewer cells in the bone marrow are committing to the lymphocyte lineage with age, which is also consistent with what has been reported in the literature[151].

3.2 Monocyte populations appear to decline with age

Next I wanted to profile how the myeloid compartment of the immune system changed with age. Monocytes are circulating myeloid cells that differentiate into the two main types of antigen presenting cells, known as macrophages and dendritic cells. In order to profile these cells, I again used flow cytometry analysis. I stained the bone marrow, spleen and blood with an antibody for the myeloid marker CD11b, an integrin expressed on monocytes, macrophages, granulocytes and immature myeloid cells. An example of the gating strategy used for cells from the spleen is shown in **Fig. 3.3**. I first excluded doublets and dead cells, as described previously, and then gated cells on CD11b expression (**Fig. 3.3B**). Within this gate, I used the two markers Ly6C and Ly6G to identify monocytes and granulocytes, respectively. Four populations could be identified with this staining. $Ly6C^{hi}Ly6G^{-}$ cells are known as inflammatory monocytes, $Ly6C^{-}$ $Ly6G^{hi}$ cells are granulocytes, $Ly6C^{dim}Ly6G^{dim}$ cells are known as immature myeloid

cells and finally cells that are Ly6C^{dim}Ly6G^{-}are known as patrolling monocytes (**Fig. 3.3C**). Using this analysis, I assessed the number of these cell populations as well as total CD11b+ cells in the blood, spleen and bone marrow from young, middle-aged and old mice of 6, 15 and 23 months of age.

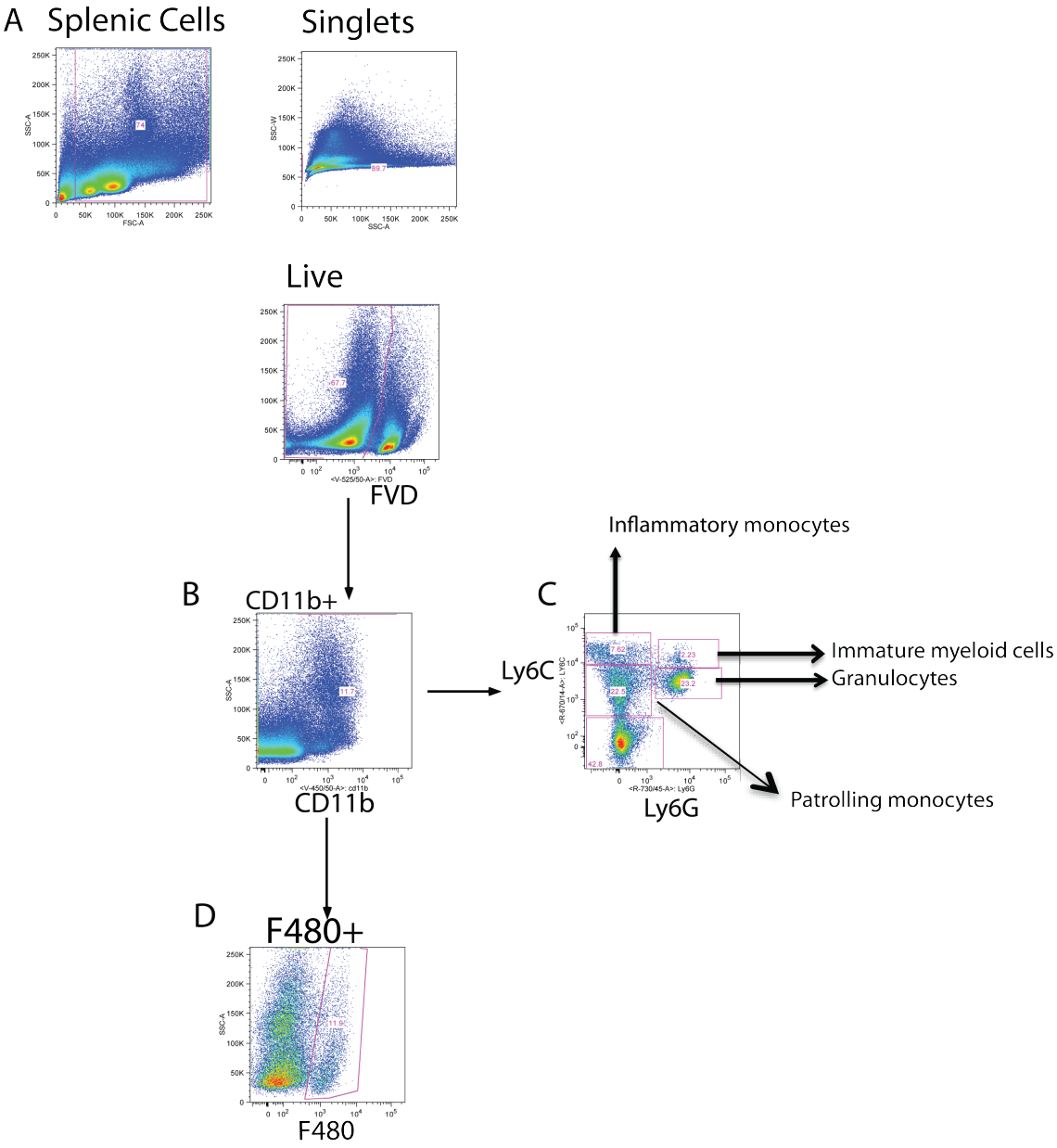

Figure 3.3 Gating strategy used to profile myeloid cells in the spleen. A) Cells are first gated by their size (forward scatter) and granularity (sideward scatter), then doublets are excluded by gating on cells by their sideward area against their sideward width. Dead cells are excluded by using a viability dye that stains dead cells. **B)** Myeloid cells are identified based on their expression of the integrin CD11b. **C)** Different populations of myeloid cells are defined based on their expression levels of Ly6C and Ly6G. Four populations could be identified with this staining. Ly6C^{hi}Ly6G^{-} cells are known as inflammatory monocytes, Ly6C^{-}Ly6G^{hi} cells are granulocytes, Ly6C^{dim}Ly6G^{dim} cells are known as immature myeloid cells and finally cells that are Ly6C^{dim}Ly6G^{-}are known as patrolling monocytes. **D)** Macrophages in the spleen identified based on their expression of the macrophage specific marker F4/80.

Unfortunately, I was not able to collect data from the blood of old mice due to problems with the staining. Nonetheless, I found that the number of CD11b+ cells in the blood between the age of 6 and 15 months did not change; this was also true for the CD11b+ cells in the spleen (**Fig. 3.4A**). However, in the bone marrow the number of CD11b+ cells appeared to be maintained until middle age, before significantly decreasing between the ages of 15 and 23 months, from almost 70% of total live cells to approximately 40% (**Fig. 3.4A**). The difference between the 3-month and 23-month old mice was statistically significant with a p value<0.001 and between 15 and 23 months with a p value <0.01 (**Fig. 3.4A**).

I also analysed the total number of granulocytic cells and found that these cells decreased with increasing age, particularly in the spleen. This trend, however, was not significant (**Fig 3.4C**).

The total number of immature myeloid cells, expressing intermediate levels of both Ly6C and Ly6G, was also analysed. Immature myeloid cells are thought to have immunosuppressive properties and are sometimes described as myeloid derived suppressor cells. In a healthy mouse, these cells are not very abundant and constitute between 2-5% of CD11b+ cells in the spleen, blood and bone marrow. In cancer, however, these cells can expand and suppress T cells and other immune functions[152]. In my cohort of mice, it appeared that the overall total number of immature myeloid cells decreased across all compartments measured. This difference though was only significant in the bone marrow with a p value<0.001 between the 6 and 23-month age group and p value<0.01 between 6 and 15 months of age (**Fig 3.4B**).

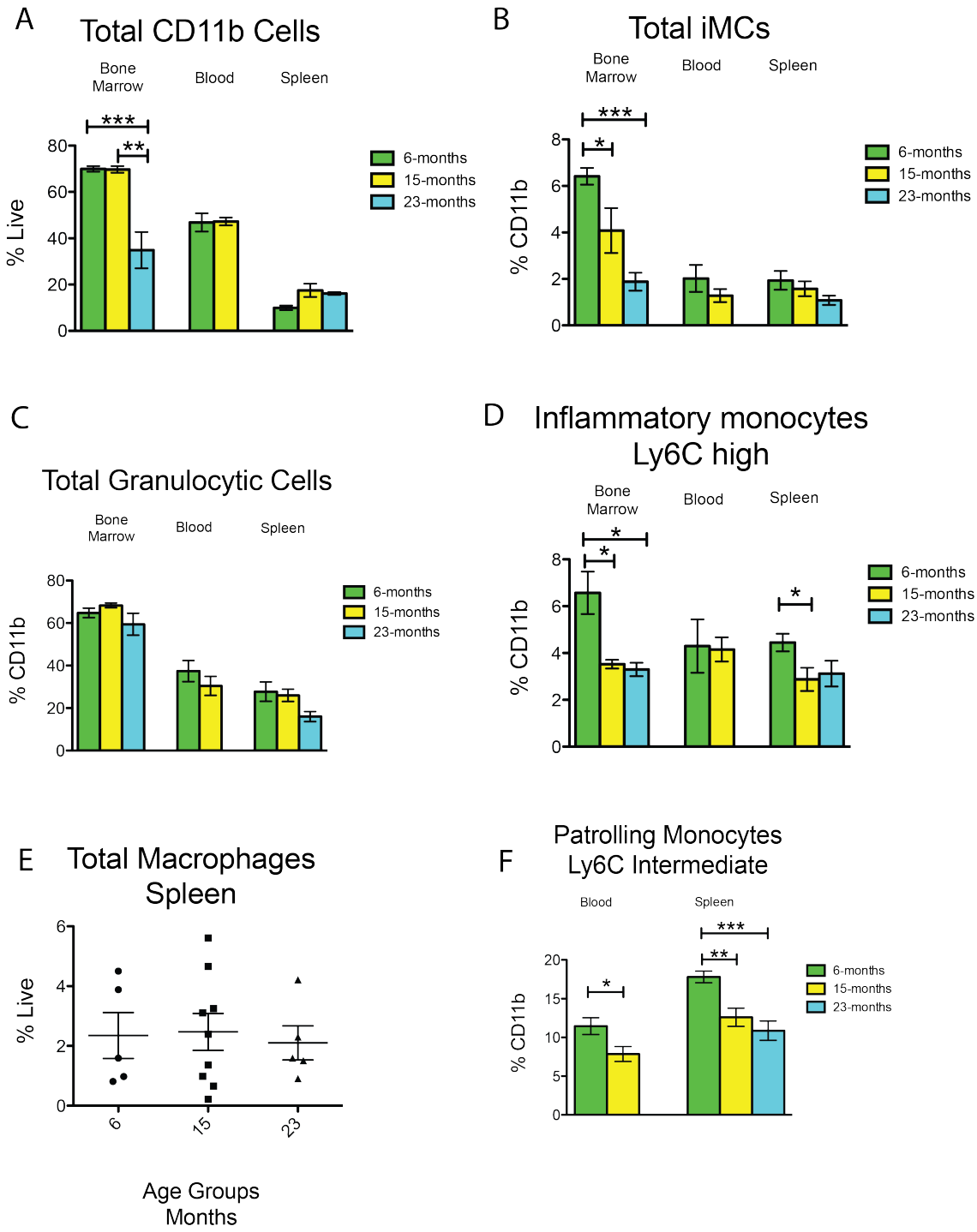

Figure 3.4 Myeloid populations appear to decline with age. The blood, spleen and bone marrow from 6, 15 and 23-month old mice was taken for flow cytometry analysis and stained for the myeloid marker, CD11b, the monocyte marker, Ly6C, the granulocyte marker, Ly6G, and the macrophage marker, F480. **A)** Total CD11b cells in spleen, bone marrow and blood shown as a % of live cells. **B)** Total immature myeloid cells (intermediate Ly6C and Ly6G expression), shown as a % of CD11b+ **C)** Total granulocytic cells (Ly6G high) as a % of CD11b+ **D)** Total inflammatory monocytes (Ly6C high) as a % of CD11b+ **E)** Total F4/80 positive macrophages in the spleen shown as a % of total live cells. **F)** Total patrolling monocytes in blood, spleen and bone marrow shown as a % of CD11b cells. The data shown are from one experiment, where n=5 for each group and * $p<0.05$, **$p<0.01$, *$p<0.001$. Significance was calculated using the unpaired two tailed student T-test between individual groups.

There are two main monocyte populations in the adult mouse that can be broadly divided by the expression of Ly6C. Monocytes in the blood that express very high levels of Ly6C are called inflammatory monocytes and the cells that express lower levels are called patrolling monocytes[153]. The two populations of Ly6C monocytes are easily distinguishable in both the spleen and blood by the gating strategy illustrated in **Fig. 3.3C**. In the bone marrow, there is only a $Ly6C^{hi}$ population.

Both monocyte populations decreased in all organs with ageing (**Fig. 3.4D** and **3.4F**). For the $Ly6C^{hi}$ population, the most striking differences were in the bone marrow with a dramatic drop by 15 months of age compared to 6 months of age with a p value<0.05, a decrease that was maintained at 23 months of age (**Fig 3.4D**). No differences were observed in the blood but, in the spleen, the decrease was evident by 15 months with a p value <0.05 (**Fig. 3.4D**). For $Ly6C^{dim}$ patrolling monocytes, a decrease in cell number with age was more evident in the blood and was statistically significant between the 6 and 15-month age group. A similar reduction in $Ly6C^{dim}$ patrolling monocytes was observed in the spleen between 6 and 15 months of age ($p<0.01$), with an even more pronounced change between 6 and 23 months of age ($p<0.001$, **Fig. 3.4F**).

Not many studies have addressed changes in macrophages with age. Therefore, I analysed the total number of macrophages in the spleen using the macrophage specific marker F4/80, as shown by the gating strategy in **Fig. 3.3D**. No differences were detected, however, in splenic macrophages (**Fig. 3.4E**). This finding does not rule out that changes might be seen in other tissue resident macrophages.

3 Discussion

Understanding how the immune system changes with age is an important aspect of ageing research. This is because the immune system is essential for maintaining health throughout lifespan. Many age-related illnesses have a strong immune component, most notably cancer, where the immune system influences both the initiation and progression of the disease[154]. In the course of my PhD, I wanted to firstly reproduce some of the findings that have already been described in the field of Immunosenescence, most notably regarding T cells. T cells mature in the thymus, however, this organ undergoes a significant involution over time, a phenomenon associated with a dramatic decrease in the output of naïve T cells[155], especially cytotoxic CD8 T cells[156]. My results agreed with the literature, with a significant decline in the number of CD8 T cells with age but unaltered numbers of CD4 T cells. I have also shown that the expression of the naïve T-cell marker CD62L decreases with age in both CD4 and CD8 T cells, most notably in the spleen. This would indicate that the T cells residing in this organ are predominantly of an effector or effector memory phenotype, but I should have included additional markers of memory T cells such as CD44 to confirm this finding. This overall change in the naïve/memory T-cell ratio has important implications for the immune response, as it could potentially compromise overall ability to clear new infections[156]. In conclusion, my findings on T lymphocytes are consistent with the literature and indicate a decline with age.

Given the interest in inflamm-ageing and the low-grade pro-inflammatory phenotype that accompanies the ageing process, I was particularly interested in assessing the myeloid compartment for possible changes. Myeloid cells were profiled in the blood, spleen, and bone marrow from young, middle-aged and old mice. The most striking observation was the significant decline in monocytes. This was true for both inflammatory monocytes and patrolling monocytes but also for immature myeloid cells. These results are in contrast to what has been previously reported in the literature, indicating that haematopoiesis is skewed towards the myeloid lineage with age[157]. It has

been shown previously that the number of myeloid-derived suppressor cells increases in the spleen, blood and bone marrow in aged mice[158]. The mice used in these studies were Balb/c, whereas the mice I analysed here were C57BL/6, furthermore the markers used to define myeloid-derived suppressor cells were different. These differences may account for the contrasting results obtained.

Despite the observed decrease in monocytes, particularly in the spleen, the number of splenic macrophages appeared unaffected by age. There is a paucity of reports on tissue-resident macrophages in ageing. It has been published that there is an overall reduction in the response to TLR stimulation in macrophages with age, which results in a reduced inflammatory response[159]. Additional studies have addressed the impact of ageing on macrophage phagocytosis, showing that aged macrophages have impaired phagocytic abilities. Also, it has been shown that microglia internalised less amyloid beta when isolated from old mice compared to young ones[160], however other studies in humans have shown that this response is unchanged with age[161]. One interesting study isolated peritoneal macrophages form young and aged mice and showed that phagocytosis of fluorescent particles was impaired[162]. Given their impaired ability to clear debris, maybe it is not surprising that the wound healing ability of macrophages also appears defective with increasing age: one study showed that VEGF, an essential angiogenic factor in wound healing, was produced significantly less by macrophages from old mice[163].

There are limitations to representing the data as a percentage of CD45 immune cells or CD11b myeloid cells, as you only obtain a change in proportion of a particular cell type. In the data presented here, for example, the proportion of inflammatory myeloid cells appears to decrease with age. It would be important to establish if the inflammatory monocytes are in fact decreasing. This could be done by showing the data as absolute cell counts to understand if there are less inflammatory monocytes in the blood and spleen with age. The limitations of using proportions rather than absolute cell counts is if another population is increasing within the CD11b population, the changes observed for the monocyte populations may just be a reflection of this. Therefore if these experiments were repeated, it would be important to use absolute cell counts and show plots as percentage live rather than percentage CD45 or CD11b.

3 Conclusion

The profiling carried out in the course of this project was limited and only gives an indication of what happens to myeloid cells with age. It would be very interesting to assess the characteristics of these cells in more detail. For example, I could stain for markers of macrophage polarisation, such as MHC II (M1 marker), or the mannose receptor (M2 marker) as well as markers of activation such as CD40, CD80 and CD86. It would also be important to isolate macrophages from the spleen or monocytes from the blood and look at how their function changes with age, similar to some of the studies described above (phagocytosis, wound healing). In terms of TLR signalling and overall inflammatory capacity, the literature is limited to the use of the TLR4 agonist LPS. It would be important to test a range of TLR ligands that would mimic both bacterial and viral infections and to analyse a range of cytokines that characterise inflammatory responses.

Chapter 4: RNA sequencing of the microglia transcriptome from the ageing brain

Following on from phenotyping of the ageing myeloid populations in the blood, spleen and bone marrow, we decided to focus on the myeloid cells of the brain known as microglia. We wanted to gain as much information as possible on how microglia change with age so we decided to use RNA sequencing, a method that would allow us to look at the entire transcriptome. This would enable us to identify key pathways or genes that were deregulated with age and provide important information about how the brain ages.

Although there have been studies that have described how the microglia transcriptome changes with age[91,95-97,164,165], the novelty of our study is defined by the fact that we used microglia cells from the whole brain, rather than the retina or cortices, we used a new system for RNA sequencing, using low amounts of starting RNA, and finally we used three age groups of mice that would allow us to gain insight into the progressive changes that occur in microglia as the whole brain ages.

4.1 Microglia Isolation

4.1.1 Florescence Activated cell sorting was essential for obtaining microglia purity over 95% in aged mice

In order to isolate microglia with a high degree of purity and sufficient yield from both the adult and aged brain, a purification protocol was optimised. The standard protocol for isolating microglia from the mouse brain involves two steps; firstly, the brain is digested with a cocktail of enzymes (dispase and collagenase) and secondly the cells are suspended in different Percoll gradients (30%, 37% and 70%), as depicted in **Fig. 4.1, Protocol 1**. This is a well-described method that results in approximately 70-80% purity of microglia[54]. This purity was, however, too low for an RNA sequencing experiment and I aimed to achieve values above 95%, as even a 10% contamination of another cell type could dramatically bias the results.

Therefore, I tested a number of other methods for isolating microglia. I began using a dissociation technique for digesting the brain tissue developed by Miltenyi Biotec. Using a cocktail of enzymes that included papain, the mouse brains were placed in C-tubes and processed through a dissociator with intermittent pulses for 30 minutes. Following the digestion/dissociation, I enriched for microglia using CD11b magnetic microbeads. The use of microbeads for the isolation of immune cells is a well-established protocol. This technique, though, depicted in **Fig. 4.1, Protocol 2** resulted in even worse purity (less than 30%) than using percoll gradients in **Protocol 1**.

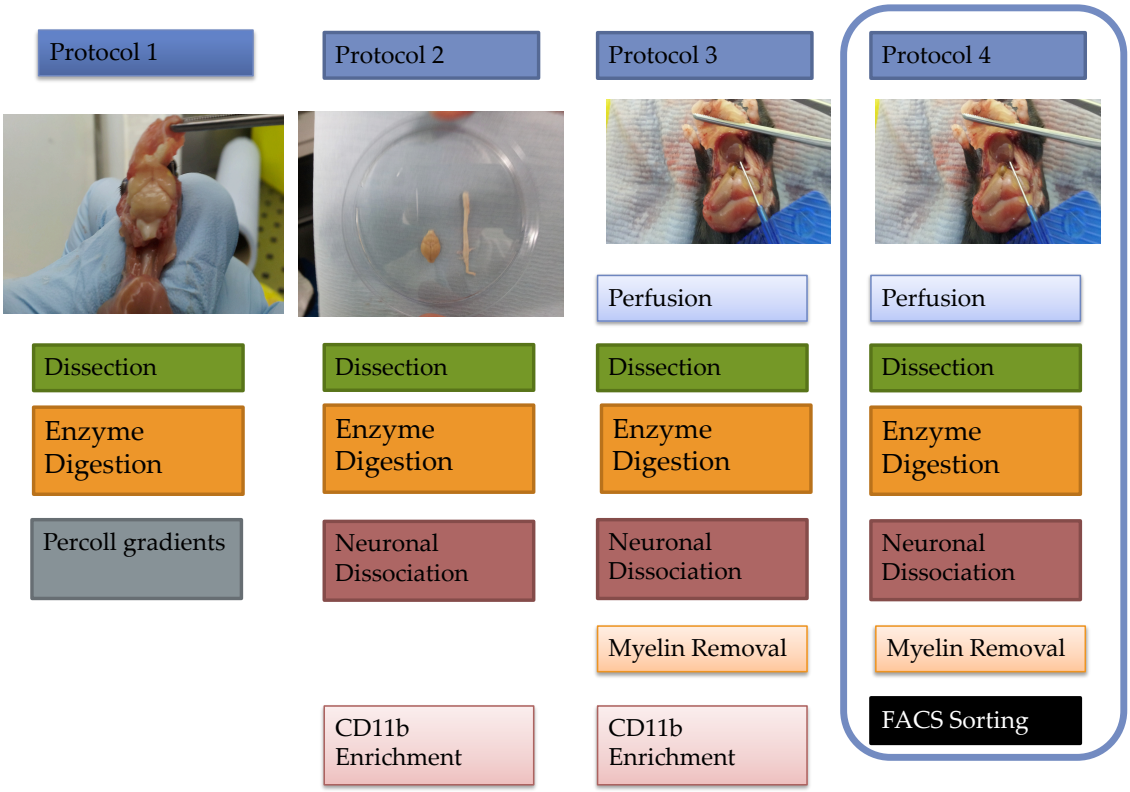

Figure 4.1 Schematic of the four protocols used to isolate microglia from the aged brain. Each protocol included dissection of the brain and enzyme digestions. In **Protocol 1**, percoll gradients were used to separate microglia from other brain cells. **In Protocol 2**, CD11b enrichment was used after the brain was digested and dissociated. In **Protocol 3** an extra step was used before CD11b enrichment to remove myelin. **Protocol 4** is highlighted, as it is the technique finally used for the RNA sequencing experiments, this protocol differs from **Protocol 3,** only in the final microglia isolation step, which was carried out using FACS sorting based on CD11b staining rather than using CD11b microbeads.

The reason for such poor purity using **Protocol 1** was found to be the large amount of myelin, a mixture of proteins and phospholipids that insulate nerve fibres and is abundant in the adult brain. Indeed, the additional step of removing the myelin in

Protocol 3 had drastic affects on the overall purity of cells (greater than 90%). An example of the purity of microglia, obtained from an adult brain, using **Protocol 3**, is shown in **Fig. 4.2A**, in which cells are first gated by their forward and side scatter, parameters that represent the size and granularity of the cells, respectively. Cells can often form clumps and stick together which can lead to misinterpreting their fluorescent labelling, therefore duplet cells were excluded by gating on the width against the area of the cells. Dead cells can stick non-specifically to antibodies and also auto-fluoresce, so it was also important to exclude them. Here I used a viability dye that stains dead cells and can be used before fixation; therefore dead cells were excluded by gating on the negative population. Finally, the number of cells that are CD11b+ and therefore microglia were obtained by gating on this marker compared to an unstained control. In this example, 96.5% of cells obtained were positive for CD11b (**Fig. 4.2A).**

I now had an established protocol (**Fig. 4.1, Protocol 3**) to obtain high purity and sufficient yield of microglia from the adult brain (2-8 x 10^6). However, I found that purity could be variable, between 85 and 95%, so I decided to use flow sorting, based on the microglia markers CD11b and CD45. The gating strategy used for FACS sorting is depicted in **Fig. 4.2B**, sample purity was checked after every sort (**Fig. 4.2C),** ensuring that every sample used for RNA sequencing had purity above 95%.

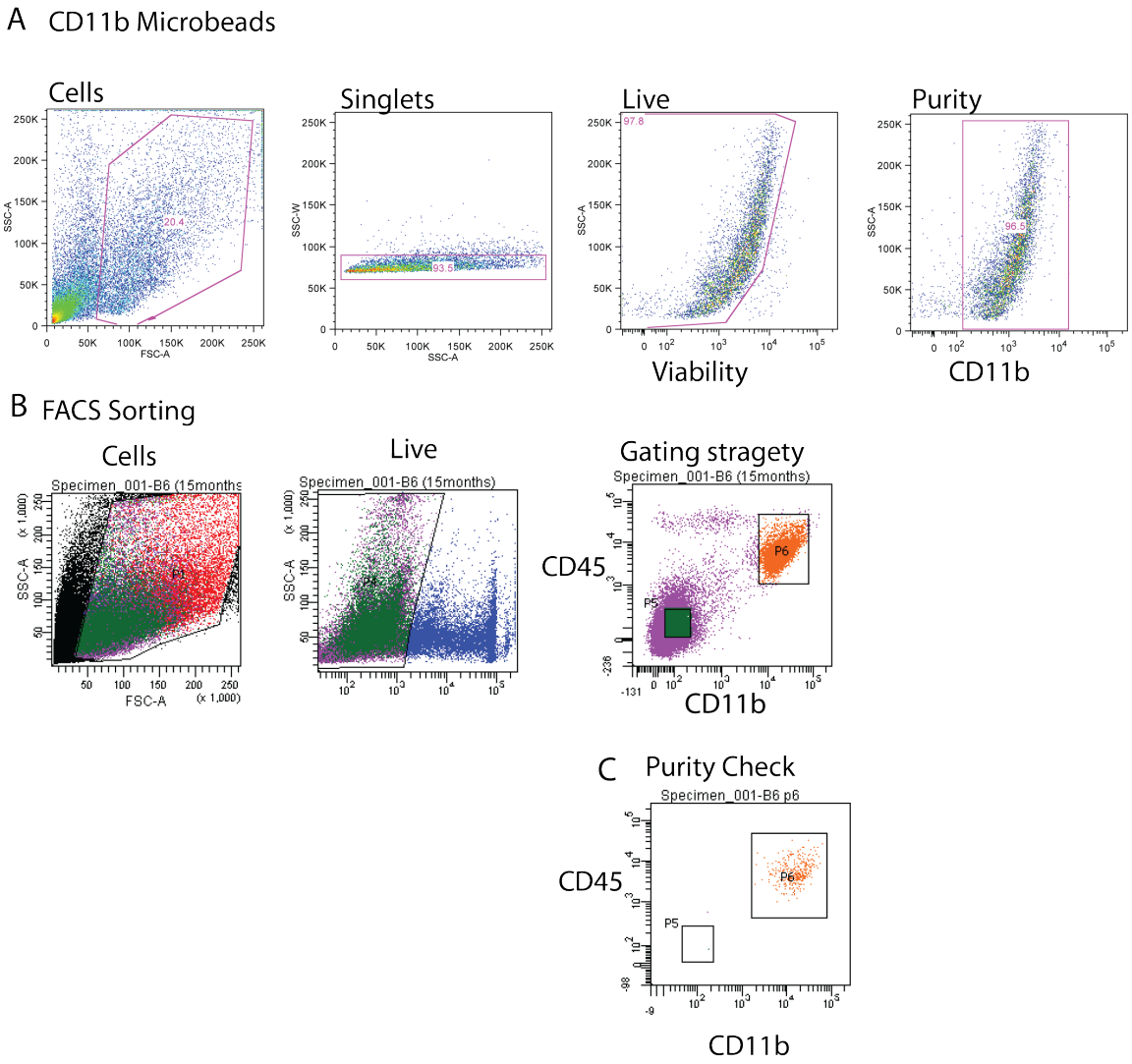

Figure 4.2 Microglia isolated using CD11b and FACS sorting yielded cells with a high degree of purity (>95%). The gating strategy is shown for microglia cells isolated using myelin removal and CD11b microbeads. **A)** Cells were first gated by forward and side scatter and then duplets and dead cells were excluded, finally cells were gated based on their expression of CD11b relative to an unstained control. **B)** Gating strategy for microglia cells isolated by FACS sorting, based on their expression of CD11b and CD45 **C)** An example of a purity check run after the sort to assess purity.

Microglia were isolated using FACS sorting, as described above, from three different age groups of mice. The age groups chosen were 6 months, 15 months and 23 months, reflecting young, middle and old age, respectively. All mice were female, ex-breeders and on a C57BL/6J background to try to minimise other variables besides their different age. For each of the nine biological replicates, microglia cells were pooled from three different mice. On average I obtained 100,000 microglia cells by FACS sorting from one whole brain. Each sample was lysed in RLT buffer and then the three lysed samples

were pooled together just before RNA extraction, to represent one biological replicate as described in **Tab 4.1**.

Group	Age (M)	Gender	Background	Breeding status	Pooled	Reps	Total mice
Young	6	Female	C57BL/6J	Ex-Breeder	3	3	9
Middle	15	Female	C57BL/6J	Ex-Breeder	3	3	9
Old	23	Female	C57BL/6J	Ex-Breeder	3	3	9

Table 4.1. Summary of the experimental design used to obtain RNA from the microglia of different age groups of mice to be used for RNA sequencing. The age, gender, background and breeding status are all given for each of the three age groups corresponding to young, middle and old age. The number of samples that were pooled for each replicate is also given.

The profile of the microglia cells before sorting between age groups was similar. It was found that the MFI of the marker CD11b was increased with age but this has also been observed in the literature[82].

4.1.2 RNA isolated from microglia of aged mice was of high quality

The integrity of RNA is an important consideration for any large-scale expression data. Using degraded RNA can introduce biases into experiments; meaning RNA of a high integrity must be used. The integrity of the RNA can be measured using the Agilent 2100 Bioanalyzer. The system is based on electrophoretic separation, where each RNA sample is placed on a microchip and is then detected by a laser. The software will generate an electropherogram, which is based on the ratio between the 18S and 28S ribosomal subunits. If the RNA is degraded, there will be a decrease in the 18S to 28S ratio. The software generates a RNA integrity number (RIN) based on this ratio with 1 being the most degraded and 10 having the best integrity. When carrying out the RNA extraction and testing the quality of the RNA using the Agilent system, peripheral blood mononuclear cells (PBMCs) were used as a control. It was found that both the control PBMC sample and the sorted microglia samples contained RNA with a high integrity. Examples of RIN numbers obtained for microglia RNA are given for each age group in **Fig. 4.3,** whereby samples obtained from microglia isolated from young mice is shown in **Fig. 4.3A**, middle aged in **Fig. 4.3B** and old in **Fig. 4.3C**. All samples (except for one-Y2) were of high quality**,** indicated by a RIN number of >8. The quantity of RNA obtained ranged from 13-126 ng. All RIN numbers and amounts of RNA obtained are given for every replicate in the table in **Fig. 4.3**. All nine samples were sent to the

company Oxford Gene Technology (OGT), where they performed the RNA integrity analysis again. They found that all samples including sample Y2 had a RIN value >8 so this sample was included in the RNA sequencing.

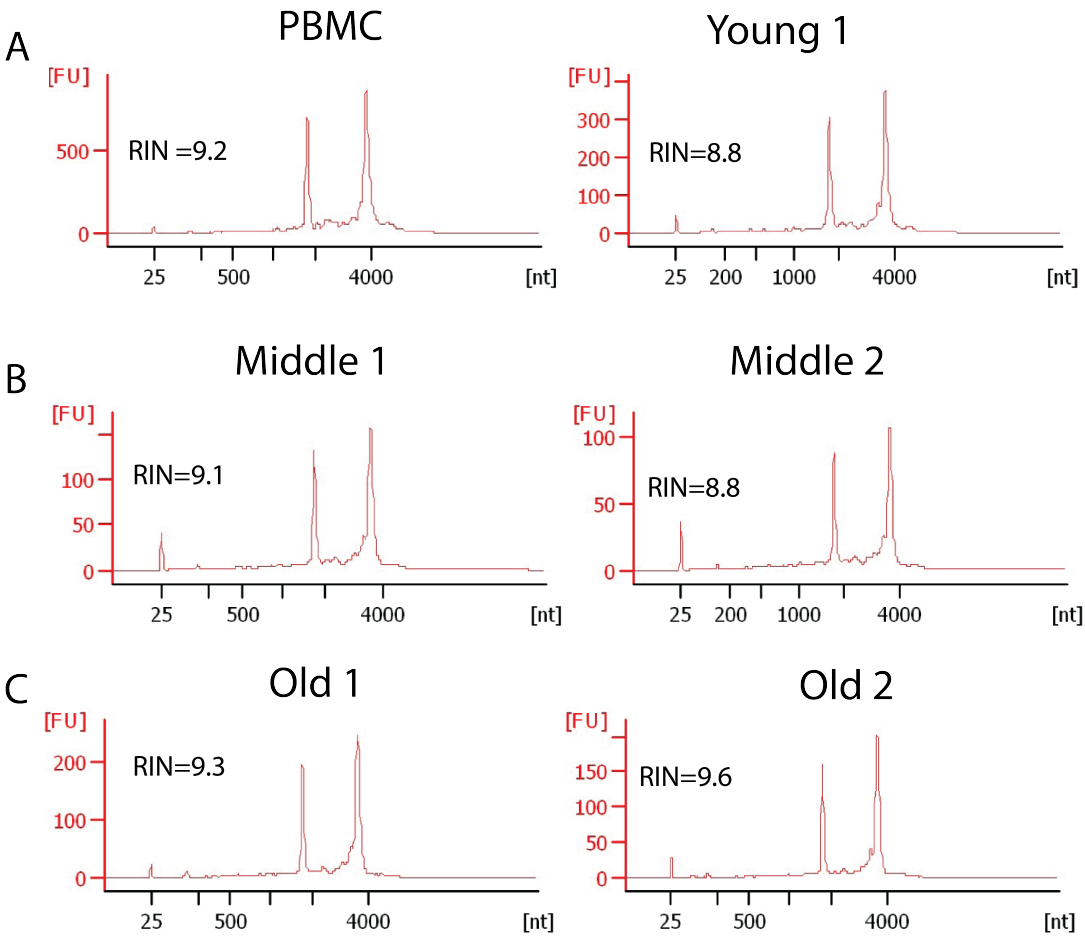

Group	Age (Month)	Sample	Total RNA (ng)	RIN Number
Young	6	Y1	51	8.8
Young	6	Y2	126	N/A
Young	6	Y3	57	8.7
Middle	15	M1	25	9.1
Middle	15	M2	16	8.8
Middle	15	M3	12	9.2
Old	23	O1	27	9.3
Old	23	O2	25	9.6
Old	23	O3	13	9.4

Figure 4.3 Quality of RNA isolated from aged microglia. Examples of RNA profiles measured using an Agilent RNA 6000 Pico Chip.5.2 are given for **A)** PBMC control and microglia obtained from young mice **B)** middle aged and **C)** old aged mice. The RNA integrity number is shown for every sample and is a measure of the overall integrity of the RNA with 1 being very degraded and 10 being fully intact RNA. The table summarises RIN numbers and quantities of RNA obtained for each replicate for RNA sequencing.

4.2 Differential expression analysis and pathway analysis

4.2.1 ANOVA analysis of aged microglia revealed eight distinct subsets of genes with similar behaviours.

After establishing a technique to isolate microglia with sufficient purity and yield and obtaining RNA of high quality, I sent my nine biological samples for RNA sequencing to the company called Oxford Gene Technology (OGT). On receiving the raw data, all subsequent bioinformatics analysis was carried out by a senior postdoctoral assistant in our lab, Dr. Raphael Zollinger. We named the three young samples mGLIA.Y1, mGLIA.Y2 and mGLIA.Y3; three middle aged samples mGLIA.M1, mGLIA.M2 and mGLIA.M3; finally the three old samples mGLIA.O1, mGLIA.O2 and mGLIA.O3. The expression of genes, based on RNA sequencing, is defined by the fragments per kilobase of transcript per million mapped reads also known as the FPKM expression values. We first looked at the expression of a number of genes that were microglia specific or specific to other cells of the brain. This would allow us to determine if our samples truly represented microglia cells. We found that in all three age groups there was a high expression of the microglia specific marker known as purinergic receptor 12 (*P2ry12*) and also of *Itgam* (CD11b, **Fig. 4.4**). We also found that *Padi4*, a gene expressed in macrophages at a higher level than in microglia, was less expressed relative to *Itgam* and *P2ry12*. Finally, we found that markers of other brain cells, such as neurons (*Eno2*), oligodendrocytes (*Mog*) and astrocytes (*Gfap*) were not expressed in any of our samples (**Fig. 4.4**). This indicated that we did not have contaminations from these cells types in our microglia preparations.

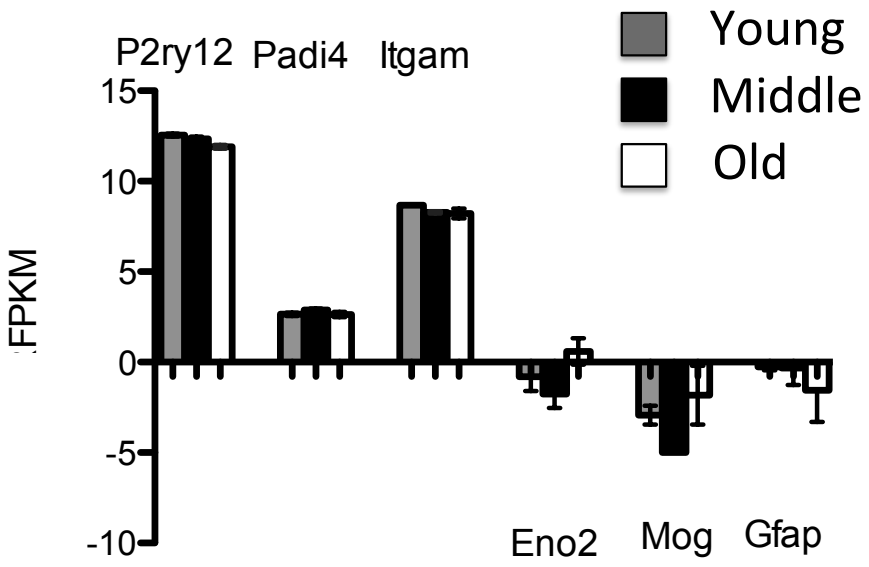

Figure 4.4 The raw FPKM expression values are given for 6 cell-specific genes. Each age group is represented by a bar graph. The genes described are *P2ry12* (microglia specific), *Itgam* (myeloid specific), *Padi4* (macrophage specific), *Eno* (neuron specific), *Mog* (oligodendrocyte specific) and *Gfap* (astrocyte specific).

The RNA sequencing of microglia from young, middle-aged and old mice identified 367 transcripts that were regulated in at least one of the three age groups using the following three criteria: 1) uncorrected 1-way ANOVA p value<0.05, 2) Fold change between highest and lowest expression >2, 3) Group with highest average FPKM value >1.We chose these criteria as they are similar to what has been published in another study on the microglia transcriptome[91]. For example, Ma *et al.* also used an uncorrected 1-way ANOVA and a p value<0.05, but they used a fold change cut off of >1.5[91]. For this analysis we decided to be more stringent, in order to identify important genes with a more robust change in gene expression. We then used hierarchical clustering on these 367 genes, using Spearman correlation and complete linkage to identify groups of genes with similar behaviours among the samples.

We identified eight distinct subgroups of genes within our hierarchical clustering analysis as depicted by the heat-map in **Fig. 4.5**. A heat map is a graphical representation of the FPKM expression values for each of the 367 transcripts, identified to differ in at least one of the three age groups. Expression values are represented by colours with red indicating an upregulation of a gene and green a downregulation of a

gene. Purple lines separate the eight subgroups and the number of transcripts belonging to each group is indicated.

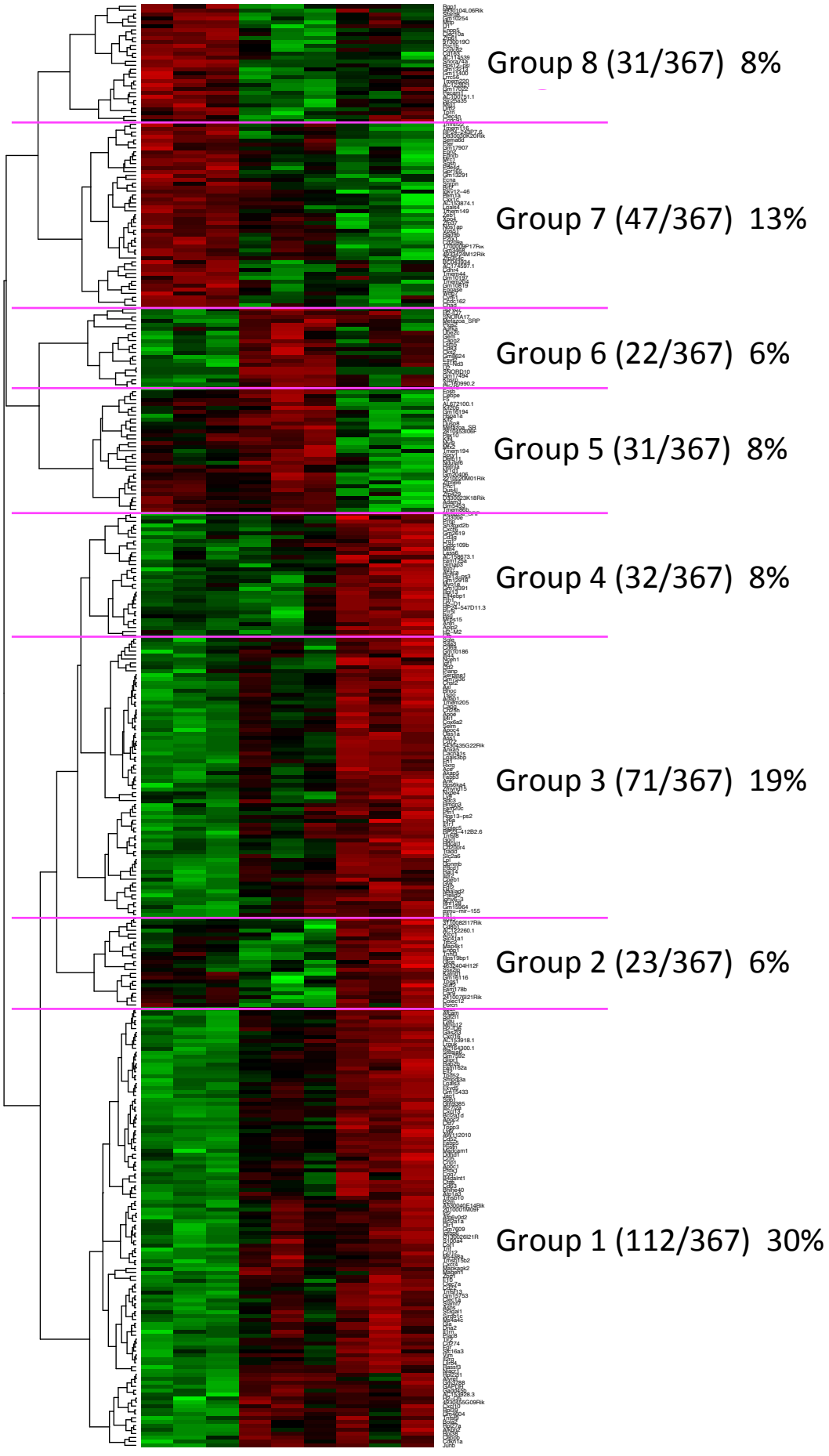
Group 8 (31/367) 8%
Group 7 (47/367) 13%
Group 6 (22/367) 6%
Group 5 (31/367) 8%
Group 4 (32/367) 8%
Group 3 (71/367) 19%
Group 2 (23/367) 6%
Group 1 (112/367) 30%
mGlia.Y1
mGlia.Y2
mGlia.Y3
mGlia.M1
mGlia.M2
mGlia.M3
mGlia.O1
mGlia.O2
mGlia.O3

Figure 4.5 There were eight distinct sets of genes with different behaviours in young, middle-aged and old microglia. Hierarchical clustering heat map of the 367 transcripts differentially expressed in one of the two age group comparisons (fold change >2, uncorrected p values<0.05, groups are young vs. middle aged; young vs. old; middle aged vs. old.) obtained using an uncorrected 1-way ANOVA. Each column represents one replicate from each age group; each row represents a single gene. Red indicates an upregulation of the gene and green indicates a downregulation of the gene.

Changes in each of these eight groups are shown in **Fig. 4.6**. The patterns of change of some of these groups of genes were similar, in some cases. For example for group 1, 3, and 4, genes were increasing in a monotonic pattern from young to middle aged and then from middle aged to old. These three groups alone made up 57% of the total genes (**Fig. 4.6)**. There were also sets of genes that demonstrated a monotonic decrease in expression from young to old as shown in-group 7 (47). There were sets of genes that decreased in expression from young to middle aged but then increased from middle aged to old, this was the case for group 2 (23) and similarly group 8 (31). Another trend of interest was shown in groups 5 and 6, where sets of genes were increased in middle-aged mice compared to both young and old, suggesting that their peak of expression was at middle age. These groups collectively demonstrate that there are significant progressive changes in microglia as the brain ages. It must also be considered that some of these groups are quite similar to one another and may form separately because there may be an outlier. This could be true for example for group 8 and group 7 because the pattern of gene expression for mGLIA.01 and mGLIA.02 appear similar in both these groups but mGLIA.03 has a different expression for both groups and this variability may be why group 7 and 8 appear to group differently.

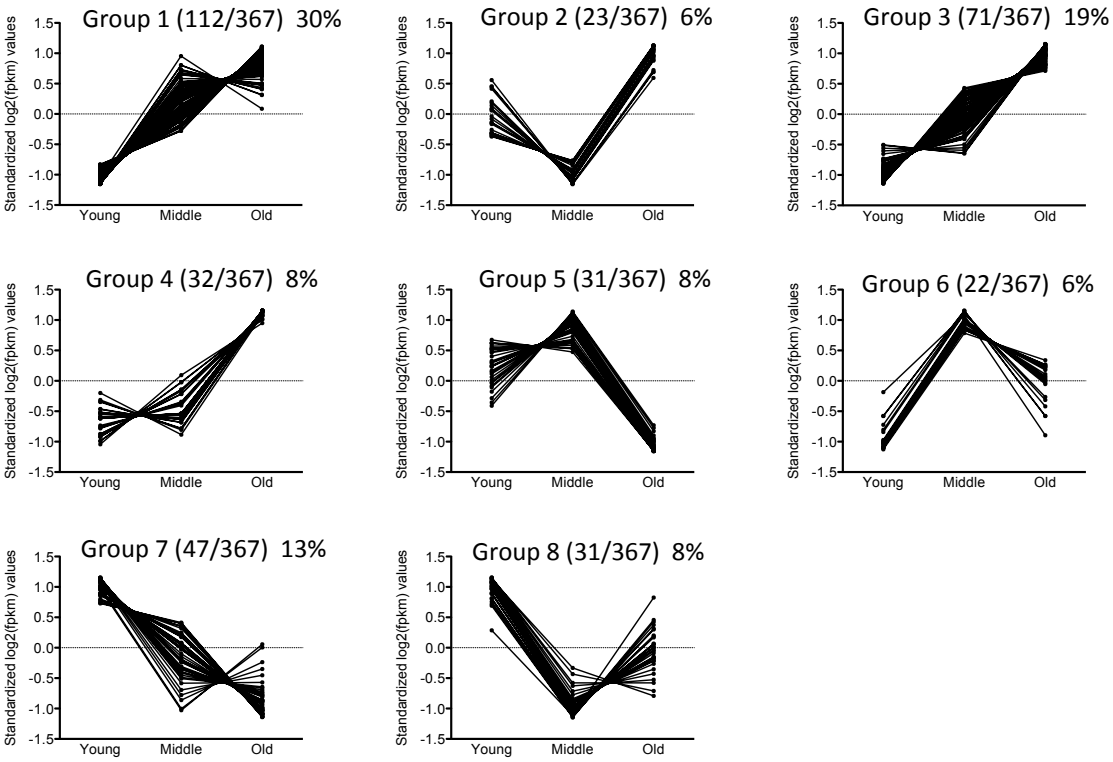

Figure 4.6 There are eight distinct sets of genes with different behaviour in young, middle and old microglia. Visualisation of the profiles by group clustering subgroup, as defined by the hierarchical clustering. Each graph represents a set of genes with a distinct behaviour over the three age groups termed young, middle and old. The number of genes represented in each group is given.

4.2.2 Glycoprotein *Gpnmb* and chemokine *Cxcl13* are among the top genes differentially expressed in aged microglia.

While an ANOVA test is a powerful tool for identifying changes in gene expression among three or more groups, it does not give any information about where the significant change is occurring; is the gene significantly different between young vs. old, young vs. middle aged or middle aged vs. old? Therefore, to gain more specific information about what genes/transcripts were significantly different between specific groups, we carried out three pairwise comparison t-tests and used the same criteria as the 1-way ANOVA previously described i.e. 1) p value <0.05, 2) Fold change between highest and lowest expression > 2, 3) Group with highest average FPKM value >1.The top 50 genes upregulated in old mice vs. young are shown in **Fig. 4.7**. Each gene identified is expressed as a Log2 fold change and the values for both old and middle-

aged groups are shown relative to the young group. This allows an easy visual comparison between the middle-aged and old groups.

Interestingly, and similarly to what was discussed in the previous paragraph, the majority (37 out of 50 genes) were already increased in the middle–aged group to some extent and then increased further in the old group. Among the top differentially expressed genes was the glycoprotein, *Gpnmb*, and the neuroinflammatory chemokine *Cxcl13*. *Gpnmb* was dramatically upregulated in middle-aged microglia by 16-fold and this was further increased to a 32-fold change in old microglia. *Cxcl13* was only moderately upregulated by 2-fold and then dramatically upregulated by another 30-fold in old microglia.

Another gene of interest was *Spp1*, known as secreted phosphoprotein 1 or osteopontin. *Spp1* is a cytokine whose upregulation has been described as characteristic of central nervous system pathologies[166]. This gene has also been shown to be highly induced by macrophages upon inflammatory activation and is associated with the inflammatory response[167]. This gene was also significantly upregulated in both the middle- and old-age groups, with a 32-fold increase in old vs. young microglia.

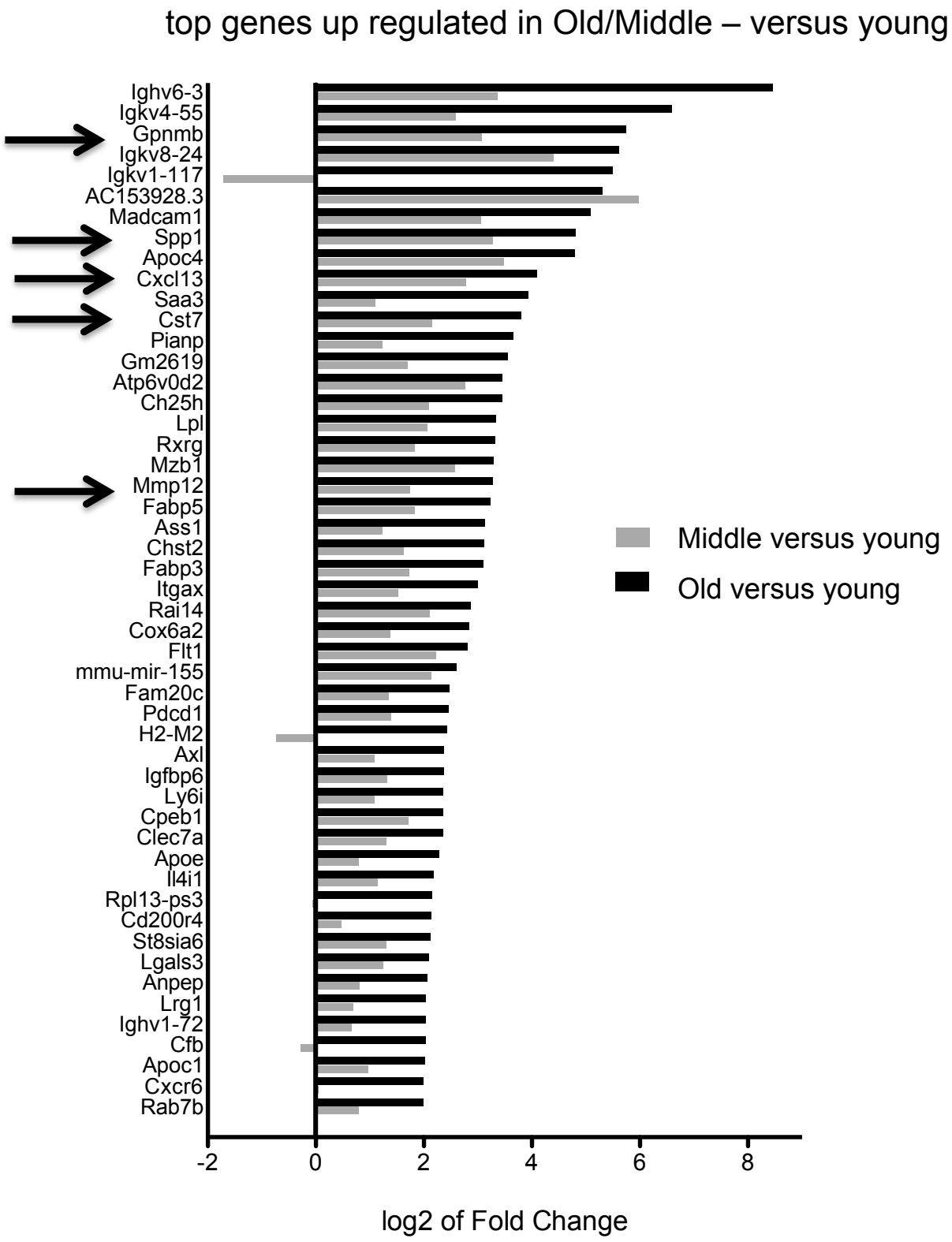

Figure 4.7. Profiles of age-associated gene expression changes in isolated microglia. Top 50 genes that were upregulated in old vs. young microglia (black bar) and middle-aged vs. young microglia (grey bar). Values shown as Log2 fold changes and calculated using pairwise comparison analysis where $p<0.05$ and fold change >2.

This gene was closely followed by cystatin F, *Cst7*, a papain-like lysosomal cysteine protease inhibitor. This is an interesting gene, as its expression in microglia has recently been associated with acute demyelination[168], and is also dramatically upregulated with age (**Fig. 4.7)**. Furthermore, the metallopeptidase 12, known as *Mmp12*, was the most upregulated Mmp with age, 8-fold increase in old vs. young microglia. Mmp12 has recently been associated with the ageing brain and neuroinflammation, with one study showing that Mmp12 is upregulated in microglia with age, consistent with our RNA sequencing study. This study also showed that Mmp12 -/- mice had considerably less inflammation in the brain with age[169].

Using the same criteria, we identified the top 50 genes downregulated in microglia from the young brain vs. the middle-aged and old brain. Similarly to upregulated genes, 35 out of the 50 most downregulated genes are decreased in a monotonic fashion i.e. we observed a steady decrease in gene expression in the middle-aged group and this decrease was even more apparent in the old group. Among the most downregulated genes were the chemokine *Ccl25* and the proteoglycan *Prg2*, as illustrated in **Fig. 4.8**.

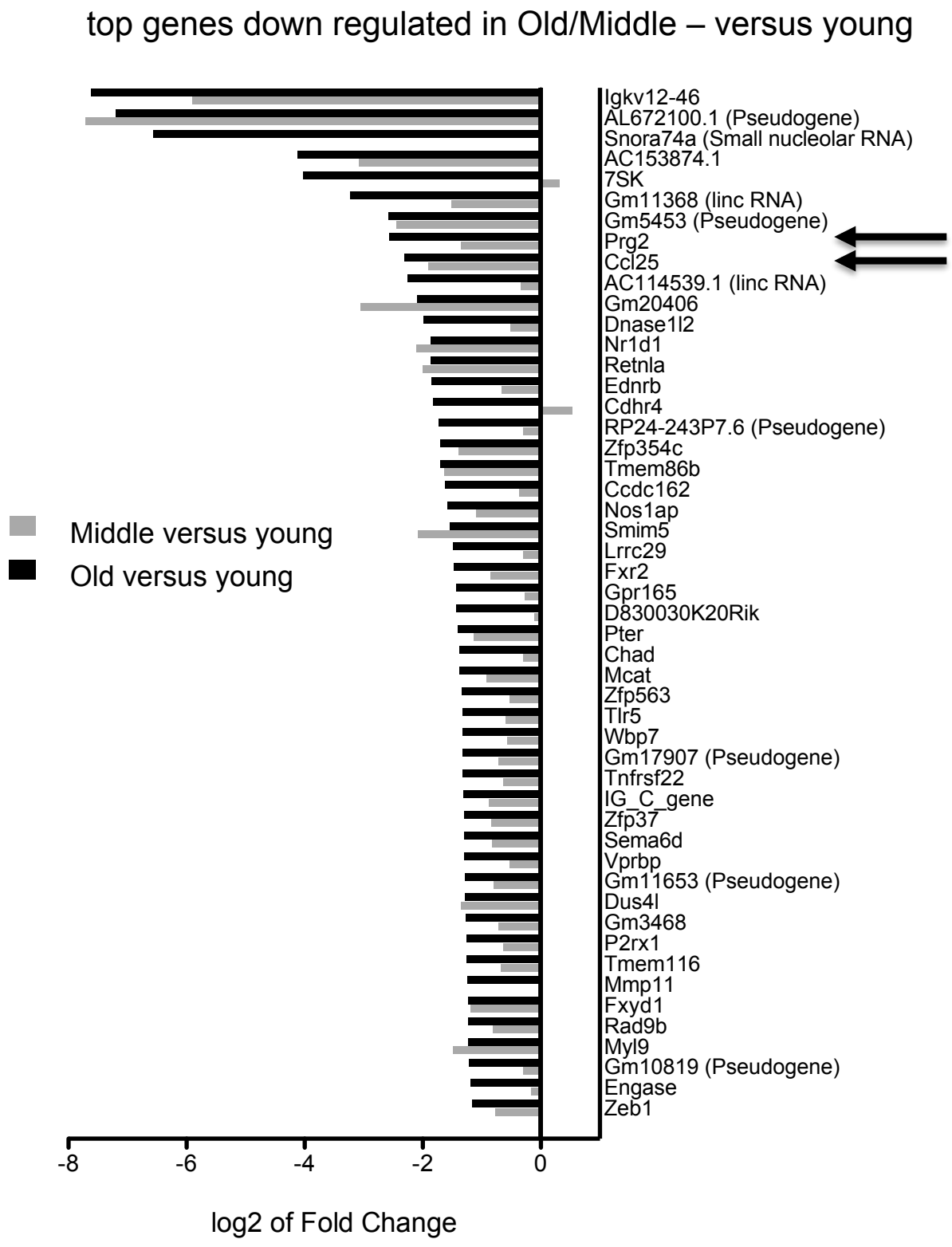

Figure 4.8 Profiles of age-associated gene expression changes in isolated microglia. Top 50 genes that were downregulated in old vs. young (black bar) and middle-aged vs. young microglia (grey bar). Values shown as Log2 fold changes and calculated using pairwise comparison analysis where $p < 0.05$ and fold change >2.

4.2.3 Regulated genes are enriched in age-related pathways

We identified 367 genes that were differentially expressed in at least one of the two age group comparisons using >2 fold change at p value<0.05 and uncorrected 1-way ANOVA, as described in **Fig. 4.6**. Using this data set, we performed gene ontology analysis, which is based on the classification of genes by their functional characteristics. Using this bioinformatics tool we identified several pathways that were deregulated with age. The top five pathways and the genes involved are shown in **Tab. 4.2**. They included the immune response, defence response, response to wounding, inflammatory response and cell adhesion. The p value for each pathway is given, as well as the percentage of genes that are represented by each pathway. For example, the immune response had a very significant p value of 2.123 E09 and includes 9.1% of all genes differentially expressed, suggesting that this pathway is significantly deregulated with age in microglia.

Term	Pvalue	% of genes	Genes
Immune response	2.123E-09	9.1	IL1R1, TNF, ENPP1, H2-D1, TLR2, TNFSF13, CCL5, PRDX1, FTH1, B2M, CXCL10, GM15753, H2-Q5, CD8B1, OLR1, H2-M2, CFB, IL1RN, CD300E, COLEC12, H2-Q6, TNFSF9, H2-Q7, CLEC4N, TNFSF8, CCL12, CXCL13, LILRB4, OAS1A, CLEC7A
Defense response	3.173E-06	7.2	IL1R1, TNF, OLR1, CEBPE, FGR, CFB, H2-D1, TLR2, CHST2, SAA3, CCL5, H2-Q6, PRDX1, H2-Q7, CD163, B2M, CXCL10, CCL12, P2RX1, CXCL13, GM15753, DEFB11, CLEC7A, FN1
Response to wounding	4.501E-05	5.7	TNF, F10, OLR1, CFB, TLR2, CHST2, SAA3, ANXA5, CCL5, CD163, CXCL10, CCL12, F5, P2RX1, CXCL13, PECAM1, CLEC7A, FN1
Inflammatory response	7.009E-05	4.4	TNF, OLR1, CFB, CHST2, SAA3, TLR2, CCL5, CD163, CXCL10, CCL12, P2RX1, CXCL13, CLEC7A, FN1
Cell adhesion	0.0001016	7.2	OLR1, CDHR4, GM13213, POSTN, LY9, ALCAM, LGALS3BP, F5, ITGAX, SIGLEC5, ITGA5, ITGB7, PECAM1, CD2, CD22, MADCAM1, CLEC7A, SSX2IP, GPNMB, MLLT4, CYR61, SPP1, FN1

Table 4.2 Pathways that are enriched in microglia from old vs. young mice. Gene ontology enrichment analysis (GSEA) of 367 genes that were differentially expressed in one of the two age group comparisons (fold change >2, p value<0.05, calculated by 1-way ANOVA).

We wanted to specifically look at the affected pathways between young and old microglia, rather than among the three groups. To this end, we decided to use a pairwise comparison t-test between the young and old groups. For this analysis, we lowered the fold change threshold to >1.5 with a p<0.05. We reasoned that a lower fold change could identify pathways in which many genes are subtly changed, which functionally might be more important than a few genes being highly differentially expressed. The analysis with the fold change >1.5 identified 888 differentially expressed genes. Ingenuity pathway analysis (IPA) was carried out on this dataset, in order to identify

pathways and biological functions differentially regulated between young and old microglia. The top 15 enriched pathways are shown in **Tab. 4.3**, with individual genes annotated. Interestingly, the top three pathways 1) EIf2 signalling 2) mTOR signalling and 3) regulation of eIf4 and p70S6K signalling are all related to the serine/threonine kinase mTOR, a key modulator of ageing and age-related disease[30]. The genes differentially expressed in these three pathways are mainly the ribosomal proteins that make up the ribosomal subunits. All of these genes were slightly upregulated in old vs. young microglia with an average fold change between 1.5-2.5. These subtle, yet consistent, changes in gene expression of genes relating to mTOR signalling may indicate that this pathway is more active in microglia with age.

Ingenuity Canonical Pathways	-log(p-value)	Genes
EIF2 Signaling	3.03E+01	RPL11,RPL22,RPL27A,RPS23,RPS7,EIF2AK1,PABPC1,RPL36A/RPL36A-HNRNPH2,RPL37,RPL23A,RPL10A,RPS4X,RPL39,RPS15,RPS25,RPL41,RPLP1,RPS27A,RPL24,RPS18,PIK3R5,RPL22L1,RPS8,RPS13,RPL14,RPS21,RPL35A,RPL6,RPL35,RPLP2,RPS5,RPL31,RPL29,RPL13,RPS24,RPL37A,EIF3H,RPS2,RPL17,RPL30,RPS19,RPL21,RPL23,RPS27L,RPL9,RPS12,RPS16,RPS26,UBA52,RPL32,RPL38
mTOR Signaling	9.54E+00	RPS18,PIK3R5,RPS13,RPS8,RPS21,HIF1A,PRR5L,RPS23,EIF4EBP1,RPS7,RPTOR,RPS5,PRKCA,RPS24,PLD3,EIF3H,RHOC,RPS2,RPS19,RPS27L,RPS12,RPS4X,RPS16,RPS26,RPS15,RPS6KA4,RPS25,RPS27A
Regulation of eIF4 and p70S6K Signaling	9.17E+00	PABPC1,EIF3H,RPS2,RPS18,PIK3R5,RPS19,ITGA5,RPS8,RPS13,RPS21,RPS27L,RPS23,RPS12,EIF4EBP1,RPS7,RPS4X,RPS16,RPS26,RPS15,RPS25,RPS5,ITGA4,RPS27A,RPS24
Agranulocyte Adhesion and Diapedesis	7.85E+00	FN1,CCL5,ITGB7,CXCL10,CXCL13,CCL2,CCL25,MMP11,MMP12,Ccl6,ITGA4,CXCR4,PF4,ITGA5,IL1R1,MADCAM1,MYL9,CXCL16,CCL4,IL1RN,PECAM1,CCL3L1/CCL3L3,IL1B,CD34,TNF
Granulocyte Adhesion and Diapedesis	7.73E+00	HRH2,CXCR4,PF4,ITGA5,CCL5,IL1R1,SDC3,ITGAL,ITGB3,CXCL10,CXCL16,CCL4,CCL2,CXCL13,IL1RN,CCL25,PECAM1,CCL3L1/CCL3L3,IL1B,MMP11,MMP12,TNF,Ccl6,ITGA4
Communication between Innate and Adaptive Immune Cells	6.06E+00	B2M,HLA-B,CD83,CCL5,CD8B,TNFRSF17,CXCL10,TLR2,CCL4,TLR5,IL1RN,TNFSF13,CCL3L1/CCL3L3,IL1B,TNF
Antioxidant Action of Vitamin C	5.00E+00	SLC2A5,PLCB2,PLD3,SLC2A1,PLCG1,PLCL2,GSTO1,IKBKG,NFKBIA,PLA2G2D,PLA2G4B,TXN,CHUK,TNF
Role of Pattern Recognition Receptors in Recognition of Bacteria and Viruses	4.38E+00	OAS1,C3,PIK3R5,C1QC,C1QA,CCL5,TLR2,CLEC7A,IRF7,TLR5,IL1B,TNF,PRKCA
Altered T Cell and B Cell Signaling in Rheumatoid Arthritis	4.22E+00	TLR2,SPP1,TLR5,CXCL13,CSF1,IL1RN,TNFSF13,IL1B,CHUK,TNF,FAS,TNFRSF17
Atherosclerosis Signaling	3.87E+00	APOE,CXCR4,APOC4,APOC2,APOC1,PLA2G2D,CCL2,CSF1,IL1RN,LPL,PLA2G4B,IL1B,TNF,ITGA4
Differential Regulation of Cytokine Production in Macrophages and T Helper Cells by IL-17A and IL-17F	3.45E+00	CCL4,CCL2,IL1B,CCL5,TNF
TREM1 Signaling	3.45E+00	TLR2,CCL2,TLR5,TYROBP,PLCG1,ITGA5,IL1B,CD83,TNF,ITGAX
Virus Entry via Endocytic Pathways	3.44E+00	B2M,HLA-B,PIK3R5,PLCG1,ITGA5,ITGAL,ITGB7,AP2S1,ITGA4,PRKCA,ITGB3
TNFR2 Signaling	3.38E+00	TANK,IKBKG,NFKBIA,TNFAIP3,CHUK,TNF

Table 4.3 Pathways that are enriched in microglia from old vs. young mice. Ingenuity pathway analysis showing pathways differentially regulated between young and old microglia, using 888 genes identified by pairwise comparison.

Finally using this list of 888 genes we looked at the potential upstream regulators using the Ingenuity software. This database gives an indication of the stimuli that may be responsible for regulating subsets of genes among the 888 differentially expressed. The

top regulators are shown in **Tab. 4.4**, together with their function**.** Interestingly, many of the upstream regulators relate to the inflammatory response including cytokines such as Tnf and the bacterial cell wall component LPS.

Molecule Type	Predicted Activation State	p-value
transcription regulator	Activated	7.06E-26
chemical drug	Activated	7.98E-25
chemical drug	Inhibited	7.49E-24
transcription regulator	Activated	2.41E-22
chemical - endogenous mammalian	Activated	1.37E-21
cytokine	Activated	2.09E-21
cytokine		4.03E-21
chemical drug	Inhibited	2.15E-20
cytokine	Activated	2.21E-20
cytokine	Activated	3.07E-19
enzyme	Activated	4.30E-19
chemical toxicant	Activated	8.06E-18
cytokine	Activated	3.56E-16
transmembrane receptor	Activated	1.26E-15
chemical reagent	Activated	1.37E-15
growth factor	Activated	3.04E-15
chemical - endogenous mammalian		3.87E-15

Table 4.4 Pathways enriched in microglia from old vs. young mice. Ingenuity pathway analysis showing potential regulators upstream of genes that were differentially expressed in old compared to young microglia calculated by pairwise comparison.

4.2.4 Transcription factors relating to differentially expressed genes appear to be mTOR related

Given that the top upregulated pathways in old microglia were related to the mTOR pathway, we interrogated our dataset to assess if the differentially expressed genes were under the control of mTOR-related transcription factors. A number of transcription factors are known targets of mTOR, either directly or indirectly. As a result, we used the EnrichR database to determine what transcription factors were associated with the gene changes observed with ageing. The top hits are shown in **Tab 4.5**.

Transcription factor	P-value	Adjusted P-value
TFAP2A	1.43126E-09	2.21129E-07
PPARG	1.12045E-09	2.21129E-07
NR5A2	2.68755E-08	2.76818E-06
NFKB1	5.62201E-08	4.343E-06
YY1	4.36321E-07	1.82142E-05
NRF1	4.71566E-07	1.82142E-05
PITX2	2.60186E-07	1.60795E-05
E2F1	4.47016E-07	1.82142E-05
SREBF1	1.49749E-06	4.20657E-05

Table 4.5 Transcription factors that are enriched in microglia from old vs. young mice based on the differentially expressed genes. EnrichR analysis showing the transcription factors that are potentially deregulated based on the 888 genes identified by pairwise comparison.

The top transcription factors that appeared to be responsible for the 888 genes that were differentially expressed between young and old microglia identified by ErichR analysis were *Tfap2a*, *Pparg*, *Nr5a2* and *Nfkb1*. *Pparg* (peroxisome proliferator-activated receptor gamma) and *Nfkb1* (nuclear factor of kappa light polypeptide gene enhancer in B cells 1) are both targets of the mTOR pathway[98,170]. This could indicate that mTOR activation in microglia from the ageing brain may be responsible for some of the transcriptome changes we observe through activation/inhibition of various transcription factors.

4.3 Microglia function

4.3.1 Age – related changes in key inflammatory genes

In order to assess whether immune functions changed in microglia with ageing, we designed specific gene lists based on reviews/reports from the literature. More general gene lists such as phagocytosis or antigen presentation were obtained from the pathway focused, PCR array profiler lists generated by Qiagen. We first looked at the key mediators of inflammation including cytokines, chemokines and their receptors.

We made four gene lists and used the software R, which is a programming language used for statistical and graphical analysis, to generate graphs showing changes in gene expression in microglia from the aged brain relative to microglia from the young brain.

Using this programme, we were able to generate graphs that indicated when a gene reached the significance threshold (p value<0.05) by an asterisk. Fold changes were represented as Log2 fold changes and a grey line represented where a gene had a reached a fold change of 2.

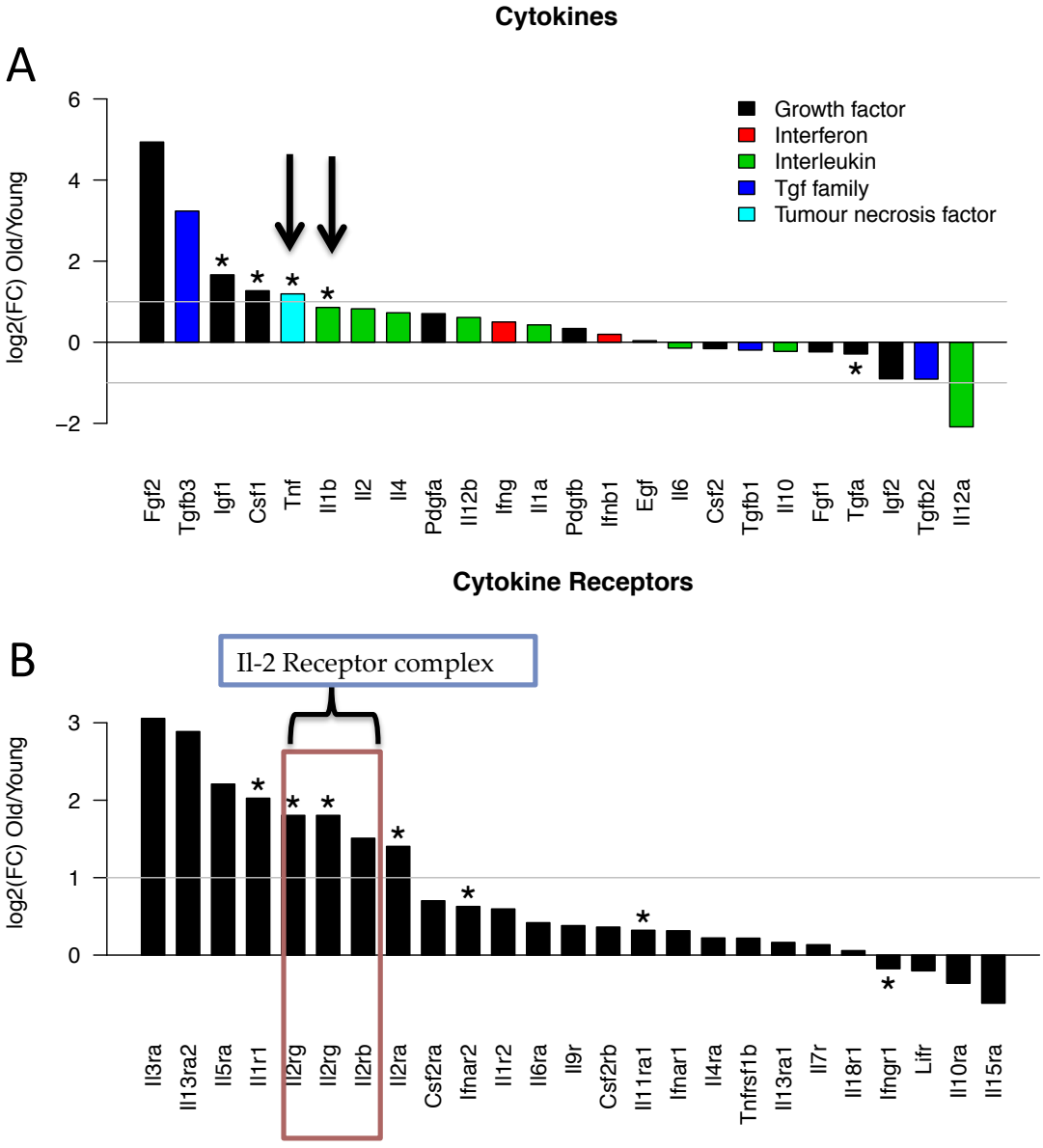

Figure 4.9 Cytokines related to inflammation differentially expressed in old vs. young microglia. **A**) Cytokines; **B)** Cytokine receptors; grey line represents genes over a fold change of 2 (log of fold change >1 or <-1) and * represent genes with t-test p value <0.05.

We examined a variety of cytokines, including members of the interferon, interleukin, tumour growth factor and tumour necrosis factor families. We found that several genes

relating to inflammation were significantly upregulated in old vs. young microglia and included the pro-inflammatory cytokines *Tnf*, *Il-1b* and *Csf1* (**Fig. 4.9A)**. *Il-2* cytokine was also significantly up regulated but was just below a 2-fold change (**Fig. 4.9A)**. Lastly, the insulin like growth factor 1 (*Ilgf1*) was significantly upregulated. *Igf1* is of interest as its production by microglia has recently been suggested to be neuroprotective[171]. It is worth noting that the Il-1β receptor, *Il1r* was also significantly upregulated (**Fig. 4.9B)**. Other cytokine receptors upregulated with age included Il-2 receptor alpha (*Il2ra*), beta (*Il2rb*) and gamma chain (*Il2rg*). Together these genes constitute the high-affinity Il-2 receptor. Both *Il2ra* and *Il2rg* were significantly increased, while *Il2rb* did not reach significance. Nevertheless, all three genes were increased by more than 2-fold (**Fig. 4.9B)**.

Chemokines play a pivotal role in inflammation by directing the movement of leukocytes to sites of injury[172]. In the brain, chemokines and their receptors also play an important role in cell-cell communication, particularly between neurons and microglia[173]. Here we looked at the two main groups of chemokines, the CC and CXC families. We found that many of them were differentially expressed with age, mostly upregulated. Three members of the CX family of chemokines were particularly over expressed in old compared to young microglia: *Cxl13* (16-fold), *Cxcl14* and *Cxcl16* (4-fold, **Fig. 4.10A)**. Other chemokines that were statistically different included many CC chemokines, such as *Ccl12*, *Ccl5*, *Ccl3* and *Ccl4* (**Fig. 4.10A)**. Interestingly, *Cxcl16* is the chemokine ligand for *Cxcr6*, which was also up regulated in old microglia by approximately 4-fold (**Fig. 4.10A).** This is a particularly interesting observation, as a recent study showed that Cxcl16 could drive neuron-microglia crosstalk to promote neuroprotective mechanisms, similarly to Cx3cr1[174].

Ccl25 was the only significantly downregulated chemokine in old vs. young microglia by almost 4-fold (**Fig. 4.10A)**. Its receptor, *Ccr9*, was also the only chemokine receptor that was significantly downregulated by a 2-fold change (**Fig. 4.10B)**. Interestingly, the chemokine *Cx3cr1,* which has been reported to be downregulated with age[96], also appeared to be downregulated in our study, however, not significantly (**Fig. 4.10B)**.

Overall, old microglia showed an upregulation of different inflammatory mediators, which may indicate they are more inflammatory than young counterparts.

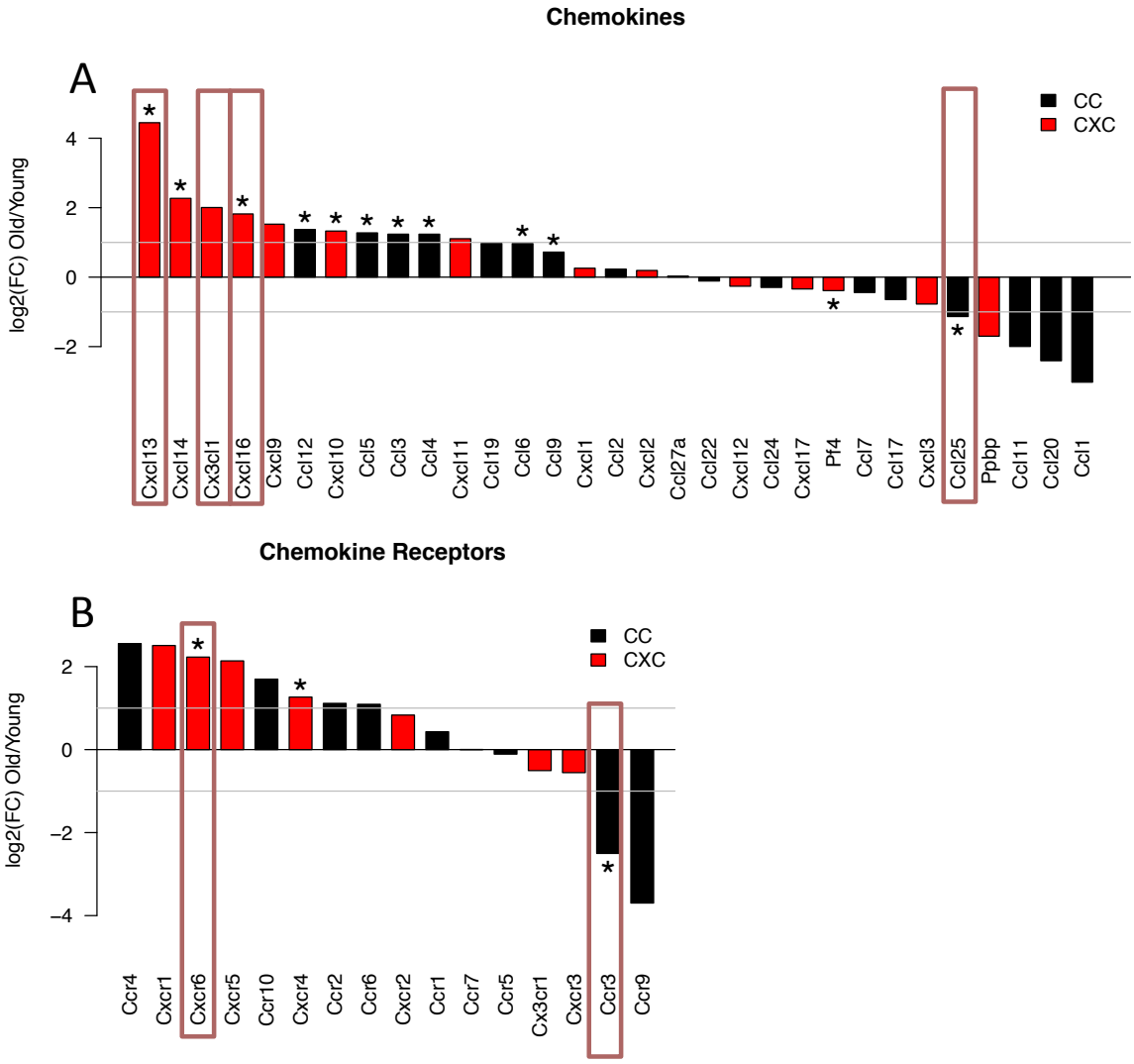

Figure 4.10 Chemokines related to inflammation that were differentially expressed in old vs. young microglia. **A**) Chemokines; **B**) Chemokines receptors, grey line represents genes over a fold change of 2 (log of fold change >1 or <-1) and * represent genes with t-test p value <0.05.

4.3.2 Age-related changes in key genes involved in phagocytosis and antigen presentation

The processes of phagocytosis and antigen presentation are both important functions carried out by innate immune cells.

Macrophage phagocytosis is essential for the uptake and the degradation of dead cells and microbes. Phagocytosis can play an important role in regulating the immune response, often resulting in the activation of the adaptive response. In order to understand if this process was more or less activated in microglia with age, we designed a list of genes known to be involved in phagocytosis. Genes included in this list could broadly be divided into; a) receptors involved in phagocytosis, b) genes involved in recognition and engulfment and c) genes involved in signal transduction. We used the R programme to interrogate our dataset and found a number of genes relating to phagocytosis to be differentially expressed in microglia from the aged brain. Among these genes were receptors associated with phagocytosis, for example, the pattern recognition receptor *Clec7a* that recognises a variety of β-1,3-linked and β-1,6 linked glucans[175] (**Fig. 4.11)**. This gene was four times more expressed in microglia from old mice than from young ones. Another receptor that was differentially expressed was the death receptor *Fas*. Additional genes involved in antigen recognition and phagocytosis were differentially expressed. These included the glycoprotein *CD44* and *Sirpb1a*, a gene shown to positively regulate phagocytosis in macrophages[176], which was upregulated, albeit not significantly (**Fig. 4.11)**.

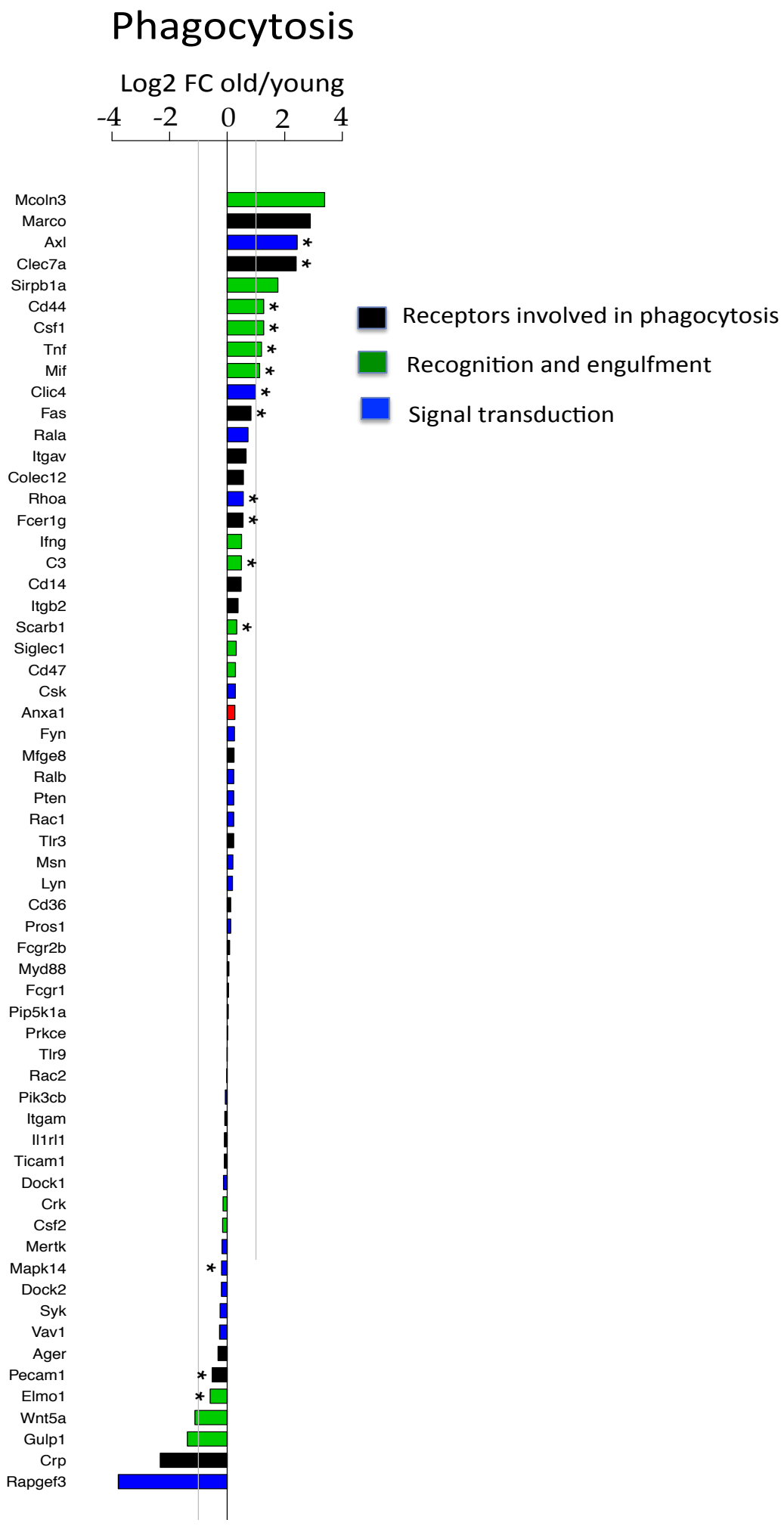
Phagocytosis
Log2 FC old/young
-4
-2
0
2
4
Mcoln3
Marco
Axl
Clec7a
Sirpb1a
Cd44
Csf1
Tnf
Mif
Clic4
Fas
Rala
Itgav
Colec12
Rhoa
Fcer1g
Ifng
C3
Cd14
Itgb2
Scarb1
Siglec1
Cd47
Csk
Anxa1
Fyn
Mfge8
Ralb
Pten
Rac1
Tlr3
Msn
Lyn
Cd36
Pros1
Fcgr2b
Myd88
Fcgr1
Pip5k1a
Prkce
Tlr9
Rac2
Pik3cb
Itgam
Il1rl1
Ticam1
Dock1
Crk
Csf2
Mertk
Mapk14
Dock2
Syk
Vav1
Ager
Pecam1
Elmo1
Wnt5a
Gulp1
Crp
Rapgef3
Receptors involved in phagocytosis
Recognition and engulfment
Signal transduction

Figure 4.11 Genes related to phagocytosis that were differentially expressed in old vs. young microglia identified by pairwise comparison t-test. Grey line represents genes over a fold change of 2 and * represent genes that were statistically significant and have a p value <0.05.

Microglia and macrophages are also antigen-presenting cells (APCs), together with dendritic cells. APCs capture antigens, process them and then present them on MHC molecules in order to prime T cells. Similarly to phagocytosis, understanding if microglia upregulate antigen presentation may be an indication of the activation state of the cells with age. We therefore designed a gene list for antigen presentation that included genes relating to a) antigen uptake; b), antigen presentation; c) cell differentiation and d) chemotaxis. Compared to the phagocytic genes, fewer genes were differentially expressed (**Fig. 4.12**). Most of the significantly upregulated genes were chemokines or chemokine receptors that are involved in chemotaxis associated with antigen presentation such as *Ccl5*, *Ccr2*, *Ccl19* and *Ccr1*. Most genes associated with antigen presentation, specifically the co-stimulatory molecules *Cd80*, *Cd86*, *Cd40* and *Cd209a*, were either unchanged or downregulated. The only genes significantly upregulated were *Cd8a*, and *Tapbp*, a transmembrane glycoprotein (**Fig. 4.12**).

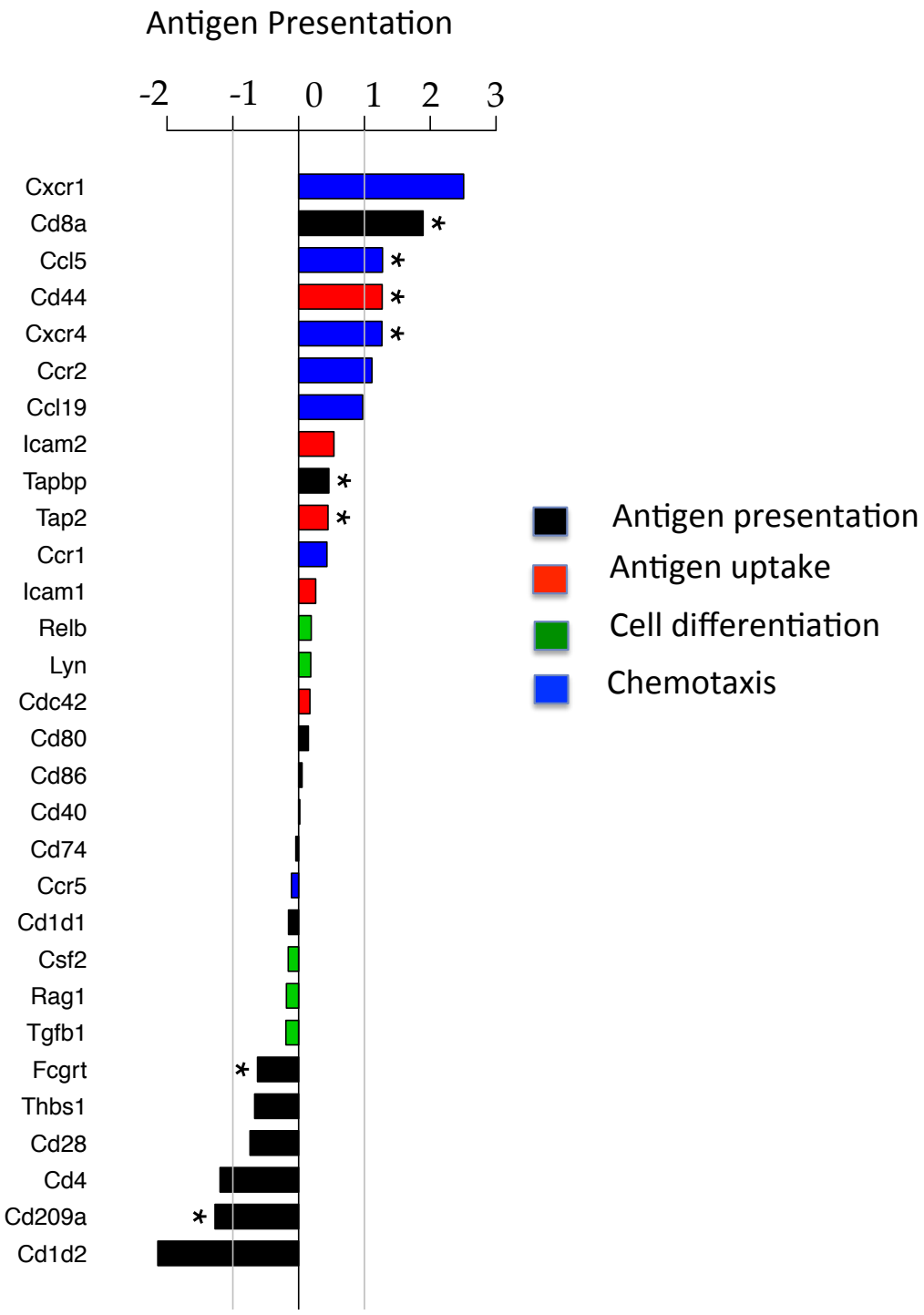

Figure 4.12 Genes related to antigen presentation that were differentially expressed in old vs. young microglia identified by pairwise comparison t-test. Grey line represents genes over a fold change of 2 and * represent genes that were statistically significant and have a p value <0.05.

4.4 Microglia and environmental sensing

4.4.1 Age-related changes in receptor genes involved in sensing the neural environment

In 2013 Hickman *et al.* showed that microglia have a unique transcriptome compared to tissue macrophages that included the expression of genes relating to sensing the neural environment. They also showed that with age, microglia appear to downregulate transcripts relating to the sensing of endogenous ligands and upregulate transcripts relating to host defence[96]. In order to understand if our data indicate similar changes in the sensome genes, we assessed levels of expression of a number of receptors used by microglia to sense changes in their environment. These include purinergic receptors, adenosine receptors, neurotransmitter receptors, innate immune receptors, neuromodulator receptors and pattern recognition receptors.

We compiled gene lists for each of these categories to generate graphs containing information regarding fold change and significance, similarly to those relating to antigen presentation and phagocytosis. In order to obtain a comprehensive picture of all the different changes taking place in microglia from aged mice, we combined the gene lists for innate immune receptors, pattern recognition receptors, purinergic and adenosine receptors, neurotransmitter receptors and neurohormone receptors in a heat-map (**Fig. 4.13A**). Genes which expression was either significantly different or above a 2-fold change were used to generate a categorised heat map**.** This heat map indicated that there are many receptors in the ageing brain that were differentially expressed from all categories. The two most striking observations that can be deducted from the heat-map were that many neurotransmitter receptors, particularly the gabaergic receptors, were downregulated in old and middle aged, compared to young, and secondly that many innate immune receptors, which will be showed in more detail below, were upregulated in middle-aged mice and to a greater extent in old mice (**Fig. 4.13A**).

The pattern recognition receptors included a broad list of innate immune receptors that included intracellular Tlrs, extracellular Tlrs, Nucleotide-binding oligomerization domain receptors (Nod receptors), Nod-like receptors (Nlr), Nlr-related apoptosis inhibitory protein receptors (Naip). All these receptors are involved in the recognition of pathogen associated molecular patterns (PAMPs), expressed by invading pathogens[177]and danger associated molecular patterns (DAMPs). Results are shown in **Fig. 4.13B**. The only gene significantly upregulated with age was *Tlr2*, an important receptor in microglia function that will be discussed in the next section. Interestingly, the only receptor significantly downregulated was *Tlr5*, the receptor for flagellin.

The innate immune receptors included a) Fc receptors which bind immunoglobulins and are important for regulating immune responses[178] b) interferon-induced transmembrane proteins, i.e. IFITMs, which are involved in inhibition of pathogenic viruses[179] and c) sialic acid binding Ig-like lectins (Siglecs), which bind sialic acid and play an important role in cell-cell interactions[180]. The genes that were differentially expressed from this list are shown in **Fig. 4.13C**. The most striking observation is that many of the *Ifitm* genes are upregulated in microglia with age and that many of the *Siglec* genes were downregulated. These two observations are similar to the findings of Hickman *et al.* which may confirm their view that microglia with age, upregulate receptors that are important for sensing pathogens[96].

A

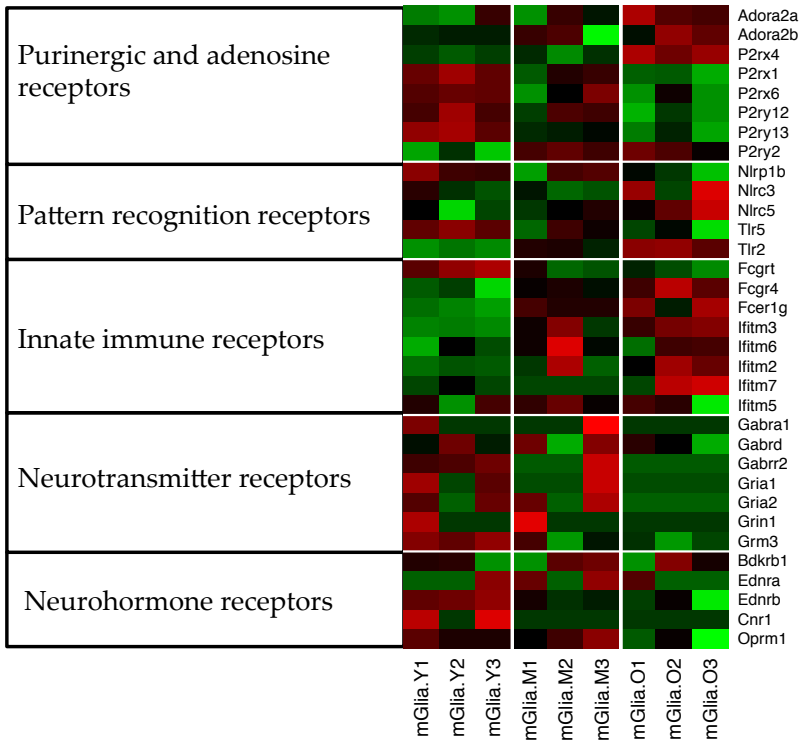
Purinergic and adenosine receptors
Pattern recognition receptors
Innate immune receptors
Neurotransmitter receptors
Neurohormone receptors
Adora2a
Adora2b
P2rx4
P2rx1
P2rx6
P2ry12
P2ry13
P2ry2
Nlrp1b
Nlrc3
Nlrc5
Tlr5
Tlr2
Fcgrt
Fcgr4
Fcer1g
Ifitm3
Ifitm6
Ifitm2
Ifitm7
Ifitm5
Gabra1
Gabrd
Gabrr2
Gria1
Gria2
Grin1
Grm3
Bdkrb1
Ednra
Ednrb
Cnr1
Oprm1
mGlia.Y1
mGlia.Y2
mGlia.Y3
mGlia.M1
mGlia.M2
mGlia.M3
mGlia.O1
mGlia.O2
mGlia.O3

B

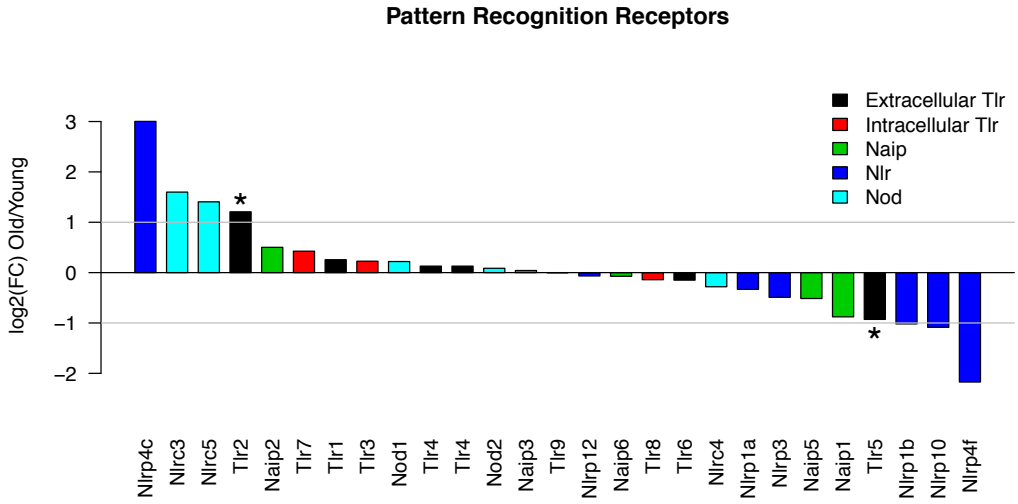
Pattern Recognition Receptors
log2(FC) Old/Young
Extracellular Tlr
Intracellular Tlr
Naip
Nlr
Nod
Nlrp4c
Nlrc3
Nlrc5
Tlr2
Naip2
Tlr7
Tlr1
Tlr3
Nod1
Tlr4
Tlr4
Nod2
Naip3
Tlr9
Nlrp12
Naip6
Tlr8
Tlr6
Nlrc4
Nlrp1a
Nlrp3
Naip5
Naip1
Tlr5
Nlrp1b
Nlrp10
Nlrp4f

C

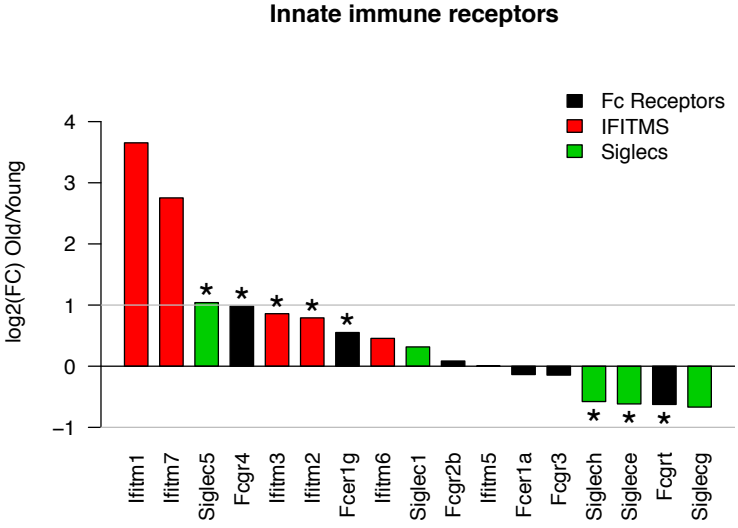
Innate immune receptors
log2(FC) Old/Young
Fc Receptors
IFITMS
Siglecs
Ifitm1
Ifitm7
Siglec5
Fcgr4
Ifitm3
Ifitm2
Fcer1g
Ifitm6
Siglec1
Fcgr2b
Ifitm5
Fcer1a
Fcgr3
Siglech
Siglece
Fcgrt
Siglecg

Figure 4.13 Genes involved in sensing changes in the neural environment that were differentially expressed in old vs. young microglia identified by pairwise comparison t-test. **A**) Categorised heat map of pattern recognition receptors, innate immune receptors, purinergic receptors, adenosine receptors, neurotransmitter receptors and neurohormone receptors. Each column represents one replicate from each age group; each row represents a single gene. Red indicates upregulated genes and green downregulated ones. **B**) Pattern recognition receptors; including intracellular and extracellular *Tlrs, Nod, Nlr* and *Naip* receptors; **C**) Innate immune receptors including *Fc* receptors, *Ifitms* and *Siglec*s; grey line represents genes over a fold change of 2 and * represent genes that were statistically significant ($p<0.05$).

4.4.2 *Tlr2* and *Tlr2*-pathway genes are differentially expressed in aged microglia

The upregulation of *Tlr2* in aged microglia seemed to us particularly interesting, since this toll-like receptor has been implicated in neurodegenerative disorders such as Alzheimer's disease and Parkinson's disease[181].

To investigate this pathway further, we generated a list for *Tlr2*-related genes, based on a study in *Nature Communications*, which investigated the role of neuron-released α-synuclein as an agonist of Tlr2[182]. We compared genes from our dataset to genes described by the authors in a hypothetical network of microglia activated by α-synuclein. We found that many of the genes they predicted as being affected by a Tlr2 agonist were also differentially expressed in microglia from the aged brain. These genes fell into several categories regulated by Tlr pathways including: cell migration and motility, inflammation, Jak-Stat signalling and genes relating to integrin signalling. We found that the integrin *Itgax*, encoding CD11c, was the most upregulated gene, which was 8-times more expressed in microglia isolated from the aged brain (**Fig. 4.14A**). Two additional integrins were also upregulated; *Itga5* and *Itga1*, and no members of this family appeared to be downregulated with age. Several signalling molecules implicated in Tlr2 signalling were differentially expressed, as were other genes relating to inflammation (**Fig. 4.14A**). The gene for *Tlr2* itself was significantly upregulated by at least 2-fold in old vs. young microglia and interestingly *Clec7a*, a receptor that cooperates with *Tlr2* in macrophage phagocytosis[175], was also significantly upregulated by 4-fold.

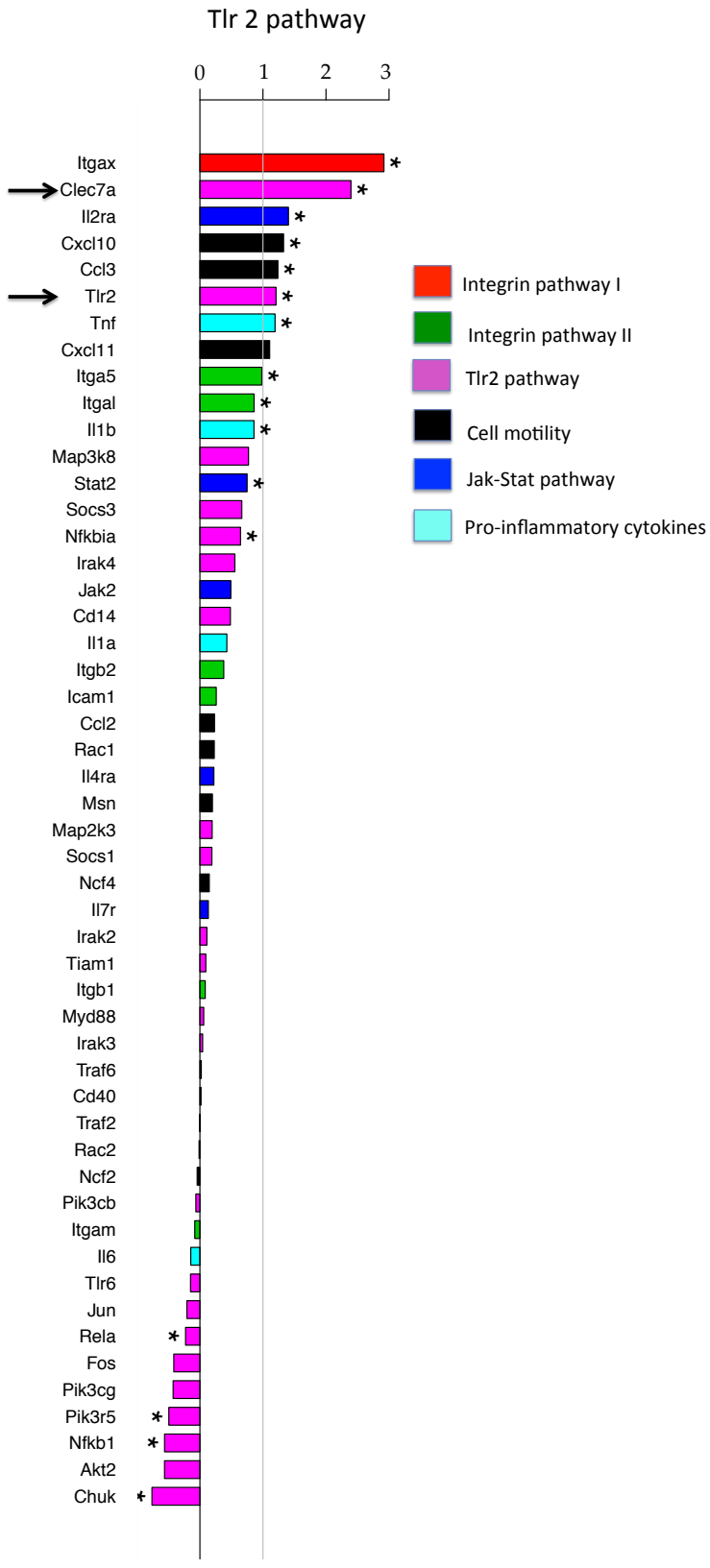

Figure 4.14 Genes related to the Tlr2 pathway identified by pairwise comparison t-test between old and young microglia. Grey line represents genes over a fold change of 2 and * represent genes that were statistically significant and have a p value <0.05.

Based on these profiles, and our interest in this pathway, we wanted to validate both *Tlr2* and *Clec7a* by quantitative real time PCR. To this end, we used the same protocol as the RNA sequencing experiments to obtain microglia RNA but used a new cohort of young, middle-aged and old mice. We also prepared lysates from a number of controls, which included: whole brain from young mice, the microglia cell line BV-2, un-stimulated BMDMs, macrophages stimulated with LPS and finally we used the negative fraction from our sorting, called here 'other brain cells'. These experiments confirmed the results from the RNA seq. data showing a steady increase in both receptors from young to middle aged and a further increase in old aged mice (**Fig. 4.15A** and **4.15B**).

We went on to validate *Tlr2* and *Clec7a* on a protein level, using flow cytometry in young and old mice. We found a striking upregulation in both receptors in old vs. young microglia, similar to what we had observed by qPCR and in the RNA sequencing analysis (**Fig. 4.15E** and **4.15F**).

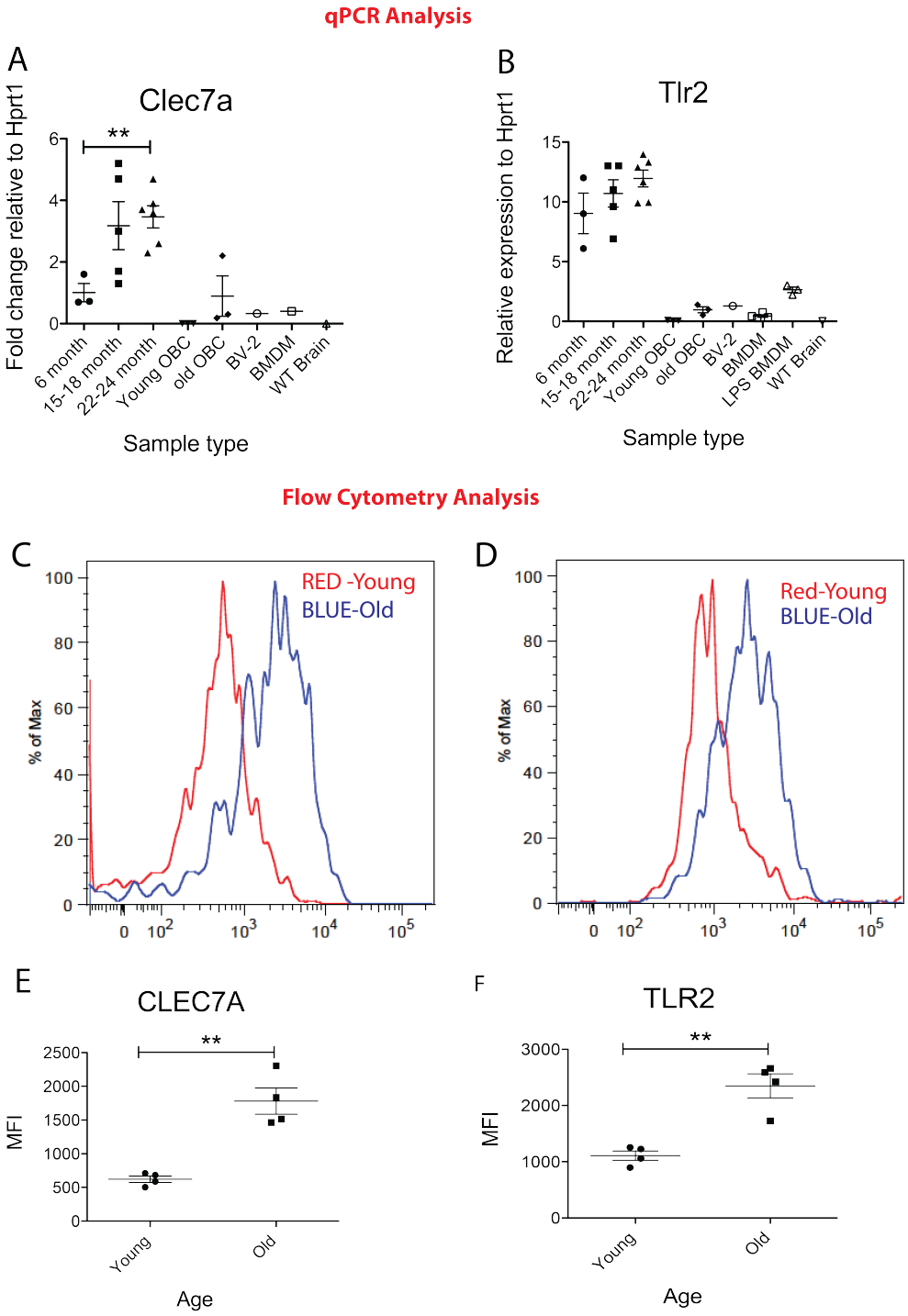

Figure 4.15 Age-related changes in gene expression quantified by qPCR. **A)** *Clec7a* and **B**) *Tlr2* expression are shown relative to Hprt1 expression. Overlay of flow cytometry analysis gated on CD11b+ microglia between one young (6 months – red line) and one old (24 months- blue line) for Clec7a (**C**) and Tlr2 (**D**). Quantification defined by a change in mean fluorescence intensity (MFI) for Clec7a (**E**) and Tlr2 (**F**). Data shown are from one experiment where n=3 for each group (qPCR) and n=4 for each group (flow cytometry), * $p<0.05$, ** $p<0.01$. Significance was calculated using the unpaired two tailed student t-test between individual groups.

4.4.3 Changes in adenosine and purinergic receptor expression may indicate microglia activation during ageing

As reported in **Fig. 4.13C**, several purinergic and adenosine receptors were differentially expressed in aged microglia. Microglia express a variety of purinergic receptors that can be categorised into two families, P2x and P2y, which primarily recognise ATP/ADP. These receptors have been proposed to have many important roles in microglia including activation, migration and response to injury[183].

Extracellular adenosine can be produced by cells following injury or damage and can bind to a number of G-protein-coupled receptors known collectively as adenosine receptors[184]. Recently, it has been shown that these receptors can play an important role in the control of the inflammatory response[185].

We combined a gene list that included all known purinergic receptors divided into these two subtypes and that also included the adenosine receptors. We found that several were differentially expressed in old vs. young microglia. *P2ry12*, which has recently been described as a microglia specific marker in the adult brain[186], was significantly downregulated with age (**Fig. 4.16A**). This downregulation has been proposed as a marker of microglia activation in response to injury or damage[187]. *P2ry13* was also significantly downregulated, as were two P2x receptors, *P2rx6* and *P2rx1*. Several receptors were upregulated, including the two adenosine receptors *Adora2b* and *Adora2a*, albeit not significantly (**Fig. 4.16A**). Recently, the upregulation of Adora2a, concomitantly to the downregulation of P2ry12, has been implicated in the retraction of cellular processes during inflammation, further indicating that it constitutes a marker of microglia activation. We proceeded to validate *P2ry12* and *P2ry13* by qPCR using the same controls and conditions as described for *Tlr2* and *Clec7a* validation (**Fig. 4.16A** and **Fig. 4.16B**). Interestingly, none of our selected controls expressed either purinergic receptors, further confirming that these genes are specific to primary microglia and are not expressed by macrophages or the WT brain[186]. We observed a similar downregulation of *P2ry12* and *P2ry13* in microglia isolated from the new cohort of aged mice when compared to microglia isolated from young mice. These changes were significant for both receptors (**Fig. 4.16B** and **4.16C**).

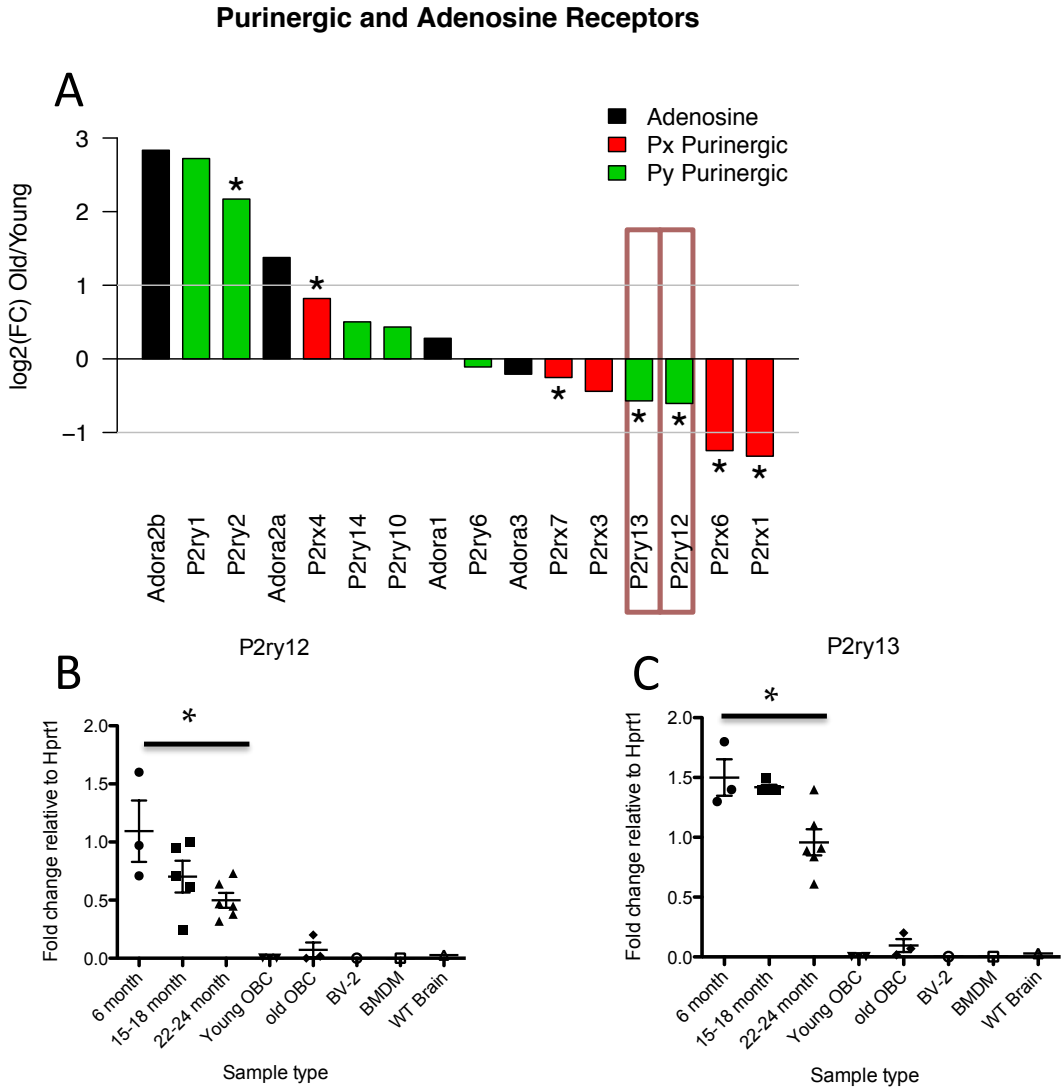

BV-2- Microglia cell line
OBC- Other brain cells
BMDM-Bone-marrow derived macrophages

Figure 4.16 Changes in purinergic and adenosine receptors and validation of purinergic receptor genes. A) Purinergic and adenosine receptors identified by pairwise comparison t-test between old and young microglia. Grey line represents genes over a fold change of 2 and * represent genes that were statistically significant and have a p value of <0.05. Age-related changes in gene expression quantified by qPCR for **B**) *P2ry12* and **C**) *P2ry13* relative to *Hprt1* expression. Data shown are from one experiment where n=3 for each group, * p<0.05, ** p<0.01. Significance was calculated using the unpaired two tailed student t-test between individual groups.

4.5 Age-related changes in genes associated with metabolism

Energy metabolism can change significantly with age and in macrophages, changes in glucose metabolism and upregulation of glycolysis are known to be important to maintain an inflammatory phenotype[188]. Therefore, we assessed whether there were any metabolic changes in microglia from aged mice. We compiled lists of genes that are involved in the main metabolic pathways, including the pentose phosphate pathway, the tricarboxylic acid cycle (TCA), glycolysis, gluconeogenesis and oxidative phosphorylation (OXPHOS).

We found that very few genes were differentially expressed in all the key metabolic pathways except for the OXPHOS pathway (**Fig. 4.17A**), in which we found 23 genes differentially expressed. Strikingly, all these genes were upregulated and were all members of complex IV and V of the electron transport chain. We picked the two most differentially expressed genes from the 23 OXPHOS gene for validation by qPCR, *Atp6v1b2* and *Cox6a2*, which were upregulated by 16-fold and 8-fold, respectively. In the qPCR assays, from a new cohort of young, middle-aged and old mice, we found that both *Cox6a2* and *Atp6v1b* steadily increased from young to middle aged and from middle aged to old, as previously observed in the RNA sequencing data (**Fig. 4.17B**). These data suggest that although some metabolic pathways may be increased in microglia with age, overall, little change was observed between young and old microglia.

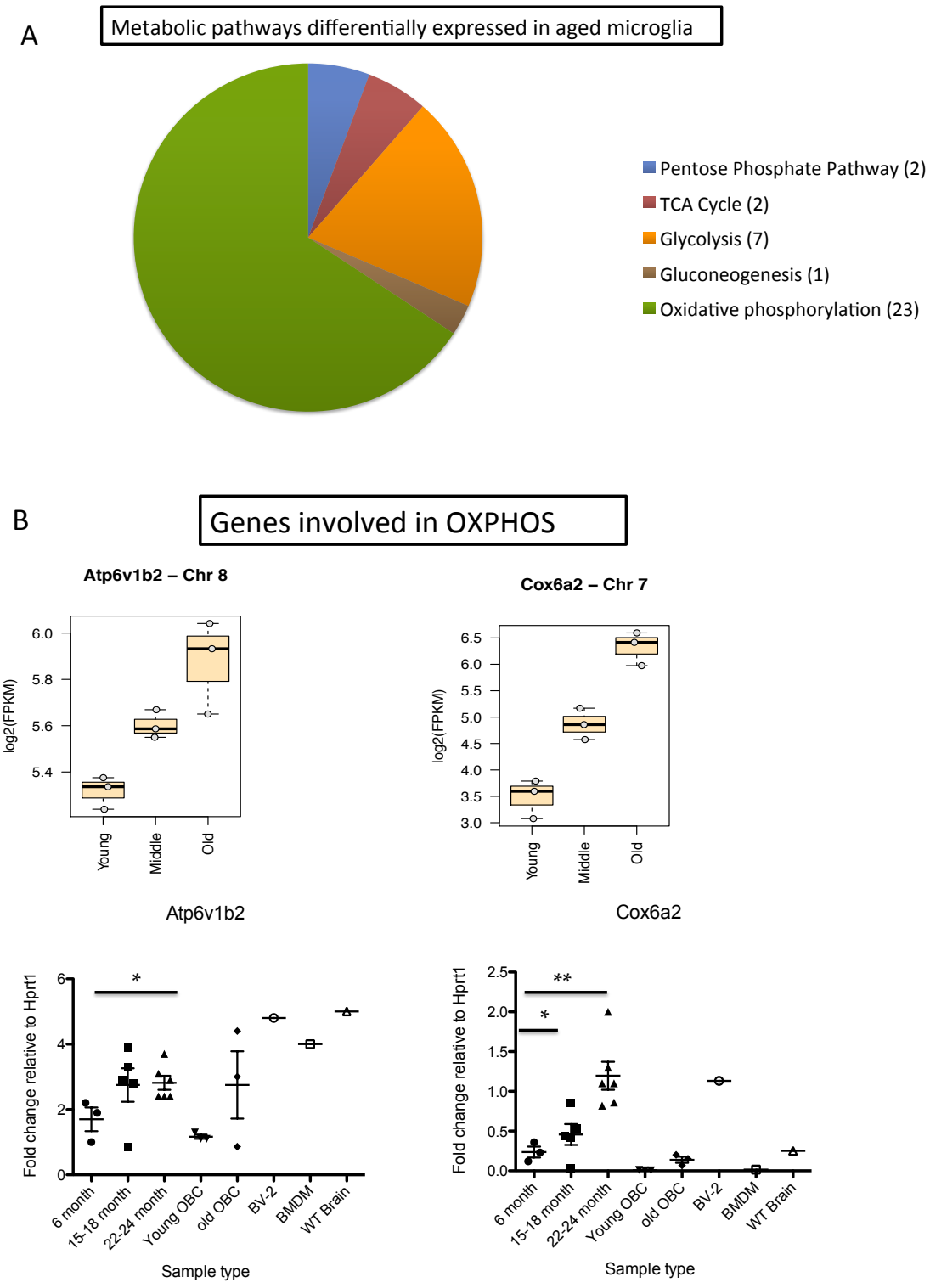

Figure 4.17 Age-related changes in genes associated with key metabolic pathways. **A**) Pie chart showing the number of genes that were differentially expressed in each of the metabolic pathways. **B**) Log2 RNA sequencing FPKM expression profiles from RNA

sequencing experiments are shown for two of the genes relating to OXPHOS; *Atp6v1b2* and *Cox6a2,* as well as age-related changes in gene expression quantified by qPCR relative to *Hprt1* expression. Data are from one experiment where n=3 for each group,* $p<0.05$, ** $p<0.01$. Significance was calculated using the unpaired two tailed student t-test between individual groups.

4 Discussion

4.1 Why the transcriptome of microglia in ageing is important

Given that microglia have been implicated in several pathologies that affect the central nervous system, including many types of cancer, neurodegenerative diseases and mental illnesses, it has been suggested that they also play a key role in the ageing of the brain. The literature indicates that microglia in the ageing brain are morphologically distinct from their younger counterparts, becoming more amoeboid in shape. However, it is still relatively unclear whether these cells reflect a senescent or activated phenotype or perhaps both. In my project I addressed the following question - do microglia in the ageing brain have an age-associated change in gene expression? This is an important question in trying to understand the role that microglia play in the ageing brain, including whether they become neurotoxic or neuroprotective. Considering that so many diseases of the CNS are age-associated, understanding what happens during this process may give insight into the pathogenesis of neurodegenerative diseases.

4.2 The isolation technique and the clontech ultralow RNA sequencing system

To study microglia in ageing, I first had to optimise a technique to isolate microglia from the ageing brain. It was extremely difficult to establish a technique that allowed the isolation of microglia with sufficient purity, particularly from brains over 18-months of age. This proved problematic but an important challenge to address, as even a 5-10% contamination with another cell type can severely distort gene expression results. Therefore, when considering doing large-scale gene expression, such as RNA sequencing, we needed a reliable method that allowed the isolation of microglia with purity of >95%. I found that in order to accomplish this, I had to first remove the

myelin with myelin removal microbeads and then flow sort the cells based on their expression of CD11b and CD45. While this technique proved to be reliable and robust, it had one major disadvantage; it reduced the yield in cell numbers dramatically. As a result, even by pooling three mice per replicate in each group, we still did not obtain sufficient quantities of RNA for standard RNA sequencing protocols. Therefore, a relatively novel system was used in which the quantity of the starting RNA can be as low as 10 pg. However, it needs to be considered that starting with such low amounts of RNA may introduce some bias into the experiment, particularly when considering genes or transcripts that are differentially expressed at low levels. This could potentially explain why so many genes that were differentially expressed were upregulated rather than downregulated in my data set. If some genes were subtly downregulated, it may have been difficult to measure this if the starting amount of RNA was already low this could possibly be introducing a bias. One was of overcoming this potential bias would be to increase the starting amounts of RNA or the depth of sequencing.

4.3 ANOVA analysis of aged microglia revealed eight distinct subsets of genes with similar behaviours

Our first analysis of the RNA seq. data was aimed at categorising the changes observed and whether there were any patterns. We first showed that there are distinct sets of genes, with expression profiles that change with age in a similar fashion. This is a major advantage to having a middle-aged group. Many studies, that have investigated microglia in the ageing brain, have only used a young and an old group [95,96]. In our study, having this additional age group, has allowed us to draw some interesting observations. Many of the changes we see in gene expression in the old group are also changed in the middle-aged group. This reflects the ageing process as it is generally defined as a gradual decline and functional deterioration of the body[4], the monotonic changes we observe from young to middle aged and from middle aged to old may mirror this gradual decline. It would have been interesting to look at an even earlier age group, for example 9 or 12 months, to try and understand when these changes in the microglia transcriptome start to appear in the brain.

We also observed that the majority of differentially expressed genes were upregulated, rather than downregulated, in the aged brain and that many of these genes were related to inflammation. There were also sets of genes where the peak of expression was observed in the middle-aged group. On deeper inspection of this set of genes, they do not appear to belong specifically to any pathway or functional group, making it difficult to interpret what this upregulation in middle age might mean.

4.4 Differential expression analysis

Our differential expression analysis revealed some interesting results. Many of the genes that appeared in our top 50 lists were genes related to inflammation. This is not surprising, given that ageing is associated with a low grade pro-inflammatory phenotype and senescent cells have been reported to secret inflammatory cytokines, known as the SASP[17]. We also saw changes in genes related to translation, metabolism, pathogen recognition and cell adhesion. The most differentially expressed gene in our dataset was the type 1 transmembrane glycoprotein *Gpmnb*, which has been implicated in a number of biological roles including inflammation. While the majority of research on Gpmnb has been in relation to its role in glioblastoma as a potential therapeutic target[189], there are two studies that have investigated its potential role in mediating inflammatory responses in microglia. Huang *et al.* showed that under basal conditions, Gpnmb was widely expressed in several regions of the brain and the majority of this expression co-localised with the microglia marker CD11b. They also found that the intensity and number of Gpnmb positive microglia increased upon intra-peritoneal injection of LPS, which is an accepted model of neuroinflammation. They suggested that Gpnmb was up regulated in microglia, following treatment with LPS[190]. This was further supported by an additional study by Shi *et al.* which showed that both the expression of *Gpnmb* and the production of pro-inflammatory cytokines Tnf-α and Il-1β increased in the BV-2 microglia cell line upon LPS treatment, however, Gpnmb knock down by siRNA dramatically reduced this pro-inflammatory response. They suggested that Gpnmb might stimulate excessive inflammatory responses in microglia, at least *in vitro*[191]. With regard to our study, it is interesting that a proven mediator of the inflammatory response in microglia is so upregulated in both middle-aged and old microglia. It would also be interesting to further explore the possible role of this glycoprotein in microglia in the ageing brain.

Another gene that was upregulated with age was the chemokine *Cxcl13*. Interestingly, *Cxcl13* was only moderately upregulated (2-fold) in middle-aged mice and this dramatically increased in old age (16-fold). Cxcl13 has been implicated in neuroinflammation particularly in multiple sclerosis[192] and recently it has been linked to microglia activation in a study that investigated the activation status of microglia in different age groups of mice. In this article, the authors assessed the brain response to inflammation by injecting a cocktail of cytokines, which included Il-12, Tnf-α and Il-1β, into the hippocampus of mice aged 6-24 months. They then performed gene expression profiling and found that, across all age groups, *Cxcl13* was significantly upregulated[193]. This study may have implications for our data presented here, especially given that *Tnf* and *Il1b* were upregulated in aged mice and that this upregulation was more pronounced in old mice compared to middle-aged ones. So, it would be interesting to determine if these cytokines induce the upregulation of *Cxcl13* in the ageing brain, or if additional factors are involved. It would also be important to understand the effect of high levels of this chemokine (if any) in the ageing brain. Cxcl13 in MS has been described as an attractant of B cells into the CNS[194] but given that the blood-brain-barrier should be intact in the ageing brain[195], it might have additional roles in this scenario.

4.5 Functions that may be affected by age

The analysis of chemokine, cytokine genes and their receptors provided some interesting observations. As expected, many of these genes were differentially expressed. What was interesting is that in some cases, for example Il-1β, both the cytokine and its receptor, *Il*1r, were upregulated. Cytokines and chemokines are also known to act in an autocrine fashion, where the cell both produces and responds to the cytokine/chemokine, or in a paracrine fashion, where one cell type produces the chemokine/cytokine that acts on another cell in its vicinity[196]. In our study, we observe a number of differentially expressed cytokine-receptor pairs, indicating that potentially these cytokines, such as Il-1β-Il1r, are acting in an autocrine fashion on microglia. An example of a potential chemokine autocrine loop could be *Cxcl16* and its receptor *Cxcr16,* both upregulated in aged mice. In the case of *Tnf*, for example, the cytokine is upregulated, unlike the receptor. This may indicate that Tnf is acting in a paracrine

fashion on neighbouring neurons or glia cells. In general, the differential expression of so many mediators of inflammation is a clear indication that the pathway is deregulated in the ageing brain.

4.6 Microglia sensing of the neural environment

4.6.1 The Tlr pathway

Overall, our data indicate that microglia from the ageing brain have a more activated inflammatory phenotype and may reflect a more primed status. It has been suggested that extrinsic factors in the ageing brain may be responsible for inducing changes in morphology and function in microglia. These may include stimuli such as neurotransmitters, ATP released from dying cells or astrocytes, cell debris, hormones, oxidative stress, or the build up of abnormal aggregates such as amyloid beta[80]. Our data supports this idea to a degree, given the differential expression of so many receptors that are responsible for sensing changes in the neural environment. These include *Tlr2* and *Clec7a*. Given the clear up-regulation of *Tlr2* and that signalling downstream of toll-like receptors such as Tlr2 can trigger the production of inflammatory cytokines and also increase phagocytic activity, we performed an additional analysis of possible *Tlr2* target genes. To this end, we used a hypothetical pathway list of genes, generated from a previous study in which authors used α-synuclein as Tlr2 agonist[182]. We found that many of the genes shown to be regulated by Tlr2 activation in this paper, were also upregulated in our aged microglia. We also found that *Clec7a*, which has been shown in many studies to co-localise with Tlr2, was also significantly upregulated in our data. Yadav *et al.* showed that Clec7a was required for Tlr2 mediated production of Tnf-α in macrophages infected with *Mycobacterium avium* or *M smegmatis*[175].

Tlr2 is of particular interest because several studies have shown that the amyloid plaques that are associated with Alzheimer's disease and that build up as the illness progresses can trigger Tlr2[197]. Given that amyloid plaques are also present in the aged brain, albeit to a lesser extent, they may be partly responsible for the inflammatory phenotype we observe in the aged microglia. Depending on the potential stimuli, it is

possible that Clec7a is upregulated simultaneously, as it may be required for Tlr2 mediated responses. Our data on *Tlr2* fits with the current literature on the ageing brain. Hickman *et al.* carried out a similar study using young and old mice and direct RNA sequencing and they also showed that the only significantly upregulated toll-like receptor in aged microglia was *Tlr2*[96]. This was further supported by an earlier study in 2006, in which *in situ* hybridisation was used to show that *Tlr2* is upregulated in microglia form aged rats compared to young counterparts [84].

4.6.2 The purinergic receptors

It is interesting that we see so many genes involved in sensing the neural environment being differentially expressed, for example many endogenous sensing genes, such as neurotransmitter receptors, were downregulated in aged microglia, perhaps to dampen microglia response to these stimuli. It is known that inflammation can be associated with the release of nucleotides, particularly ATP, which is recognised by purinergic receptors[183]. P2ry12 has been shown to be downregulated after microglia activation[187]. During inflammation microglia retract their cellular processes and downregulate this receptor, its downregulation coincides with the upregulation of the A2 (A) adenosine receptor. This switch in receptor expression is proposed as a "hallmark of CNS inflammation" by the authors[198]. Therefore, it is very interesting that in our study we see the same pattern of receptor expression in old vs. young microglia, which may be another indication of CNS inflammation and microglia activation in the ageing brain. It is also worth to note that *P2ry13* (in the same family as P2ry12) is also downregulated and that the other adenosine receptor *A*dora2b is upregulated, suggesting a potential role also for these receptors in CNS inflammation. The downregulation of the purinergic receptors is further supported by our validation data, obtained from a separate cohort of mice and supported by the Hickman *et al.* ageing study[96]. It would be important to validate some of these receptors on a protein level. Given the unavailability of antibodies that can be used for imaging, this is technically very difficult at present.

4.7 Interpretation of our data

When interpreting and analysing our data, we need to consider the use of the Clontech system and the input of such low amounts of starting RNA. The fact that we were able to validate many of our candidate genes by qPCR, in which the RNA was not amplified

using the Clontech system, indicates that this technique does not seem to have introduced any major biases into our experiment. However, many genes of interest are upregulated, in some cases with a substantial fold change, but are not statistically significant. This may be due to the fact that one of the three replicates from the old mice had very small amount of total RNA, with the smallest being just 13 ng. This may have introduced some differences among our replicates, which may increase the standard deviation and reduce the statistical significance. Therefore, for some genes with a high fold change but a p value over 0.05, it may still be worthwhile, if they are of interest, to validate them in a new cohort of mice to see if the differences were significant. This may be true for example for the *Sirpbl1* gene, which has been shown to be a positive regulator of phagocytosis in macrophages[176] and for which we observe a 2-fold increase between young and old microglia but the p value is 0.06.

This is also an indication of the possible disadvantage of having only three replicates per group, as four or five replicates may have reduced the standard deviation. We did, though, have to limit our replicates to three given the difficulty in obtaining RNA from aged microglia.

4.8 How does our data compare to the field of microglia and ageing?

Since additional studies on the transcriptome of microglia in ageing have been published, it is important to compare our data to others in the microglia field. As discussed, our data show similarities with the Hickman *et al.* ageing study; this is true for many of our differentially expressed genes. Overall they report that many endogenous sensing genes are downregulated, whereas many pattern recognition transcripts are upregulated, which is similar to our data set. They do also observe an overall downregulation of the oxidative phosphorylation pathway, which has been suggested to promote neurotoxicity, whereas in our study we see an upregulation of many genes involved in the electron transport chain of oxidative phosphorylation, suggesting an overall upregulation of this pathway[96].

We also see a clear upregulation of complement related genes C3 and Cfb, which was the main finding of the retina ageing study[91]. Finally, with regard to the Orre *et al.* ageing study, which isolated microglia from the cortices of aged mice, we observe very few similarities[95].

Another study by Grabert *et al.* showed that changes in the microglia transcriptome with age were non-uniform across different brain regions. In this study microglia were isolated from different regions of the brain from young and aged mice. They identified major transcriptional networks relating to both immune function and bioenergetics that defined the microglia transcriptome from different regions of the brain. Perhaps most relevant to our study was the finding that genes relating to the immune response were induced with age in the cerebellar microglia, whereas other genes more involved in limiting excessive inflammation were mainly stable across all brain regions. Could the transcriptome changes we observe, particularly those relating to inflammation, be due to changes to cerebellar microglia rather than a general phenotype of aged microglia from the whole brain?

When comparing these studies to our data or to each other, it is important to be aware that they differ in terms of how microglia were isolated from the ageing brain, the age groups of mice that were used, the regions of the brain used, the type of gene-expression profiling carried out and how the data were analysed. Potentially, the differences in overall experiment design and procedure may reflect the variations observed among data sets.

4.9 The possible role of mTOR in microglia from the ageing brain

The two main themes emerging from our data set were the concomitant deregulation of inflammatory pathways and the mTOR pathway. This was further corroborated by the observation that transcription factors putatively upstream of the genes differentially expressed in age were related to mTOR, such as *Pparg* and *Nfkb*1. Maybe, it is not

surprising that the mTOR pathway is more active in microglia with age, given that its activation has been associated with ageing in a number of tissues[199]. In fact, inhibiting the pathway has also been shown to extend lifespan in a number of genetic models[30] . What is not known however, is what role this activation may possibly have in microglia with age. Could it possibly be regulating some of the transcription changes we observe with ageing? It has been shown to negatively regulate NF-kB in primary monocytes and that mTOR inhibition in this setting actually leads to a more pronounced inflammatory response[129]. Could mTOR activation in the ageing brain be preventing excessive inflammation or, on the contrary, be modulating microglia priming?

4 Conclusion

In conclusion, our results show that overall microglia from mice as young as 15 months of age display a global change in gene expression and that this change is often further increased, as the mice get older. These changes appear to relate to genes involved in microglia function, such as phagocytosis or inflammation, and may be a reflection of a more primed activated cell that seems to have an increased ability to sense changes in its environment. Nevertheless, the upregulation of the mTOR pathway with age may be an attempt to counterbalance excessive inflammation with age. The role of mTOR in ageing microglia clearly warrants further investigation.

Chapter 5: mTOR inhibition regulates inflammatory responses in microglia from the ageing brain

As explained in the introduction, mTOR is a serine/threonine kinase of the PI3K related family and a master regulator of cellular growth and metabolism, which is deregulated in a number of human diseases, including type 2 diabetes and cancer[98]. Unsurprisingly, there is a strong interest around mTOR in the ageing field, since its inhibition, either genetically or with rapamycin, has been shown to extend lifespan in a number of model organisms[30].

I was particularly interested in the mTOR pathway, given that it appeared upregulated in microglia from the ageing brain. Weichhart *et al.* had previously described how mTOR inhibition in primary monocytes could lead to an increase in inflammatory responses through the activation of NF-κB[129], therefore I hypothesised that, in the ageing brain, mTOR might be activated in microglia to prevent excessive inflammation in the brain.

The *Csf1r-Cre; Rheb f/f* mouse model

Rheb is a small GTPase upstream of mTORC1 signalling and activates it when bound to GTP[102]. This activation leads to phosphorylation of the downstream targets S6K1 and 4E-BP1. Therefore, when Rheb is knocked out, the mTOR pathway is inhibited and phosphorylation of mTORC1 downstream targets are blocked. To investigate the potential link between mTOR and inflammation in microglia, I used a mouse model in which Rheb was deleted under the control of the Csf1r promoter. In this model, LoxP sites flank both Rheb alleles and the gene is deleted by the Cre recombinase. This occurs in cells that express Csf1r, which are primarily monocytes, macrophages and microglia, since Csf1 signalling is important for their differentiation and development[200]. This model made it possible to study the effect of mTOR inhibition in microglia and macrophages both *in vivo* and *in vitro*. The *Rheb f/f* model has been used previously, crossed with a T-cell Cre recombinase mouse model, which showed that Rheb was important for the differentiation of T cells into Th1[201].

5.1 *In vitro* stimulation of BMDMs with LPS reveals the mTOR pathway is inhibited in *Csf1r-Cre*; *Rheb f/f* cells

I first wanted to assess if the mouse model was working correctly. To this end, I differentiated macrophages from the bone marrow of both control and *Csf1r-Cre; Rheb f/f* mice (called Rheb KO for simplicity). Control mice were *Rheb f/f* and negative for *Csf1r-Cre* (called WT for simplicity). I decided to use this strategy in order to use littermates as controls. Given that the mouse line is on a mixed background, partly 129, partly FVB/N and partly C57BL/6J – backcrossed three times to C57BL/6J – it was important that controls had a similar background. Once macrophages were generated, they were stimulated with LPS at different time points to induce phosphorylation of S6, which is mediated by the kinase S6K1; therefore, it is directly downstream of mTORC1. I observed a complete deletion of the Rheb protein in Rheb KO BMDMs, as shown in **Fig. 5.1A**.

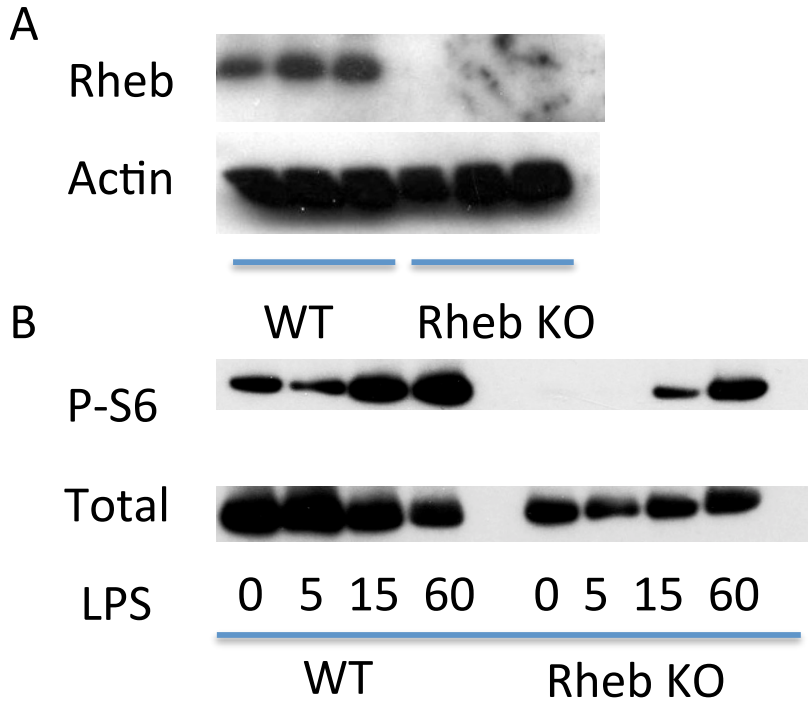

Figure 5.1 Immunoblots showing that the mTOR pathway is inhibited in *Csf1r-Cre; Rheb f/f* – Rheb KO – BMDMs. BMDMs were differentiated for 6 days and then re-plated overnight in complete media. **A)** Immunoblot for the GTPase Rheb from the whole cell lysate of three WT and three Rheb KO mice. **B)** BMDMs were stimulated with 200 ng/ml of LPS for the indicated time points (in minutes). Data are representative of three independent experiments.

Upon LPS stimulation, there was a clear induction of p-S6 in WT cells, suggesting that LPS strongly activates the mTOR pathway, as previously published in the literature[129]. However, p-S6 levels were significantly reduced in Rheb KO BMDMs (**Fig. 5.1B)**.

5.2 The number of myeloid cells is not affected by Rheb deletion *in vivo*

It was important to understand if Rheb KO mice had similar numbers of myeloid cells compared to littermate controls, as this would be important for *in vivo* experiments to measure their inflammatory responses. To this end, I assessed CD11b+ cells in the bone marrow and the spleen from both young and old WT and Rheb KO mice using flow cytometry analysis. As described in chapter 3, CD11b is an integrin that is expressed on all myeloid cells. I found that there was no difference in the number of myeloid cells between WT and Rheb KO mice. This was the case for both young and old mice in the bone marrow (**Fig. 5.2A**) and similarly in the spleen (**Fig. 5.2B**).

I also found that there were no differences in the total number of cells obtained from the bone marrow (**Fig. 5.2C**), spleen (**Fig. 5.2D**) or blood (**Fig. 5.2E)**. Finally, a similar number of microglia cells were purified from WT and Rheb KO brains (**Fig 5.2F**). It would be important to confirm that there weren't any changes in the number of microglia or the distribution of these cells in the brain in Rheb KO mice by using a microglia marker such as IBA-1 to stain brain sections form both Rheb KO and WT brains.

Nevertheless, it would appear that the deletion of Rheb in myeloid cells does not have an effect on myeloid cell numbers *in vivo*. Both WT and Rheb KO mice were kept to a maximum age of 22 months and Rheb KO mice did not display any obvious phenotype compared to WT mice. It must also be mentioned that I did notice, however, impairment in the growth of Rheb KO BMDMs *in vitro*. I found, in general, that I obtained fewer BMDMs from Rheb KO cultures compared to WTs.

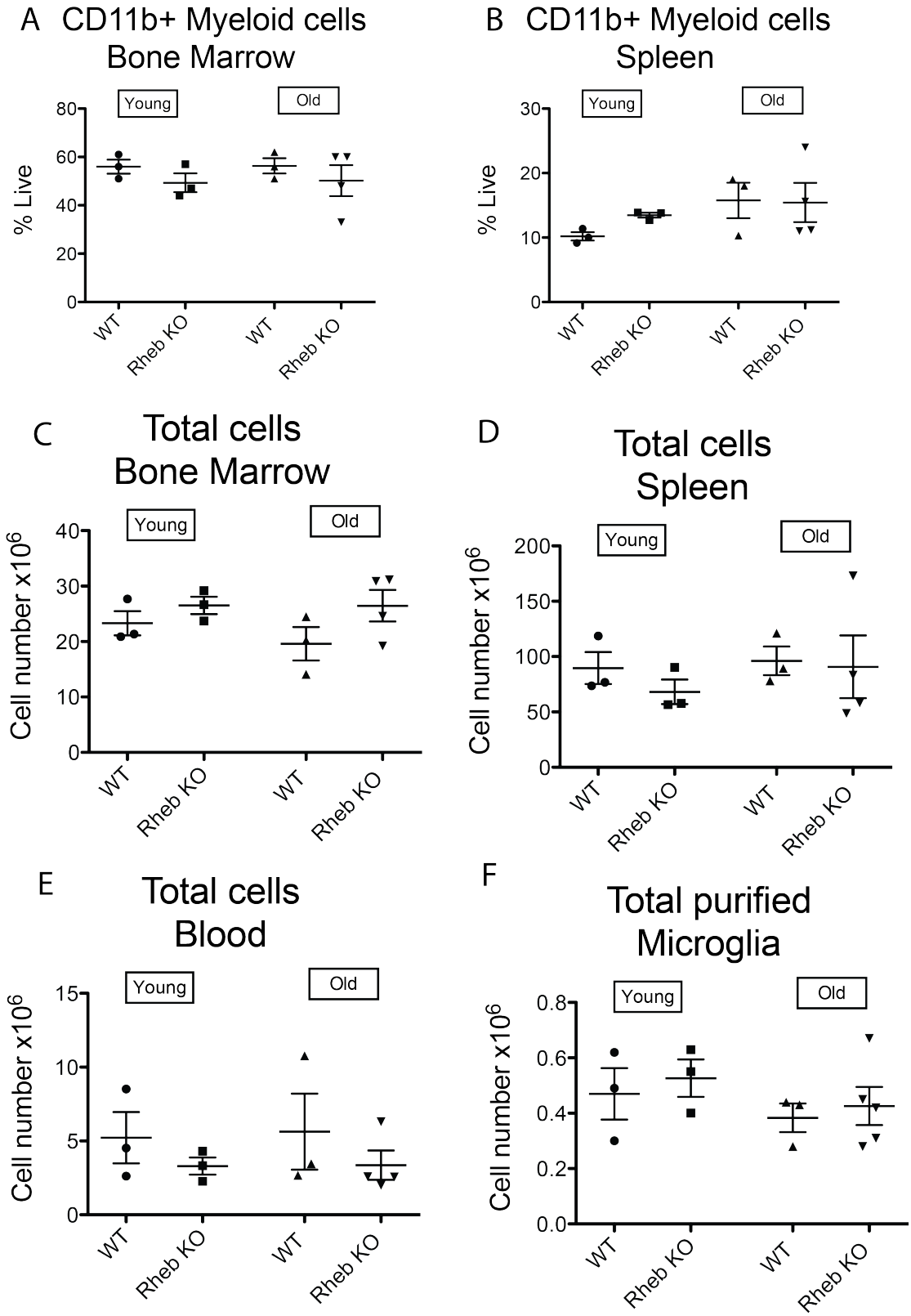

Figure 5.2 Myeloid cell numbers are not affected by Rheb deletion *in vivo.* The spleen and bone marrow from young (3 months) and old (22 months), Rheb KO and WT mice were assessed by flow cytometry analysis for CD11b expression. **A)** Percentage of CD11b+ cells in the bone marrow **B)** Percentage of CD11b+ cells in the spleen. **C**) Total number of cells in the bone marrow, **D**) total number of cells in the spleen **E**) total number of cells in the blood. **F)** The number of microglia obtained by purification is also shown**.** The data shown is from one experiment where n=3 for each group.

5.3 mTOR inhibition in BMDMs leads to an upregulation of inflammatory cytokine genes upon LPS stimulation *in vitro*

It has been described in the literature that inhibition of the mTOR pathway by rapamycin leads to an increase in cytokine production, in response to bacterial infection[129]. Therefore, after establishing that the mTOR pathway was inhibited in BMDMs upon Rheb deletion, I wanted to establish if this inhibition would affect the inflammatory response, as previously described in chapter 4.

To test this hypothesis, BMDMs were stimulated with 200 ng/ml of LPS for six hours to determine the effect of mTOR inhibition on the expression of pro-inflammatory cytokine genes, known to be regulated by NF-κB. It appeared that key inflammatory genes were upregulated in Rheb KO BMDMs upon LPS stimulation. These changes were consistent among inflammatory cytokines *Tnf* (**Fig. 5.3A**), *Il1b* (**Fig. 5.3B**) *Il6 (***Fig. 5.3C**) and *Il12a* (**Fig. 5.3D)** when mTOR was inhibited. Finally, I also looked at the expression of *Tlr2* (**Fig. 5.3E**), one of the genes significantly upregulated with age in microglia, as described in chapter 4. *Tlr2* expression also appeared increased in Rheb KO BMDMs upon LPS stimulation. Statistical analysis was not carried out on this dataset, as the number of replicates was equal to two and therefore more replicates would be needed for this analysis.

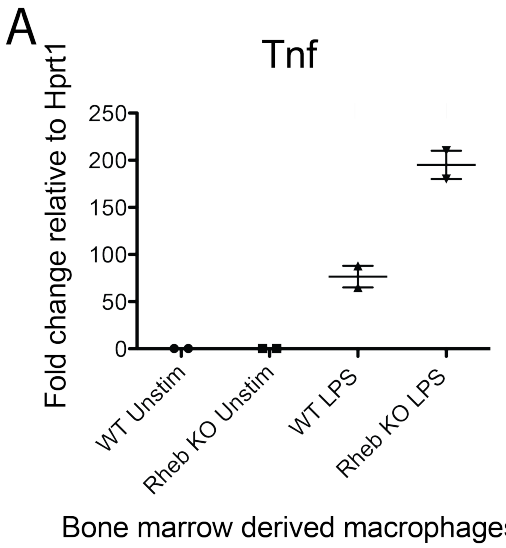
A
Tnf
Fold change relative to Hprt1
250
200
150
100
50
0
WT Unstim
Rheb KO Unstim
WT LPS
Rheb KO LPS
Bone marrow derived macrophages

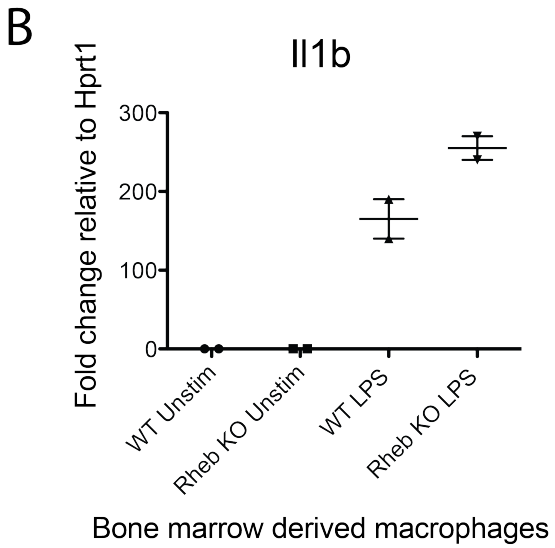
B
Il1b
Fold change relative to Hprt1
300
200
100
0
WT Unstim
Rheb KO Unstim
WT LPS
Rheb KO LPS
Bone marrow derived macrophages

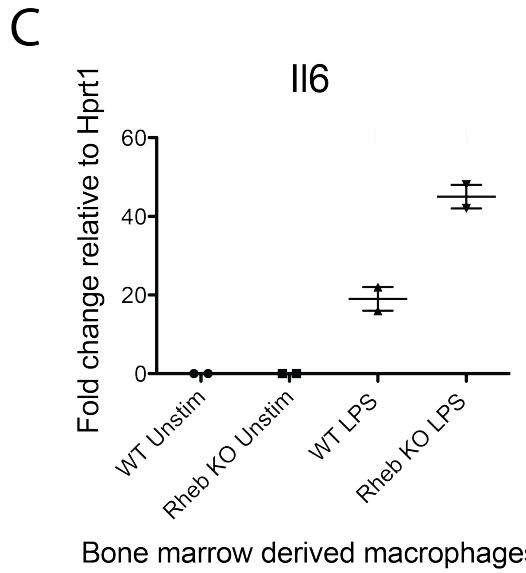
C
Il6
Fold change relative to Hprt1
60
40
20
0
WT Unstim
Rheb KO Unstim
WT LPS
Rheb KO LPS
Bone marrow derived macrophages

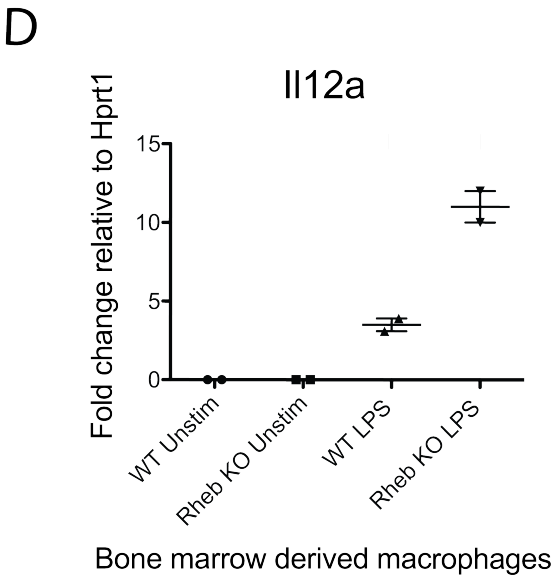
D
Il12a
Fold change relative to Hprt1
15
10
5
0
WT Unstim
Rheb KO Unstim
WT LPS
Rheb KO LPS
Bone marrow derived macrophages

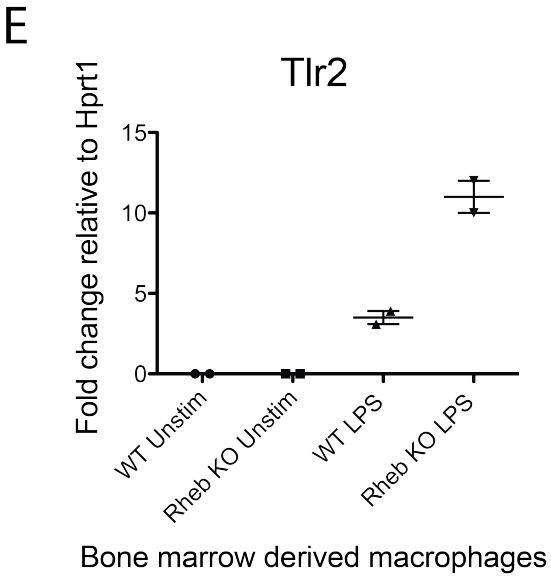
E
Tlr2
Fold change relative to Hprt1
15
10
5
0
WT Unstim
Rheb KO Unstim
WT LPS
Rheb KO LPS
Bone marrow derived macrophages

Figure 5.3 Inhibition of mTORC1 signalling increases transcription of inflammatory genes in BMDMs *in vitro*. BMDMs were differentiated for 6 days before being re-plated overnight in complete media. They were then treated with 200 ng/ml of LPS for six hours, or media only as control, shown here as un-stimulated. Expression of inflammatory genes was determined using qPCR with fold changes being shown relative to the housekeeping gene *Hprt1* for **A**) *Tnf*, **B**) *Il1b*, **C***) Il6*, **D**) *Il12a* and for **E**) *Tlr2*. The data shown is from one experiment, where n=2 for each group.

5.4 mTOR inhibition in primary adult microglia leads to an upregulation of inflammatory cytokine genes upon LPS stimulation *in vitro*

Following the observation that mTOR inhibition by Rheb deletion resulted in an increase in inflammatory cytokine genes in BMDMs upon LPS stimulation, I wanted to test if this would also be the case in primary microglia. To this end, I isolated microglia from the adult brain of both WT and Rheb KO mice and incubated them for two hours with LPS. A shorter time point was chosen because adult microglia are more sensitive to stress and apoptosis. Nevertheless, even at a shorter time point, the Rheb KO microglia showed an upregulation of inflammatory genes such as *Tnf* (**Fig. 5.4A**) and *Il1b* (**Fig. 5.4B**) although this was only significant for *Il1b*. Other inflammatory cytokines such as *Il6* appeared only slightly upregulated (**Fig. 5.4C**), however, this could be due to the shorter time point used. It must be noted that, particularly for *Tnf*, the un-stimulated cells were expressing high levels already, which is probably due to their overall stress levels at the time of stimulation. Finally, the gene for *Tlr2* was also upregulated upon LPS stimulation in Rheb KO microglia cells (**Fig. 5.4D**).

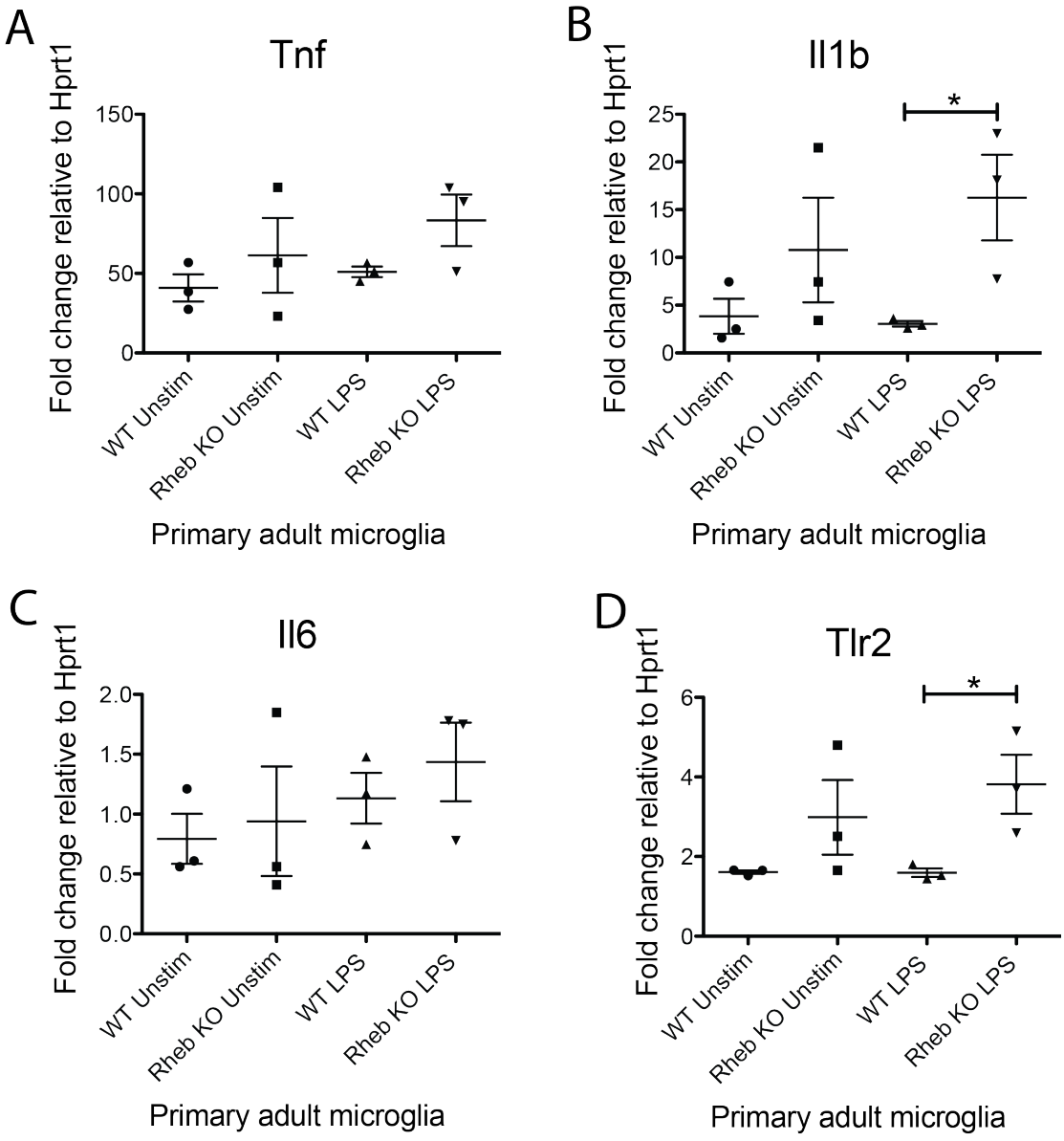

Figure 5.4 Inhibition of mTORC1 signalling affects inflammatory responses *in vitro* in primary adult microglia. Primary microglia were isolated from the adult brain and stimulated directly with 200 ng/ml of LPS for two hours. Expression of inflammatory genes was determined by qPCR for **A**) *Tnf*, **B**) *Il1b*, **C**) *Il6* and **D**) *Tlr2*. The data shown are representative of two independent experiments, where n=3 for each group and * $p<0.05$. Significance was calculated using the unpaired two tailed student t-test between individual groups.

5.5 Optimisation of LPS stimulation conditions to be used for *in vivo* ageing studies

Following my *in vitro* observations that inhibiting the mTOR pathway by Rheb deletion lead to an increase in inflammatory cytokines upon LPS stimulation, I wanted to test if

this would also be the case *in vivo*. Furthermore, given my transcriptome data showing an upregulation of mTOR signalling in microglia with age, I wanted to understand what would be the effect of inhibiting mTORC1 in ageing in response to an LPS challenge. This is an important question, since mTOR inhibitors are being tested as anti-ageing interventions. If a more profound inflammatory response is a consequence of mTOR inhibition, when an infection is encountered, for example, this could have major implications for neuroinflammation and neurotoxicity.

Lipopolysaccharide–induced neuroinflammation is a well-studied and accepted model of neuroinflammation, both *in vivo* and *in vitro*[202]. The route of administration, however, dose and age of animals all need to be considered in the study design.

In order to optimise a dose and duration of LPS treatment *in vivo,* I carried out a small pilot study in which I administered young WT mice either 1 mg/kg or 5 mg/kg of LPS for 4 or 24 hours. In addition, I used one aged mouse (24 months) to assess the tolerability of the higher dose. All mice received LPS by intraperitoneal injection, in order to model the scenario of an elderly individual contracting a peripheral infection.

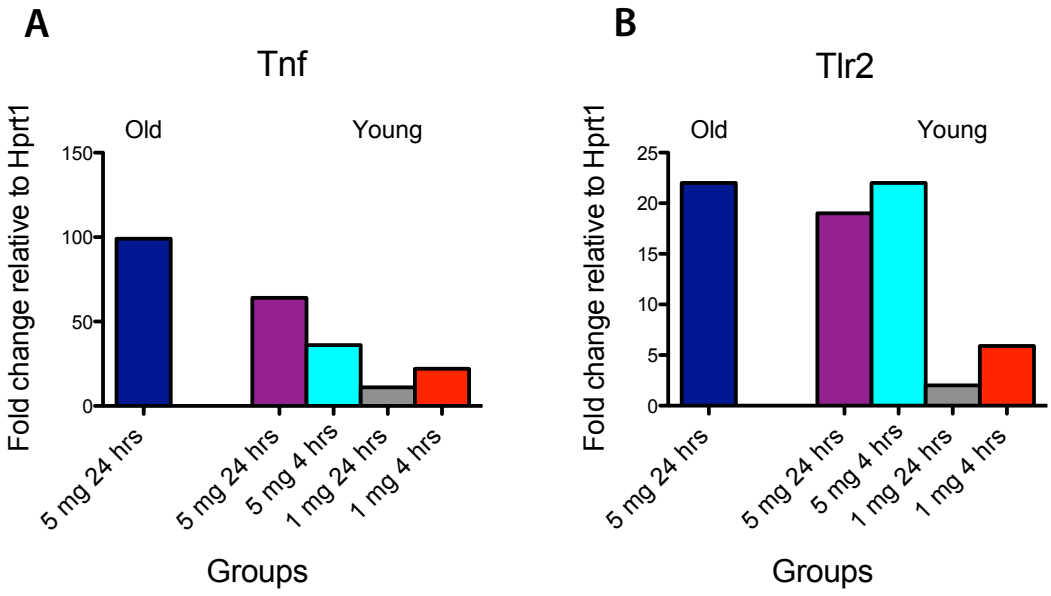

Figure 5.5 Optimisation of LPS dose and time-point for *in vivo* challenge. WT mice received LPS by intra-peritoneal injection for either 4 hours or 24 hours. The doses of LPS used were either 5mg/kg or 1 mg/kg at the time points indicated. Microglia were isolated from the brain using CD11b microbeads and the induction of inflammatory genes was measured by qPCR. Fold changes shown as relative to the housekeeping gene *Hprt1* for **A**) *Tnf* and **B**) *Tlr2*. Data shown are from one experiment, n=1 for all groups.

Microglia were isolated following LPS challenge, and qPCR was carried out on the key inflammatory gene *Tnf* (**Fig. 5.5A)** and the age-related gene *Tlr2* (**Fig. 5.5B)**. Both genes should be strongly induced in microglia following an LPS challenge. I found that the strongest induction of *Tnf* in microglia, for both young and old mice, was observed with 5 mg/kg LPS after 24 hours (**Fig 5.5A)**. A weaker induction of *Tnf* was observed at 4 hours with this dose and an even lower one with 1 mg/kg of LPS for 4 and 24 hours.

At the higher dose of LPS, after 24 hours, both the young and particularly the old mouse were extremely ill, therefore I deemed it inhumane to use this dose and time point for future experiments. The higher dose of LPS but the shorter time point of four hours was therefore used for future experiments.

5.6 mTORC1 inhibition in the ageing brain

In order to assess if mTORC1 inhibition leads to an increased inflammatory response in microglia from the ageing brain, I aged Rheb KO mice and WT littermate controls. Once mice were 18-months old (old group) and 4-months old (young group), they were divided into groups and given the sub lethal dose of LPS of 5 mg/kg intraperitoneally for 4 hours or PBS, as described in the schematic in **Fig. 5.6.** Following the *in vivo* stimulation, microglia were isolated, RNA extracted, and qPCR was conducted for a number of inflammatory and age-related genes.

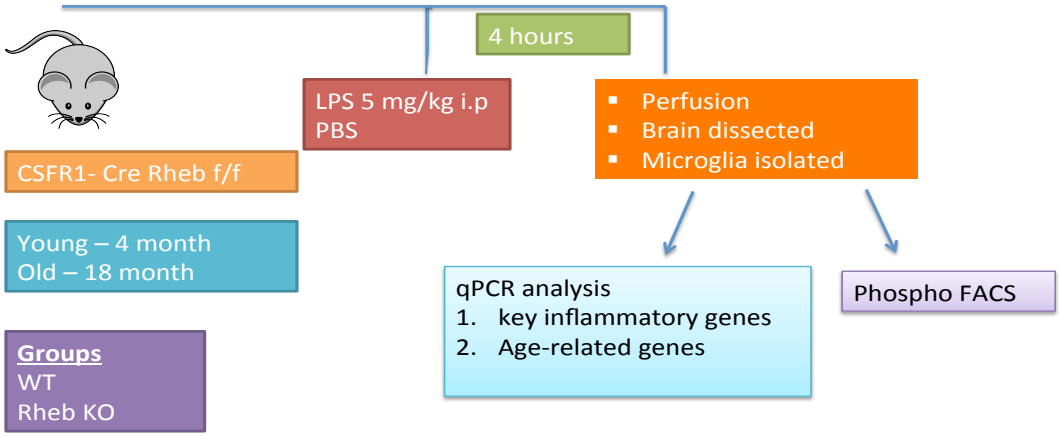

Figure 5.6 Experimental design for *in vivo* LPS challenge. Young and aged mice were used in this experiment and given a peripheral injection of PBS as control or LPS (5mg/kg) for four hours. Microglia were isolated using magnetic beads and used for phospho-flow cytometry, to assess mTORC1 inhibition, and qPCR analysis.

5.7 Phosphorylation of p-S6 is reduced in microglia from aged Rheb KO mice compared to WT mice upon LPS stimulation *in vivo*

In order to test that our *in vivo* model was working correctly, i.e. that there was a deletion of Rheb in microglia under the *Csf1r-Cre*, I assessed levels of p-S6 using a phospho-specific flow cytometry antibody (phospho-S6-Alexa 488). The use of flow cytometry was necessary, given that a low number of microglia can be recovered from each brain and was not sufficient for a western blot analysis. Following the LPS injection (5 mg/kg i.p. for four hours), brains were digested and myelin removed as previously described in chapter 4. Following myelin removal, the remaining glia cells were stained for p-S6 and the microglia specific markers CD11b and CD45. An example of the p-S6 levels in microglia comparing WT and Rheb KO cells is shown in **Fig. 5.7A.** There was a clear shift of p-S6 in the WT cells (green line) upon LPS stimulation that was not as pronounced in Rheb KO microglia cells (red line). A quantification of p-S6 levels from different mice is reported in **Fig. 5.7B**, which shows p-S6 levels were significantly lower in Rheb KO microglia.

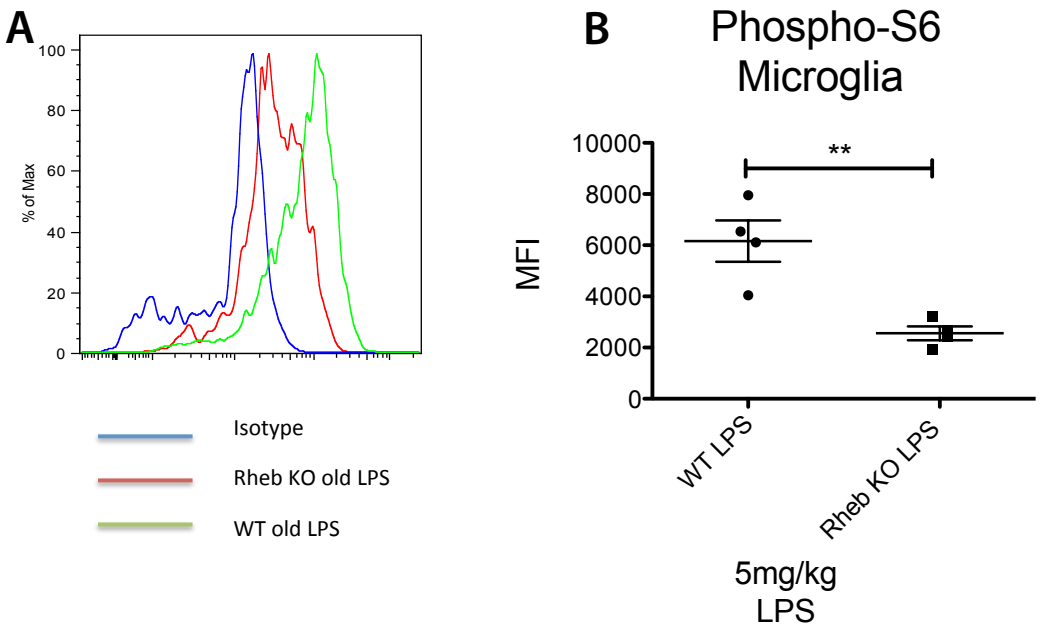

Figure 5.7 Phospho flow cytometry reveals that the mTOR pathway is inhibited in Rheb KO microglia. Aged WT and Rheb KO mice were given a peripheral injection of LPS (5 mg/kg) for four hours. The brains were digested and myelin was removed. The cell suspension was stained for p-S6 after paraformaldehyde (PFA) fixation and methanol permeabilisation. **A**) Representative flow cytometry plots comparing p-S6 levels in microglia from an aged Rheb KO (red) and WT mouse (green), the isotype control is in blue. **B**) Quantification of p-S6 in microglia, expressed as median fluorescence intensity (MFI) from different mice. The data shown is from one experiment, where n=4 for each group and **p<0.01. Significance was calculated using the unpaired two tailed student t-test between individual groups.

5.8 mTOR inhibition leads to an upregulation of inflammatory genes in microglia upon LPS injection *in vivo*

Microglia cells from LPS-challenged mice were isolated and expression levels of pro-inflammatory and age-related genes were quantified by qPCR.

Figure **5.8** depicts the qPCR results for the pro-inflammatory genes *Tnf* (**Fig. 5.8A**), *Il1b* (**Fig. 5.8B**), *Il12a* (**Fig. 5.8C**) and *Il6* (**Fig. 5.8D**) in microglia from both young and aged WT and Rheb KO mice. Regarding the young mice, consistent with what I observed in BMDMs and adult microglia *in vitro*, there was an upregulation of all four inflammatory genes upon LPS stimulation in Rheb KO microglia (**Fig 5.8A-D**). These results were statistically significant for all genes ($p<0.05$), except *Il1b* (**Fig. 5.8B**), which showed a similar trend. No differences were observed in the PBS controls.

I also detected an upregulation of all four genes in microglia from aged Rheb KO mice that was statistically significant for *Il1b* (**Fig. 5.8B**), *Il12a* (**Fig. 5.8C**) and *Il6* (**Fig. 5.8D**) with $p<0.05$ and *Tnf* with $p<0.01$. The upregulation of pro-inflammatory genes in Rheb KO microglia was consistent between young and aged mice, however it was significantly stronger with age. Indeed, *Tnf* (**Fig. 5.8A**), *Il1b* (**Fig. 5.8B**) and *Il6* (**Fig. 5.8D**) showed a significant increased expression in aged Rheb KO microglia compared to young counterparts, whereas *Il12a* (**Fig. 5.8C**) showed a similar trend. This, though, did not reach statistical significance. Overall it appeared that, consistent with the literature and our *in vitro* data, inhibition of the mTOR pathway in microglia led to an increase in the expression of pro-inflammatory genes upon LPS injection *in vivo* and that this increase appeared to be stronger with age.

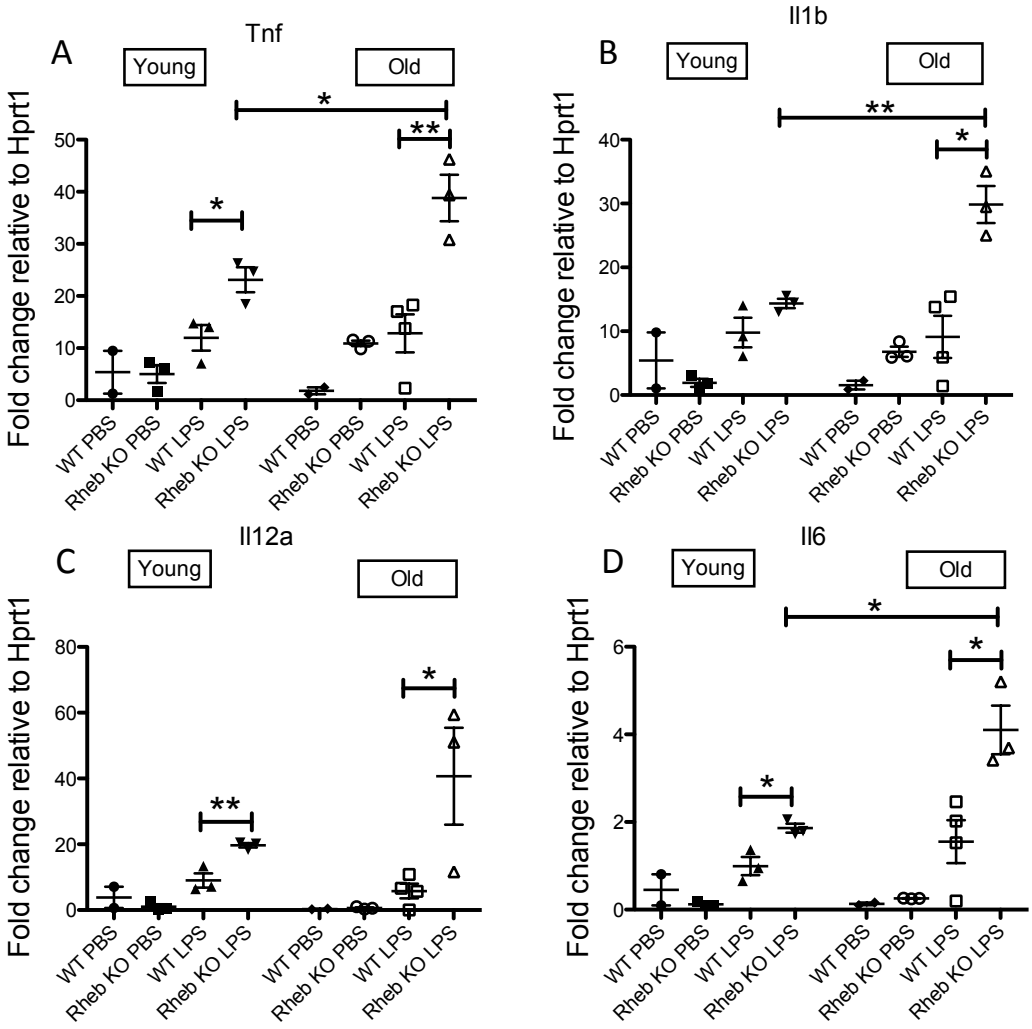

5.8 mTOR inhibition leads to an upregulation of inflammatory genes in microglia upon LPS injection *in vivo*. Young (4 months) and old (18 months) WT and Rheb KO mice were given a peripheral injection of LPS 5mg/kg or PBS for four hours. Mice were perfused and the brains were removed, digested and myelin was removed, before microglia were isolated using magnetic beads. The induction of inflammatory genes was determined using qPCR with fold changes shown relative to the housekeeping gene *Hprt1* for **A)** *Tnf,* ***B)*** *Il1b* **C)** *Il12a* and **D**) *Il6*. Data shown is representative of 2 independent experiments, * $p<0.05$, ** $p<0.01$. Significance was calculated using the unpaired two tailed student t-test between individual groups.

5.9 mTOR inhibition leads to an upregulation of age-associated and sensing genes *Tlr2* and *Clec7a*

In the RNA sequencing data described in the previous chapter, I found an upregulation of both inflammatory pathways and the mTOR pathway in microglia from the ageing brain under basal conditions. This led to the hypothesis that the mTOR pathway could be regulating some of the transcriptional changes observed with ageing, possibly through regulation of transcription factors such as NF-κB. To test this hypothesis, I assessed some of the genes found upregulated with age in Rheb KO microglia such as *Tlr2* and *Clec7a*.

Tlr2 has been implicated in Alzheimer's disease, where it is thought to be a ligand for amyloid beta[197] and in other neurodegenerative disorders[182]. Clec7a, or Dectin-1, is also a pattern recognition receptor thought to function together with Tlr2 to mediate the inflammatory response[175].

Figure **5.9** shows the RNA sequencing results for these two age-related genes, *Tlr2* and *Clec7a*. Both these genes were found to steadily increase with age in microglia, as shown by the FPKM expression values in **Fig. 5.9A** and **Fig. 5.9B**. In the LPS *in vivo* experiments, it was found that especially *Tlr2* (**Fig. 5.9C**) but also *Clec7a* (**Fig. 5.9D**) were upregulated in Rheb KO microglia from young mice. A further increase was observed in the aged group for *Clec7a* ($p<0.001$) between young Rheb KO microglia and old Rheb KO microglia (**Fig. 5.9D**). However, this was not the case for *Tlr2*, where the age of the KO did not seem to affect its pattern of expression (**Fig 5.9C**).

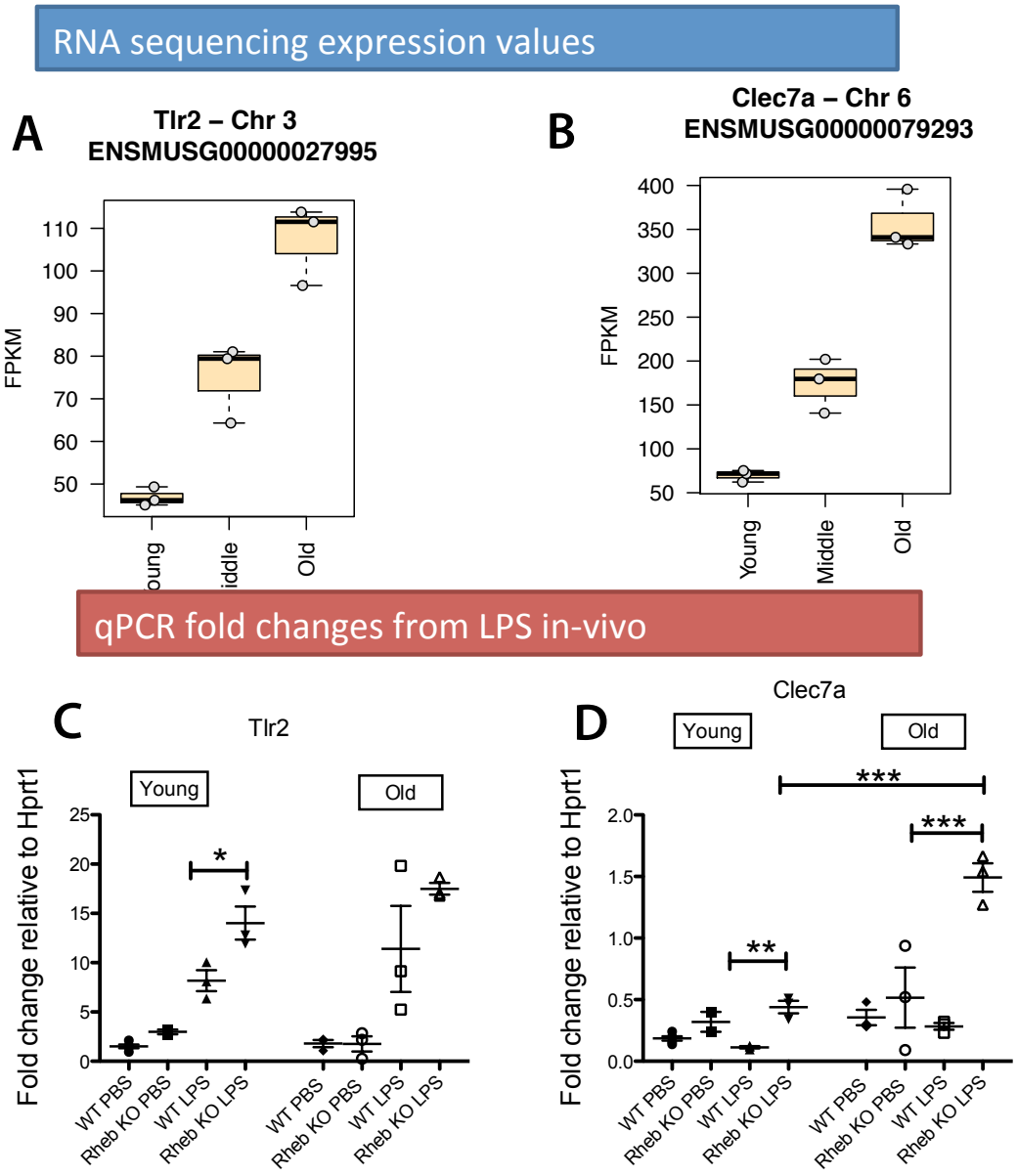

Fig. 5.9 *In vivo* mTOR inhibition leads to an upregulation of age-associated genes *Tlr2* and *Clec7a* in microglia. Microglia isolated from young and aged mice was used for RNA sequencing analysis. The expression values for **A)** *Tlr2* and **B)** *Clec7a* are shown. **C)** and **D)** Young and old Rheb KO and WT mice were given a peripheral injection of LPS 5mg/kg or PBS and culled after four hours. Mice were perfused and the brains were removed, digested and myelin was removed before microglia were isolated using magnetic beads. The induction of **C)** *Tlr2* and **D)** *Clec7a* was determined using qPCR, shown as fold change relative to the housekeeping gene *Hprt1*. Data shown are representative of 2 independent experiments, * $p<0.05$, *** $p<0.001$. Significance was calculated using the unpaired two tailed student t-test between individual groups.

5.10 The mTOR pathway regulates the expression of other age-associated genes upon LPS injection *in vivo*

I examined a range of other genes that appeared to be deregulated with age, especially genes most differentially expressed with age or linked to inflammation. These included the glycoprotein, *Gpnmb*, previously discussed in chapter 4. This gene was one of the most upregulated genes with age in microglia. I found an increase in the expression of this gene in Rheb KO microglia compared to WTs. This appeared to be at steady state, as it was observed in both the PBS controls and did not increase further upon LPS stimulation. These differences were only evident in young mice, with no differences being observed in any of the groups with age (**Fig. 5.10A**). *Cxcl13* (**Fig. 5.10B**), the most upregulated chemokine with age, and *Ccl25* (**Fig. 5.10C**), one of the most down-regulated chemokines in microglia with age, were also examined. There was no difference in expression of these genes in any of the groups tested, suggesting that mTOR inhibition did not appear to regulate their expression in either young or aged mice. The same was true for the age-related gene *Apoe4*, also known as alpoliprotein C4 (**Fig. 5.10D**).

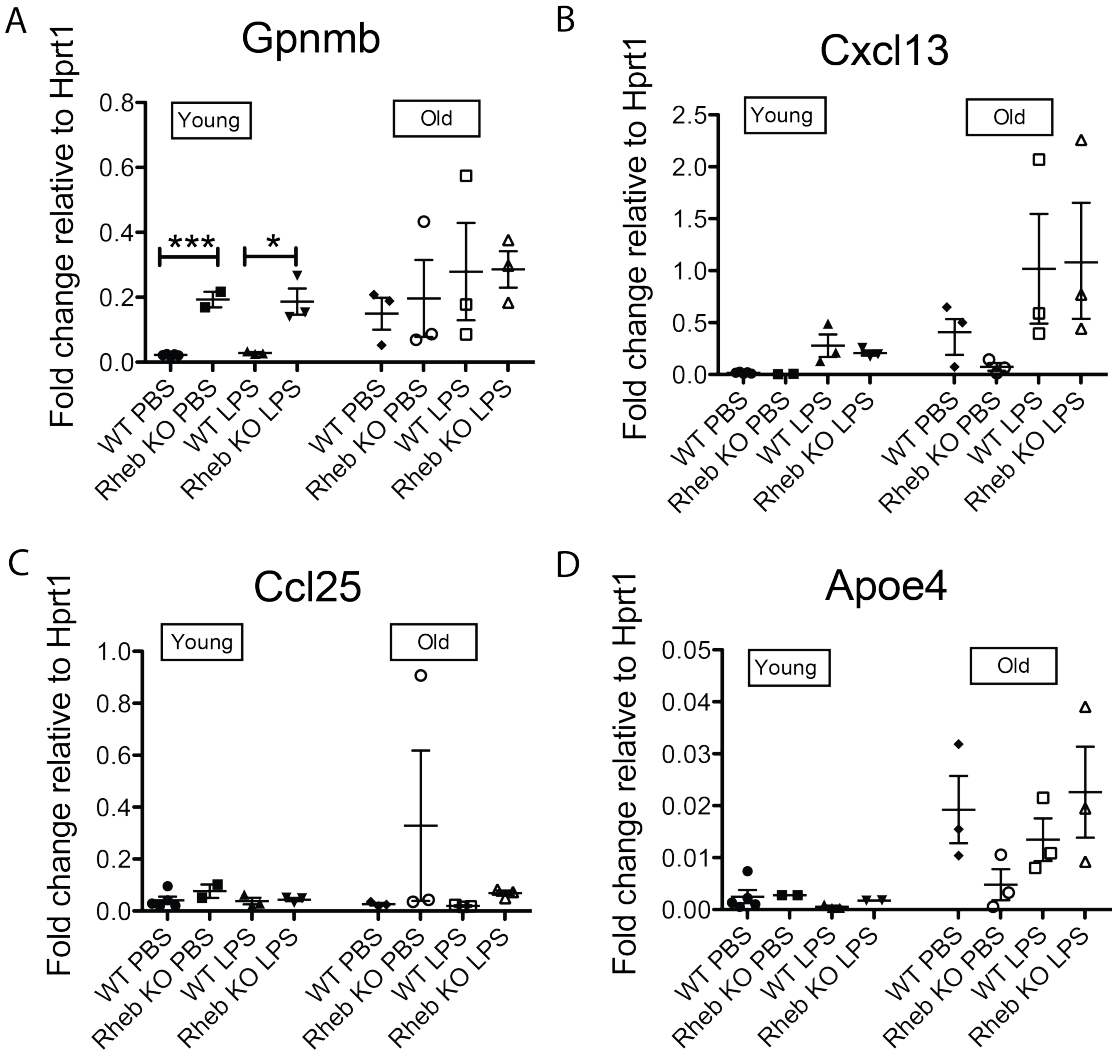

Figure 5.10 *In vivo* mTOR inhibition does not regulate the expression of all age-related genes. Young and old Rheb KO and WT mice were given a peripheral injection of LPS 5mg/kg or PBS and culled after four hours. Mice were perfused and the brains were removed, digested and myelin removed, before microglia were isolated using magnetic beads. The induction of **A)** *Gpnmb*, **B)** *Cxcl13,* **C)** *Ccl25* and **D)** *Apoe4* was determined using qPCR, shown as fold change relative to the housekeeping gene *Hprt1*. Data shown are representative of 2 independent experiments, * $p<0.05$, ***$p<0.001$. Significance was calculated using the unpaired two tailed student t-test between individual groups.

The age-related genes *Spp1, Cst7* and *Mmp12*, however, were significantly affected by loss of Rheb in microglia (**Fig. 5.12A-C**). Spp1, secreted phosphoprotein 1 or osteopontin is a cytokine upregulated in a number of central nervous system pathologies[166]. Its expression appeared to be strongly mediated by mTOR, as its inhibition lead to an increase in *Spp1* expression in microglia from both young and aged mice (**Fig. 5.11D)**.

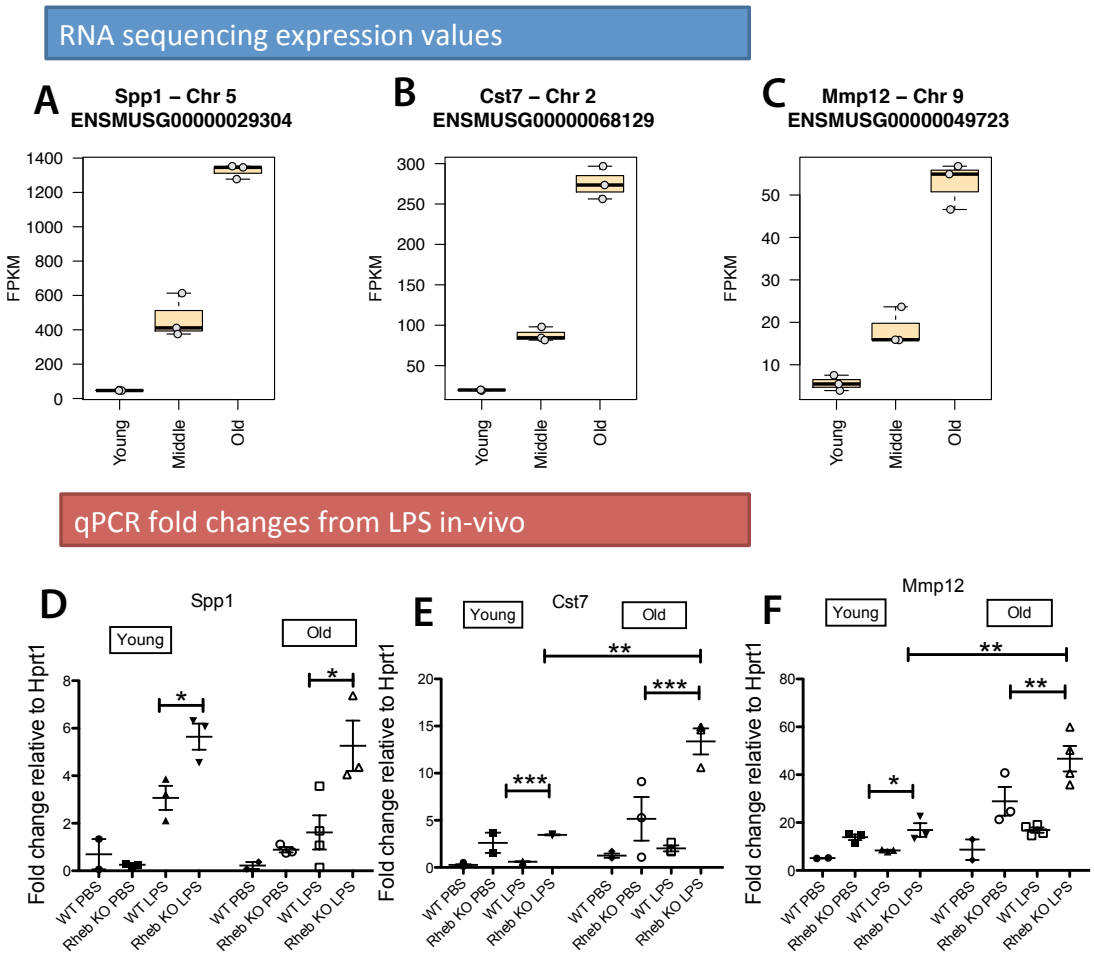

Figure 5.11 mTOR inhibition *in vivo* leads to an upregulation of age-associated genes *Spp1*, *Cst7* and *Mmp12* in microglia. Microglia isolated from young and aged mice were used for RNA sequencing analysis. The expression values for three genes that were upregulated with age are shown: **A**), *Spp1*, **B)** *Cst7* and **C)** *Mmp12*. **D**) to **F**) Young and old WT and Rheb KO mice were given a peripheral injection of LPS 5mg/kg or PBS and culled after four hours. Mice were perfused and the brains were removed, digested and myelin removed before microglia were isolated using magnetic beads. The induction of **D**) *Spp1* **E)** *Cst7* and **F**) *Mmp12* was determined using qPCR and shown as fold change relative to the housekeeping gene *Hprt1*. The data shown are representative of two independent experiments, *p<0.05, **p<0.01, *p<0.001. Significance was calculated using the unpaired two tailed student t-test between individual groups.

Next I looked at Cystatin F, *Cst7*, a papain-like lysosomal cysteine protease inhibitor. This is an interesting gene, as its expression in microglia has recently been associated with acute demyelination[168]. Similarly to *Spp1*, its expression is significantly increased in microglia with mTOR inhibition (p<0.001; **Fig. 5.11E)**. Unlike *Spp1*, its expression seems to be exaggerated with age upon LPS challenge (p<0.01).

Lastly I looked at the Metallopeptidase 12 known as *Mmp12*. Mmps play multiple roles in signalling, migration and extracellular matrix remodelling. Mmp12 has recently been associated with ageing of the brain and neuroinflammation[169]. It was also the most upregulated *Mmp* in the RNA sequencing data. Its pattern of expression upon mTOR inhibition is similar to *Cst7,* with an upregulation in Rheb KO microglia in both age groups and a more exaggerated effect with age (**Fig. 5.11F).**

In conclusion, it appears that mTOR plays a role in regulating expression of some age-related genes but not all. Overall, it seems to negatively regulate the expression of a number of age-related genes, since its loss in Rheb KO microglia leads to their upregulation. This observation is difficult to reconcile with the upregulation of mTOR signalling in aged microglia. It is possible to speculate that the upregulation of mTOR with age is not responsible for the increased expression levels of inflammatory and age-related genes but rather is an attempt of microglia cells to counteract the pro-inflammatory phenotype associated with age.

5.11 Possible regulators of inflammation affected by mTOR inhibition

It has been shown previously that mTOR inhibition with rapamycin in human monocytes leads to an upregulation of inflammatory genes through an activation of NF-κB, suggesting that mTOR is a negative regulator of NF-κB[129]. I observed a similar upregulation of inflammatory genes when the pathway was inhibited by Rheb deletion. Therefore, I monitored the expression of the NF-κB gene, *Rela,* which encodes p65, to assess whether it was deregulated in Rheb KO microglia. P65 forms a complex with p50 and IKβα. Once IKβα becomes phosphorylated, it is targeted for degradation and this leads to the translocation of the p65/p50 complex into the nucleus, where it can drive the transcription of a number of NF-κB target genes, including inflammatory ones.

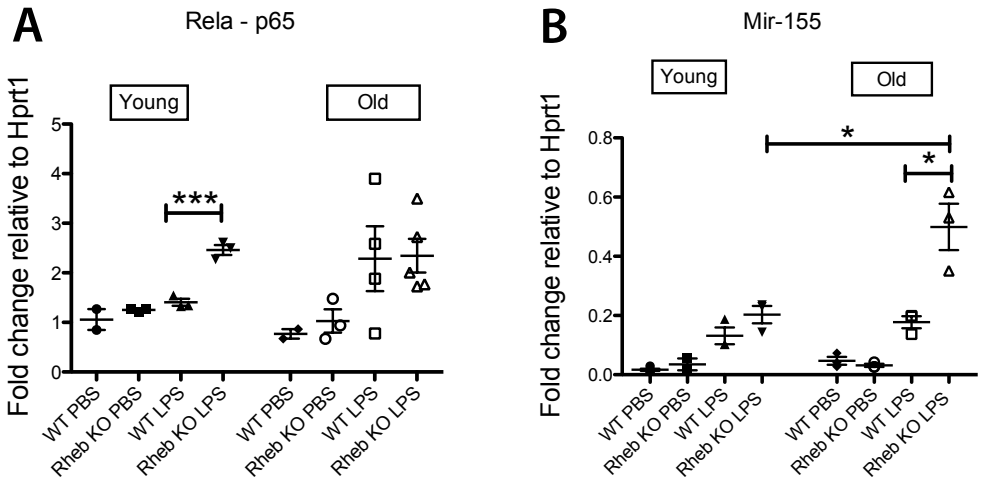

5.12 mTOR inhibition *in vivo* leads to an upregulation of regulators of inflammation in microglia. Young and old WT and Rheb KO mice were given a peripheral injection of LPS 5mg/kg or PBS and culled after four hours. Mice were perfused and the brains were removed, digested and myelin removed before microglia were isolated using magnetic beads. The induction of **A**) *Rela* (encoding p65) and **B**) *Mir-155* was determined using qPCR. The data shown are representative of 2 independent experiments, * $p<0.05$, ***$p<0.001$. Significance was calculated using the unpaired two tailed student t-test between individual groups.

There was a clear upregulation of p65 expression upon LPS injection in microglia from young mice when mTOR was inhibited ($p<0.001$). I did not, however, observe the same increase in gene expression in aged mice (**Fig. 5.12A**).

I also monitored the gene coding for the microRNA, *mir-155*. I was interested in this gene because it was highly upregulated in the RNA sequencing data of microglia from the ageing brain and it has been implicated in pro-inflammatory responses in a number of models[203]. Interestingly, it was found to have a similar pattern of expression as many of the age-related genes and inflammatory genes, showing to be upregulated upon LPS injection in microglia from Rheb KO mice compared to WTs, an effect further exaggerated with age (**Fig. 5.12B).**

5 Discussion

5.1 Questions to be addressed

mTOR activation has been observed in a number of tissues with age and overall the pathway has been accepted as a major regulator of ageing[30]. This comes from a long list of studies that have shown that both genetic and pharmacological inhibition of the pathway leads to lifespan extension in a number of model organisms[31]. As a result, mTOR inhibitors are being considered as potential ageing interventions.

Given the association of mTOR activation with ageing, it is not surprising that this pathway appears to be upregulated in microglia from the ageing brain. What remains to be addressed is the role played by mTOR activation in microglia, i.e. how is it affecting the function of these cells? One suggestion is that it may be involved in regulating senescence, particularly the secretion of the SASP, as rapamycin appears to attenuate this phenotype in senescent fibroblasts[142]. Other studies have shown that inhibiting the mTOR pathway in primary human monocytes actually leads to NF-κB activation and an increase in inflammatory cytokines[129]. While these reports appear conflicting, they do indicate that mTOR is an important regulator of inflammation, possibly exerting different functions depending on the signals it receives. These studies lead us to ask a number of questions, such as - what role is mTOR playing in microglia from the ageing brain? Could it be regulating some of the transcriptional changes I have observed, particularly those relating to inflammation? Could mTOR be involved in microglia priming? Could mTOR be important for regulating neuroinflammation in age-associated pathologies?

5.2 Increase in pro-inflammatory cytokine genes in microglia from *Csf1r-Cre; Rheb f/f* mice

In order to answer some of these questions, I decided to use a model of LPS-induced brain inflammation via a peripheral injection. I hypothesised that if mTOR was involved in microglia priming and regulating inflammatory responses with age, this should be further increased or attenuated in a model of neuroinflammation. I found that upon *i.p.* LPS injection, the mRNA expression of pro-inflammatory cytokines *Tnf*, *Il6*,

Il12a and *Il1b* were all upregulated in microglia from Rheb KO mice. The fact that I found that phospho-S6 was downregulated in microglia from Rheb KO mice compared to WT microglia would give an indication that mTOR was inhibited in these cells and that mTOR may play a role in regulating inflammation in microglia. However it cannot be ruled out that phospho-S6 might have been downregulated in Rheb KO microglia as a consequence of mTOR being inhibited in other myeloid cells and therefore a result of changes in peripheral cytokine levels.

One way to address this question in the future is to consider the use of another mouse model. I have used the *Csfr1*-Cre model in my study as it's well used for the study of myeloid cells and it was the most readily available model in my lab. However, this model has some disadvantages most notably, not being able to decipher between resident macrophage populations in the brain and microglia and also not being able to discount perpetuations in the periphery due to the affects on monocyte populations. This is because these populations also express Csfr1. Other models used to study specific gene deletions in microglia use promoters such as CD11b or CX3CR1, however these markers are also expressed by other myeloid population and therefore do not offer a better alternative. Goldman *et al.* recently developed a novel Cre-LoxP-based system that can be used to target microglia but not monocyte derived macrophages. This system is induced using the estrogen antagonist tamoxifen (TAM)[204]. While the use of TAM will induce the deletion in both microglia and other CX3CR1+ monocytes and macrophages, these cells are known to be relatively short lived and constantly replaced by the bone marrow whereas microglia remain permanently modified[205]. Therefore it would be really interesting to cross this model with the Rheb f/f mice in order to determine if the results I have observed are microglia specific. This is an important consideration for the ageing *in vivo* studies where is has to be considered that the deletion is in all the myeloid cells and also present for the entire lifespan of the mouse. It would also be interesting therefore, to delete Rheb in microglia at different points during the lifespan to understand if this would lead to similar results.

This work is also consistent with reports that inhibition of the pathway in primary monocytes leads to an increase in cytokine production[129]. I also saw a consistent upregulation of these cytokines in microglia isolated from the aged brain, but what is really interesting, is that the effect was exaggerated with age. I can speculate that if

mTOR activation is important for regulating microglia priming, then it is conceivable that the cells become even more primed when the pathway is inhibited and, therefore, even more over-responsive to an inflammatory stimulus such as LPS. These observations lead to some relevant questions, discussed below:

1) Are the transcriptome changes observed in Rheb KO microglia being translated?

Given that the main function of mTOR is to regulate translation and cell growth in cells, it is important to understand if these changes at the transcriptome level are being translated. Activation of mTOR leads to phosphorylation of S6 and 4E-BP1, which influence initiation and elongation of translation, respectively[114]. There are conflicting reports about whether rapamycin affects mTOR-mediated translation, since there are rapamycin-resistant functions of mTORC1[115]. This is important, specifically with regards to the studies showing that mTOR inhibition with rapamycin leads to an increase in inflammatory cytokines[129]. In this study, the authors show that cytokines are upregulated at transcriptome and protein levels[129]. This may not be the case in our model, where the pathway is genetically inhibited through loss of Rheb. This can be tested in a variety of ways. Firstly, a protein lysate can be made from the tissues from the LPS *in vivo* study described in this chapter and can be used to perform ELISA to quantify the amounts of pro-inflammatory cytokines in KO versus WT tissue. This would indicate if there is more tissue inflammation in the Rheb KO mice upon LPS-stimulation. It would be particularly relevant to use brain lysates. Secondly, I can perform *in vitro* studies with Rheb KO BMDMs or primary microglia, whereby the cells are stimulated with LPS and then the amount of pro-inflammatory cytokines are measured in the supernatant, also by ELISA. Thirdly, I can measure cytokines in the plasma from our LPS *in vivo* study to assess cytokine production.

Inflammation in elderly people can result in delirium, where the person becomes confused and agitated, as well as experiencing a range of other cognitive symptoms. Delirium is thought to be mediated by infections in the periphery having secondary effects in the brain[206]. One way of assessing the effect of inflammation in our KO mice would be to use the open-field test to assess how sick the mice become. While this simple test is not suitable to define delirium, it can give information on locomotor activity and anxiety behavior and is a good measure of systemic inflammation[87]. It

would also give an indication of whether these cytokine changes observed on a transcriptome level are in fact being translated.

2) What is the potential mechanism regulating these transcriptome changes?

Weichhart *et al.* showed that mTOR inhibition with rapamycin leads to an increased inflammatory phenotype in macrophages via NF-κB activation; the mechanism could be different, however, in a model where the pathway is inhibited genetically and therefore NF-κB involvement would have to be confirmed. This could be done by staining for the NF-κB subunit, p65, in microglia. p65 localises to the nucleus rather than the cytoplasm when the pathway is active. Another way to confirm NF-κB activation upon Rheb deletion would be performing time-course experiments using BMDMs and looking at key proteins involved in NF-κB signalling such as p-IKKα, and p-IKβα[207], both should be stronger if NF-κB is more strongly activated (followed by an earlier degradation of p-IKβα). If it appears that NF-κB is indeed more active in our model, it would be interesting to understand the intracellular pathways that link mTOR inhibition and NF-κB activation, as these remain unclear. Some potential pathways that intersect with mTOR could be:

A. Activation of AMP kinase[208], which could result in increased p38 activation[209], leading to NF-κB activation[210].
B. Other potential candidates may include members of the autophagy pathway as autophagy activation is a consequence of mTOR inhibition and has also been linked to inflammasome activation[211].

5.3 Age-related genes

I also examined a number of differentially expressed genes from the RNA sequencing data i.e. genes that were deregulated with age in microglia that were not key inflammatory genes. Interestingly, I found that 5 out of the 10 genes analysed appeared to be regulated by mTOR. Of these 5 genes – *Tlr2*, *Clec7a*, *Mmp12*, *Cst7* and *Spp1* – three are known targets of NF-κB, such as *Tlr2*, *Cst7* and *Spp1*. This evidence further supports the notion that NF-κB activation is increased in Rheb KO microglia and may

also support the idea that mTOR activation in microglia in the ageing brain may be a mechanism to limit the upregulation of some of these genes.

5.4 Limitations

When examining our data, it is important to acknowledge some of the limitations of both the cells and models used. While BMDMs are an accepted model to look at macrophage function and molecular signalling, they may behave differently to microglia cells. It was important to confirm that the upregulation of inflammatory cytokines upon LPS stimulation *in vitro* in BMDMs lacking Rheb was also evident in primary microglia. I wanted to use adult microglia as they would be the closest model to our ageing data but they are difficult to culture. Therefore, I isolated primary microglia from the adult brain and stimulated them for a short period of time *in vitro*. While the qPCR data was consistent with the BMDM data, it must be acknowledged that, in the un-stimulated microglia cells, there was already a high basal level of inflammatory cytokines, particularly *Tnf*. This indicates that the cells were not in a good condition. It would be important to repeat both the signalling experiment with p-S6 and the qPCR in primary microglia isolated from neonate mice. These cells are obtained by culturing whole brain tissue on poly-d-lysine for 10 days, therefore microglia grow on a feeder layer of astrocytes and can then be recovered for *in vitro* culture experiments. This is a more established method for *in vitro* experiments, using primary microglia, and will be carried out in the future to support our current data[212].

I must also consider the limitation of using a peripheral injection of LPS as a model of inflammation. While this approach was chosen to mimic the effect of a peripheral infection in the elderly, it also complicates the interpretation of results. This is particularly true for our model, given that the *Csf1r-Cre* will cause Rheb deletion in microglia but also monocytes and macrophages in the organism. There may be more peripheral inflammation present in our Rheb KO model that could be contributing to the priming of the microglia with age, rather than a direct effect of Rheb deletion on the microglia. In order to assess the relevance of mTOR signalling in microglia from aged Rheb KO mice, I performed phospho-flow cytometry analysis, which showed an increase in phospho-S6 in aged WT microglia and a reduction in Rheb KO microglia.

This evidence supports the notion that the effect on inflammatory cytokines is specific to mTOR inhibition in microglia, rather than a secondary affect from the periphery. I cannot, however, exclude that the peripheral environment contributes to microglia inflammation in our mouse model.

5 Conclusion

In conclusion, it appears that mTOR inhibition by Rheb deletion leads to an increase in inflammatory cytokine gene expression upon LPS stimulation in both BMDMs and microglia. This is evident both *in vitro* and *in vivo***.** This upregulation is further increased with age, suggesting that the mTOR pathway plays a role in microglia priming. Surprisingly, mTOR inhibition also regulated the gene expression of additional age-related genes, suggesting that mTOR regulates at least some of the transcriptome changes observed in our RNA sequencing analysis. While more work is needed to clarify the role of mTOR in microglia with age, this data would support the hypothesis that it is a key player of inflammation in ageing.

Chapter 6: Sickness behaviour and cytokine production in *Csf1r-Cre; Rheb f/f* mice

As described in the previous chapter, *Csf1r-Cre; Rheb f/f* (Rheb KO) mice showed increased expression of inflammatory genes upon LPS stimulation compared to WT controls. Thus, I wanted to investigate if these changes were also observed at protein level and whether the increased inflammation in the brain had an impact on neurological functions.

6.1 Increased gene expression of pro-inflammatory genes in Rheb KO BMDMs is not accompanied by an increase at protein level

In order to assess if the increase in gene expression of inflammatory genes was translated into the corresponding proteins, I used BMDMs derived from both WT and Rheb KO mice. Bone marrow cells were purified from adult mice and differentiated into macrophages by a 6-day culture in the presence of M-Csf. Once differentiated, cells were re-plated and treated with LPS at three different time points; 3, 6 and 24 hours. Following LPS stimulation, secreted cytokines were measured by ELISA in the culture supernatant, whereas cells were lysed, RNA was extracted and quantitative PCR (qPCR) was carried out on key inflammatory genes.

The genes measured were *Tnf, Il1b*, *Il6* and *Il12*. TNF is one of the first cytokines to be produced under inflammatory conditions and can amplify and prolong the inflammatory response by activating other cytokines such as IL-1[213]. By qPCR analysis of mRNA levels, I found that in WT cells this gene was induced at 3 hours post LPS treatment, with similar levels observed at 6 hours before a decline by 24 hours (**Fig. 6.1A**). As expected, there was considerably more *Tnf* production in the Rheb KO BMDMs at 3 hours post LPS, however, its levels were comparable to WT cells at 6 and 24 hours (**Fig. 6.1A**), similarly to what I observed in Rheb KO microglia after *in vivo* LPS stimulation**.** Surprisingly, measurement of Tnf protein by ELISA showed an opposite trend to that observed by qPCR analysis. While protein levels were similar at 3 hours,

the Rheb KO BMDMs were producing considerably less Tnf at 6 hours post LPS treatment compared with WT controls (**Fig. 6.1B**). By 24 hours, Tnf levels were again similar in WT and Rheb KO cells.

I also assessed levels of the cytokine gene *Il1*b. Again, as expected, Rheb KO BMDMs stimulated with LPS had an increased expression of *Il1b* compared to WTs, as measured by qPCR, with a peak of expression for both WTs and Rheb KO BMDMs at 6 hours (**Fig. 6.1C**). An ELISA on Il-1β in the supernatant was also carried out. It is well documented that macrophages must first be primed with interferon-γ overnight before being treated with LPS in order to stimulate the production of Il-1β. This is because two distinct steps, priming and activation, are required for the generation of Il-1β. First, expression of the proform of Il-1β is induced, which is subsequently cleaved by caspase-1 activated by the inflammasome, into its active form[214]. However, in my experimental conditions, I stimulated cells with LPS only and as such I expected to see much less Il-1β production compared to Tnf. Nevertheless, IL-1β levels were comparable to Tnf, with less Il-1β in Rheb KO BMDMs compared to WTs at 6 hours post LPS stimulation (**Fig. 6.1D**).

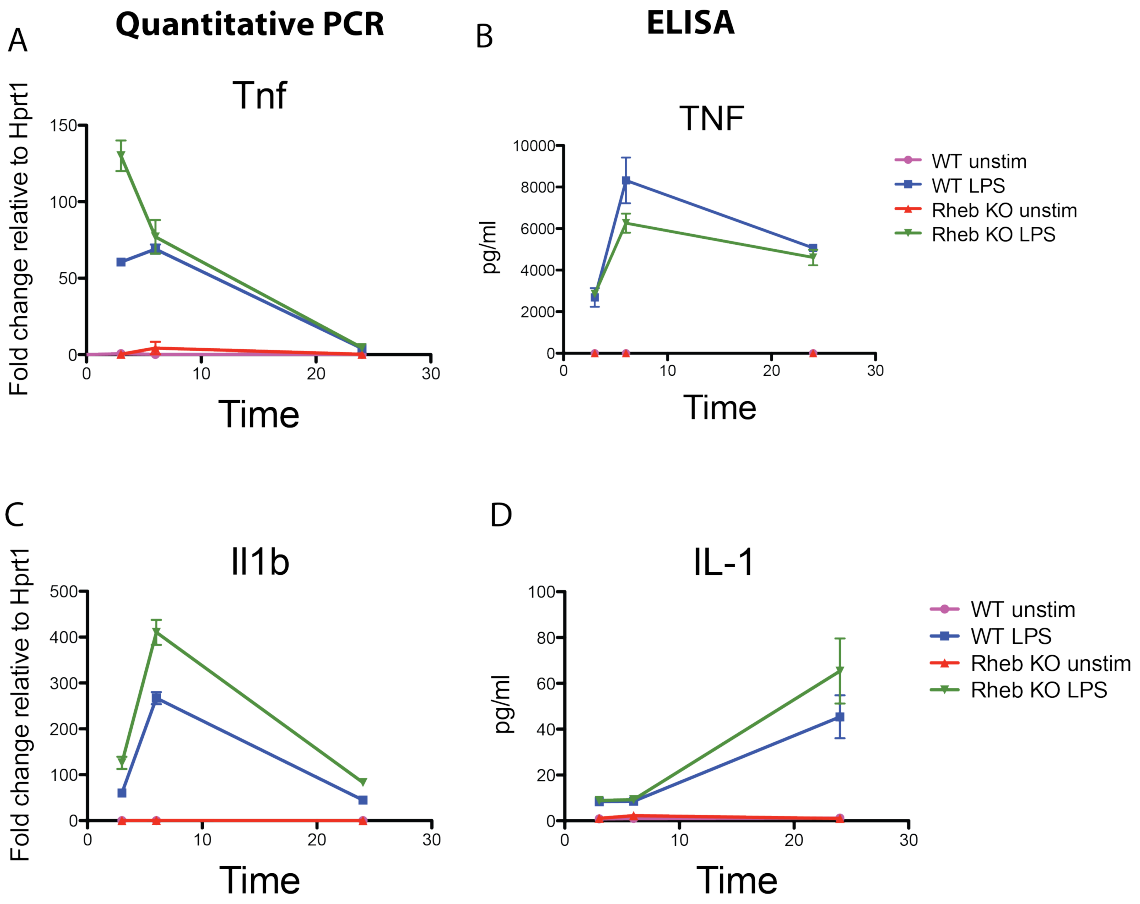

Figure 6.1 Increases in gene expression of pro-inflammatory genes *Tnf* and *Il1b* in Rheb KO BMDMs are not consistent with secreted protein levels. Rheb KO and WT macrophages were obtained from the bone marrow and differentiated for 6 days with 20 ng/ml of M-Csf to generate BMDMs. BMDMs were then re-plated on day 6 and left to rest overnight. The following day, they were stimulated with 200 ng/ml of LPS for 3, 6 and 24 hours. The induction of **A)** *Tnf* and **C)** *Il1b* was determined using qPCR, results are shown as fold change over the housekeeping gene *Hprt1*. **B)** Tnf and **D)** Il-1β secreted in the culture supernatants were assessed by ELISA. Data shown is from one experiment, where n=2 for all time-points and conditions shown.

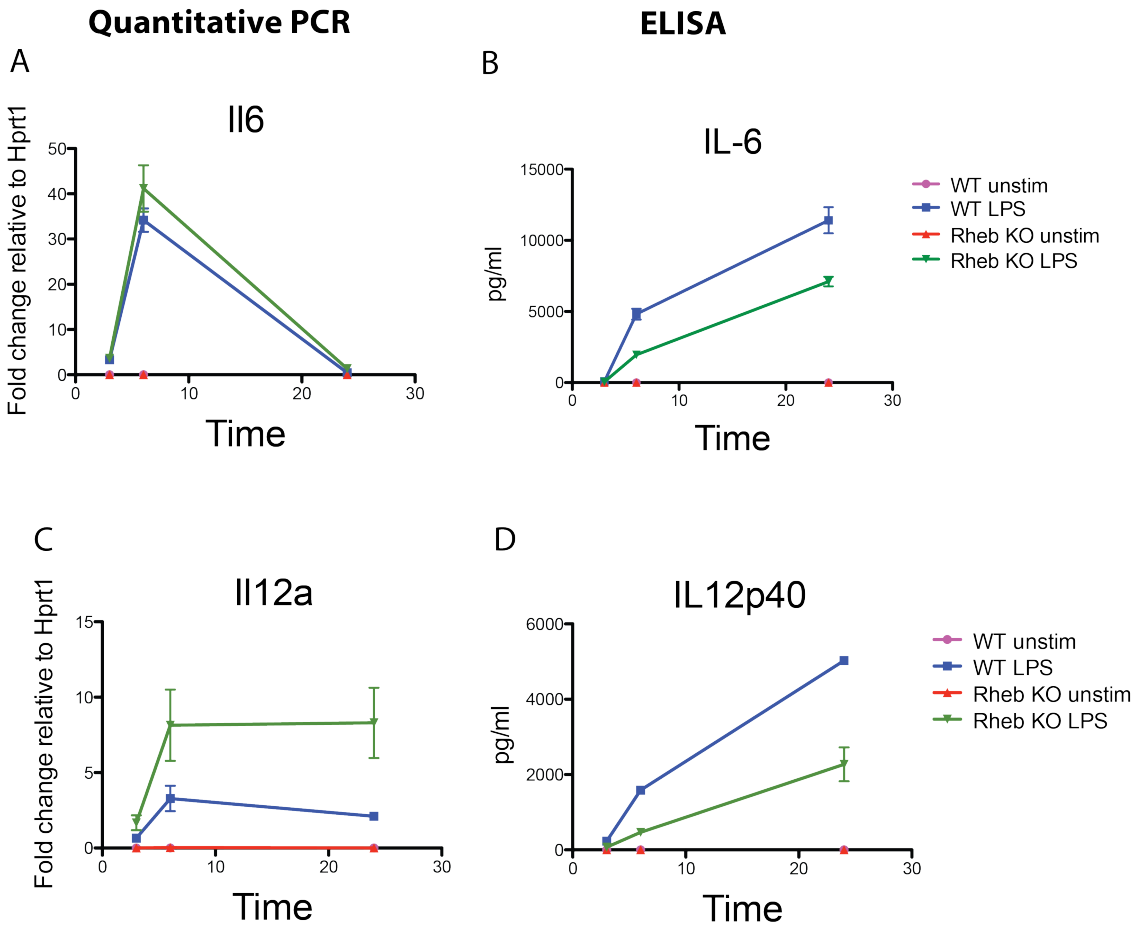

Figure 6.2 Increased gene expression of pro-inflammatory genes *IL6* and *IL12a* in Rheb KO BMDMs is not consistent with secreted protein levels. Cells were obtained from the bone marrow of WT and Rheb KO mice and differentiated in culture for 6 days with 20 ng/ml of M-Csf, in order to generate BMDMs. BMDMs were then re-plated on day 6 and stimulated with 200 ng/ml of LPS for 3, 6 and 24 hours. The induction of **A)** *Il6* and **C)** *Il12a* was determined by qPCR, results are shown as fold change relative to the housekeeping gene *Hprt1*. **B**) Il-6 and **D)** Il12p40 secreted in the culture supernatant were assessed by ELISA. Data shown is from one experiment, where n=2 for all time-points and conditions shown.

Given that this result was quite striking, I next assessed whether Il-6 and Il-12p40 behaved in a similar fashion. *Il6* was only slightly increased in Rheb KO cells compared to WT, whereas *Il12a* was significantly increased at both 6 and 24 hours, as measured by qPCR (**Fig. 6.2A** and **6.2C**). Proteins secreted in the supernatant were measured, and both Il6 and Il12p40 were decreased in the supernatant of Rheb KO cells at 6 and 24 hours (**Fig 6.2B** and **6.2D**), a result in direct contrast to the gene expression data. Statistical analysis could not be carried out on this set of data as the n number only equalled two and therefore additional replicates would be needed to test significance. Nonetheless, this experiment indicated that Rheb KO macrophages behaved differently to rapamycin-inhibited macrophages[129] upon LPS stimulation.

6.2 Inflammation was not induced above baseline in Rheb KO mice after *in vivo* LPS stimulation compared to WT controls

Given that cytokine production appeared to be decreased in Rheb KO BMDMs, despite the increase in gene expression, I wanted to test if this was also the case *in vivo*. To this end, I took lung tissue from mice, which had received a single intraperitoneal injection of LPS at a dose of 5 mg/kg. I selected the lung as this organ is known to contain a high number of macrophages. Protein lysates from frozen lung tissue were prepared and used for ELISA in order to measure Tnf. Indeed, there was decreased Tnf in the lungs of Rheb KO mice compared to WT controls (**Fig. 6.3**). Differences were evident in both young and aged mice, although they appeared more striking in the younger age group. However, differences were not significant, perhaps because of the variability observed in the Rheb KO samples.

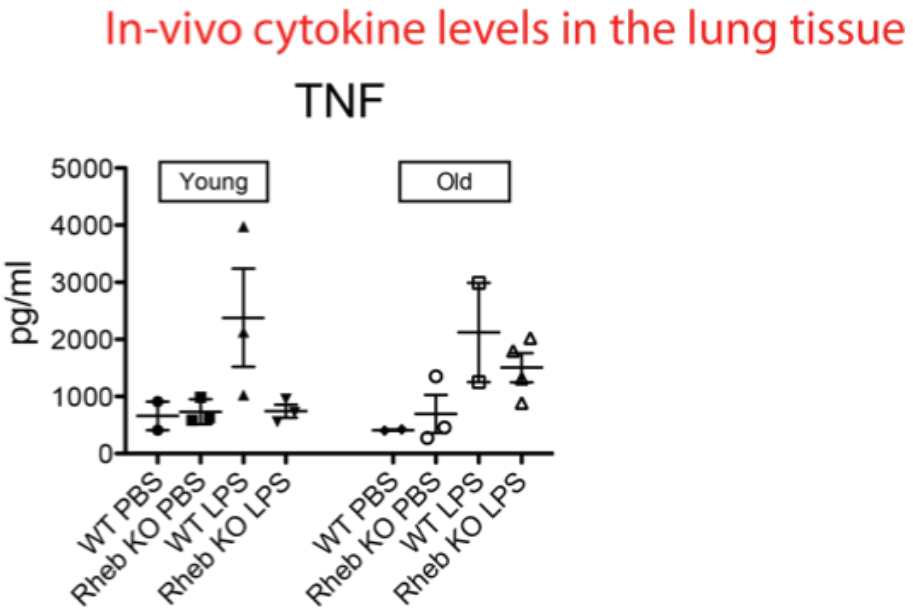

Figure 6.3 Reduced Tnf protein levels in the lungs of Rheb KO mice treated with LPS. Young and old Rheb KO and WT mice were given an i.p. injection of LPS, 5mg/kg and culled 4 hours later. Protein lysates were prepared from the lung tissue and Tnf was measured by ELISA. Data are from one experiment, where n=3 for each group.

Both the *in vitro* and *in vivo* data suggested that cytokines were not being translated in the Rheb KO mice. I wanted to further confirm this finding *in vivo*. To this end, I used a new cohort of Rheb KO and WT mice and gave them an i.p. injection of LPS (5

mg/kg). However, instead of perfusing the animals as in previous experiments, mice were culled by cardiac puncture in order to collect blood. This way, I was able to quantify the amount of Tnf (**Fig. 6.4A**) and Il12p70 (**Fig. 6.4B**) in the plasma from both young (4 month) and old (22 month) Rheb KO and WT mice. While it appeared that there was less Tnf (**Fig. 6.4A**) and Il12p70 (**Fig. 6.4B**) in young Rheb KO mice compared to controls, the differences were not significant (Tnf, p=0.08 and Il12p70, p=0.09). On the other hand, there was a robust induction of both cytokines with age in the WT control groups, which was not observed in the aged Rheb KO mice. This result was striking for both cytokines (**Fig. 6.4A** and **Fig. 6.4B**) and was highly significant in both cases with a p value <0.001.

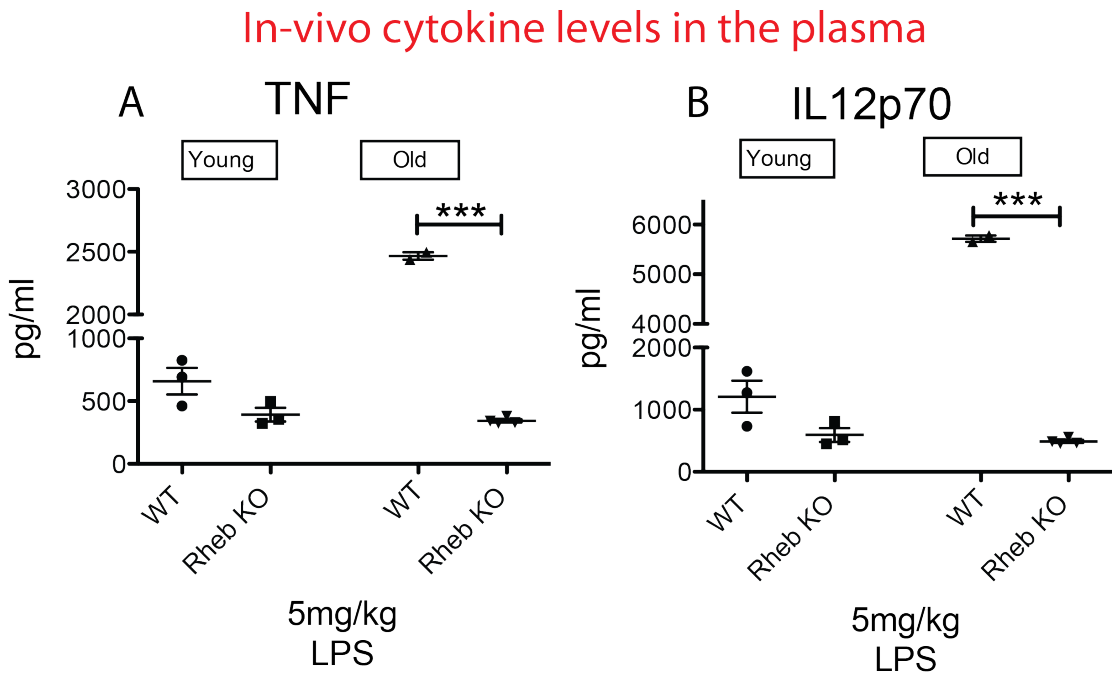

Figure 6.4 Cytokines are not translated in aged Rheb KO mice upon LPS stimulation. Young and old Rheb KO and WT mice were given an i.p. injection of LPS, 5mg/kg and culled 4 hours later by cardiac puncture. Plasma was obtained from blood and then cytokines were measured using the legendplex mouse inflammatory panel from Biolegend. The amount of **A)** Tnf and **B)** Il12p70 is shown. Data shown are from one experiment, where n=3 for all groups and ***p<0.001. Significance was calculated using the unpaired two tailed student t-test between individual groups.

6.3 Optimisation of an *in vivo* experiment to assess sickness behaviour

The *in vitro* and *in vivo* results so far suggested that Rheb KO mice may have less overall inflammation upon LPS stimulation compared to WT mice, the opposite of what

I hypothesised based on the increased transcription levels of pro-inflammatory cytokines. In order to elucidate the overall effect on the host response, I carried out an additional experiment with a lower dose of LPS of 0.33 mg/kg. Mice are not terminally sick with this dose of LPS[87] and behavioural tests can be carried out after the LPS injection, in order to measure sickness behaviour. If overall inflammation was decreased in Rheb KO mice upon LPS stimulation, mice should be less sick.

Sickness behaviour was measured with an open-field test. The test was carried out by placing each mouse into an empty 15-square gridded box and observing its behaviour for 5 minutes. Several parameters can be measured: the distance travelled and number of rears, which give an indication of the locomotor ability. The time spent in the middle of the box, and time delay before the mouse enters the squares in the middle of the box, which provide a measurement of stress and anxiety[215]. Sicker mice are expected to have impaired locomotion and increased anxiety, resulting in reduced movement, rears and time spent in the middle of the box.

I could not use the 5 mg/kg high dose of LPS previously described, as the mice became too sick too quickly, therefore I chose a lower dose of LPS (0.33 mg/kg), as previously reported[216]. I carried out a pilot experiment using this dose of LPS and simultaneously measured a number of different parameters in WT mice, in order to assess the feasibility of the experimental design. Mice were given an i.p. injection of 0.33 mg/kg LPS and the open-field test was conducted at 6 hours.

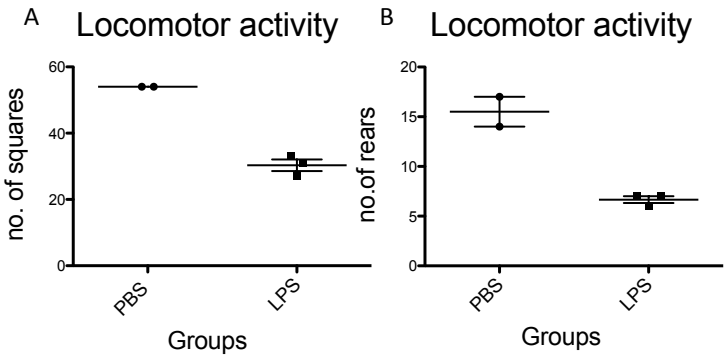

Figure 6.5 Locomotor activity is measurable at 6 hours post low dose LPS treatment. WT mice were given a peripheral injection of either a low dose of LPS (0.33 mg/kg) or PBS before being assessed in an open-field test 6 hours post injection. During the 5-minute test in a 15-square gridded box, locomotor activity was determined by **A**) distance travelled, measured as the number of squares the mouse passes through (with all four paws) and **B**) the number of times the mouse rears up (both front paws) during the 5-minute period.

I found that at 6 hours post LPS injection, there was a clear difference in the locomotor activity of LPS injected mice compared to PBS injected mice. This was measured by two parameters. Firstly, the distance travelled was calculated based on the number of squares each mouse passed through (all four paws had to be in each square). There was a clear decrease in this parameter with LPS (**Fig. 6.5A**). Secondly, locomotor activity was calculated based on the number of times the mouse reared up, both paws, which was also decreased with LPS (**Fig. 6.5B**). Therefore, LPS-treated mice, as expected, were sicker and consequently moved less than the PBS control group.

I could adequately measure sickness behaviour using this dose of LPS and I subsequently wanted to determine if I could still measure some inflammatory parameters after 48 hours with such a low dose of LPS, since it would have been helpful to repeat the open-field test also at a later time-point. I isolated microglia from the brain of these mice (48 hours post LPS) and carried out qPCR analysis on key inflammatory genes. I also isolated Ly6C monocytes from the spleen; I was interested in this cell type because these are the inflammatory cells in the blood that are recruited into the brain during neuroinflammation[217]. I found there were still detectable levels of both *Tnf* and *Il1b* in microglia measured by qPCR (**Fig. 6.6A** and **6.6C**). This was not the case for *Il6* and *Il12a*, which were not much expressed at this time point relative to the house keeping gene (**Fig. 6.6E** and **6.6G**). These observations were not consistent between microglia isolated from the brain and Ly6C monocytes isolated from the spleen, which showed little difference between the LPS and PBS groups (**Fig. 6.6B, 6.6D, 6.6F** and **6.6H**). Furthermore, it appeared that after 48-hours low-dose LPS stimulation, there was still some persistent inflammation in the microglia that was not present in the monocytes.

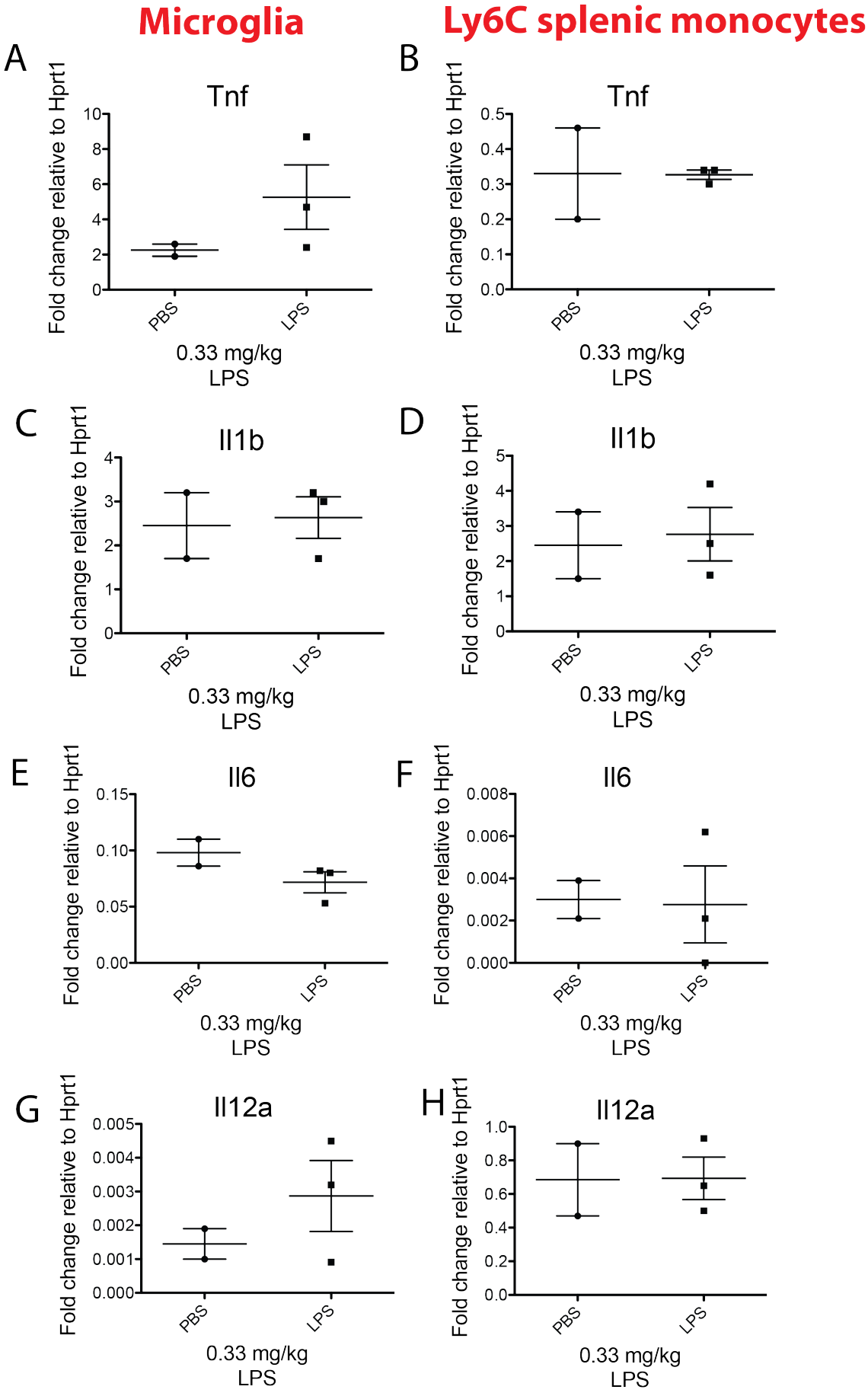
Microglia
Ly6C splenic monocytes
A
Tnf
Fold change relative to Hprt1
10
8
6
4
2
0
PBS
LPS
0.33 mg/kg
LPS
B
Tnf
Fold change relative to Hprt1
0.5
0.4
0.3
0.2
0.1
0.0
PBS
LPS
0.33 mg/kg
LPS
C
Il1b
Fold change relative to Hprt1
4
3
2
1
0
PBS
LPS
0.33 mg/kg
LPS
D
Il1b
Fold change relative to Hprt1
5
4
3
2
1
0
PBS
LPS
0.33 mg/kg
LPS
E
Il6
Fold change relative to Hprt1
0.15
0.10
0.05
0.00
PBS
LPS
0.33 mg/kg
LPS
F
Il6
Fold change relative to Hprt1
0.008
0.006
0.004
0.002
0.000
PBS
LPS
0.33 mg/kg
LPS
G
Il12a
Fold change relative to Hprt1
0.005
0.004
0.003
0.002
0.001
0.000
PBS
LPS
0.33 mg/kg
LPS
H
Il12a
Fold change relative to Hprt1
1.0
0.8
0.6
0.4
0.2
0.0
PBS
LPS
0.33 mg/kg
LPS

Figure 6.6 *Tnf* and *Il1b* gene expression are still detectable in microglia 48 hours post low dose LPS challenge. WT mice were given a peripheral injection of LPS, 0.33 mg/kg, or PBS for 48 hours. Mice were culled by cardiac puncture and the brains were removed and digested before microglia were isolated using magnetic beads. The spleens were also removed and Ly6C monocytes were isolated with magnetic beads similarly to microglia. The induction of inflammatory genes was determined using qPCR for both microglia and splenic monocytes with fold changes relative to the housekeeping gene *Hprt* for *Tnf (***A** and **B**), *Il1b* (**C** and **D**), *IL6* (**E** and **F**) and *IL12a* (**G** and **H**). Data shown are from one experiment, where n=3 for LPS group and n=2 for PBS group.

I also monitored at the expression of the activation markers CD11b and Tlr2 on microglia using flow cytometry analysis and found that both markers were still detectably upregulated with this dose of LPS after 48 hours as shown by their MFI (**Fig. 6.7A** and **6.7B**).

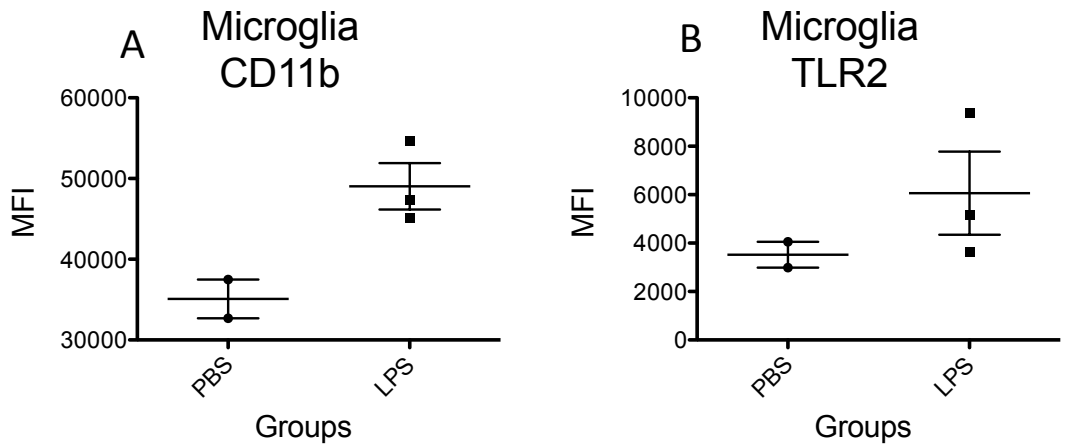

Figure 6.7 Flow cytometry analysis of markers of microglia activation. WT mice were given a peripheral injection of LPS, 0.33 mg/kg, or PBS for 48 hours. Mice were culled by cardiac puncture and the brains were removed and digested before microglia were isolated using magnetic beads. Microglia were then stained with the activation markers **A)** CD11b and **B)** Tlr2**.** Data shown are from one experiment where, n=3 for LPS treated group, and n=2 for PBS group.

6.4 Less pronounced sickness behaviour in Rheb KO mice

I decided to use the low dose of LPS 0.33 mg/kg to study sickness behaviour in the Rheb KO mice as I was able to detect markers of inflammation (either by qPCR or FACS) in microglia using this dose and time frame. The experimental design used for these experiments is depicted in **Fig. 6.8.** I first had to carry out a baseline open-field, two weeks prior to LPS stimulation. It was important to take into consideration sample

size and gender when designing these behavioural experiments. Ideally, a large sample size is required and using mice of the same gender is desirable. This is why I carried out these experiments at first in males and then in females. All mice received an LPS challenge, rather than splitting them into the two groups LPS and PBS, in order to keep the sample size large. Following 0.33 mg/kg LPS injection, the open-field test was carried out at 6 hours, as in my pilot study. I also choose an additional time point of 30 hour post LPS, in order to gain information about sickness behaviour in Rheb KO mice during the recovery phase. After 48 hours, all mice were culled by cardiac puncture, and plasma was obtained from the blood. Microglia were isolated from the brain but I did not isolate monocytes from the spleen, given that I found it difficult to detect changes in gene expression in these cells after 48 hours.

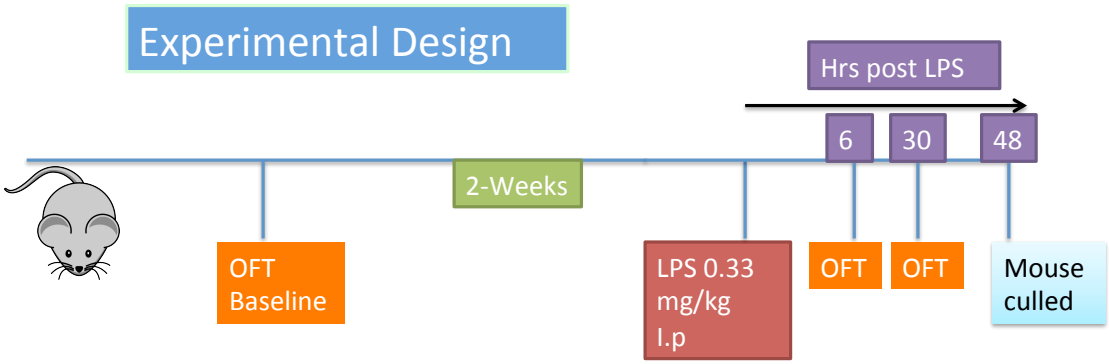

Figure 6.8 Experimental design for low dose LPS experiments, using Rheb KO and WT mice. All mice were subjected to a 5-minute open-field test, two weeks prior to the start of the experiment to assess baseline locomotion. Rheb KO and WT mice were then given a peripheral injection of 0.33 mg/kg of LPS. The open-field test was carried out 6-hours and 30-hours post LPS challenge and all mice were culled at 48 hours.

6.5 Baseline results

I found that Rheb KO mice and WT mice appeared to travel approximately the same distance during the 5-minute open-field test, passing through between 40 and 60 squares (**Fig. 6.9A**). Overall, I found no difference in the number of rears (**Fig. 6.9B**) or in the time it took for each mouse to rear (**Fig. 6.9C**), with each mouse rearing at approximately 20-30 seconds after the start of the experiment.

The open-field test can also give an indication of stress, measured by the number of times a mouse enters the three central squares of the gridded box. Mice go into the centre when they are less stressed and less fearful of their environment. I therefore assessed at which point the mice first passed through any of the three central squares. I found that, in general, Rheb KO mice passed through the centre earlier compared to WT controls, suggesting that these mice may have a lower baseline for stress. However, this was not statistically significant (p=0.17, **Fig. 6.9D**). I also found no difference in how often mice go into the central squares (**Fig. 6.9E**). As a result, I can conclude that there are no major differences in behaviour associated with either movement or stress between the Rheb KO and WT mice.

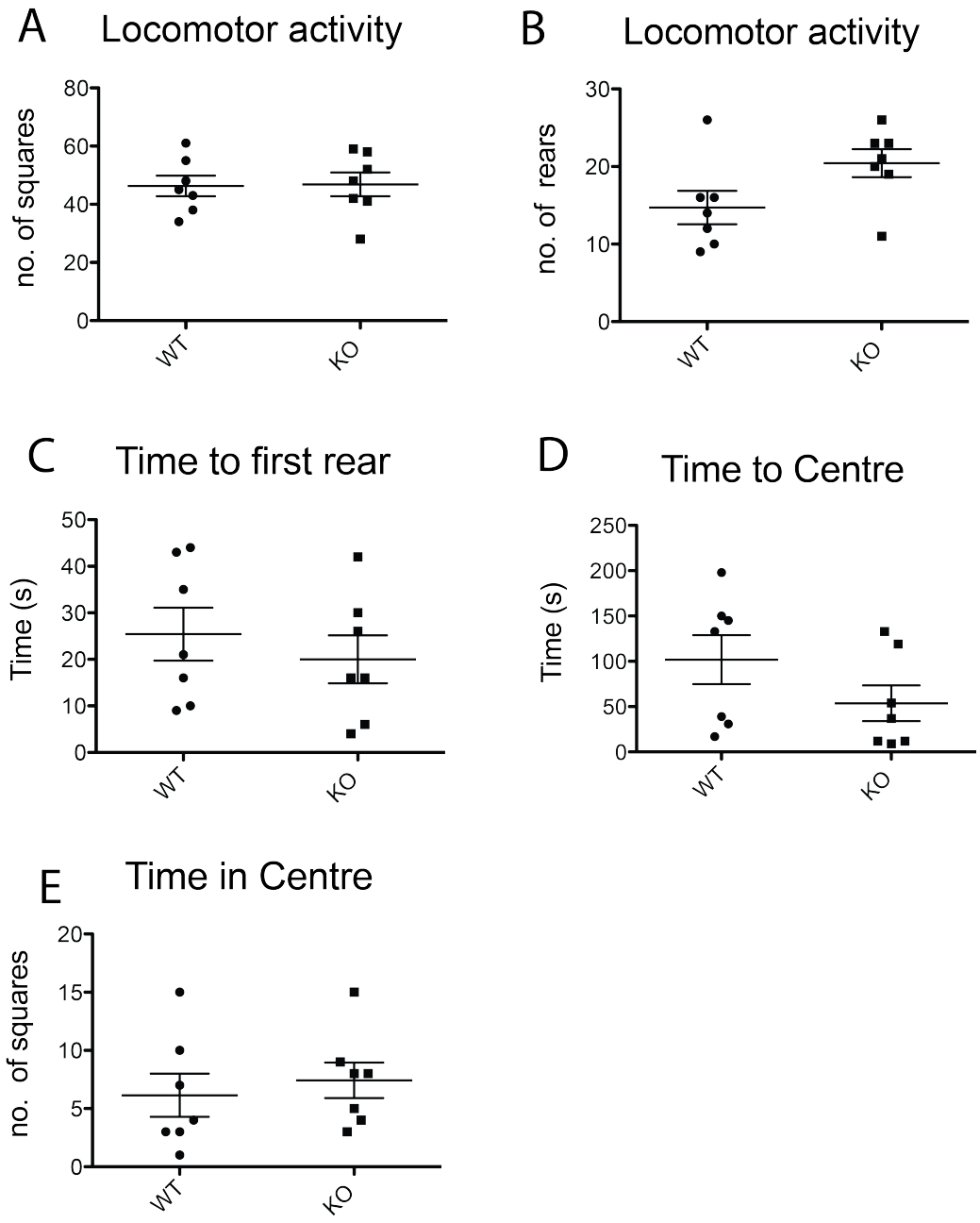

Figure 6.9 Baseline analysis of sickness behaviour parameters in Rheb KO vs. WT mice as measured by the open-field test. Mice were placed into a 15-square gridded rat cage for a 5-minute period. Each test was recorded and later analysed blind. The overall movements of each mouse were assessed by three parameters; **A)** the distance travelled measured by the number of squares each mouse passes through during the test, **B)** locomotor activity measured by the number of times the mouse rears (both paws) during the test and **C)** the first time the mouse rears. The overall amount of stress experienced by each mouse was also measured by two parameters; **D)** Time to centre: the first time the mouse passes though any of the 3-centre squares, and **E)** Time in Centre: number of times the mouse passes through these 3-centre squares. All mice used were male and between the ages of 3 and 6 months, n=6 for WT group and n=7 for Rheb KO group.

6.6 Sickness behaviour following *in vivo* LPS stimulation

6.6.1 Males

Two weeks following the assessment of the baseline parameters with the open-field test, I injected mice with a low dose of LPS (0.33 mg/kg) as described in **Fig. 6.8.** I found that, at 6 hours post LPS challenge, Rheb KO mice appeared more mobile (**Fig. 6.10A**). Consistent with this finding, Rheb KO mice also appeared to rear more (**Fig. 6.10D**). The differences for both these parameters were significantly different. These results show that the Rheb KO mice move more than their WT counterparts, indicating they were less sick. This is perhaps not surprising, given that pro-inflammatory cytokines such as Il-6 and Tnf are known to be important in inducing sickness behaviour. Therefore, this data is consistent with the hypothesis that Rheb KO mice appear to have less overall inflammation after *in vivo* LPS challenge.

In addition, I observed a similar trend at 30 hours post LPS-treatment, with the Rheb KO mice continuing to travel through more squares (**Fig. 6.10C**) and rear more than WT controls (**Fig. 6.10D**). However, neither of these parameters was significantly different at this time point (distance travelled p=0.2, locomotor activity p=0.3).

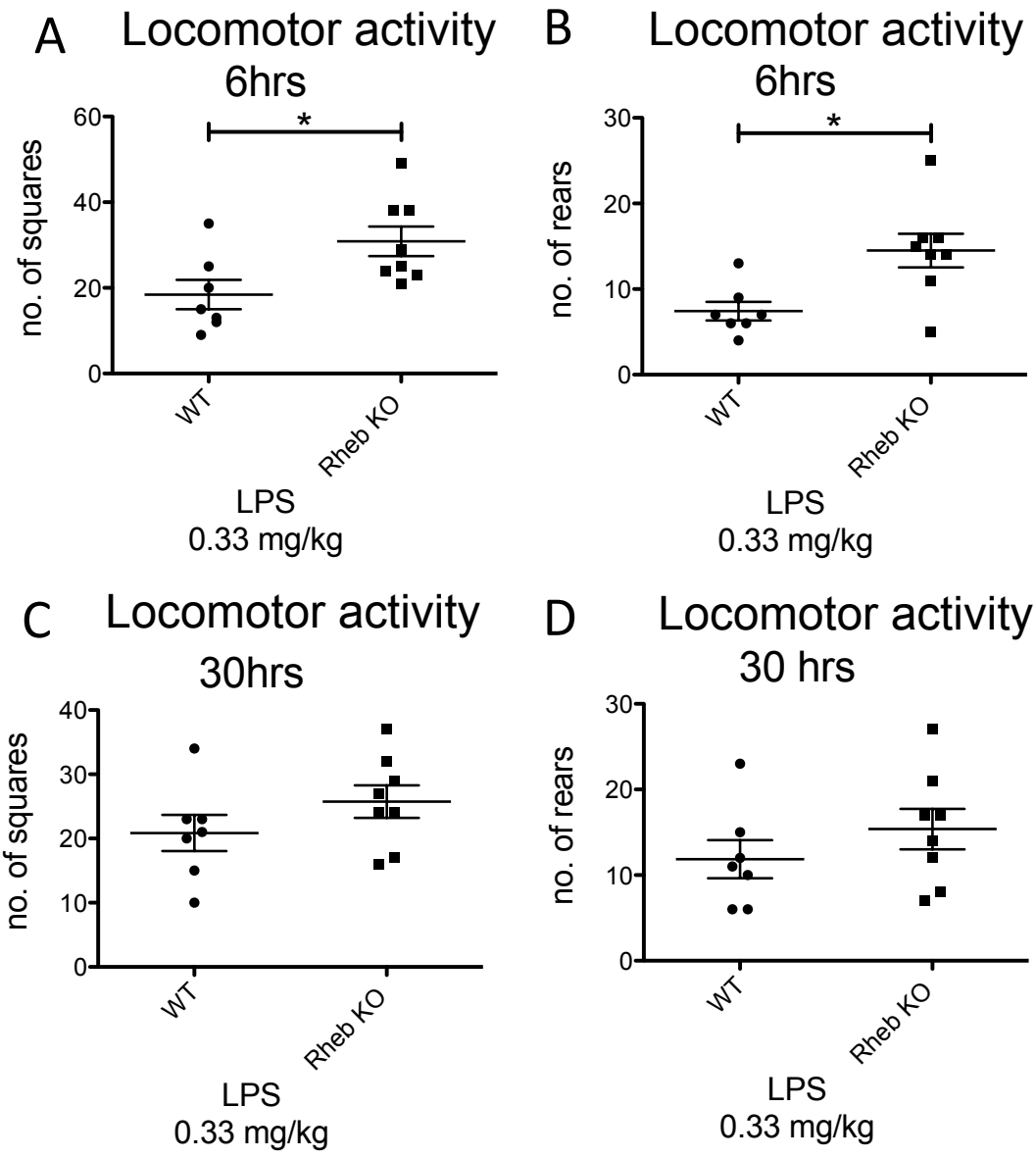

Figure 6.10 Male Rheb KO mice appear less sick compared to WT controls after low dose LPS treatment. Sickness behaviour was measured by assessing locomotor activity 6 and 30 hours post LPS treatment (0.33 mg/kg). Mice were subjected to a 5-minute open-field test in a 15-square gridded box at these two time points. Locomotor activity was determined by distance travelled at **A**) 6-hours and **B**) 30-hours post LPS challenge. Locomotor activity was also determined by the number of times the mouse rears during the 5-minute period at **D**) 6-hours and **E)** 30-hrs post LPS challenge. The experiment was carried out on male mice between the ages of 3 and 6 months, n=6 for WT group and n=7 for Rheb KO group, * $p<0.05$. Significance was calculated using the unpaired two tailed student t-test between individual groups.

6.6.2 Females

I wanted to repeat this study on female mice, in order to understand whether gender was a factor contributing to the improved performance of Rheb KO mice after LPS challenge. I found that, consistent with the male study, female Rheb KO mice appeared to move more during the open-field test at 6-hours post injection. This was not statistically significant for the distance travelled ($p=0.17$, **Fig. 6.11A**) but significant for the number of rears ($p<0.05$, **Fig. 6.11B**). I also observed a similar trend at 30-hours post LPS, however, these differences were not statistically significant for either parameters (**Fig. 6.11A** and **6.11B**). Overall, it appeared that Rheb KO female mice were less sick compared to their WT counterparts, which was consistent with what was observed in male mice.

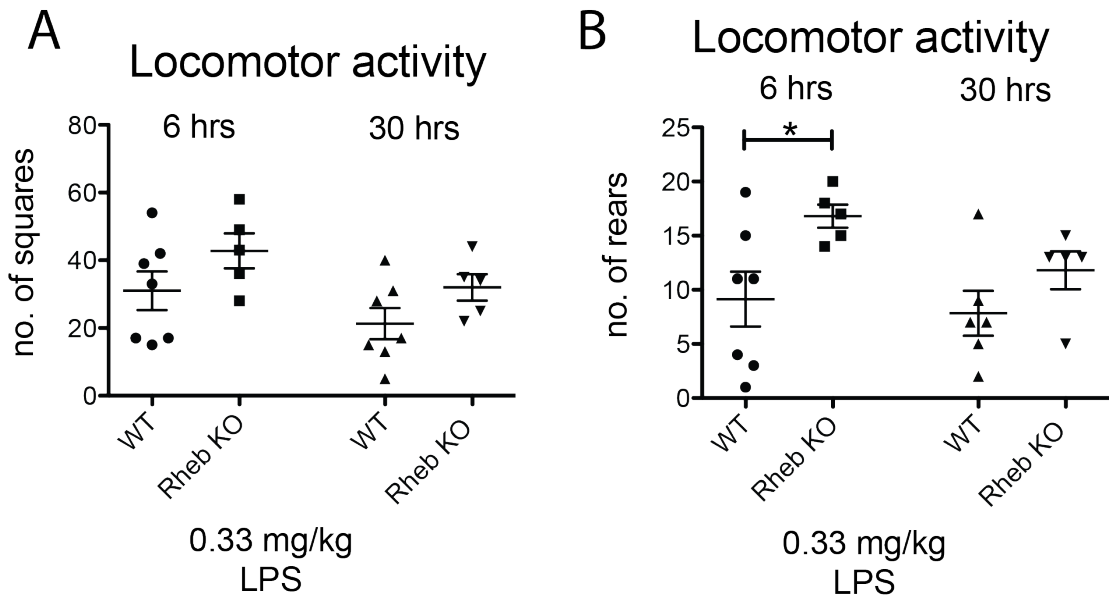

Figure 6.11 Female Rheb KO mice appear less sick compared to WT controls after low-dose LPS treatment. Sickness behaviour was measured by assessing locomotor activity 6 and 30 hours post LPS treatment (0.33 mg/kg). Mice were subjected to a 5-minute open-field test in a 15-square gridded box at these two time points. Locomotor activity was determined by distance travelled at **A**) 6-hours and 30-hours post LPS challenge. This was assessed by calculating the number of squares the mouse passes through during the 5-minute test. **B)** Locomotor activity was also determined by the number of times the mouse rears during the 5-minute period at 6-hours and 30-hours post LPS challenge. The experiment was carried out on female mice between the ages of 3 and 6 months, n=5 for WT group and n=7 for Rheb KO group, * $p<0.05$. Significance was calculated using the unpaired two tailed student t-test between individual groups.

6.7 Stress/anxiety in males and females

With the open-field test I assessed also at which point the mice went into any of the three central squares, termed here "time to centre" and found that there was no difference between male Rheb KO and WT mice post LPS challenge (**Fig. 6.12A**). Female Rheb KO mice did appear to go into the centre more quickly than WTs, although this observation was not statistically significant (**Fig. 6.12B**). The finding that mice move into the centre more quickly could indicate that the mice are less stressed, although more behavioural tests would be needed to establish this point unequivocally.

Additionally, I measured how many times each mouse passed through any of the three central squares, termed "time in centre" and found that there was no difference at either time points for the male mice (**Fig. 6.12C**) or the female mice (**Fig. 6.12D**).

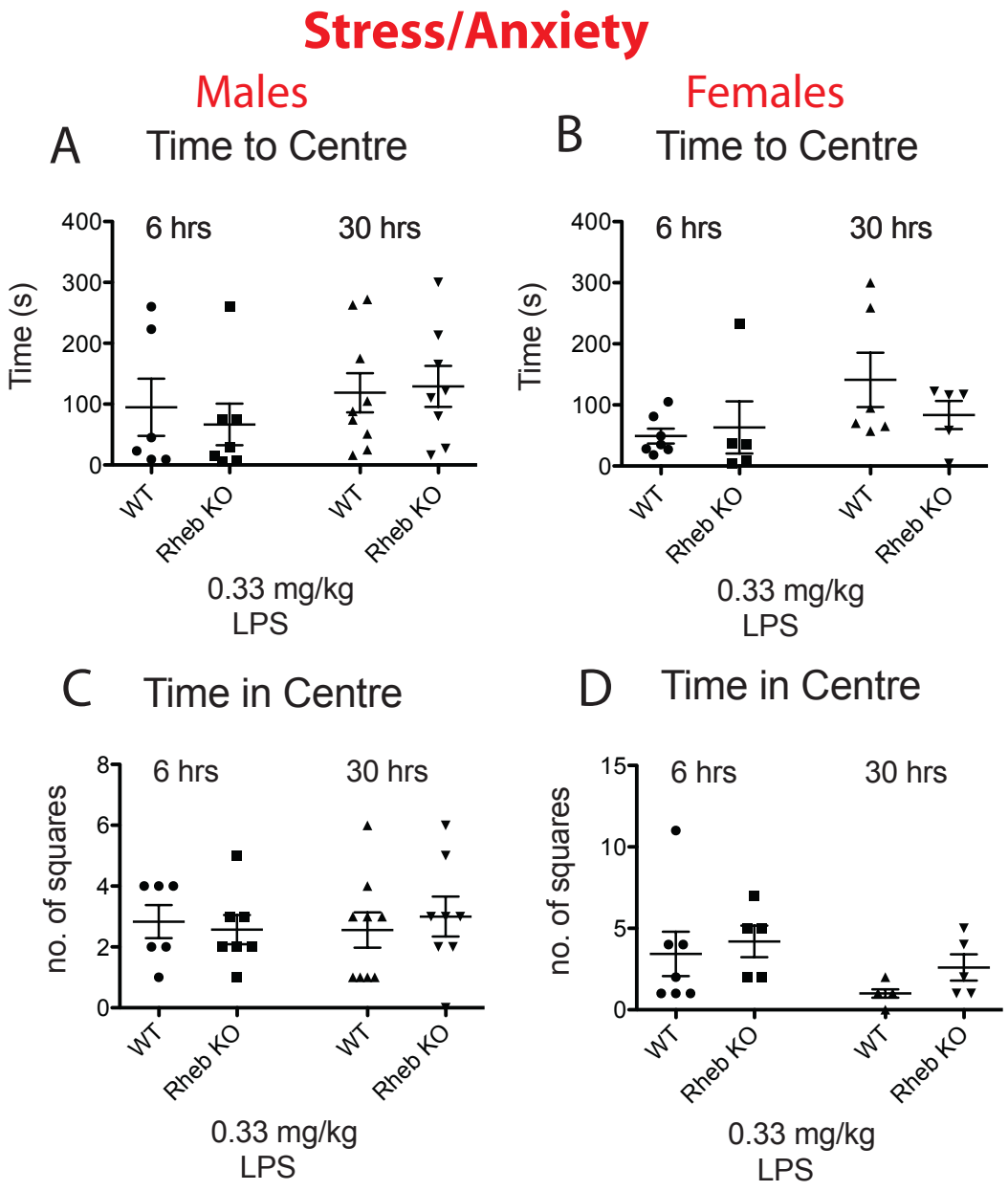

Figure 6.12 No differences in stress behaviour between Rheb KO and WT mice post LPS challenge. Mice were placed into a 15-square gridded rat cage for a 5-minute period. Each test was recorded and later analysed blind. The overall amount of stress experienced by each mouse was measured by two parameters; The first time the mouse passes though any of the 3-centre squares, shown in seconds for **A)** males and **B)** females and the number of times the mouse passed through the 3-centre squares, measured for **C)** males and **D)** females. All mice used were between the ages of 3 and 6 months n >5 for all groups.

6.8 Rheb KO microglia appear to have an increase in the transcription of inflammatory genes at low dose *in vivo* LPS challenge

Sickness behaviour results for both male and female Rheb KO mice appeared to be consistent, indicating that the mice had less overall inflammation. These findings are not that surprising, given the lower inflammatory cytokines measured by ELISA. Nonetheless, I wanted to confirm if in this cohort of mice and using this dose and timeframe of LPS, I still observed an increase in inflammatory gene expression in Rheb KO microglia. I carried out qPCR analysis on key inflammatory genes and age related genes, as previously described in chapter 5. I found that for *Tnf* (**Fig. 6.13A***), Il1b* (**Fig. 6.13B**) and *Il12b* (**Fig**. **6.13C**) there was a statistically significant upregulation in Rheb KO microglia, consistent with previous findings ($p<0.05$ for all three genes). I also measured *Il10* expression. I expected it to be downregulated in Rheb KO microglia cells. This is due to the fact that it has been reported in the literature that mTOR positively regulates Stat3 and Il10 production[129], thus Il10 production should be inhibited in the absence of Rheb. Consistent with the literature, I found there was a significant downregulation of the *Il10* gene in Rheb KO microglia ($p<0.01$, **Fig. 6.13D**). On the other hand, there were no significant differences in expression of *Il6* or *Il12a* (**Fig. 6.13F** and **Fig. 6.13G**). This was similar to what I observed in the pilot study (**Fig. 6.5E** and **Fig. 6.5F**). Furthermore, I found that there was an upregulation of the age-related genes *Spp1* and *Cst7* in the Rheb KO microglia, as previously observed (**Fig. 6.13G** and **Fig. 6.13H**). These differences were highly significant for both genes ($p<0.001$).

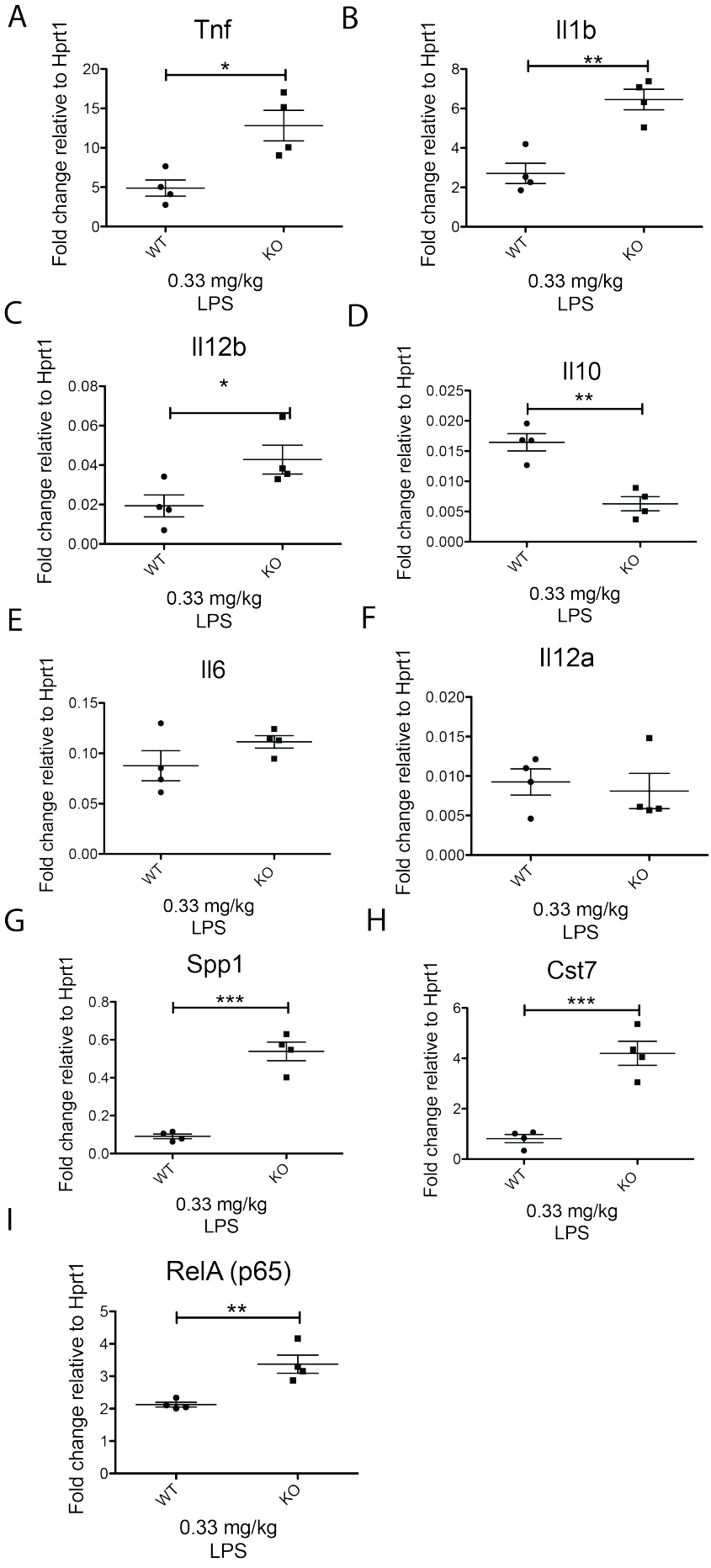
A
Tnf
Fold change relative to Hprt1
*
WT
KO
0.33 mg/kg
LPS
B
Il1b
**
C
Il12b
*
D
Il10
**
E
Il6
F
Il12a
G
Spp1
***
H
Cst7
***
I
RelA (p65)
**

Figure 6.13 Inflammatory and age-related genes are upregulated in microglia from Rheb KO mice upon low-dose LPS challenge. WT and Rheb KO mice were given a peripheral injection of LPS, 0.33 mg/kg. Mice were culled by cardiac puncture 48 hours later and the brains were removed and digested before microglia were isolated using magnetic beads. The induction of inflammatory genes was determined using qPCR with fold changes being expressed relative to the housekeeping gene *Hprt.* **A-F**) inflammatory genes and **G-I**) age-related genes. The data are from one experiment, where n=4 for both groups, * $p<0.05$, **$p<0.01$, ***$p<0.001$. Significance was calculated using the unpaired two tailed student t-test between individual groups.

Finally, I measured the induction of the NF-κB subunit, p65, as I was interested in the association between the mTOR pathway and NF-κB activation and found that this gene was significantly upregulated in Rheb KO microglia ($p<0.01$, **Fig 6.13I**). These data are consistent with what I observed with higher doses of LPS described in Chapter 5 and show that despite the Rheb KO mice appearing to be less sick, likely as a consequence of having reduced overall cytokine production, there is a stronger upregulation of inflammatory genes at transcription level**.**

Finally, I measured the expression of CD11b and Tlr2 by flow cytometry, as they are associated with microglia activation. I found that microglia from Rheb KO mice expressed significantly less CD11b ($p<0.01$) compared with WT controls (**Fig. 6.14A**). Nonetheless, there did not appear to be a difference between the two groups for Tlr2 expression (**Fig. 6.14B**).

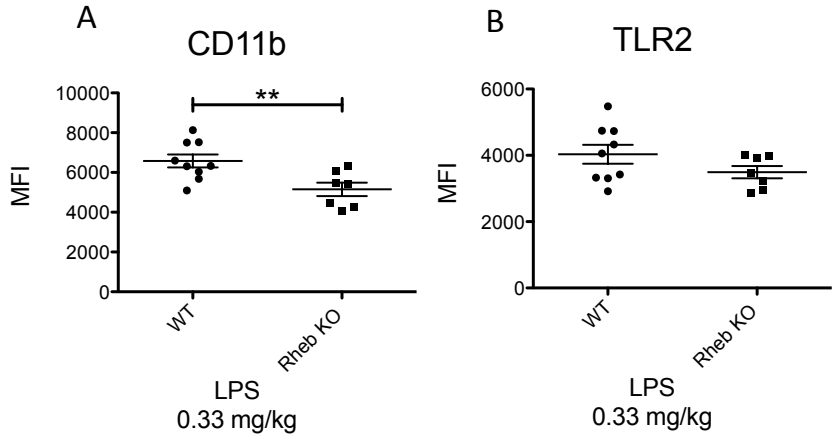

Figure 6.14 Flow cytometry analysis of markers of microglia activation after low-dose LPS challenge. WT and Rheb KO mice were given a peripheral injection of LPS, 0.33 mg/kg for 48 hours. Mice were culled by cardiac puncture and the brains were removed and digested before microglia were isolated using magnetic beads. Microglia were then stained with the activation markers **A)** CD11b and **B)** Tlr2**.** Data are from one experiment where n=9 for

WT group, n= 8 for Rheb KO group and **p<0.01. Significance was calculated using the unpaired two tailed student t-test between individual groups.

6 Discussion

The main question I wanted to address in this chapter was; what are the potential consequences of the increased microglia-mediated inflammation in the Rheb KO mice? Before approaching this question, I had to confirm that the transcriptional changes observed in microglia and BMDMs from Rheb KO mice were also observed at a protein level. The most straightforward way to measure cytokines produced by BMDMs from Rheb KO and WT mice treated with LPS was by ELISA. Surprisingly, protein levels were very different to gene expression changes. While there was a clear upregulation of the transcripts for pro-inflammatory cytokines such as *Tnf* and *Il6*, there were significantly lower levels of cytokines being produced and released from these cells. This was a very interesting result as it was in contrast to Weichhart *et al.* where they observed the same changes at transcript and protein level when mTOR was inhibited in BMDMs or peripheral human monocytes[129]. The major difference between our experimental approaches is the mode by which mTORC1 is inhibited. Weichhart *et al.* use the mTORC1 inhibitor rapamycin to inhibit the pathway, while in our model the pathway is inhibited by genetic loss of the positive regulator of mTORC1, Rheb. Therefore, it is conceivable that the downstream consequences could be very different.

6.1 Effects on translation

One of the major functions of mTORC1 is to regulate translation through its two main substrates, 4E-BP1 and S6, which mediate the initiation and elongation stages of cap-dependent translation, respectively. There has been a lot of controversy regarding whether rapamycin inhibits mTOR-mediated translation, and if so, to what extent. In 2009, the Sabatini lab reported the development of a small molecule inhibitor called Torin1, an ATP-competitive inhibitor of both mTORC1 and mTORC2. They showed that a number of mTORC1 functions were rapamycin resistant. They mainly focused on cap-dependent translation and used 35S methionine/cysteine incorporation to show that protein synthesis was inhibited by Torin1 to a greater extent than by rapamycin[115]. While S6K activity is completely inhibited by rapamycin[115], this is not the case for the

other main mTORC1 substrate 4E-BP1. 4E-BP1, when phosphorylated at four residues (Thr-37, Thr-46, Ser-65 and Thr-70), can dissociate from its binding partner eIf4E, allowing it to form complexes with other eIf proteins and initiate translation[32]. Thoreen *et al.* found that some of these phosphorylation events, mainly the phosphorylation at T37/46, were not affected by rapamycin treatment, however, they were completely inhibited by Torin1, suggesting this mechanism is behind the increased potency of Torin1 in inhibiting protein translation[114].

This paper was further supported by a follow-up study conducted by the same group and published in 2012, which showed that a subset of mRNAs specifically regulated by mTORC1 contained 5'terminal oligopyrimidine (TOP) motifs. Loss of 4E-BP1 was sufficient to inhibit the translation of these TOP and TOP-like transcripts. Again these findings were only observed in the presence of Torin1 but not rapamycin[115].

These studies may shed light on why I observe reduced cytokine production in our Rheb KO cells compared to the Weichhart *et al.* paper. In this paper, the authors used relatively low doses of rapamycin (10-100 nM) and for relatively short periods of time (20-22 hours *in vitro*, 3 days *in vivo*)[129]. As a result, it is possible that rapamycin was sufficient to activate NF-κB (through a yet to be identified mechanism). However, given its lack of effect on protein initiation through 4E-BP1, it was not affecting protein synthesis and therefore cytokine production. Alternatively, in our model, deletion of Rheb caused a stronger inhibition of mTORC1, with consequences also on protein translation. Indeed, Rheb has been shown to be essential for the regulation of translation[218]. It is likely that in our model the initiation of cap-dependent translation is impaired, causing a reduction in translation of pro-inflammatory cytokines. There are several ways I could test this hypothesis. Similarly to Thoreen *et al.* I could measure 35S methionine/cysteine incorporation in Rheb KO cells, as this would give an idea of the extent of inhibition of protein synthesis. I could also measure the level of phosphorylation of 4E-BP1 at the different phosphorylation sites, particularly T37/46, to see if these are inhibited in the Rheb KO cells compared to WT or rapamycin treated BMDMs. Lastly, I could investigate the binding of 4E-BP1 to eIF-4E in Rheb KO cells as this binding will prevent eIF-4E forming a complex with other eIF proteins to initiate translation. Perhaps the best way to assess this would be to measure polysome

associated transcripts (which are the ones being translated into proteins) and check if there is a reduction in inflammatory cytokines in Rheb KO cells.

While these experiments could answer the question concerning why I observe significantly reduced protein levels of Tnf, Il6 and Il12p40 compared WT controls, it does not address why I observe the opposite on a transcript level. As discussed in the previous chapter, Weichhart *et al.* showed that the increase in cytokine production upon mTOR inhibition was mediated by activation of NF-κB, specifically showing increased DNA binding of NF-κB subunit p65. It is possible that in Rheb KO mice, a similar increase in NF-κB activation is taking place. In spite of this, I cannot exclude that given the impairment in protein synthesis; the mechanism responsible for changes in mRNA levels may be different. For example, is there a compensatory mechanism that causes an upregulation of mRNA inflammatory genes if proteins are not produced? If this was the case, I would expect to observe differences in the kinetics of mRNA upregulation, i.e. that the upregulation of mRNA in Rheb KO cells occurred at a later time point, in response to loss of a feedback mechanism initiated by increased protein levels. However, this does not appear to be the case, as the peak of cytokine mRNA expression is similar in WT and Rheb KO cells. In order to test if the mechanism responsible for increased NF-κB activation following mTOR inhibition is the same, whether the inhibition is mediated by rapamycin or genetic loss of Rheb, BMDMs could be treated with rapamycin and an inhibitor of protein synthesis such as cycloheximide, in order to assess if NF-κB activation is dependent on new protein synthesis or not.

It's also important to acknowledge that measuring the cytokines present in the supernatant may not be the most optimal way of determining the inflammatory capacity of Rheb KO cells. This is because this is a measurement of only what is secreted by the cell. Therefore if there is a defect in the secretion in the Rheb KO BMDMs this could be a potential reason why I observed less production of Tnf, Il-6 and ll-12. To try to understand if the decrease of these inflammatory genes on a protein level is due to a defect in translation rather than secretion, it would be important to carry out an ELISA on protein lysates obtained from Rheb KO and WT BMDMs stimulated with LPS and measure how much of these cytokines are present within the cell. If I still observed less of these cytokines it would be a clearer indication that the cell is not able to make these cytokines as efficiently as WT cells.

6.2 Sickness behaviour

After observing that reduced overall cytokine production was occurring in Rheb KO BMDMs and that this was also evident *in vivo* upon LPS stimulation, I wanted to assess the consequences of impaired cytokine production and decided to study sickness behaviour.

Communication between the immune system and the brain is necessary for responses to pathogens and adequate immune activation. As previously discussed, the ability of the immune system to respond to pathogens has been shown to decline with age, furthermore and possible as a consequence, infections in the elderly are associated with alterations in both behaviour and cognition[219]. For example, it has been shown that peripheral infections such as those affecting the urinary tract can cause a state of delirium in the elderly, often resulting in a more pronounced sickness behaviour[206].

Sickness behaviour occurs during a peripheral infection when cells of the innate immune system are activated and produce inflammatory cytokines such as Tnf, Il6 and Il1b. These signals are then transmitted across the blood brain barrier (BBB), where they activate glia cells such as microglia. These cells then produce an array of cytokines, prostaglandins and secondary mediators, which will then act on neuronal cells to elicit the symptoms of sickness behaviour[220].

Accordingly, in our model of low dose LPS *in vivo* stimulation, I hypothesised that lower levels of cytokines would be produced in Rheb KO mice and, for this reason, they would exhibit reduced sickness behaviour. Indeed, this was what I observed: mice appeared less lethargic and moved more, as measured in the open-field test.

I must consider that the open-field test is not a comprehensive way of measuring sickness behaviour. Sickness behaviour is characterised by a variety of symptoms that include fever, reduced locomotor activity, depressive-like behaviour, reduction in social exploratory behaviour, increased sleep and reduced appetite[221]. Consequently, it would have been more powerful if more tests were carried out, for example using a rectal

probe to measure changes in body temperature or by performing a social exploratory test, in which a test mouse is placed in a cage with a subject mouse and the amount of time the test mouse spends investigating the subject mouse is measured.

Although I was able to assess that sickness behaviour in Rheb KO was not affected by gender, it would have been extremely interesting to carry out this experiment also in elderly Rheb KO mice. Given that I observed an increase in the transcript levels of the pro-inflammatory cytokines in old Rheb KO microglia compared to young Rheb KO microglia, as described in chapter 5, it would have been important to understand if this increase in gene transcripts had any effect on the overall inflammation in the brain. Considering that there were significantly less Tnf and Il12p70 in the plasma of aged Rheb KO mice, I could hypothesise that elderly Rheb KO mice would be even more protected from the induction of sickness behaviour than their younger counterparts. Nonetheless, this point will need to be tested.

6.3 Relevance for immune responses to infections

It is important to consider the overall consequences of having reduced cytokine production, particularly in an ageing context. Cytokine production is an important part of clearing an infection. For example, Balb/c mice are unable to mount an effective Th1 response and are therefore more susceptible to infections such as *L. major*, which can be rescued by the administration of IL-12. Fakao *et al.* showed that inhibition of PI3K in DCs led to an increase in IL-12 production, and PI3K-/- mice infected with *L. major* had enhanced resistance to the infection, confirmed by a significant reduction in the number of parasites in the popliteal lymph nodes 6 weeks post infection[126]. This is consistent with a report by Aksoy *et al.* who showed that DCs from mice with a knock-in mutation in the p110δ isoform of PI3K had augmented cytokine production[128]. The authors went on to explain that this is due to differences in Tlr4 internalisation and downstream consequences on alternative TLR signalling. Whether a similar mechanism contributes to the effect observed in Rheb KO mice remains to be elucidated. Weichhart *et al.* showed that rapamycin treated Balb/c mice were protected from infection with *L.monocytogenes* through an increase in the production of IL-12[129]. Therefore in Rheb KO mice, I may hypothesise that they are more susceptible to similar infections

compared to WT controls, however, they would be protected from endotoxic shock during sepsis.

It would be interesting to challenge older mice with infectious agents such as *L. Major* or influenza, in order to mimic what happens in elderly individuals and assess the overall impact of mTORC1 inhibition in this context. Would it cause an improvement in cognitive and locomotion functions during infections? In elderly rodents, LPS injections cause an amplified cytokine response[216] and a decline in both spatial memory[222] and contextual memory[223]. Nonetheless, could it increase susceptibility to succumb to infections? Moreover, could it protect elderly individuals undergoing sepsis? What would be the consequences on inflamm-ageing?

Inflamm-ageing is thought to underlie many age-related illnesses such as Alzheimer's and cancer; correspondingly, in the Rheb KO mice, a reduction in the overall production of cytokines could reduce inflamm-ageing in older mice. It would be intriguing to assess the baseline levels of Tnf, Il6, Il1b and Il12 in the plasma of old Rheb KO mice compared to controls, as this would give an overall indication of the systemic inflammation that accumulates with age. However, given that the mouse model used here has a deletion of Rheb specifically in myeloid cells, I might not be able to observe a systemic effect, since the SASP can be produced by other cells in the organism [18] and they would not be affected.

6 Conclusion

Overall, my data suggest that inhibition of mTORC1 by deletion of Rheb in myeloid cells leads to reduced inflammatory cytokine production, which is associated with improved sickness behaviour as measured by the open-field test. These results raise further questions, most notably, what could long term mTOR inhibition mean for the ageing host? A number of studies have shown that long-term mTOR inhibition increases lifespan in a number of model organisms, more recently rapamcyin itself was shown to extend lifespan in mice[31]. I therefore wanted to ask the question; what would happen if I treated young and aged mice long-term with rapamycin and then challenged them with a peripheral injection of LPS? Would I observe the same transcriptional

changes in microglia observed in the Rheb KO mice? Would I see these effects at protein level? Would mice be less or more sick after an LPS challenge?

Chapter 7: The effect of long-term rapamycin treatment on the LPS-induced inflammatory response in ageing mice

Given that rapamycin is being considered as an anti-ageing intervention, I wanted to understand the impact of long-term rapamycin treatment on the inflammatory response, especially in microglia. I also wanted to understand if the effect (if any) of rapamcyin treatment was similar in young and aged individuals. At the time of starting this experiment, I was aware that Rheb KO microglia expressed higher levels of inflammatory cytokines at the mRNA level, with previous reports observing an increased inflammatory response in both rapamycin-treated mice and *in vitro* rapamycin-treated macrophages. Therefore, I wanted to assess whether long-term rapamycin treatment could result in exaggerated inflammatory responses in the event of an infection. I designed an experiment using all female mice as depicted in **Fig 7.1**, using LPS to mimic a peripheral infection**.**

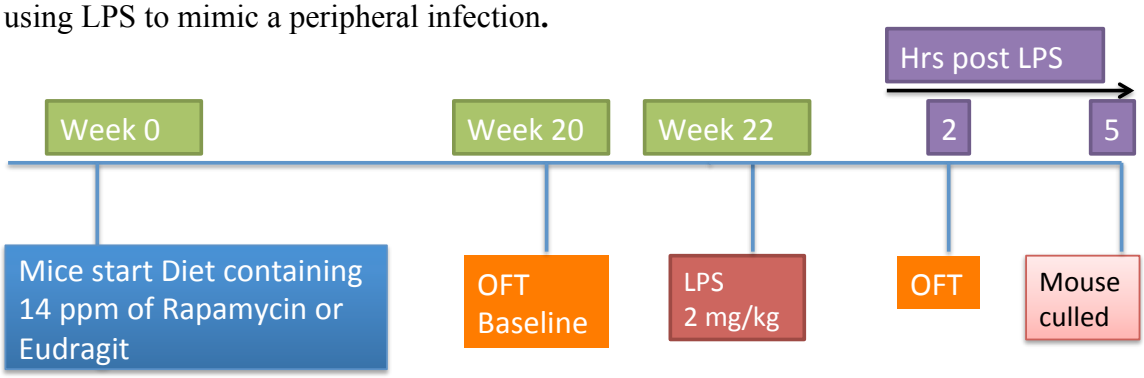

Group	Age	Gender	Diet	No. of Mice
1	6-months	female	Eudragit	8
2	6-months	female	Rapamycin	9
3	18-months	female	Eudragit	7
4	18-months	female	Rapamycin	9

Figure 7.1 Experimental design to assess inflammatory responses after long-term rapamycin treatment. Mice used were female and either young (6 months) or old (18 months). These groups were sub divided into two groups; one receiving a diet containing 14 parts per million (ppm) of encapsulated rapamycin and one receiving only the material used to encapsulate the drug, known as eudragit, as the control group. The mice were kept on this diet for 22 weeks, after which they were injected i.p. with 2 mg/kg of LPS and culled after five hours. The baseline open-field test was conducted after 20 weeks on the diet. A second open-

field test was conducted two hours post LPS injection in order to assess changes in sickness behaviour. Mice were 11 and 23 months at the time of the LPS injection.

I used both young (6 month) and aged mice (18 months), which were each split into two groups that received a diet containing either encapsulated rapamycin or only the material used to encapsulate it, known as eudragit, as the control group. Eudragit is a polymer used to coat drugs to prevent their premature degradation in the stomach, thanks to the fact that the polymer can only be broken down at an adequate pH in the gastrointestinal (GI) track. The diet used was similar to the one used in other ageing studies, including the 2012 Harrison *et al.* study in *Nature* showing that rapamycin extended lifespan in mice. The amount of rapamycin incorporated into the diet corresponded to 14 parts per million (PPM) that equates to approximately 2.2 mg/kg of rapamycin per day. Mice were placed on both diets at 6 and 18-months of age and 22 weeks later they were challenged with a dose of LPS of 2mg/kg, then culled 5 hours later. The open-field test was conducted two weeks prior to this challenge, to assess changes in baseline behaviour and was also conducted two hours post LPS injection, in order to determine the effect of rapamycin on LPS-induced sickness behaviour.

7.1 Rapamycin treatment did not affect baseline behaviour of young or aged mice

Firstly, I determined if there were any differences in the baseline behaviour of mice treated with rapamycin before challenging them with LPS. To this end, I carried out an open-field test after 20 weeks of rapamycin/eudragit diet, when mice were 11 months (middle aged) and 23 months old (old). I measured a number of parameters associated with both locomotion and stress. I found that the distance travelled, i.e. the number of squares each mouse passed through during the 5-minute test, was similar between eudragit and rapamycin-treated groups, in both age groups (**Fig. 7.2A**). This result was consistent with other measurements of locomotor ability, including rearing (**Fig. 7.2B**) and time to first rear (**Fig. 7.1C**).

It appeared that for the 11-month old rapamycin-treated mice, the time interval before traversing one of the three central squares was shorter than the eudragit-treated group, although this difference was not statistically significant ($p=0.07$). There was no difference in this parameter for the older age group (**Fig. 7.2D**). I also measured how

many faecal boli were present in the box at the end of the test, as this is also a measure of stress and anxiety and found that there were no differences (**Fig. 7.2E**).

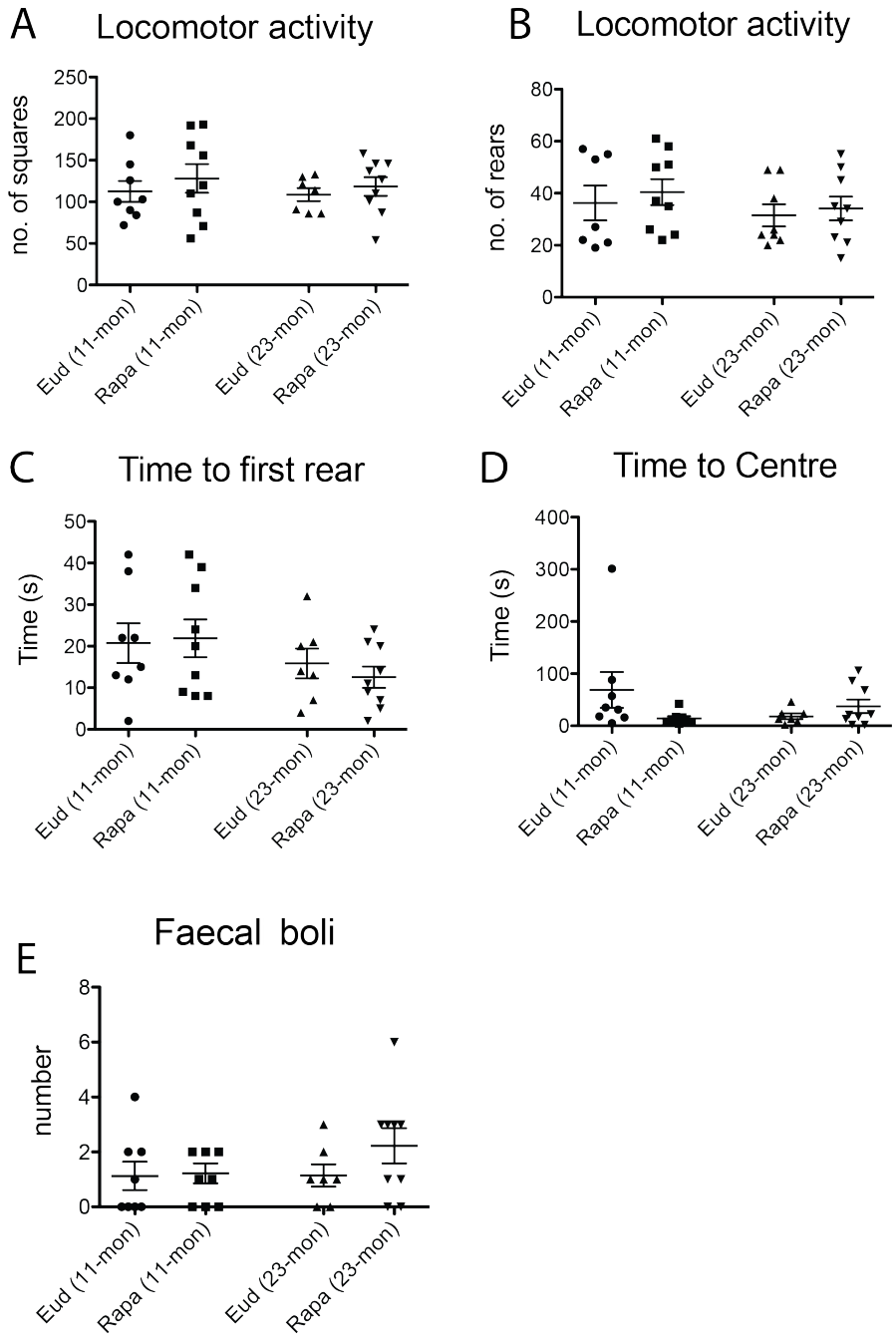

Figure 7.2 Baseline analysis of locomotor ability and stress levels in rapamycin-treated versus eudragit-treated mice, as measured by the open-field test. Mice were placed into a 15-square gridded rat cage for a 5-minute period. Each test was recorded and later analysed blind. Locomotor ability was assessed by three parameters; **A)** distance travelled, measured by the number of squares traversed during the test **B**) number of rears (both paws), **C**) time to first rear. Stress levels were measured by two parameters; **D**) time delay before the mouse crossed one of the 3 squares in the centre **E)** number of faecal boli present in the box after each test**.** All mice used were female of 11- or 23-months of age, $n \geq 7$ for all groups, data are representative of one experiment. Eud = Eudragit and Rapa=Rapamycin.

7.2 Long-term rapamycin treatment does not affect sickness behaviour after LPS challenge

Twenty-two weeks after starting the rapamycin/eudragit diet, mice were challenged with a peripheral injection of 2 mg/kg LPS for 5 hours. While I used a higher dose for Rheb KO experiments descried in chapter 5 (5 mg/kg), I decided to use a lower dose of LPS in order to carry out a sickness behaviour test, as well as assess cytokine levels in microglia and in the blood. With 5 mg/kg of LPS, mice rapidly became too unwell and would not have been able to withstand an open-field test.

In order to assess if the 2 mg/kg dose of LPS would be suitable for assessing sickness behaviour as well as induce a strong cytokine response, I performed a pilot experiment with either 1 mg/kg or 2 mg/kg of LPS and found that the latter was the most appropriate to measure tissue inflammation and conduct the open-field test two hours post LPS injection. Due to the relatively small size of my cohort of mice on the rapamycin/eudragit diet, I decided to inject all mice with LPS and not to have PBS-injected controls. I reasoned that it was better to have a larger sample size as both the open-field test and cytokine responses might show a greater variability, compared to Rheb KO mice.

Overall, I found no major differences in sickness behaviour in any of the groups tested. In terms of locomotor activity, there was a trend for the rapamycin-treated middle-aged group (11 month) to cross more squares (**Fig. 7.3A**) and rear more (**Fig. 7.3B**), suggesting these mice were less sick. The differences, however, were not statistically significant.

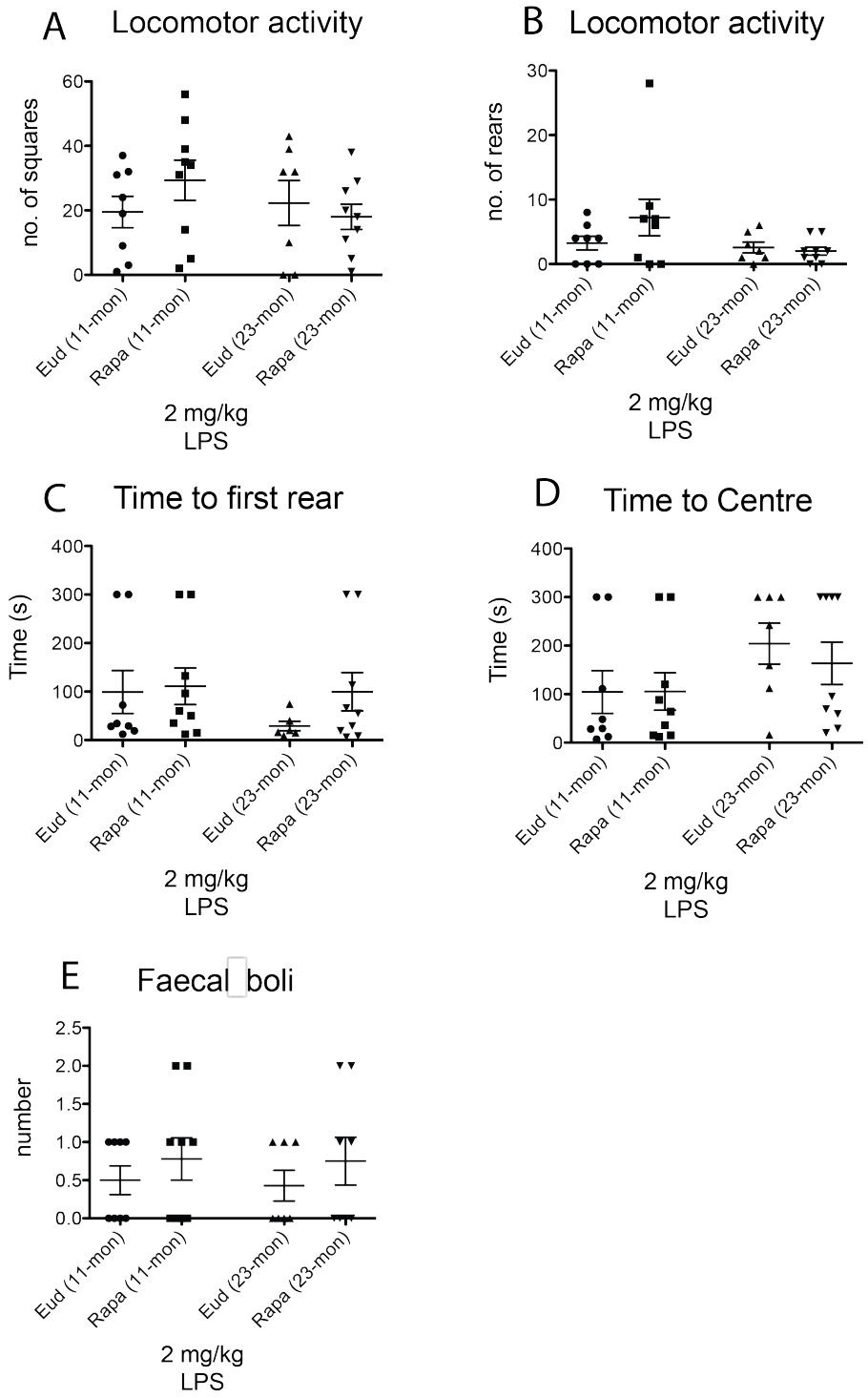

Figure 7.3 Sickness behaviour in rapamycin-treated vs. eudragit-treated mice as measured by the open-field test. Mice were placed into a 15-square gridded rat cage for a 5-minute period. Each test was recorded and later analysed blind. Locomotor ability was assessed by three parameters; **A)** distance travelled, measured by the number of squares traversed during the test **B**) number of rears (both paws), **C**) time to first rear. Stress levels were measured by two parameters; **D**) time delay before the mouse crossed one of the 3 squares in the centre **E)** number of faecal boli present in the box after each test. All mice used were female of 11- or 23-months of age, n ≥ 7 for all groups, data are representative of one experiment. Eud = Eudragit and Rapa=Rapamycin.

No differences were observed in the older age group for distance travelled or the number of rears (**Fig. 7.3A** and **7.3B**). I also found there were no differences between any of the groups for the last parameter of locomotion measured, time to first rear **(Fig. 7.3C**).

I also measured the two parameters relating to stress and anxiety and found again that there were no differences for any of the groups: all mice appeared to traverse one of the 3-centre squares at the same time (**Fig. 7.3D**) and also the number of faecal boli was similar across all groups (**Fig. 7.3E**).

7.3 Middle-aged rapamycin-treated mice but not older ones show a minor reduction in pro-inflammatory genes

I next assessed inflammatory genes induced in microglia after LPS injection. Since Weichhart *et al.*[129] reported that a short treatment with rapamycin induced a stronger inflammatory response and given the observation in Rheb KO mice, which showed an increase of inflammatory cytokines at transcript level, I hypothesised that rapamycin treatment would cause an increase in pro-inflammatory genes at least at mRNA levels. Furthermore, given the evidence that microglia from old mice appear to be primed, I expected the inflammatory response to be further exaggerated with age. Therefore, I isolated microglia from all four groups of mice and performed qPCR analysis similar to Rheb KO experiments described in chapter 4. Surprisingly, the results were quite different to what I expected. There was a clear downregulation of pro-inflammatory cytokines in microglia from the middle-aged rapamycin-treated group. This trend was just below the significance threshold for *Tnf* ($p=0.06$, **Fig. 7.4A**) but was significant for both *Il6* ($p<0.05$, **Fig. 7.4E**) and *Tlr2* ($p<0.05$, **Fig. 7.4F**). A similar trend was observed for *Il1b* (**Fig. 7.4D**) but differences were not statistically significant.

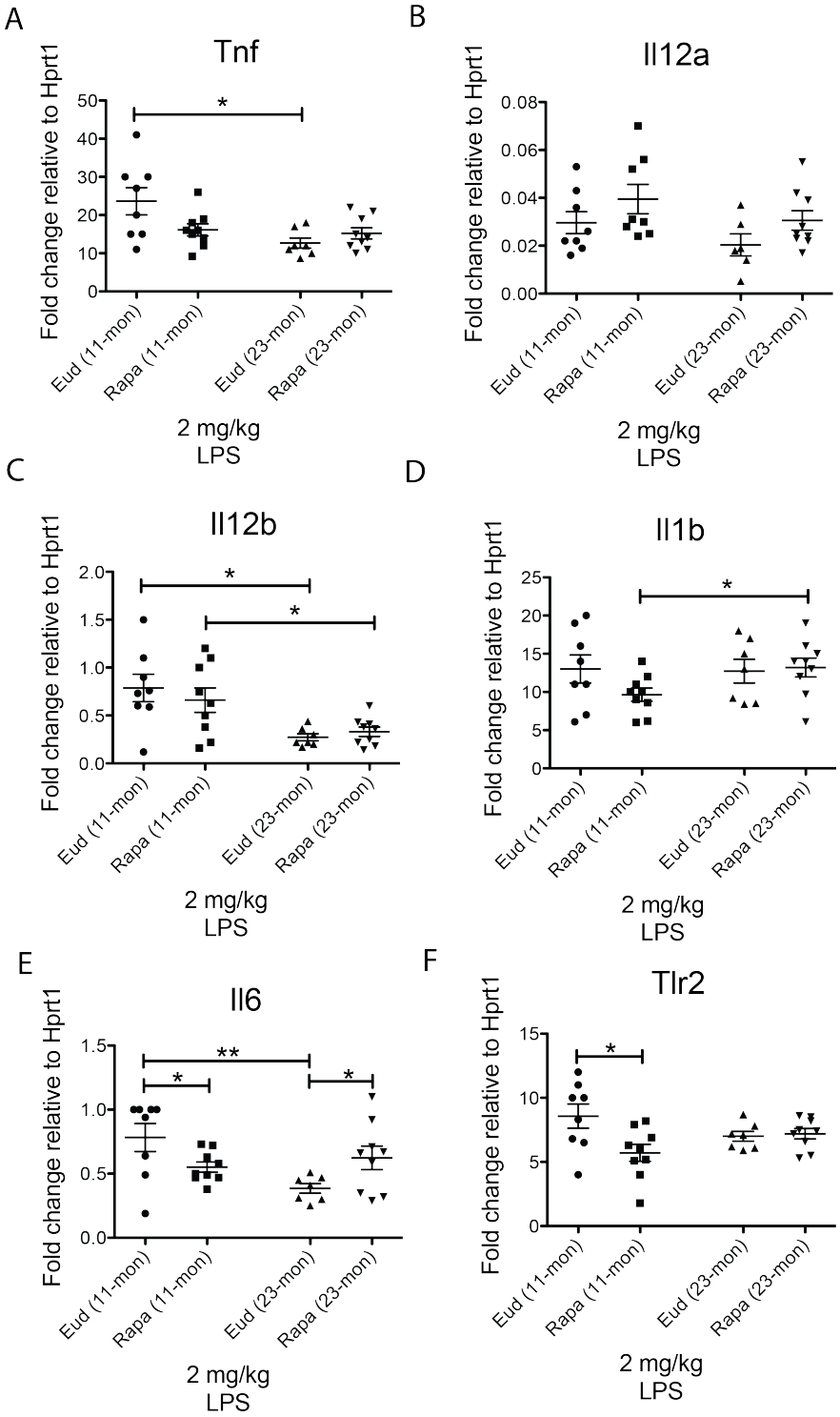

Figure 7.4 Downregulation of inflammatory genes in microglia isolated from middle-aged mice treated with rapamycin. Young (6 month) and aged mice (18 month) mice were fed a diet containing 14 ppm of rapamycin or eudragit control for 22 weeks, prior to being challenged with a peripheral injection of LPS (2 mg/kg). After five hours, mice were culled by cardiac puncture and brains were removed**.** Microglia were isolated using magnetic beads. The induction of inflammatory genes was determined using qPCR and results are reported as fold change relative to the housekeeping gene *Hprt1*. Genes analysed were **A)** *Tnf,* **B)** *Il12a* **C)** *Il12b*, **D)** *Il1b*, **E)** *Il6,* **F)** *Tlr2*. All mice used were female and n≥7 for all groups, * p<0.05, **p<0.01, data are from one individual experiment. Significance was calculated using

the unpaired two tailed student t-test between individual groups. Eud = Eudragit and Rapa=Rapamycin.

While the rapamycin diet seemed to be anti-inflammatory in middle-aged mice, no differences were observed in older mice (**Fig. 7.4 A-D** and **Fig. 7.4F**). Nonetheless, there was a significant upregulation of the *Il6* gene in the older mice (23 month) after rapamycin treatment ($p<0.05$), which was in direct contrast to what was observed in the 11-month age group, in which the gene appeared to be downregulated (**Fig. 7.4E**).

The most striking result was the difference between the two different eudragit control groups post LPS injection. As explained earlier, it has been reported in the literature that microglia become primed with age, i.e. they become over responsive to an LPS challenge and produce more inflammatory cytokines compared to their younger counterparts[224]. As a result, in this experiment, I expected to see a stronger induction of pro-inflammatory cytokines in the 23-month old control group compared to the 11-month one. I observed the opposite; there was a clear down regulation of key inflammatory genes with age in the eudragit-treated group after LPS injection. This was evident for *Tnf* and *Il12b* (**Fig 7.4A** and **7.4C**), for which differences were statistically significant ($p<0.05$). The downregulation was even more striking for *Il6* ($p<0.01$, **Fig 7.4E**).

Finally, there were also differences between the 11 and 23-month old rapamycin-treated groups. These differences were not consistent across the different genes tested. For example, *Il12b* was reduced in the old group after rapamycin treatment ($p<0.05$, **Fig. 7.4C**), whereas the opposite was true for *Il1b*, which was enriched in the rapamycin-treated old mice compared to middle-aged mice ($p<0.05$, **Fig 7.4D**).

7.4 Middle-aged rapamycin-treated mice exhibited reduced cytokine production at protein level

I further assessed cytokine production in rapamycin-treated mice by ELISA, in order to verify whether the protein levels correlated with the mRNA levels measured in microglia. To this end, I analysed the plasma for TNF α and IL-12p40 by ELISA. Similarly to what I observed in microglial mRNAs, inflammatory cytokines were lower in middle-aged rapamycin-treated mice compared to those on the eudragit control diet. TNF α and IL12p40 followed this trend, although the decrease in middle-aged rapamycin-treated mice was only significant for IL12p40 ($p<0.05$, **Fig. 7.5A** and **7.5B**). There were no differences between the rapamcyin and eudragit treatments in the 23-month old groups. Furthermore, there were also no differences between the control groups (middle aged vs. old) and rapamycin-treated group (middle-aged vs. old, **Fig. 7.5A** and **7.5B**) at protein level.

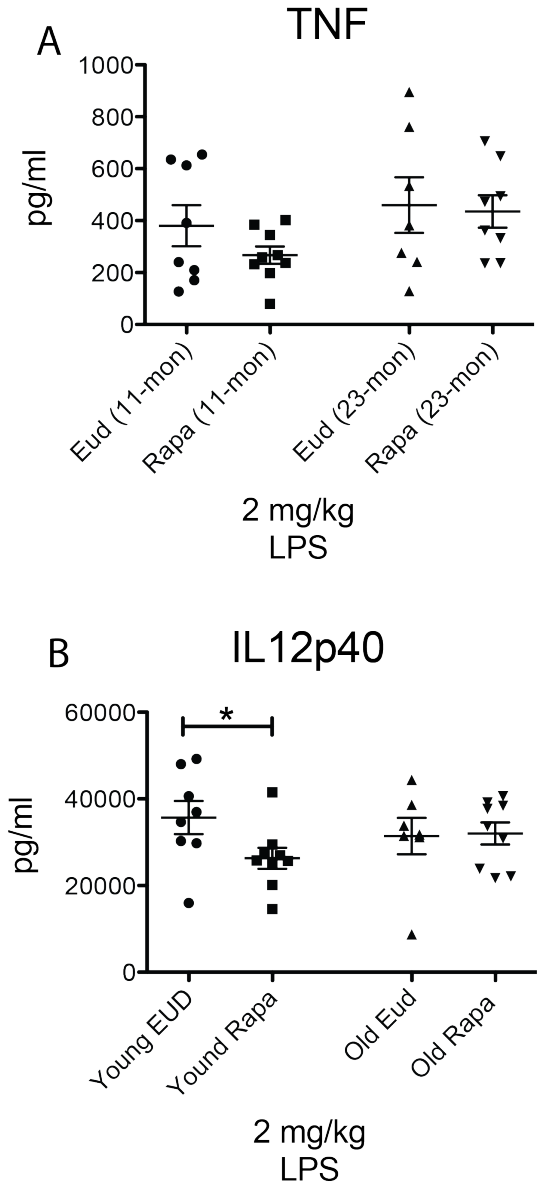

Figure 7.5 Rapamycin-treated middle-aged mice showed reduced levels of IL-12p40 in plasma. Plasma levels of **A)** TNFα and **B)** IL12p40 as measured by ELISA using the plasma of middle-aged and old mice on rapamycin or eudragit diets injected with 2mg/kg LPS i.p. and culled five hours later. All mice were female, n≥7 for all groups, * $p<0.05$, data are from one individual experiment. Eud = Eudragit and Rapa=Rapamycin. Significance was calculated using the unpaired two tailed student t-test between individual groups.

7.5 Is the mTOR pathway inhibited in older (23 months) rapamycin-treated mice?

Given that I only observed changes in cytokine transcript levels (microglia) and cytokine protein levels (plasma) in the younger 11-month old group of mice and not in the older group following rapamycin treatment, I asked the question; is the mTOR pathway inhibited in these older mice? To answer this, I carried out phospho flow cytometry analysis assessing the status of p-S6. Staining was done on the whole blood, using CD11b and CD45 as markers for myeloid (CD11b) and immune cells (CD45). I found that there was a reduction in the phosphorylation of S6 in CD11b+ myeloid cells (**Fig. 7.6A**) and in CD45+ immune cells (**Fig. 7.6B**) in the 11-month age group, although these differences were not statistically significant. In the old mice (23 months), the levels of phospho-S6 appeared lower overall, however, no differences were observed between the rapamycin-treated and control groups. This was the case for both CD11b+ cells (**Fig. 7.6A**) and for CD45+ immune cells (**Fig. 7.6B**).

To assess if the mTOR pathway was inhibited in the older age group of mice, protein lysates were made from the heart tissue of both rapamycin- and eudragit-treated groups. No difference in p-S6 levels between these two groups were observed (**Fig. 7.6C**), however, p-S6 levels were not assessed in the 11-month old mice, therefore it was not possible to make a comparison.

These results do not clarify if the mTOR pathway was inhibited in the 23-month rapamycin-treated group. It is possible that the pathway was not inhibited because mTOR activation is already reduced in aged peripheral myeloid cells and heart tissue, therefore cannot be reduced further by rapamycin treatment. Furthermore, the heart may not be the most appropriate tissue to test p-S6 levels and it would be important to check p-S6 levels in other tissues to confirm mTOR inhibition.

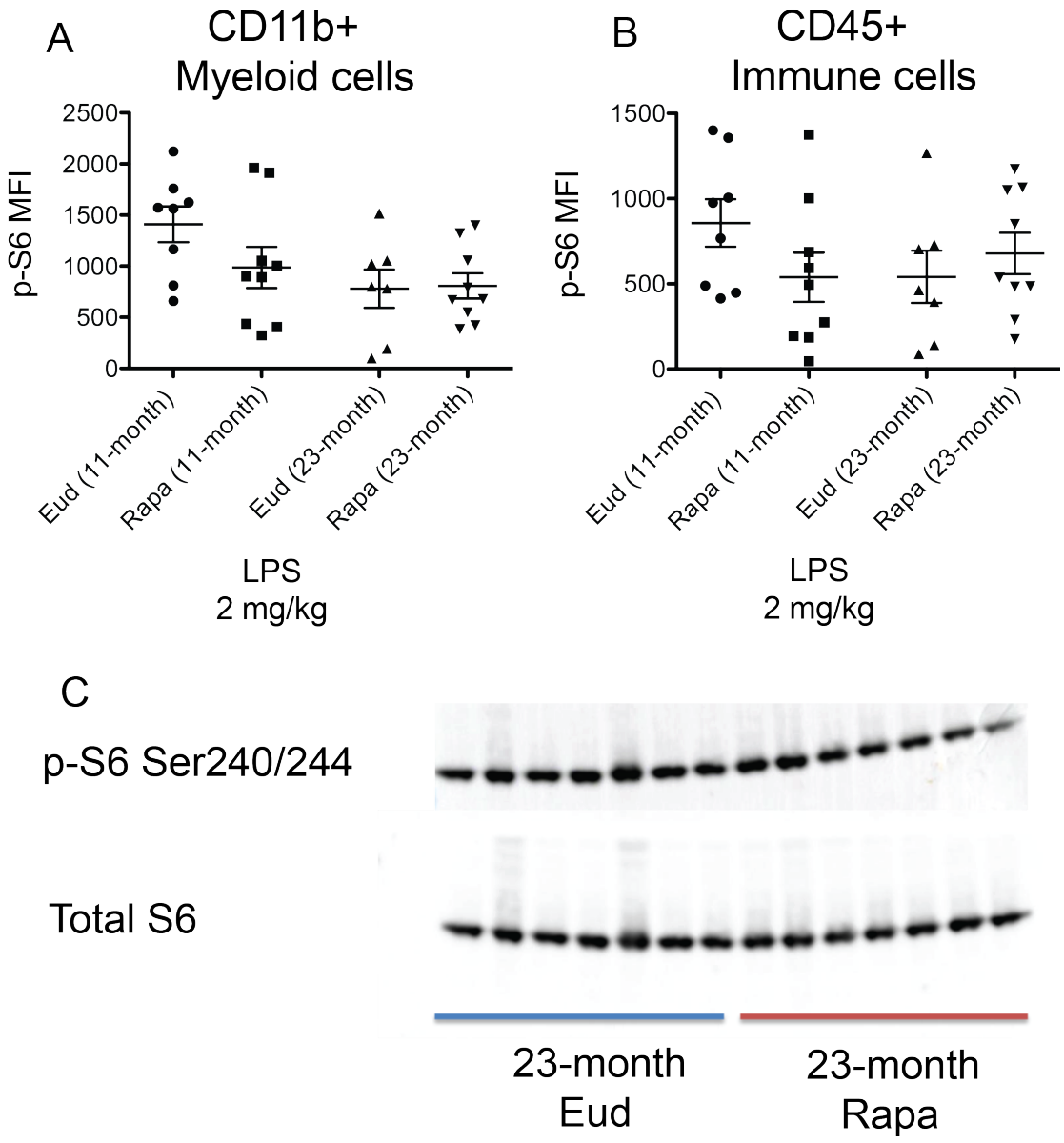

Figure 7.6 The mTOR pathway may not have been inhibited in 23-month old rapamycin treated group. Young (6 month) and aged mice (18 month) mice were fed a diet containing 14 ppm of rapamycin or eudragit control for 22 weeks, prior to being challenged with a peripheral injection of LPS (2 mg/kg). After five hours, mice were culled by cardiac puncture and 100 ul of blood was fixed immediately in PFA and later stained for p-S6, CD11b and CD45. The median fluorescence intensity (MFI) for p-S6 is shown for **A)** CD11b+ myeloid cells and **B)** CD45+ immune cells from whole blood. **C)** Protein lysates were prepared from the heart tissue of seven 23-month eudragit-treated mice and eight 23-month rapamycin-treated mice and immunoblot for p-S6 was carried out. Eud = Eudragit and Rapa=Rapamycin.

7 Discussion

In this chapter, I describe my efforts to understand if long-term rapamycin treatment would have an effect on the inflammatory response. To this end, I fed mice with a rapamycin-containing diet for 22 weeks and then challenged them with a peripheral injection of 2 mg/kg of LPS. I hypothesised that the mice on rapamycin would have a stronger inflammatory response compared to eudragit controls and that this effect might be further increased in the older age groups. The results were quite different to what I expected and they raise a number of questions that will need to be addressed in the future.

7.1 Length of rapamycin treatment and effect on mTOR signalling

The most striking observation in this data set is that the only difference due to rapamycin was observed in the group that received it from 6 months of age, with relatively no differences in any of the parameters measured in the older group. This observation leads to the question; was the pathway equally inhibited in both age groups of mice? Was 22-weeks on rapamycin a sufficiently long treatment? Our preliminary data would suggest that the pathway may be at least be partly inhibited in myeloid cells from the younger group of mice, but this did not seem to be the case from the older age group. P-S6 levels in the heart tissue obtained from the older group of mice also further support the idea that the pathway was not inhibited in this group. To try to reconcile these findings and to determine if the heart was the best tissue to test levels of p-S6, I examined the literature on mTOR activation in different tissues with ageing.

It has been generally thought that mTORC1 signalling increases with age and that rapamycin exerts some, if not all, of its anti-ageing properties by inhibiting mTOR[225]. Recent evidence, however, has suggested this may not be entirely true. Indeed, Houtkooper *et al.* showed that there was a reduction in mTORC1 signalling with age (2 v 24 month mice) as marked by a decrease in phosphorylation of S6K1 in muscle tissue[226]. This was similar to a human study that profiled transcriptional changes in the blood between young and aged individuals and found a general decrease in mTOR related transcripts with age[227]. However, a number of studies with C57BL/6 mice have

reported an increase in mTORC1 signalling with age, for example in the lung[228] and the liver[229]. It is possible that the discrepancies in the literature are linked to sex differences, age groups or models used.

Baar *et al.* conducted a study that is most relevant to our research. The authors examined both mTORC1 and mTORC2 signalling in male and female C57BL/6J at 6 months and 22 to 26 months. From the different organs examined, it was found that there was a 30% decrease in mTORC1 signalling in the liver in both male and female mice with age, as measured by phosphorylation of S6. In the skeletal muscle, there was twice as much phosphorylation of S6 in males with age but no changes were observed in the skeletal muscle of females. There was no increase in mTORC1 signalling in the heart with age in either males or females. The most striking increases in pS6 was in the adipose tissue, where a 3-fold increase was observed in males and a 6-fold increase was observed in females with age[230]. Based on this evidence, I should check if the pathway was inhibited in the adipose tissue in my cohort of mice after rapamycin treatment, as this appears to be the only tissue majorly affected in female C57BL/6J mice. This could be tested by carrying out a western blot with the adipose tissue cell lysate and measuring phosphorylation of S6, similarly to what I have shown with the heart tissue. In the Harrison *et al. Nature* paper that first showed an extension of lifespan in mice with rapamycin, the authors show a clear inhibition of phosphorylation of S6 in the visceral fat pads of both male and female mice. However, these mice were fed rapamcyin for 420 days[31]. It would also be important to clarify if therapeutic levels of rapamycin were present in the blood of these mice. This could be done similarly to the Harrison *et al.* study that used high performance liquid chromatography to quantify the amount of rapamycin in the blood of each animal.

Could it be that longer treatment is needed to fully inhibit the pathway in the older age group? Given that lower levels are observed in p-S6 in myeloid cells from older mice?

It would also be important to determine what affect the rapamycin diet had on mTOR signalling in microglia from the ageing brain. I have previously described in chapter 4 that the mTOR pathway is upregulated in microglia from 23-month old female mice, as determined by RNA sequencing. An important question would be; even if mTOR inhibition is not evident in the tissues from the 23-month rapamycin-treated mice, could

rapamycin levels be sufficient to inhibit the mTOR pathway in microglia? The best way to test this would be to look at the levels of pS6 in the microglia by immunofluorescence in the brains of these mice.

7.2 Microglia priming

Regarding the qPCR analysis of inflammatory genes, when comparing the middle-aged and old eudragit control groups I expected to observe a clear upregulation of inflammatory genes in the old group upon LPS challenge. This was not the case, as I observed many of the inflammatory genes to be downregulated in the old control group, compared to the middle-aged one. This is not in line with what has previously been reported in the literature, showing microglia are primed with age and tend to be over responsive to inflammatory stimuli[3]. In our experiment, microglia appeared to be tolerised rather than primed with age. Tolerance and priming are well-described mechanisms in macrophages and depend on which stimuli the cells are exposed to and the order of exposure. For example, macrophages exposed to LPS become tolerised and respond to a second inflammatory stimulus with a reduced production of inflammatory cytokines, compared to "naïve macrophages". On the other hand, if macrophages are exposed to beta-glucan, they become primed and produce more inflammatory cytokines when later challenged with a second stimulus. These responses were shown to be due to epigenetic reprogramming[231]. Given what I observed in my experiment, in which microglia appear to produce lower levels of inflammatory cytokines with age, it is possible to speculate that these mice were exposed to a pathogen or endotoxin, which lead them to become tolerised and less responsive. Mice were purchased from Charles River prior to commencing the experiment; therefore the old group had spent a considerable length of time in a different environment, before being transferred to our facility.

While this is one possible explanation, it also cannot be ruled out that the material used to encapsulate the rapamycin, eudragit, could be having an effect on the inflammatory response in the microglia. Therefore, it would be important to repeat this experiment with a group of mice that do not receive the eudragit control diet, to rule out any potential effects. It would also be important to use PBS controls if the experiment was repeated, in order to see if rapamycin affected the baseline levels of inflammatory genes

in microglia and systemically in ageing. Unfortunately, I did not have sufficient mice to include PBS controls in this experiment, as I thought it would be more important to have a larger cohort of mice to examine sickness behaviour and be certain about the LPS results. This is a major limitation in interrupting the results presented in this chapter as not having PBS controls means I could not determine changes from the baseline. This is true for example when trying to understand if LPS has induced an inflammatory response, as this is also difficult to determine without having a baseline reference. Another limitation is not being able to determine the affect of the Eudragit (if any) on this cohort of mice, as again we cannot compare it to baseline.

Although I still need to verify that rapamcyin was administered at a sufficiently high concentration to attain mTOR inhibition, I did observe an affect in the middle-aged group of mice, which suggests that, at least in the middle-aged group, rapamycin concentrations were therapeutically relevant. However, as a result of rapamycin treatment I observed a decrease in the inflammatory response, both at transcript (in microglia) and protein levels (in the plasma). The fact that I detected a decrease in gene expression indicates that a different mechanism is in place, compared to Rheb KO mice, possibly rapamycin is causing inhibition of NF-κB, rather than its activation or there is a different effect on FOXO1, another transcription factor implicated in the inflammatory response that is regulated by mTOR[137]. Our results are in direct contrast to Weichhart *et al.* who *s*howed that rapamycin treatment *in vivo* lead to a stronger inflammatory response to *L. monocytogenes* pathogen in Balb/c mice. It is possible that differences in mouse strains used or the extent of rapamycin treatment plays an important role. It remains unknown what is the effect of inhibiting both mTORC1 and mTORC2 complexes for such a long period of time on the downstream signalling and global changes at organism level, such as changes in whole body metabolism.

The idea that treatment with rapamycin in an ageing context may be anti-inflammatory is supported by other reports in the literature. In one study, Flynn *et al.* showed a reduction in heart-related inflammation when mice were treated with rapamycin in a similar fashion to our study[232]. An overall reduction in both the induction of SASP-related genes and secreted proteins was reported with *in vitro* treatment of senescent cells with rapamycin. Importantly, in this paper, SASP-related genes, including *Il6* and *Il1b*, were downregulated in the liver of mice treated with rapamycin long term[233]. In

these studies, the molecular mechanism governing these changes were not described and more work regarding the effect on downstream signalling with long-term rapamycin treatment is needed to clarify this point.

7 Conclusion

Overall, our results suggest that rapamycin treatment starting at a relatively young age (6 months) may lead to a reduction in the inflammatory response when mice are later challenged with LPS, whereas rapamycin treatment starting in old age (18 month) does not seem to have any significant effect. It is important to carry out control experiments to verify the validity of these findings and repeat this work in both male and female mice to see if their responses are similar.

8: Discussion and plans for future work

The main aim of this thesis was to understand how microglia change with age and to use this information to decipher the molecular mechanisms underpinning these changes. The work presented in this thesis has lead to a number of novel findings summarised below:

1. **Microglia from the ageing brain have a very distinct transcriptome signature;**
2. **The mTOR and inflammatory pathways are deregulated in microglia with age;**
3. **Inhibition of the mTOR pathway in microglia by Rheb deletion leads to an upregulation of key inflammatory genes at mRNA level;**
4. **This is further exaggerated with age;**
5. **These transcriptome changes are not translated into protein both *in vitro* or *in vivo*;**
6. **As a consequence, *Csf1r-Cre; Rheb f/f* mice appear to have less overall inflammation;**
7. **Long-term treatment with rapamcyin *in vivo* leads to a very different phenotype, with a decrease in inflammation at transcript and protein level but the effect is evident in middle-aged and not old mice;**
8. **These results differ from previously published evidence in which mTOR inhibition by short-term rapamycin treatment results in increased inflammation[129].**

8.1 Role of mTOR in inflammation

While activation of NF-κB is a well-established event occurring downstream of TLR or cytokine receptor signalling, the role of the mTOR pathway in NF-κB activation and more broadly its role in inflammation is less well defined. It has been suggested that mTORC1 is a negative regulator of NF-κB and therefore can increase the inflammatory response when inhibited[234] but the results presented in this thesis may indicate that the

mechanism of action of how mTORC1 co-ordinates the inflammatory response in myeloid cells can vary depending on how mTORC1 inhibition is achieved.

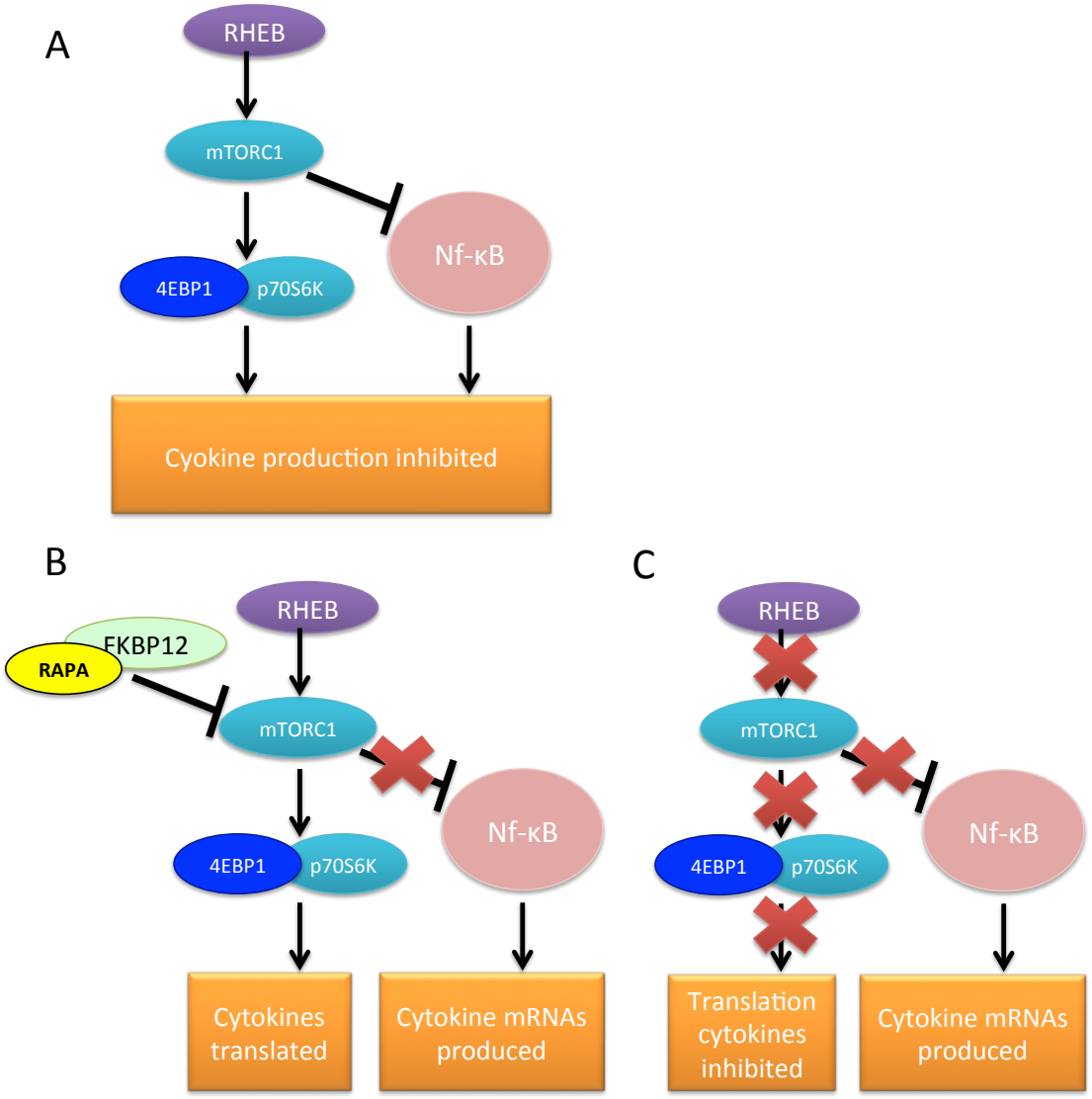

Figure 8.1 Schematic depicting the potential mechanisms governing the inflammatory response in microglia following mTOR inhibition. **A)** mTORC1 negatively regulates NF-κB and therefore is inhibited when mTORC1 is active and cytokine production is limited. **B)** Rapamycin inhibits mTORC1 leading to activation of NF-κB and production of cytokines, both at transcript and protein levels. **C)** Hypothesised effect of Rheb deletion on mTORC1 functions regulating NF-κB and protein translation.

Based on previous findings[234], we hypothesised that inhibition of mTORC1 would result in activation of NF-κB, however, it seems that if the mode of inhibition is rapamycin, it does not affect mTORC1 regulation of translation and, as result, more NF-κB dependent cytokines may be produced at a protein level, causing a stronger inflammatory response (**Fig. 8.1B**). On the other hand, if the mode of inhibition is the genetic deletion of Rheb, it seems to affect mTORC1 regulation of translation more

severely, as well as causing activation of NF-κB, therefore although there is an increase in the gene expression of cytokines, they seem to be not translated into proteins: overall this results in a weaker inflammatory response (**Fig. 8.1C**). As discussed in the discussion in chapter 6, I hypothesised that in Rheb KO cells both 4E-BP1 and S6 phosphorylation are inhibited and this could be the reason for the impairment in the translation of cytokines. One study indicates that Rheb may be very important for the regulation of protein synthesis[218]. In this study, Tyagi *et al.* showed that deletion of Rheb by small hairpin RNA (shRNA) in HEK293 cells lead to a reduction in p-4E-BP1 and p-S6 and speculate that this would inhibit protein synthesis. However, they also elucidate another molecular pathway by which Rheb can regulate protein synthesis, through the phosphorylation of another eukaryotic initiation factor called eIF2α. When Rheb was over expressed, it increased the phosphorylation of this factor and inhibited protein synthesis. Therefore both Rheb downregulation and Rheb overexpression can impair protein synthesis. The authors suggest that Rheb may act as a molecular switch between the stimulation and inhibition of protein synthesis[218]. It would be interesting in my model to check the phosphorylation state of eIF2α although the fact that I observed an inhibition of protein synthesis when Rheb is deleted suggests the effect is 4E-BP1 mediated. Nevertheless this study does highlight the importance of Rheb in regulating protein synthesis. These findings are important as they may shed light on the contradictory results on whether mTOR inhibition leads to a pro versus an anti-inflammatory response. They also provide useful information about the effect of targeting different arms of the pathway. mTOR inhibitors are under investigation as a treatment for a number of diseases with an inflammatory component and to extend lifespan, therefore understanding what affect these drugs would have on inflammation is very important.

Overall, my results show that mTOR is a key regulator of the inflammatory response of macrophages and microglia.

8.2 Role of mTOR in ageing

My results may have implications also for the use of mTOR inhibitors to extend lifespan. Rapamycin was recently shown to boost immune responses, specifically antibody titres, after influenza vaccinations in a group of elderly people[235]. However, a

6-week pre-treatment with rapamycin may have very different effects compared to long-term chronic use of the drug. The rapamycin data presented in my study would suggest that long-term use of this drug could result in a reduction in the inflammatory response. This could have both positive and negative implications for the ageing host. It is well documented that the immune system declines with age and that elderly people can often succumb to basic infections. Therefore if rapamycin treatment was to result in a defective ability to produce important inflammatory cytokines, this could potentially have deleterious consequences for the clearance of basic bacterial or viral infections.

Analogs of rapamcyin (rapalogs) are being investigated as potential anti ageing treatments as well as other possible mTORC1 inhibitors. It would be important to investigate the specific effect of each of them on the inflammatory response. For example, too much inflammation in the elderly could lead to an increase in age-related diseases, endotoxic shock or tissue damage. In my data obtained with rapamycin, it appeared that the effects on the inflammatory response only occurred when mice were fed the drug from an early age. While these experiments would need to be repeated, they do indicate that giving rapamycin later in life may not affect inflammatory responses.

It must be considered that the majority of ageing studies conducted in mice using the drug rapamycin have been done in a relatively clean environment. This is true for the Harrison *et al*. study where specific pathogen free (SPF) mice were used at three independent sites to assess the affects of rapamycin on lifespan[31]. While there have been many other studies to date where both age and age-related illness have been assessed in mice treated long-term with rapamycin, these studies would also have been carried out on WT laboratory mice housed in clean conditions. This therefore leads to the question would the anti-ageing affect of rapamycin be observed in mice in a "dirtier" environment. This is perhaps a particularly important question when studying the immune system, in the context of rapamycin treatment, given a recent publication in *Nature* that showed that standard laboratory housing conditions had profound effects on the immune system[236]. The most striking observation was that laboratory mice lacked effector-differentiated memory T cells, a compartment that was present in WT mice obtained from pet shops and barns. This compartment could be induced effectively in laboratory mice by co-habiting them with these pet shop/barn mice. Given that many

age-related illnesses are believed to have a strong immune component, it must be considered that rapamycin given to these types of WT mice could have very different results to there SPF WT counterparts. One study that might overcome the environmental bias associated with laboratory mice is a study being conducted by Kaeberlein *et al*. in which dogs are being treated with rapamycin[237]. The dogs that have been recruited in these studies are pets and therefore share the same environment as their human owners including, for example, contaminants in the water or exposure to pathogens. Therefore the results of these types of studies will be extremely informative. Early results reported suggest that rapamycin has lead to improvements in heart function, however it will be several years till it is clear if it has similar effects on canine longevity[237].

The use of rapamycin has been associated with a long list of side effects including ulcers, rash, hair and nail disorders, alopecia and reduced male fertility[238]. While the majority of these side effects have been described in transplant or renal cell carcinoma patients, they do raise the important question of whether a drug with these side effects is a valid treatment to prevent ageing[238]. However, it must also be considered that the doses used in transplant and renal cell carcinoma of rapamycin is considerably higher than the doses that are being proposed for human ageing studies. For example, in renal cell carcinoma patients are routinely given approximately 25 mg/kg of rapamycin or a rapamycin analog[239] whereas the proposed dose for human studies is considered to be within the 0.5-5 mg/kg range[235].

8.3 Implications of mTOR inhibition in microglia cells on neurodegeneration

One of the most interesting results from my data was that the mTOR pathway appeared to be upregulated in microglia with age. However, it is important to confirm this upregulation at protein level in order to show that the changes observed are not an artefact of the RNA sequencing experiment. I am therefore, currently trying to validate that the mTOR pathway is upregulated with age in microglia by using immunofluorescence staining of p-S6 and Iba-1, a microglia-specific marker. Considering my hypothesis that mTOR is activated with age to limit excessive

inflammation, it would also be important to look at the nuclear localisation of NF-κB p65 in aged microglia, as a measure of NF-κB activation. These experiments are important for understanding my rapamycin experiment data, especially in order to understand how much rapamycin is therapeutically necessary to inhibit the mTOR pathway in microglia with age.

The first indication that rapamycin could be beneficial in the treatment of Alzheimer's was published in 2010 by Caccamo *et al*. The authors used the 3 x Tg-AD mouse model, which develops the key features of the disease such as the build up of amyloid plagues and tau tangles. Using this model, it was shown that a 13-week treatment with rapamycin was sufficient to protect Tg mice from cognitive decline, as measured by the morris water maze[240]. The finding that rapamycin could improve cognition was confirmed by a second group in another model of Alzheimer's, the hAPP model[241]. In both studies, the authors showed that rapamycin treatment lead to the induction of autophagy and this was suggested as the potential mechanism behind the beneficial effects.

While there is no clear agreement on the role of inflammation in the pathogenesis of Alzheimer's disease, it is generally accepted that the number of microglia increases in the disease and that these cells present a more activated phenotype[242]. Majumder *et al.* showed that there was a clear reduction in the number of activated microglia in the hippocampus of 3 x Ttg-AD mice that had received rapamycin, compared to 3 x Tg-AD control mice, suggesting that rapamcyin was also having an effect on microglia activation[243]. However it is still relatively unknown to what extent the microglia phenotype is affected in these models. It has been suggested that this reduction in microglia activation may correlate with a decrease in brain inflammation[244] but this has not been shown conclusively.

These studies provide evidence for the use of rapamyin as an anti ageing therapy, since age is a major risk factor for Alzheimer's. Using a drug like rapamycin as a preventable measure for neurodegenerative diseases would be an attractive prospect. However, it is plausible to speculate from my data from Rheb KO mice that microglia from the ageing brain upregulate the mTOR pathway to try and limit excessive inflammation, which is further supported by the fact that many of the age-related genes altered in aged

microglia were regulated by mTOR. If this hypothesis was true, then using a drug that inhibits this pathway in microglia could potentially have negative consequences, causing excessive inflammation. However, this is not supported by my results from the *in vivo* rapamycin experiment. Therefore, it remains to be elucidated how mTOR inhibition would affect inflammation in ageing and if different mTOR inhibitors are likely to play different roles.

There are several lines of evidence in the data described in this thesis that may indicate that mTOR activation is important to limit inflammation in microglia with age. The changes in the transcriptome of microglia with age suggests that the mTOR pathway is upregulated and the fact that a number of transcription factors with a known association to mTOR are implicated using the differentially expressed genes, again would suggest a possible role of mTOR in microglia with age. However based on the transcriptome data alone it is not apparent if mTOR is activated as a consequence of age in microglia or if it plays a role in the transcriptome changes itself. The data I have obtained using the Rheb KO model may partly answer this question. This data showed that on a transcript level, inhibition of mTOR led to an upregulation of many inflammatory and age-related genes suggesting that mTOR may be used as a control mechanism for some inflammatory and age-related factors. The fact that Rheb KO macrophages display these changes on RNA but not protein level adds another layer of complexity to how mTOR may potentially control these responses. However while these findings may indicate that mTOR in ageing microglia may be controlling some of the transcriptome changes, without protein data from microglia in the ageing brain it is difficult to conclusively say how much mTOR may be controlling these changes. Also it would be important to validate that mTOR is actually active in these cells with age.

Evidence in the past suggested that microglia become more inflammatory with age and this was generally associated with more of a neurotoxic phenotype[224]. However the Hickman *et al*. study where microglia were isolated from young and aged mice and directly RNA sequenced suggested otherwise. They suggest that microglia upregulate pathways associated with neuroprotection and downregulated those associated with neurotoxicity[96]. This would indicate that the changes they observe could be a reflection of an adaptive response. The hypothesis presented in this thesis that the mTOR pathway is upregulated to try and limit excessive inflammation may also suggest a potentially

protective response. It has been reported in the literature that microglia become primed due to a change in the brain microenvironment as it ages. Therefore it could be hypothesised that the changes observed on the transcriptome level both in my study and the Hickman *et a*l. study could be a reflection of the microglia trying to cope with a changing environment. This is supported by the fact that microglia with age downregulate receptors that would be activated by endogenous ligands and upregulate those that sense exogenous ligands potentially trying to limit their activation to changes in the brain environment while also maintaining an immune-vigilant state[96,97]. However, it must also be considered that these cells do appear to be more inflammatory and that this can have negative consequences for example triggering apoptosis in neurons[55]. The production of inflammatory mediators could be a direct consequence of a changing environment and therefore influenced by age-related changes. However they could also potentially be due to intrinsic changes within the cells or a combination of both. It was shown recently that macrophages undergo epigenetic modifications that had a profound affect on the macrophage phenotype determining if the cells became primed or tolerised. This ultimately led to an effect on the cytokines produced by the cells in response to a number of ligands[231]. It is therefore conceivable that during lifespan, microglia become epigenetically modified depending on the endogenous/exogenous ligands they encounter. This may explain how the microglia become primed and are then over responsive in the changing environment of the brain. Therefore it is possible that both intrinsic and extrinsic factors influence how microglia change with age.

8.4 Future work

My work still leaves many questions unanswered; most notably the molecular mechanisms that are responsible for the phenotype observed in Rheb KO mice after LPS stimulation. I have attempted to carry out experiments to define the signalling in Rheb KO myeloid cells, however, they have been technically challenging, due to inconsistent growth of BMDMs derived from Rheb KO mice. There are a number of alternative ways to study cell signalling and they will be discussed below. I would also like to answer the following questions:

1. Does mTOR inhibition in microglia affect neurotoxicity?

2. What are the effects of inhibiting mTOR at different levels on the host's ability to clear infections? How is age affecting this process?
3. Are the results obtained from my long-term rapamycin ageing study reproducible? Could the effect depend on variables such as mice being tolerized or their microbiota?

8.4.1 Molecular mechanism of increased NF- κB. activation

The main aim of my future work is to understand the molecular mechanisms that govern the phenotype of Rheb KO mice. As described in **Fig. 8.1B**, I want to understand if the transcript changes we observe are due to NF-κB activation and if the cytokines are not translated because of broad or specific block in translation, most likely linked to 4E-BP1 phosphorylation. Since the growth of BMDMs appears to be affected by the deletion of Rheb, as well as using BMDMs, which require a differentiation step *in vitro*, I will use primary microglia obtained from neonatal mice. These cells are grown on a feeder layer of astrocytes for 10 days and it is possible that their growth may not be as affected as BMDMs. I will also use macrophages already differentiated, obtained from the peritoneum. Given that the growth of myeloid cells did not appear to be affected *in vivo*, peritoneal macrophages may be a useful alternative to cultured cells.

I plan to compare the signalling events that occur after LPS stimulation in Rheb KO cells and cells treated with rapamycin or Torin1, in order to understand their different effects on signalling and NF-κB activation.

8.4.2 mTOR inhibition and neurotoxicity

I will also generate neuronal cultures from day 18 embryonic tissue by dissecting the hippocampus and establishing cultures for 10-12 days on poly-D-lysine. I will treat Rheb KO microglia, rapamycin-treated, Torin1-treated or WT microglia with 200 ng/ml of LPS for 20-24 hours in order to induce the production and secretion of pro-inflammatory and neurotoxic factors. I will then use this culture media to assess if different modes of mTOR inhibition in microglia lead to more or less neurotoxicity. Neuronal cell death can be assessed using the MTT assay. I can also use blocking antibodies or inhibitors to block certain neurotoxic factors, if more neurotoxicity was

observed. For example, I could use an inhibitor for Il-1 β, in order to see if blocking this cytokine could reverse a potential increased neurotoxicity when mTOR is inhibited in microglia.

8.4.3 The effect of mTOR inhibition on clearing infections in the elderly

It would be really interesting and relevant to ageing research to understand what effect the different modes of mTOR inhibition would have on the ability of the host to clear infections. To answer this question, I could use young and aged Rheb KO or WT mice pre-treated with rapamycin/Torin 1 and then expose them to a basic infection often encountered by the elderly, for example influenza. It has been well documented that elderly people have increased susceptibility to this disease and it has been shown that elderly mice infected with the virus have increased mortality compared to their younger counterparts. I could then measure overall survival, as well as viral titers in the lungs and overall inflammation. It would be more relevant to do this study using long-term treatments with rapamycin or Torin1, however using a short 3-day pre-treatment similar to other studies might be necessary to distinguish the effect of long-term and short-term mTOR inhibition.

8.4.4 Questions unanswered from the rapamycin *in vivo* experiment

It would also be important to understand if the results obtained in my long-term rapamycin ageing study are reproducible, since it is possible that they are affected by the past history of infections in mice (if there was one) and/or by their microbiota. To this end, it would be important to repeat the experiment on a new cohort of young and aged mice. It would also be important to use both male and female mice to eliminate any gender-specific differences and to include both LPS and PBS treated groups, in order to gain information about changes to the baseline level of inflammatory cytokines when rapamycin is used long term.

I also need to establish if all the mice used in my original study received equal amounts of rapamycin, by measuring it in the blood using targeted mass spectrometry. If my results are reproducible and an overall reduction in the inflammatory response occurs at

transcript and protein level when rapamycin is used long term, it would be interesting to understand why this differs to short-term rapamycin treatment, which caused a more pronounced inflammatory response in Balb/c mice[234]. Why does long-term rapamycin treatment result in the opposite response? Could it be through and additional effect on mTORC2 or PI3K signalling as discussed above? Or an overall systemic adaptation to rapamycin treatment, i.e. are the metabolic changes caused by rapamycin affecting the inflammatory response? Are these differences strain specific?

In this respect, it would be useful to have an *in vitro* system to mimic long-term rapamycin treatment, which might be technically challenging. One potential strategy could be to inhibit the mTOR pathway in a macrophage-like cell line, for example the RAW 264.7. It would be interesting to compare long-term inhibition, for example 14 days, with short-term inhibition (24 hours) and see if the two treatments cause similar distinct effects on the inflammatory response

References

1 Oeppen, J. & Vaupel, J. W. Demography. Broken limits to life expectancy. *Science* **296**, 1029-1031, doi:10.1126/science.1069675 (2002).

2 Statistics, O. f. N. National Life Table, United Kingdom 2012-2014. (2015).

3 Nations, U. Changing balance between age groups *Population Division, DSEA, Unite Nations* (2015).

4 Lopez-Otin, C., Blasco, M. A., Partridge, L., Serrano, M. & Kroemer, G. The hallmarks of aging. *Cell* **153**, 1194-1217, doi:10.1016/j.cell.2013.05.039 (2013).

5 Harman, D. The aging process: major risk factor for disease and death. *Proc Natl Acad Sci U S A* **88**, 5360-5363 (1991).

6 International, A. s. D. The Global Impact of Dementia, an analysis of prevalence, incidence, costs and trends. *World Alzheimer Report 2015* (2015).

7 Bourzac, K. Interventions: Live long and prosper. *Nature* **492**, S18-20, doi:10.1038/492S18a (2012).

8 Hanahan, D. & Weinberg, R. A. The hallmarks of cancer. *Cell* **100**, 57-70 (2000).

9 Franceschi, C. *et al.* Inflammaging and anti-inflammaging: a systemic perspective on aging and longevity emerged from studies in humans. *Mech Ageing Dev* **128**, 92-105, doi:10.1016/j.mad.2006.11.016 (2007).

10 Franceschi, C. *et al.* Inflamm-aging. An evolutionary perspective on immunosenescence. *Ann N Y Acad Sci* **908**, 244-254 (2000).

11 Rubinsztein, D. C., Marino, G. & Kroemer, G. Autophagy and aging. *Cell* **146**, 682-695, doi:10.1016/j.cell.2011.07.030 (2011).
12 Shimada, K. *et al.* Oxidized mitochondrial DNA activates the NLRP3 inflammasome during apoptosis. *Immunity* **36**, 401-414, doi:10.1016/j.immuni.2012.01.009 (2012).
13 Heneka, M. T. *et al.* NLRP3 is activated in Alzheimer's disease and contributes to pathology in APP/PS1 mice. *Nature* **493**, 674-678, doi:10.1038/nature11729 (2013).
14 Nixon, R. A. & Yang, D. S. Autophagy failure in Alzheimer's disease--locating the primary defect. *Neurobiol Dis* **43**, 38-45, doi:10.1016/j.nbd.2011.01.021 (2011).
15 Combs, C. K., Karlo, J. C., Kao, S. C. & Landreth, G. E. beta-Amyloid stimulation of microglia and monocytes results in TNFalpha-dependent expression of inducible nitric oxide synthase and neuronal apoptosis. *J Neurosci* **21**, 1179-1188 (2001).
16 van de Veerdonk, F. L., Netea, M. G., Dinarello, C. A. & Joosten, L. A. Inflammasome activation and IL-1beta and IL-18 processing during infection. *Trends Immunol* **32**, 110-116, doi:10.1016/j.it.2011.01.003 (2011).
17 Coppe, J. P., Desprez, P. Y., Krtolica, A. & Campisi, J. The senescence-associated secretory phenotype: the dark side of tumor suppression. *Annu Rev Pathol* **5**, 99-118, doi:10.1146/annurev-pathol-121808-102144 (2010).
18 Coppe, J. P. *et al.* Senescence-associated secretory phenotypes reveal cell-nonautonomous functions of oncogenic RAS and the p53 tumor suppressor. *PLoS Biol* **6**, 2853-2868, doi:10.1371/journal.pbio.0060301 (2008).
19 Coppe, J. P., Desprez, P. Y., Krtolica, A. & Campisi, J. The senescence-associated secretory phenotype: the dark side of tumor suppression. *Annu Rev Pathol* **5**, 99-118, doi:10.1146/annurev-pathol-121808-102144 (2010).
20 McCay, C. M., Crowell, M. F. & Maynard, L. A. The effect of retarded growth upon the length of life span and upon the ultimate body size. 1935. *Nutrition* **5**, 155-171; discussion 172 (1989).
21 Bordone, L. & Guarente, L. Calorie restriction, SIRT1 and metabolism: understanding longevity. *Nat Rev Mol Cell Biol* **6**, 298-305, doi:10.1038/nrm1616 (2005).
22 Colman, R. J. *et al.* Caloric restriction delays disease onset and mortality in rhesus monkeys. *Science* **325**, 201-204, doi:10.1126/science.1173635 (2009).
23 Jung, K. J. *et al.* Effect of short term calorie restriction on pro-inflammatory NF-kB and AP-1 in aged rat kidney. *Inflamm Res* **58**, 143-150, doi:10.1007/s00011-008-7227-2 (2009).
24 Chung, J. H. *et al.* Molecular mechanism of PPAR in the regulation of age-related inflammation. *Ageing Res Rev* **7**, 126-136, doi:10.1016/j.arr.2008.01.001 (2008).
25 Chung, K. W. *et al.* Recent advances in calorie restriction research on aging. *Experimental gerontology* **48**, 1049-1053, doi:10.1016/j.exger.2012.11.007 (2013).
26 Kaeberlein, M. *et al.* Regulation of yeast replicative life span by TOR and Sch9 in response to nutrients. *Science* **310**, 1193-1196, doi:10.1126/science.1115535 (2005).
27 Urban, J. *et al.* Sch9 is a major target of TORC1 in Saccharomyces cerevisiae. *Mol Cell* **26**, 663-674, doi:10.1016/j.molcel.2007.04.020 (2007).

28 Hansen, M. *et al.* A role for autophagy in the extension of lifespan by dietary restriction in C. elegans. *PLoS Genet* **4**, e24, doi:10.1371/journal.pgen.0040024 (2008).
29 Hansen, M. *et al.* Lifespan extension by conditions that inhibit translation in Caenorhabditis elegans. *Aging Cell* **6**, 95-110, doi:10.1111/j.1474-9726.2006.00267.x (2007).
30 Johnson, S. C., Rabinovitch, P. S. & Kaeberlein, M. mTOR is a key modulator of ageing and age-related disease. *Nature* **493**, 338-345, doi:10.1038/nature11861 (2013).
31 Harrison, D. E. *et al.* Rapamycin fed late in life extends lifespan in genetically heterogeneous mice. *Nature* **460**, 392-395, doi:10.1038/nature08221 (2009).
32 Ma, X. M. & Blenis, J. Molecular mechanisms of mTOR-mediated translational control. *Nat Rev Mol Cell Biol* **10**, 307-318, doi:10.1038/nrm2672 (2009).
33 Rogers, A. N. *et al.* Life span extension via eIF4G inhibition is mediated by posttranscriptional remodeling of stress response gene expression in C. elegans. *Cell Metab* **14**, 55-66, doi:10.1016/j.cmet.2011.05.010 (2011).
34 Steffen, K. K. *et al.* Yeast life span extension by depletion of 60s ribosomal subunits is mediated by Gcn4. *Cell* **133**, 292-302, doi:10.1016/j.cell.2008.02.037 (2008).
35 Kim, J., Kundu, M., Viollet, B. & Guan, K. L. AMPK and mTOR regulate autophagy through direct phosphorylation of Ulk1. *Nat Cell Biol* **13**, 132-141, doi:10.1038/ncb2152 (2011).
36 Salminen, A. & Kaarniranta, K. Regulation of the aging process by autophagy. *Trends Mol Med* **15**, 217-224, doi:10.1016/j.molmed.2009.03.004 (2009).
37 Bjedov, I. *et al.* Mechanisms of life span extension by rapamycin in the fruit fly Drosophila melanogaster. *Cell Metab* **11**, 35-46, doi:10.1016/j.cmet.2009.11.010 (2010).
38 Ransohoff, R. M. & Cardona, A. E. The myeloid cells of the central nervous system parenchyma. *Nature* **468**, 253-262, doi:10.1038/nature09615 (2010).
39 Ginhoux, F. *et al.* Fate mapping analysis reveals that adult microglia derive from primitive macrophages. *Science* **330**, 841-845, doi:10.1126/science.1194637 (2010).
40 Harry, G. J. Microglia during development and aging. *Pharmacol Ther* **139**, 313-326, doi:10.1016/j.pharmthera.2013.04.013 (2013).
41 Kettenmann, H., Hanisch, U. K., Noda, M. & Verkhratsky, A. Physiology of microglia. *Physiol Rev* **91**, 461-553, doi:10.1152/physrev.00011.2010 (2011).
42 Perry, V. H., Hume, D. A. & Gordon, S. Immunohistochemical localization of macrophages and microglia in the adult and developing mouse brain. *Neuroscience* **15**, 313-326 (1985).
43 Williams, K., Ulvestad, E. & Antel, J. Immune regulatory and effector properties of human adult microglia studies in vitro and in situ. *Adv Neuroimmunol* **4**, 273-281 (1994).
44 McGeer, P. L. & McGeer, E. G. The inflammatory response system of brain: implications for therapy of Alzheimer and other neurodegenerative diseases. *Brain Res Brain Res Rev* **21**, 195-218 (1995).
45 Aloisi, F. Immune function of microglia. *Glia* **36**, 165-179 (2001).
46 Prinz, M., Tay, T. L., Wolf, Y. & Jung, S. Microglia: unique and common features with other tissue macrophages. *Acta Neuropathol*, doi:10.1007/s00401-014-1267-1 (2014).

47 Wake, H., Moorhouse, A. J., Miyamoto, A. & Nabekura, J. Microglia: actively surveying and shaping neuronal circuit structure and function. *Trends Neurosci* **36**, 209-217, doi:10.1016/j.tins.2012.11.007 (2013).
48 Paolicelli, R. C. *et al.* Synaptic pruning by microglia is necessary for normal brain development. *Science* **333**, 1456-1458, doi:10.1126/science.1202529 (2011).
49 Marin-Teva, J. L., Cuadros, M. A., Martin-Oliva, D. & Navascues, J. Microglia and neuronal cell death. *Neuron Glia Biol* **7**, 25-40, doi:10.1017/S1740925X12000014 (2011).
50 Neher, J. J. *et al.* Inhibition of microglial phagocytosis is sufficient to prevent inflammatory neuronal death. *J Immunol* **186**, 4973-4983, doi:10.4049/jimmunol.1003600 (2011).
51 Hsieh, C. L. *et al.* A role for TREM2 ligands in the phagocytosis of apoptotic neuronal cells by microglia. *J Neurochem* **109**, 1144-1156, doi:10.1111/j.1471-4159.2009.06042.x (2009).
52 Gitik, M., Liraz-Zaltsman, S., Oldenborg, P. A., Reichert, F. & Rotshenker, S. Myelin down-regulates myelin phagocytosis by microglia and macrophages through interactions between CD47 on myelin and SIRPalpha (signal regulatory protein-alpha) on phagocytes. *J Neuroinflammation* **8**, 24, doi:10.1186/1742-2094-8-24 (2011).
53 Claude, J., Linnartz-Gerlach, B., Kudin, A. P., Kunz, W. S. & Neumann, H. Microglial CD33-related Siglec-E inhibits neurotoxicity by preventing the phagocytosis-associated oxidative burst. *J Neurosci* **33**, 18270-18276, doi:10.1523/JNEUROSCI.2211-13.2013 (2013).
54 Cardona, A. E. *et al.* Control of microglial neurotoxicity by the fractalkine receptor. *Nat Neurosci* **9**, 917-924, doi:10.1038/nn1715 (2006).
55 Sierra, A. *et al.* Microglia shape adult hippocampal neurogenesis through apoptosis-coupled phagocytosis. *Cell Stem Cell* **7**, 483-495, doi:10.1016/j.stem.2010.08.014 (2010).
56 Choi, S. H. *et al.* Non-cell-autonomous effects of presenilin 1 variants on enrichment-mediated hippocampal progenitor cell proliferation and differentiation. *Neuron* **59**, 568-580, doi:10.1016/j.neuron.2008.07.033 (2008).
57 Davalos, D. *et al.* ATP mediates rapid microglial response to local brain injury in vivo. *Nat Neurosci* **8**, 752-758, doi:10.1038/nn1472 (2005).
58 Nimmerjahn, A., Kirchhoff, F. & Helmchen, F. Resting microglial cells are highly dynamic surveillants of brain parenchyma in vivo. *Science* **308**, 1314-1318, doi:10.1126/science.1110647 (2005).
59 Chechik, G., Meilijson, I. & Ruppin, E. Synaptic pruning in development: a computational account. *Neural Comput* **10**, 1759-1777 (1998).
60 Ma, Y., Ramachandran, A., Ford, N., Parada, I. & Prince, D. A. Remodeling of dendrites and spines in the C1q knockout model of genetic epilepsy. *Epilepsia* **54**, 1232-1239, doi:10.1111/epi.12195 (2013).
61 Schafer, D. P. *et al.* Microglia sculpt postnatal neural circuits in an activity and complement-dependent manner. *Neuron* **74**, 691-705, doi:10.1016/j.neuron.2012.03.026 (2012).
62 Hoshiko, M., Arnoux, I., Avignone, E., Yamamoto, N. & Audinat, E. Deficiency of the microglial receptor CX3CR1 impairs postnatal functional development of thalamocortical synapses in the barrel cortex. *J Neurosci* **32**, 15106-15111, doi:10.1523/JNEUROSCI.1167-12.2012 (2012).

63 Dissing-Olesen, L. *et al.* Activation of neuronal NMDA receptors triggers transient ATP-mediated microglial process outgrowth. *J Neurosci* **34**, 10511-10527, doi:10.1523/JNEUROSCI.0405-14.2014 (2014).
64 Stellwagen, D. & Malenka, R. C. Synaptic scaling mediated by glial TNF-alpha. *Nature* **440**, 1054-1059, doi:10.1038/nature04671 (2006).
65 Parkhurst, C. N. *et al.* Microglia promote learning-dependent synapse formation through brain-derived neurotrophic factor. *Cell* **155**, 1596-1609, doi:10.1016/j.cell.2013.11.030 (2013).
66 Nakajima, K. & Kohsaka, S. Microglia: activation and their significance in the central nervous system. *J Biochem* **130**, 169-175 (2001).
67 Verdijk, P. *et al.* Morphological changes during dendritic cell maturation correlate with cofilin activation and translocation to the cell membrane. *Eur J Immunol* **34**, 156-164, doi:10.1002/eji.200324241 (2004).
68 Kreutzberg, G. W. Microglia: a sensor for pathological events in the CNS. *Trends Neurosci* **19**, 312-318 (1996).
69 Hanisch, U. K. & Kettenmann, H. Microglia: active sensor and versatile effector cells in the normal and pathologic brain. *Nat Neurosci* **10**, 1387-1394, doi:10.1038/nn1997 (2007).
70 Hoek, R. M. *et al.* Down-regulation of the macrophage lineage through interaction with OX2 (CD200). *Science* **290**, 1768-1771 (2000).
71 Wright, G. J. *et al.* Lymphoid/neuronal cell surface OX2 glycoprotein recognizes a novel receptor on macrophages implicated in the control of their function. *Immunity* **13**, 233-242 (2000).
72 Wakselman, S. *et al.* Developmental neuronal death in hippocampus requires the microglial CD11b integrin and DAP12 immunoreceptor. *J Neurosci* **28**, 8138-8143, doi:10.1523/JNEUROSCI.1006-08.2008 (2008).
73 Marin-Teva, J. L. *et al.* Microglia promote the death of developing Purkinje cells. *Neuron* **41**, 535-547 (2004).
74 Stevens, B. *et al.* The classical complement cascade mediates CNS synapse elimination. *Cell* **131**, 1164-1178, doi:10.1016/j.cell.2007.10.036 (2007).
75 Erblich, B., Zhu, L., Etgen, A. M., Dobrenis, K. & Pollard, J. W. Absence of colony stimulation factor-1 receptor results in loss of microglia, disrupted brain development and olfactory deficits. *PLoS One* **6**, e26317, doi:10.1371/journal.pone.0026317 (2011).
76 Pont-Lezica, L., Bechade, C., Belarif-Cantaut, Y., Pascual, O. & Bessis, A. Physiological roles of microglia during development. *J Neurochem* **119**, 901-908, doi:10.1111/j.1471-4159.2011.07504.x (2011).
77 Tremblay, M. E., Zettel, M. L., Ison, J. R., Allen, P. D. & Majewska, A. K. Effects of aging and sensory loss on glial cells in mouse visual and auditory cortices. *Glia* **60**, 541-558, doi:10.1002/glia.22287 (2012).
78 Vaughan, D. W. & Peters, A. Neuroglial cells in the cerebral cortex of rats from young adulthood to old age: an electron microscope study. *J Neurocytol* **3**, 405-429 (1974).
79 Damani, M. R. *et al.* Age-related alterations in the dynamic behavior of microglia. *Aging Cell* **10**, 263-276, doi:10.1111/j.1474-9726.2010.00660.x (2011).
80 Luo, X. G., Ding, J. Q. & Chen, S. D. Microglia in the aging brain: relevance to neurodegeneration. *Mol Neurodegener* **5**, 12, doi:10.1186/1750-1326-5-12 (2010).

81 Schuitemaker, A. *et al.* Microglial activation in healthy aging. *Neurobiol Aging* **33**, 1067-1072, doi:10.1016/j.neurobiolaging.2010.09.016 (2012).
82 Ogura, K., Ogawa, M. & Yoshida, M. Effects of ageing on microglia in the normal rat brain: immunohistochemical observations. *Neuroreport* **5**, 1224-1226 (1994).
83 Frank, M. G. *et al.* mRNA up-regulation of MHC II and pivotal pro-inflammatory genes in normal brain aging. *Neurobiol Aging* **27**, 717-722, doi:10.1016/j.neurobiolaging.2005.03.013 (2006).
84 Letiembre, M. *et al.* Innate immune receptor expression in normal brain aging. *Neuroscience* **146**, 248-254, doi:10.1016/j.neuroscience.2007.01.004 (2007).
85 Sheng, J. G., Mrak, R. E. & Griffin, W. S. Enlarged and phagocytic, but not primed, interleukin-1 alpha-immunoreactive microglia increase with age in normal human brain. *Acta Neuropathol* **95**, 229-234 (1998).
86 Ye, S. M. & Johnson, R. W. Increased interleukin-6 expression by microglia from brain of aged mice. *J Neuroimmunol* **93**, 139-148 (1999).
87 Godbout, J. P. *et al.* Exaggerated neuroinflammation and sickness behavior in aged mice following activation of the peripheral innate immune system. *Faseb J* **19**, 1329-1331, doi:10.1096/fj.05-3776fje (2005).
88 Henry, C. J., Huang, Y., Wynne, A. M. & Godbout, J. P. Peripheral lipopolysaccharide (LPS) challenge promotes microglial hyperactivity in aged mice that is associated with exaggerated induction of both pro-inflammatory IL-1beta and anti-inflammatory IL-10 cytokines. *Brain Behav Immun* **23**, 309-317, doi:10.1016/j.bbi.2008.09.002 (2009).
89 Dilger, R. N. & Johnson, R. W. Aging, microglial cell priming, and the discordant central inflammatory response to signals from the peripheral immune system. *J Leukoc Biol* **84**, 932-939, doi:10.1189/jlb.0208108 (2008).
90 Zhang, G. *et al.* Hypothalamic programming of systemic ageing involving IKK-beta, NF-kappaB and GnRH. *Nature* **497**, 211-216, doi:10.1038/nature12143 (2013).
91 Ma, W. *et al.* Gene expression changes in aging retinal microglia: relationship to microglial support functions and regulation of activation. *Neurobiol Aging* **34**, 2310-2321, doi:10.1016/j.neurobiolaging.2013.03.022 (2013).
92 Perry, V. H., Matyszak, M. K. & Fearn, S. Altered antigen expression of microglia in the aged rodent CNS. *Glia* **7**, 60-67, doi:10.1002/glia.440070111 (1993).
93 Perry, V. H. & O'Connor, V. The role of microglia in synaptic stripping and synaptic degeneration: a revised perspective. *ASN Neuro* **2**, e00047, doi:10.1042/AN20100024 (2010).
94 Bachstetter, A. D. *et al.* Fractalkine and CX 3 CR1 regulate hippocampal neurogenesis in adult and aged rats. *Neurobiol Aging* **32**, 2030-2044, doi:10.1016/j.neurobiolaging.2009.11.022 (2011).
95 Orre, M. *et al.* Acute isolation and transcriptome characterization of cortical astrocytes and microglia from young and aged mice. *Neurobiol Aging* **35**, 1-14, doi:10.1016/j.neurobiolaging.2013.07.008 (2014).
96 Hickman, S. E. *et al.* The microglial sensome revealed by direct RNA sequencing. *Nat Neurosci* **16**, 1896-1905, doi:10.1038/nn.3554 (2013).
97 Grabert, K. *et al.* Microglial brain region-dependent diversity and selective regional sensitivities to aging. *Nat Neurosci* **19**, 504-516, doi:10.1038/nn.4222 (2016).

98 Laplante, M. & Sabatini, D. M. mTOR signaling at a glance. *Journal of cell science* **122**, 3589-3594, doi:10.1242/jcs.051011 (2009).
99 Hara, K. *et al.* Raptor, a binding partner of target of rapamycin (TOR), mediates TOR action. *Cell* **110**, 177-189 (2002).
100 Peterson, T. R. *et al.* DEPTOR is an mTOR inhibitor frequently overexpressed in multiple myeloma cells and required for their survival. *Cell* **137**, 873-886, doi:10.1016/j.cell.2009.03.046 (2009).
101 Frias, M. A. *et al.* mSin1 is necessary for Akt/PKB phosphorylation, and its isoforms define three distinct mTORC2s. *Curr Biol* **16**, 1865-1870, doi:10.1016/j.cub.2006.08.001 (2006).
102 Manning, B. D. & Cantley, L. C. Rheb fills a GAP between TSC and TOR. *Trends Biochem Sci* **28**, 573-576, doi:10.1016/j.tibs.2003.09.003 (2003).
103 Potter, C. J., Pedraza, L. G. & Xu, T. Akt regulates growth by directly phosphorylating Tsc2. *Nat Cell Biol* **4**, 658-665, doi:10.1038/ncb840 (2002).
104 Vander Haar, E., Lee, S. I., Bandhakavi, S., Griffin, T. J. & Kim, D. H. Insulin signalling to mTOR mediated by the Akt/PKB substrate PRAS40. *Nat Cell Biol* **9**, 316-323, doi:10.1038/ncb1547 (2007).
105 Zhang, J., Gao, Z., Yin, J., Quon, M. J. & Ye, J. S6K directly phosphorylates IRS-1 on Ser-270 to promote insulin resistance in response to TNF-(alpha) signaling through IKK2. *J Biol Chem* **283**, 35375-35382, doi:10.1074/jbc.M806480200 (2008).
106 Harrington, L. S., Findlay, G. M. & Lamb, R. F. Restraining PI3K: mTOR signalling goes back to the membrane. *Trends Biochem Sci* **30**, 35-42, doi:10.1016/j.tibs.2004.11.003 (2005).
107 Gwinn, D. M. *et al.* AMPK phosphorylation of raptor mediates a metabolic checkpoint. *Mol Cell* **30**, 214-226, doi:10.1016/j.molcel.2008.03.003 (2008).
108 Hardie, D. G. AMP-activated/SNF1 protein kinases: conserved guardians of cellular energy. *Nat Rev Mol Cell Biol* **8**, 774-785, doi:10.1038/nrm2249 (2007).
109 Efeyan, A., Zoncu, R. & Sabatini, D. M. Amino acids and mTORC1: from lysosomes to disease. *Trends Mol Med* **18**, 524-533, doi:10.1016/j.molmed.2012.05.007 (2012).
110 Sancak, Y. *et al.* The Rag GTPases bind raptor and mediate amino acid signaling to mTORC1. *Science* **320**, 1496-1501, doi:10.1126/science.1157535 (2008).
111 DeYoung, M. P., Horak, P., Sofer, A., Sgroi, D. & Ellisen, L. W. Hypoxia regulates TSC1/2-mTOR signaling and tumor suppression through REDD1-mediated 14-3-3 shuttling. *Genes Dev* **22**, 239-251, doi:10.1101/gad.1617608 (2008).
112 Vezina, C., Kudelski, A. & Sehgal, S. N. Rapamycin (AY-22,989), a new antifungal antibiotic. I. Taxonomy of the producing streptomycete and isolation of the active principle. *J Antibiot (Tokyo)* **28**, 721-726 (1975).
113 Sarbassov, D. D. *et al.* Prolonged rapamycin treatment inhibits mTORC2 assembly and Akt/PKB. *Mol Cell* **22**, 159-168, doi:10.1016/j.molcel.2006.03.029 (2006).
114 Thoreen, C. C. *et al.* A unifying model for mTORC1-mediated regulation of mRNA translation. *Nature* **485**, 109-113, doi:10.1038/nature11083 (2012).
115 Thoreen, C. C. *et al.* An ATP-competitive mammalian target of rapamycin inhibitor reveals rapamycin-resistant functions of mTORC1. *J Biol Chem* **284**, 8023-8032, doi:10.1074/jbc.M900301200 (2009).

116 Shimobayashi, M. & Hall, M. N. Making new contacts: the mTOR network in metabolism and signalling crosstalk. *Nat Rev Mol Cell Biol* **15**, 155-162, doi:10.1038/nrm3757 (2014).
117 Kim, J. E. & Chen, J. regulation of peroxisome proliferator-activated receptor-gamma activity by mammalian target of rapamycin and amino acids in adipogenesis. *Diabetes* **53**, 2748-2756 (2004).
118 Porstmann, T. *et al.* SREBP activity is regulated by mTORC1 and contributes to Akt-dependent cell growth. *Cell Metab* **8**, 224-236, doi:10.1016/j.cmet.2008.07.007 (2008).
119 Hosokawa, N. *et al.* Nutrient-dependent mTORC1 association with the ULK1-Atg13-FIP200 complex required for autophagy. *Mol Biol Cell* **20**, 1981-1991, doi:10.1091/mbc.E08-12-1248 (2009).
120 Schieke, S. M. *et al.* The mammalian target of rapamycin (mTOR) pathway regulates mitochondrial oxygen consumption and oxidative capacity. *J Biol Chem* **281**, 27643-27652, doi:10.1074/jbc.M603536200 (2006).
121 Cunningham, J. T. *et al.* mTOR controls mitochondrial oxidative function through a YY1-PGC-1alpha transcriptional complex. *Nature* **450**, 736-740, doi:10.1038/nature06322 (2007).
122 Guertin, D. A. *et al.* Ablation in mice of the mTORC components raptor, rictor, or mLST8 reveals that mTORC2 is required for signaling to Akt-FOXO and PKCalpha, but not S6K1. *Dev Cell* **11**, 859-871, doi:10.1016/j.devcel.2006.10.007 (2006).
123 Calnan, D. R. & Brunet, A. The FoxO code. *Oncogene* **27**, 2276-2288, doi:10.1038/onc.2008.21 (2008).
124 Sarbassov, D. D. *et al.* Rictor, a novel binding partner of mTOR, defines a rapamycin-insensitive and raptor-independent pathway that regulates the cytoskeleton. *Curr Biol* **14**, 1296-1302, doi:10.1016/j.cub.2004.06.054 (2004).
125 Saunders, R. N., Metcalfe, M. S. & Nicholson, M. L. Rapamycin in transplantation: a review of the evidence. *Kidney Int* **59**, 3-16, doi:10.1046/j.1523-1755.2001.00460.x (2001).
126 Fukao, T. *et al.* PI3K-mediated negative feedback regulation of IL-12 production in DCs. *Nat Immunol* **3**, 875-881, doi:10.1038/ni825 (2002).
127 Martin, M. *et al.* Role of the phosphatidylinositol 3 kinase-Akt pathway in the regulation of IL-10 and IL-12 by Porphyromonas gingivalis lipopolysaccharide. *J Immunol* **171**, 717-725 (2003).
128 Aksoy, E. *et al.* The p110delta isoform of the kinase PI(3)K controls the subcellular compartmentalization of TLR4 signaling and protects from endotoxic shock. *Nat Immunol* **13**, 1045-1054, doi:10.1038/ni.2426 (2012).
129 Weichhart, T. *et al.* The TSC-mTOR signaling pathway regulates the innate inflammatory response. *Immunity* **29**, 565-577, doi:10.1016/j.immuni.2008.08.012 (2008).
130 Napetschnig, J. & Wu, H. Molecular basis of NF-kappaB signaling. *Annu Rev Biophys* **42**, 443-468, doi:10.1146/annurev-biophys-083012-130338 (2013).
131 Ohtani, M. *et al.* Cutting edge: mTORC1 in intestinal CD11c+ CD11b+ dendritic cells regulates intestinal homeostasis by promoting IL-10 production. *J Immunol* **188**, 4736-4740, doi:10.4049/jimmunol.1200069 (2012).
132 Gallon, L. *et al.* Cellular and molecular immune profiles in renal transplant recipients after conversion from tacrolimus to sirolimus. *Kidney Int* **87**, 828-838, doi:10.1038/ki.2014.350 (2015).

133 Brouard, S. *et al.* Comparative transcriptional and phenotypic peripheral blood analysis of kidney recipients under cyclosporin A or sirolimus monotherapy. *Am J Transplant* **10**, 2604-2614, doi:10.1111/j.1600-6143.2010.03302.x (2010).
134 Weichhart, T. *et al.* Inhibition of mTOR blocks the anti-inflammatory effects of glucocorticoids in myeloid immune cells. *Blood* **117**, 4273-4283, doi:10.1182/blood-2010-09-310888 (2011).
135 Pan, H., O'Brien, T. F., Zhang, P. & Zhong, X. P. The role of tuberous sclerosis complex 1 in regulating innate immunity. *J Immunol* **188**, 3658-3666, doi:10.4049/jimmunol.1102187 (2012).
136 Byles, V. *et al.* The TSC-mTOR pathway regulates macrophage polarization. *Nat Commun* **4**, 2834, doi:10.1038/ncomms3834 (2013).
137 Fan, W. *et al.* FoxO1 regulates Tlr4 inflammatory pathway signalling in macrophages. *EMBO J* **29**, 4223-4236, doi:10.1038/emboj.2010.268 (2010).
138 Zhu, L. *et al.* TSC1 controls macrophage polarization to prevent inflammatory disease. *Nat Commun* **5**, 4696, doi:10.1038/ncomms5696 (2014).
139 Brown, J., Wang, H., Suttles, J., Graves, D. T. & Martin, M. Mammalian target of rapamycin complex 2 (mTORC2) negatively regulates Toll-like receptor 4-mediated inflammatory response via FoxO1. *J Biol Chem* **286**, 44295-44305, doi:10.1074/jbc.M111.258053 (2011).
140 Festuccia, W. T., Pouliot, P., Bakan, I., Sabatini, D. M. & Laplante, M. Myeloid-specific Rictor deletion induces M1 macrophage polarization and potentiates in vivo pro-inflammatory response to lipopolysaccharide. *PLoS One* **9**, e95432, doi:10.1371/journal.pone.0095432 (2014).
141 Ivanov, S. S. & Roy, C. R. Pathogen signatures activate a ubiquitination pathway that modulates the function of the metabolic checkpoint kinase mTOR. *Nat Immunol* **14**, 1219-1228, doi:10.1038/ni.2740 (2013).
142 Herranz, N. *et al.* mTOR regulates MAPKAPK2 translation to control the senescence-associated secretory phenotype. *Nat Cell Biol* **17**, 1205-1217, doi:10.1038/ncb3225 (2015).
143 Jang, B. C. *et al.* Catalase induced expression of inflammatory mediators via activation of NF-kappaB, PI3K/AKT, p70S6K, and JNKs in BV2 microglia. *Cell Signal* **17**, 625-633, doi:10.1016/j.cellsig.2004.10.001 (2005).
144 Lu, D. Y., Liou, H. C., Tang, C. H. & Fu, W. M. Hypoxia-induced iNOS expression in microglia is regulated by the PI3-kinase/Akt/mTOR signaling pathway and activation of hypoxia inducible factor-1alpha. *Biochem Pharmacol* **72**, 992-1000, doi:10.1016/j.bcp.2006.06.038 (2006).
145 Chong, Z. Z., Li, F. & Maiese, K. The pro-survival pathways of mTOR and protein kinase B target glycogen synthase kinase-3beta and nuclear factor-kappaB to foster endogenous microglial cell protection. *Int J Mol Med* **19**, 263-272 (2007).
146 Dello Russo, C., Lisi, L., Tringali, G. & Navarra, P. Involvement of mTOR kinase in cytokine-dependent microglial activation and cell proliferation. *Biochem Pharmacol* **78**, 1242-1251, doi:10.1016/j.bcp.2009.06.097 (2009).
147 Verheijden, S. *et al.* Identification of a chronic non-neurodegenerative microglia activation state in a mouse model of peroxisomal beta-oxidation deficiency. *Glia* **63**, 1606-1620, doi:10.1002/glia.22831 (2015).
148 Zou, J. *et al.* Rheb1 is required for mTORC1 and myelination in postnatal brain development. *Dev Cell* **20**, 97-108, doi:10.1016/j.devcel.2010.11.020 (2011).

149 Lazuardi, L. *et al.* Age-related loss of naive T cells and dysregulation of T-cell/B-cell interactions in human lymph nodes. *Immunology* **114**, 37-43, doi:10.1111/j.1365-2567.2004.02006.x (2005).
150 Rosen, S. D. Ligands for L-selectin: homing, inflammation, and beyond. *Annu Rev Immunol* **22**, 129-156, doi:10.1146/annurev.immunol.21.090501.080131 (2004).
151 Salam, N. *et al.* T cell ageing: effects of age on development, survival & function. *Indian J Med Res* **138**, 595-608 (2013).
152 Bueno, V., Sant'Anna, O. A. & Lord, J. M. Ageing and myeloid-derived suppressor cells: possible involvement in immunosenescence and age-related disease. *Age (Dordr)* **36**, 9729, doi:10.1007/s11357-014-9729-x (2014).
153 Auffray, C., Sieweke, M. H. & Geissmann, F. Blood monocytes: development, heterogeneity, and relationship with dendritic cells. *Annu Rev Immunol* **27**, 669-692, doi:10.1146/annurev.immunol.021908.132557 (2009).
154 Quail, D. F. & Joyce, J. A. Microenvironmental regulation of tumor progression and metastasis. *Nat Med* **19**, 1423-1437, doi:10.1038/nm.3394 (2013).
155 Palmer, D. B. The effect of age on thymic function. *Front Immunol* **4**, 316, doi:10.3389/fimmu.2013.00316 (2013).
156 Moro-Garcia, M. A., Alonso-Arias, R. & Lopez-Larrea, C. When Aging Reaches CD4+ T-Cells: Phenotypic and Functional Changes. *Front Immunol* **4**, 107, doi:10.3389/fimmu.2013.00107 (2013).
157 Beerman, I. *et al.* Functionally distinct hematopoietic stem cells modulate hematopoietic lineage potential during aging by a mechanism of clonal expansion. *Proc Natl Acad Sci U S A* **107**, 5465-5470, doi:10.1073/pnas.1000834107 (2010).
158 Enioutina, E. Y., Bareyan, D. & Daynes, R. A. A role for immature myeloid cells in immune senescence. *J Immunol* **186**, 697-707, doi:10.4049/jimmunol.1002987 (2011).
159 Renshaw, M. *et al.* Cutting edge: impaired Toll-like receptor expression and function in aging. *J Immunol* **169**, 4697-4701 (2002).
160 Njie, E. G. *et al.* Ex vivo cultures of microglia from young and aged rodent brain reveal age-related changes in microglial function. *Neurobiol Aging* **33**, 195 e191-112, doi:10.1016/j.neurobiolaging.2010.05.008 (2012).
161 Fietta, A., Merlini, C., Dos Santos, C., Rovida, S. & Grassi, C. Influence of aging on some specific and nonspecific mechanisms of the host defense system in 146 healthy subjects. *Gerontology* **40**, 237-245 (1994).
162 Linehan, E. *et al.* Aging impairs peritoneal but not bone marrow-derived macrophage phagocytosis. *Aging Cell* **13**, 699-708, doi:10.1111/acel.12223 (2014).
163 Swift, M. E., Kleinman, H. K. & DiPietro, L. A. Impaired wound repair and delayed angiogenesis in aged mice. *Lab Invest* **79**, 1479-1487 (1999).
164 Beutner, C. *et al.* Unique transcriptome signature of mouse microglia. *Glia* **61**, 1429-1442, doi:10.1002/glia.22524 (2013).
165 Parakalan, R. *et al.* Transcriptome analysis of amoeboid and ramified microglia isolated from the corpus callosum of rat brain. *BMC Neurosci* **13**, 64, doi:10.1186/1471-2202-13-64 (2012).
166 Marcondes, M. C. *et al.* Osteopontin expression in the brain triggers localized inflammation and cell death when immune cells are activated by pertussis toxin. *Mediators Inflamm* **2014**, 358218, doi:10.1155/2014/358218 (2014).

167 Kahles, F., Findeisen, H. M. & Bruemmer, D. Osteopontin: A novel regulator at the cross roads of inflammation, obesity and diabetes. *Mol Metab* **3**, 384-393, doi:10.1016/j.molmet.2014.03.004 (2014).
168 Ma, J. *et al.* Microglial cystatin F expression is a sensitive indicator for ongoing demyelination with concurrent remyelination. *Journal of neuroscience research* **89**, 639-649, doi:10.1002/jnr.22567 (2011).
169 Liu, Y. *et al.* Matrix metalloproteinase-12 contributes to neuroinflammation in the aged brain. *Neurobiol Aging* **34**, 1231-1239, doi:10.1016/j.neurobiolaging.2012.10.015 (2013).
170 Laplante, M. & Sabatini, D. M. mTOR signaling in growth control and disease. *Cell* **149**, 274-293, doi:10.1016/j.cell.2012.03.017 (2012).
171 Suh, H. S., Zhao, M. L., Derico, L., Choi, N. & Lee, S. C. Insulin-like growth factor 1 and 2 (IGF1, IGF2) expression in human microglia: differential regulation by inflammatory mediators. *J Neuroinflammation* **10**, 37, doi:10.1186/1742-2094-10-37 (2013).
172 Charo, I. F. & Ransohoff, R. M. The many roles of chemokines and chemokine receptors in inflammation. *N Engl J Med* **354**, 610-621, doi:10.1056/NEJMra052723 (2006).
173 Biber, K., Vinet, J. & Boddeke, H. W. Neuron-microglia signaling: chemokines as versatile messengers. *J Neuroimmunol* **198**, 69-74, doi:10.1016/j.jneuroim.2008.04.012 (2008).
174 Rosito, M. *et al.* Trasmembrane chemokines CX3CL1 and CXCL16 drive interplay between neurons, microglia and astrocytes to counteract pMCAO and excitotoxic neuronal death. *Front Cell Neurosci* **8**, 193, doi:10.3389/fncel.2014.00193 (2014).
175 Yadav, M. & Schorey, J. S. The beta-glucan receptor dectin-1 functions together with TLR2 to mediate macrophage activation by mycobacteria. *Blood* **108**, 3168-3175, doi:10.1182/blood-2006-05-024406 (2006).
176 Hayashi, A. *et al.* Positive regulation of phagocytosis by SIRPbeta and its signaling mechanism in macrophages. *J Biol Chem* **279**, 29450-29460, doi:10.1074/jbc.M400950200 (2004).
177 Geddes, K., Magalhaes, J. G. & Girardin, S. E. Unleashing the therapeutic potential of NOD-like receptors. *Nat Rev Drug Discov* **8**, 465-479, doi:10.1038/nrd2783 (2009).
178 Nimmerjahn, F. & Ravetch, J. V. Fc-receptors as regulators of immunity. *Adv Immunol* **96**, 179-204, doi:10.1016/S0065-2776(07)96005-8 (2007).
179 Perreira, J. M., Chin, C. R., Feeley, E. M. & Brass, A. L. IFITMs restrict the replication of multiple pathogenic viruses. *J Mol Biol* **425**, 4937-4955, doi:10.1016/j.jmb.2013.09.024 (2013).
180 Crocker, P. R., Paulson, J. C. & Varki, A. Siglecs and their roles in the immune system. *Nat Rev Immunol* **7**, 255-266, doi:10.1038/nri2056 (2007).
181 Akira, S., Takeda, K. & Kaisho, T. Toll-like receptors: critical proteins linking innate and acquired immunity. *Nat Immunol* **2**, 675-680, doi:10.1038/90609 (2001).
182 Kim, C. *et al.* Neuron-released oligomeric alpha-synuclein is an endogenous agonist of TLR2 for paracrine activation of microglia. *Nat Commun* **4**, 1562, doi:10.1038/ncomms2534 (2013).
183 Idzko, M., Ferrari, D. & Eltzschig, H. K. Nucleotide signalling during inflammation. *Nature* **509**, 310-317, doi:10.1038/nature13085 (2014).

184 Blackburn, M. R., Vance, C. O., Morschl, E. & Wilson, C. N. Adenosine receptors and inflammation. *Handb Exp Pharmacol*, 215-269, doi:10.1007/978-3-540-89615-9_8 (2009).
185 Hasko, G., Linden, J., Cronstein, B. & Pacher, P. Adenosine receptors: therapeutic aspects for inflammatory and immune diseases. *Nat Rev Drug Discov* **7**, 759-770, doi:10.1038/nrd2638 (2008).
186 Butovsky, O. *et al.* Identification of a unique TGF-beta-dependent molecular and functional signature in microglia. *Nat Neurosci* **17**, 131-143, doi:10.1038/nn.3599 (2014).
187 Haynes, S. E. *et al.* The P2Y12 receptor regulates microglial activation by extracellular nucleotides. *Nat Neurosci* **9**, 1512-1519, doi:10.1038/nn1805 (2006).
188 Kelly, B. & O'Neill, L. A. Metabolic reprogramming in macrophages and dendritic cells in innate immunity. *Cell Res* **25**, 771-784, doi:10.1038/cr.2015.68 (2015).
189 Zhou, L. T. *et al.* Gpnmb/osteoactivin, an attractive target in cancer immunotherapy. *Neoplasma* **59**, 1-5, doi:10.4149/neo_2012_001 (2012).
190 Huang, J. J., Ma, W. J. & Yokoyama, S. Expression and immunolocalization of Gpnmb, a glioma-associated glycoprotein, in normal and inflamed central nervous systems of adult rats. *Brain Behav* **2**, 85-96, doi:10.1002/brb3.39 (2012).
191 Shi, F. *et al.* Induction of Matrix Metalloproteinase-3 (MMP-3) Expression in the Microglia by Lipopolysaccharide (LPS) via Upregulation of Glycoprotein Nonmetastatic Melanoma B (GPNMB) Expression. *J Mol Neurosci*, doi:10.1007/s12031-014-0280-0 (2014).
192 Aloisi, F. *et al.* Lymphoid chemokines in chronic neuroinflammation. *J Neuroimmunol* **198**, 106-112, doi:10.1016/j.jneuroim.2008.04.025 (2008).
193 Lee, D. C. *et al.* Aging enhances classical activation but mitigates alternative activation in the central nervous system. *Neurobiol Aging* **34**, 1610-1620, doi:10.1016/j.neurobiolaging.2012.12.014 (2013).
194 Kowarik, M. C. *et al.* CXCL13 is the major determinant for B cell recruitment to the CSF during neuroinflammation. *J Neuroinflammation* **9**, 93, doi:10.1186/1742-2094-9-93 (2012).
195 Popescu, B. O. *et al.* Blood-brain barrier alterations in ageing and dementia. *J Neurol Sci* **283**, 99-106, doi:10.1016/j.jns.2009.02.321 (2009).
196 Leonard, W. J. & Lin, J. X. Cytokine receptor signaling pathways. *J Allergy Clin Immunol* **105**, 877-888, doi:10.1037/mai.2000.106899 (2000).
197 Liu, S. *et al.* TLR2 is a primary receptor for Alzheimer's amyloid beta peptide to trigger neuroinflammatory activation. *J Immunol* **188**, 1098-1107, doi:10.4049/jimmunol.1101121 (2012).
198 Orr, A. G., Orr, A. L., Li, X. J., Gross, R. E. & Traynelis, S. F. Adenosine A(2A) receptor mediates microglial process retraction. *Nat Neurosci* **12**, 872-878, doi:10.1038/nn.2341 (2009).
199 Miller, R. A. *et al.* Rapamycin-mediated lifespan increase in mice is dose and sex dependent and metabolically distinct from dietary restriction. *Aging Cell* **13**, 468-477, doi:10.1111/acel.12194 (2014).
200 Elmore, M. R. *et al.* Colony-stimulating factor 1 receptor signaling is necessary for microglia viability, unmasking a microglia progenitor cell in the adult brain. *Neuron* **82**, 380-397, doi:10.1016/j.neuron.2014.02.040 (2014).

201 Delgoffe, G. M. *et al.* The kinase mTOR regulates the differentiation of helper T cells through the selective activation of signaling by mTORC1 and mTORC2. *Nat Immunol* **12**, 295-303, doi:10.1038/ni.2005 (2011).
202 Nazem, A., Sankowski, R., Bacher, M. & Al-Abed, Y. Rodent models of neuroinflammation for Alzheimer's disease. *J Neuroinflammation* **12**, 74, doi:10.1186/s12974-015-0291-y (2015).
203 Butovsky, O. *et al.* Targeting miR-155 restores abnormal microglia and attenuates disease in SOD1 mice. *Ann Neurol* **77**, 75-99, doi:10.1002/ana.24304 (2015).
204 Wolf, Y., Yona, S., Kim, K. W. & Jung, S. Microglia, seen from the CX3CR1 angle. *Front Cell Neurosci* **7**, 26, doi:10.3389/fncel.2013.00026 (2013).
205 Varol, C. *et al.* Intestinal lamina propria dendritic cell subsets have different origin and functions. *Immunity* **31**, 502-512, doi:10.1016/j.immuni.2009.06.025 (2009).
206 Cunningham, C. & Maclullich, A. M. At the extreme end of the psychoneuroimmunological spectrum: delirium as a maladaptive sickness behaviour response. *Brain Behav Immun* **28**, 1-13, doi:10.1016/j.bbi.2012.07.012 (2013).
207 Perkins, N. D. Integrating cell-signalling pathways with NF-kappaB and IKK function. *Nat Rev Mol Cell Biol* **8**, 49-62, doi:10.1038/nrm2083 (2007).
208 Habib, S. L. Mechanism of activation of AMPK and upregulation of OGG1 by rapamycin in cancer cells. *Oncotarget* **2**, 958-959, doi:10.18632/oncotarget.381 (2011).
209 Lanna, A., Henson, S. M., Escors, D. & Akbar, A. N. The kinase p38 activated by the metabolic regulator AMPK and scaffold TAB1 drives the senescence of human T cells. *Nat Immunol* **15**, 965-972, doi:10.1038/ni.2981 (2014).
210 Olson, C. M. *et al.* p38 mitogen-activated protein kinase controls NF-kappaB transcriptional activation and tumor necrosis factor alpha production through RelA phosphorylation mediated by mitogen- and stress-activated protein kinase 1 in response to Borrelia burgdorferi antigens. *Infect Immun* **75**, 270-277, doi:10.1128/IAI.01412-06 (2007).
211 Wen, H. *et al.* Fatty acid-induced NLRP3-ASC inflammasome activation interferes with insulin signaling. *Nat Immunol* **12**, 408-415, doi:10.1038/ni.2022 (2011).
212 Ni, M. & Aschner, M. Neonatal rat primary microglia: isolation, culturing, and selected applications. *Curr Protoc Toxicol* **Chapter 12**, Unit 12 17, doi:10.1002/0471140856.tx1217s43 (2010).
213 Bradley, J. R. TNF-mediated inflammatory disease. *J Pathol* **214**, 149-160, doi:10.1002/path.2287 (2008).
214 Bauernfeind, F. G. *et al.* Cutting edge: NF-kappaB activating pattern recognition and cytokine receptors license NLRP3 inflammasome activation by regulating NLRP3 expression. *J Immunol* **183**, 787-791, doi:10.4049/jimmunol.0901363 (2009).
215 Carola, V., D'Olimpio, F., Brunamonti, E., Mangia, F. & Renzi, P. Evaluation of the elevated plus-maze and open-field tests for the assessment of anxiety-related behaviour in inbred mice. *Behav Brain Res* **134**, 49-57 (2002).
216 Godbout, J. P. *et al.* Exaggerated neuroinflammation and sickness behavior in aged mice following activation of the peripheral innate immune system. *Faseb J* **19**, 1329-1331, doi:10.1096/fj.05-3776fje (2005).

217 Shi, C. & Pamer, E. G. Monocyte recruitment during infection and inflammation. *Nat Rev Immunol* **11**, 762-774, doi:10.1038/nri3070 (2011).
218 Tyagi, R. *et al.* Rheb Inhibits Protein Synthesis by Activating the PERK-eIF2alpha Signaling Cascade. *Cell Rep*, doi:10.1016/j.celrep.2015.01.014 (2015).
219 Penninx, B. W. *et al.* Inflammatory markers and depressed mood in older persons: results from the Health, Aging and Body Composition study. *Biol Psychiatry* **54**, 566-572 (2003).
220 Nguyen, M. D., Julien, J. P. & Rivest, S. Innate immunity: the missing link in neuroprotection and neurodegeneration? *Nature reviews. Neuroscience* **3**, 216-227, doi:10.1038/nrn752 (2002).
221 Konsman, J. P., Parnet, P. & Dantzer, R. Cytokine-induced sickness behaviour: mechanisms and implications. *Trends Neurosci* **25**, 154-159 (2002).
222 Chen, J. *et al.* Neuroinflammation and disruption in working memory in aged mice after acute stimulation of the peripheral innate immune system. *Brain Behav Immun* **22**, 301-311, doi:10.1016/j.bbi.2007.08.014 (2008).
223 Barrientos, R. M. *et al.* Peripheral infection and aging interact to impair hippocampal memory consolidation. *Neurobiol Aging* **27**, 723-732, doi:10.1016/j.neurobiolaging.2005.03.010 (2006).
224 Perry, V. H. & Holmes, C. Microglial priming in neurodegenerative disease. *Nature reviews. Neurology* **10**, 217-224, doi:10.1038/nrneurol.2014.38 (2014).
225 Blagosklonny, M. V. TOR-driven aging: speeding car without brakes. *Cell Cycle* **8**, 4055-4059 (2009).
226 Houtkooper, R. H. *et al.* The metabolic footprint of aging in mice. *Sci Rep* **1**, 134, doi:10.1038/srep00134 (2011).
227 Harries, L. W. *et al.* Advancing age is associated with gene expression changes resembling mTOR inhibition: evidence from two human populations. *Mech Ageing Dev* **133**, 556-562, doi:10.1016/j.mad.2012.07.003 (2012).
228 Calhoun, C. *et al.* Senescent Cells Contribute to the Physiological Remodeling of Aged Lungs. *J Gerontol A Biol Sci Med Sci* **71**, 153-160, doi:10.1093/gerona/glu241 (2016).
229 Leontieva, O. V., Paszkiewicz, G. M. & Blagosklonny, M. V. Fasting levels of hepatic p-S6 are increased in old mice. *Cell Cycle* **13**, 2656-2659, doi:10.4161/15384101.2014.949150 (2014).
230 Baar, E. L., Carbajal, K. A., Ong, I. M. & Lamming, D. W. Sex- and tissue-specific changes in mTOR signaling with age in C57BL/6J mice. *Aging Cell* **15**, 155-166, doi:10.1111/acel.12425 (2016).
231 Saeed, S. *et al.* Epigenetic programming of monocyte-to-macrophage differentiation and trained innate immunity. *Science* **345**, 1251086, doi:10.1126/science.1251086 (2014).
232 Flynn, J. M. *et al.* Late-life rapamycin treatment reverses age-related heart dysfunction. *Aging Cell* **12**, 851-862, doi:10.1111/acel.12109 (2013).
233 Herranz, N. *et al.* Erratum: mTOR regulates MAPKAPK2 translation to control the senescence-associated secretory phenotype. *Nat Cell Biol* **17**, 1370, doi:10.1038/ncb3243 (2015).
234 Weichhart, T., Hengstschlager, M. & Linke, M. Regulation of innate immune cell function by mTOR. *Nat Rev Immunol* **15**, 599-614, doi:10.1038/nri3901 (2015).
235 Mannick, J. B. *et al.* mTOR inhibition improves immune function in the elderly. *Sci Transl Med* **6**, 268ra179, doi:10.1126/scitranslmed.3009892 (2014).

236 Beura, L. K. *et al.* Normalizing the environment recapitulates adult human immune traits in laboratory mice. *Nature* **532**, 512-516, doi:10.1038/nature17655 (2016).
237 Kaeberlein, M., Creevy, K. E. & Promislow, D. E. The dog aging project: translational geroscience in companion animals. *Mamm Genome* **27**, 279-288, doi:10.1007/s00335-016-9638-7 (2016).
238 Lamming, D. W., Ye, L., Sabatini, D. M. & Baur, J. A. Rapalogs and mTOR inhibitors as anti-aging therapeutics. *The Journal of clinical investigation* **123**, 980-989, doi:10.1172/JCI64099 (2013).
239 Battelli, C. & Cho, D. C. mTOR inhibitors in renal cell carcinoma. *Therapy* **8**, 359-367, doi:10.2217/thy.11.32 (2011).
240 Caccamo, A., Majumder, S., Richardson, A., Strong, R. & Oddo, S. Molecular interplay between mammalian target of rapamycin (mTOR), amyloid-beta, and Tau: effects on cognitive impairments. *J Biol Chem* **285**, 13107-13120, doi:10.1074/jbc.M110.100420 (2010).
241 Spilman, P. *et al.* Inhibition of mTOR by rapamycin abolishes cognitive deficits and reduces amyloid-beta levels in a mouse model of Alzheimer's disease. *PLoS One* **5**, e9979, doi:10.1371/journal.pone.0009979 (2010).
242 Cameron, B. & Landreth, G. E. Inflammation, microglia, and Alzheimer's disease. *Neurobiol Dis* **37**, 503-509, doi:10.1016/j.nbd.2009.10.006 (2010).
243 Majumder, S., Richardson, A., Strong, R. & Oddo, S. Inducing autophagy by rapamycin before, but not after, the formation of plaques and tangles ameliorates cognitive deficits. *PLoS One* **6**, e25416, doi:10.1371/journal.pone.0025416 (2011).
244 Richardson, A., Galvan, V., Lin, A. L. & Oddo, S. How longevity research can lead to therapies for Alzheimer's disease: The rapamycin story. *Experimental gerontology* **68**, 51-58, doi:10.1016/j.exger.2014.12.002 (2015).